MICROCOPY RESOLUTION TEST CHART

NATIONAL BUREAU OF STANDARDS-1963-A

AFML-TR-76-241

# ASCERTAINMENT OF THE EFFECT OF COMPRESSIVE LOADING ON THE FATIGUE LIFETIME OF GRAPHITE EPOXY LAMINATES FOR STRUCTURAL APPLICATIONS

*LOCKHEED-CALIFORNIA COMPANY*
*RYE CANYON RESEARCH LABORATORY*
*BURBANK, CALIFORNIA 91520*

DECEMBER 1976

FINAL REPORT FEBRUARY 1975 - SEPTEMBER 1976

410347

Approved for public release; distribution unlimited

AIR FORCE MATERIALS LABORATORY
AIR FORCE WRIGHT AERONAUTICAL LABORATORIES
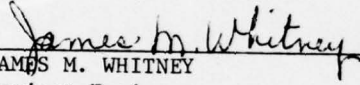AIR FORCE SYSTEMS COMMAND
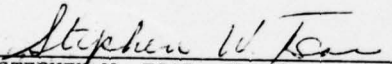WRIGHT-PATTERSON AIR FORCE BASE, OHIO 45433

JAMES M. WHITNEY
Project Engineer

FOR THE DIRECTOR

STEPHEN W. TSAI, Chief
Mechanics & Surface Interactions Branch
Nonmetallic Materials Division

# REPORT DOCUMENTATION PAGE

READ INSTRUCTIONS
BEFORE COMPLETING FORM

| 1. REPORT NUMBER | 2. GOVT ACCESSION NO. | 3. RECIPIENT'S CATALOG NUMBER |
|---|---|---|
| AFML-TR-76-241 | | |

4. TITLE (and Subtitle)

ASCERTAINMENT OF THE EFFECT OF COMPRESSIVE
LOADING ON THE FATIGUE LIFETIME OF GRAPHITE
EPOXY LAMINATES FOR STRUCTURAL APPLICATIONS

5. TYPE OF REPORT & PERIOD COVERED
Final Technical report
13 Feb 1975 — 22 Sep 1976

6. PERFORMING ORG. REPORT NUMBER

7. AUTHOR(s)

J. T. Ryder
E. K. Walker

8. CONTRACT OR GRANT NUMBER(s)

F33615-75-C-5118

9. PERFORMING ORGANIZATION NAME AND ADDRESS

Lockheed-California Company
Division of Lockheed Aircraft Corporation
Burbank, California 91520

10. PROGRAM ELEMENT, PROJECT, TASK
AREA & WORK UNIT NUMBERS

73400399

11. CONTROLLING OFFICE NAME AND ADDRESS

Air Force Materials Laboratory (MBM)
Air Force Systems Command
Wright-Patterson AFB, Ohio

12. REPORT DATE
December 1976

13. NUMBER OF PAGES
273

| 14. MONITORING AGENCY NAME & ADDRESS(if different from Controlling Office) | 15. SECURITY CLASS. (of this report) |
|---|---|
| | Unclassified |
| | 15a. DECLASSIFICATION DOWNGRADING SCHEDULE |

16. DISTRIBUTION STATEMENT (of this Report)

Approved for public release: distribution unlimited

17. DISTRIBUTION STATEMENT (of the abstract entered in Block 20, if different from Report)

D D C
AUG 22 1977
C

18. SUPPLEMENTARY NOTES

19. KEY WORDS (Continue on reverse side if necessary and identify by block number)

Composites
Graphite/Epoxy
Fatigue
Compression
Residual Strength

20. ABSTRACT (Continue on reverse side if necessary and identify by block number)

The main objective of this research investigation was the experimental determination of the effect of compressive loading on the fatigue response of graphite/epoxy laminates. The primary emphasis of the program was on the accumulation of a statistically significant data base. The data base was to be used for developing an analytical model with predictive capability to account for the effect of compressive loading. The test program included only unnotched coupons in a room temperature, laboratory air environment. The test program consisted of static tensile and compressive tests; tension-tension and tension-

DD FORM 1473 EDITION OF 1 NOV 65 IS OBSOLETE
1 JAN 73

410347

20.

compression fatigue tests; and tensile and compressive residual strength tests
of coupons tested either under tension-tension or tension-compression fatigue
loading.  The development of a large, statistically meaningful data base was
accomplished.  The general effect of compression on the fatigue response of
a graphite/epoxy composite was determined.  However, a general model with
capability to account for compressive loading was not attempted.  As an
alternate, the concept of a fatigue threshold was postulated along with
consideration of some substantiating data.  Analysis of the data showed
that due to the extent of data scatter, a model of the "wear-out" or similar
type would predict the need for unacceptably low stress levels to achieve the
high probabilities of survival required for aircraft structures.

FOREWORD

This report describes an investigation of ascertainment of the effect of
compressive loading on the fatigue lifetime of graphite/epoxy laminates
for structural applications performed by the Lockheed-California Company
under Air Force Contract F33615-75-C-5118. The Air Force Project Engineer
directing the program was Dr. J. M. Whitney of the Mechanics and Surface
Interactions Branch, Nonmetallic Materials Division, Air Force Materials
Laboratory at Wright-Patterson AFB, Ohio. Dr. J. T. Ryder was the Principal
Investigator while Mr. E. K. Walker was the Program Manager.

The program was conducted through the Structures Department of the Lockheed-
California Company. The support and contributions of Mr. W. E. Krupp,
Group Engineer, Fatigue and Fracture Mechanics Laboratory; Mr. D. E. Pettit
Dr. G. E. Bowie and Ms. K. N. Lauraitis, all of the same laboratory, and of
Mr. L. D. Fogg of the Structural Methods Group, are gratefully acknowledged
by the authors.

iii

TABLE OF CONTENTS

TABLE OF CONTENTS (Continued)

LIST OF ILLUSTRATIONS

LIST OF ILLUSTRATIONS (Continued)

LIST OF ILLUSTRATIONS (Continued)

LIST OF ILLUSTRATIONS (Continued)

LIST OF ILLUSTRATIONS (Continued)

LIST OF TABLES

LIST OF TABLES (Continued)

LIST OF TABLES (Continued)

SECTION I

INTRODUCTION

The main objective of this research investigation was the experimental deter-
mination of the effect of compressive loading on the fatigue response of
graphite/epoxy laminates.  The primary emphasis of the program was on the
accumulation of a statistically significant data base.  The intention was
to use the data base to develop an analytical model with predictive capabil-
ity to account for the effect of compressive loading.  The test program
included only unnotched coupons in a room temperature, laboratory air
environment.

The development of a large, statistically meaningful data base was accomp-
lished.  The general effect of compression on the fatigue response of a
graphite/epoxy composite was determined.  However, a general model with
capability to account for compressive loading was not attempted.  As an
alternate, the concept of a fatigue threshold was postulated and the
substantiating data presented.  The decision to explore the possibility
of a fatigue threshold was made after an extensive analysis of the
data and after appraisal of the associated implications.  The analysis
showed that the large data scatter implied the necessity of using low
fatigue stress levels to achieve the high probabilities of survival
required for aircraft structures.

The program emphasis on the accumulation of a large data base was considered
necessary for two reasons.  First, only a large set of data from more than
one laminate would allow correct resolution of the effect of compressive
loading on the fatigue properties.  Second, numerous replications were
needed to determine the reliability of any analytical model.  The latter
reason for an extensive data base was extremely important and needs to be
further elucidated.

1

In many design applications, such as "safe life" components, the cost and safety implications of a failure are so high that an acceptable probability of survival must be $P_{.99}$, $P_{.999}$, $P_{.9999}$ or, as in helicopter applications, even higher. Analytical models for predicting residual strength degradation or fatigue failures should be reliable to these probability of survival levels. Thus, the usefulness for aerospace design of residual strength and fatigue models must be judged in regards to their ability to reasonably estimate high probability of survival values.

The principal features of the sequential investigation are shown in Fig. 1. Phase 1 consisted of fabrication of unnotched specimens with as nearly consistent properties as practical. In Phase 2, initial static strength (including stress-strain curves) distributions were determined. Following this, Phase 3 established the general stress-life (S-N) behavior of the material for both tension-tension and tension-compression fatigue. The preliminary screening tests at several load levels were used to determine the general shape of the S-N curves and aid in selection of load levels at which statistically based fatigue life distributions were to be determined. Using this information, the number of cycles for each load level which would give the most useful information on the distribution of tension and compression residual strengths was determined in Phase 4, and residual strength fatigue tests conducted. Phases 1 to 4 were conducted first using a quasi-isotropic laminate and then using a 67% 0° fiber laminate.

Experimental results were analyzed and analytical models considered in Phase 5. Data analysis included estimation of Weibull parameters. Investigation of analytical models was primarily concerned with evaluation of the "wear-out" type of model where the specific rate-decay equation and limits of integration are selected based on data trends and physical evidence of mechanisms.

2

TASK I

```
┌─────────────────────────────────┐
│           PHASE 1               │
│      SPECIMEN FABRICATION       │
└─────────────────────────────────┘
                 │
                 ▼
┌─────────────────────────────────┐
│           PHASE 2               │
│         STATIC TESTING          │
└─────────────────────────────────┘
                 │
                 ▼
┌─────────────────────────────────┐
│           PHASE 3               │
│        FATIGUE TESTING          │
└─────────────────────────────────┘
                 │
                 ▼
┌─────────────────────────────────┐
│           PHASE 4               │
│    RESIDUAL STRENGTH TESTING    │
└─────────────────────────────────┘
                 │
```

TASK II

```
                 ▼
┌─────────────────────────────────┐
│           PHASE 5               │
│  DATA ANALYSIS AND FATIGUE      │
│      MODEL DEVELOPMENT          │
└─────────────────────────────────┘
```
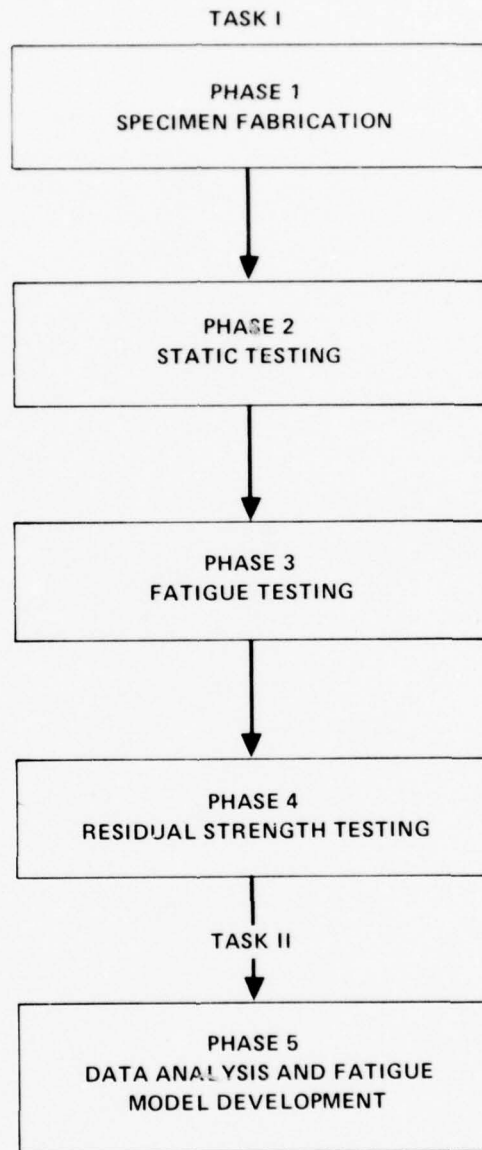
Figure 1.  Program Outline

## SECTION II

## PROGRAM OVERVIEW

This research investigation emphasized the delineation of the effect of compressive loading on the fatigue behavior of graphite/epoxy laminates. This section presents a discussion of the rationale for material selection, program test matrix, and general test procedures.

### 2.1 Material Selection Background

The number of graphite material systems which have emerged in the recent history of advanced composites and which were viable for acceptance in this program were numerous. However, changes in system designation have been more a consequence of changes in the epoxy resin system than in the graphite fiber. An in-depth review of available graphite/epoxy systems led to the conclusion that the basic material selected for use on this program should consist of a low-cost, high strength graphite fiber such as the Hercules AS type or the Union Carbide Thornel 300. The matrix material was chosen as a 177°C (350°F) cure epoxy to be selected from one of the following: Hercules 3501, Narmco 5208, or Fiberite 934. The fiber/resin combinations considered for this program were Hercules' Magnamite (AS/3501), Narmco's Rigidite (T300/5208), Fiberite's HY-E-1034C (T300/934) and HY-E-1334C (AS/934).

The selected fiber/resin system was Fiberite system HY-E-1034C (Thornel T300 Fiber/Fiberite 934 Resin). Fiber/resin systems employing the AS fiber or 3501 resin were eliminated on the basis of limited data [1] which indicated that they had excessively wide property variations at the time of the inception of this program. The Narmco Rigidite (T300/5208) system was eliminated during discussions with the Air Force Program Manager.

### 2.2 Laminate Selection

Laminates for aircraft structures are typically selected for convenience from the $0_i/\pm45_j/90_k$ orientation family. The $0°$ direction is generally oriented parallel to the principal axial loading direction; $\pm45°$ plies

5

Preceding Page Blank

provide shear strength and stiffness or buckling resistance; and 90° plies provide additional strength in the transverse direction when required.   The judicious addition of 90° plies to $(0_i/45_j)$ laminates reduces the Poisson's ratio, can be used to mitigate some of the free edge stresses, and can result in strength and stiffness benefits depending on the loading direction.  However, the 90° plies may crack at a fraction of the ultimate tensile strength of the laminates complicating the fatigue phenomenon.  Two laminates were chosen for the investigation:  a quasi-isotropic, 25% 0° fiber laminate $(0/+45/90/-45_2/90/+45/0)_s$, and a 67% 0° fiber laminate $(0/+45/0_2/-45/0_2/+45/0_2/-45/0)_s$.  The first laminate, designated 1, was chosen because of possible wide application and because the failure mode may be dominated by the matrix. The second laminate, designated 2, was chosen because the failure may be dominated by the fiber.

The selection of stacking sequences for the laminates considered the following:

(a)  Mirror symmetry about the mid-plane was maintained to minimize warping or curling during manufacture or under load.

(b)  Stacking order was considered because of the severe effects on the flexural stiffness and, consequently, the buckling behavior of the laminate.  A wide column has a maximum buckling strength when the 0° plies are at or near the outer surface.

(c)  For optimum load transfer the ply adjacent to a bonded joint was oriented with the fibers parallel to the direction of loading.

(d)  Adjacent plies were oriented (when possible) to minimize the angle between adjacent plies.  Studies [2] have shown microcracking can occur from curing stresses if adjacent plies are oriented at greater than 60°.  The same rule applies to the transfer of interlaminar shear stresses [3]. While not normally affecting static strength, this can affect fatigue strength.

6

(e) The stacking sequence can cause interlaminar normal
stresses to occur at the free edge of the laminate.
Interlaminar tension stresses can cause delamination
under both static and cyclic loading. The sign
(tension or compression) of the normal stress depends
both on the sign of the laminate in-plane loading and
the stacking sequence. A given ply set can be stacked
in such a way that maximum or minimum tension or
compression, $\sigma_z$, can be obtained.

Obviously, simultaneous satisfaction of all the above criteria for a given
structural element required compromises. Items (c) and (d) frequently
conflicted with item (b), and the development of a stacking sequence that
minimized interlaminar normal and shear stresses (item e) also conflicted
with (b) and (c). Stacking the laminate so that the normal stresses are
compressive is generally believed to increase the fatigue strength over that
of a laminate with tensile normal stresses. However, cyclically applied
loading with reversing direction results in reversal of the sign of the
normal stress. Consequently, for the fatigue coupons of this program, which
were subjected to compressive loading, laminae were stacked to minimize
normal stresses over the entire range of loading and thus minimize their
effects on fatigue strength.

A Lockheed computer program, SIGMZ, based on the method of Pagano and Pipes
[4], was used to approximate the interlaminar stresses and aid in selecting
optimum stacking sequences. Laminate ultimate strengths were calculated
using a Lockheed program, HYBRID. Material property data for Fiberite's
T300/934 graphite/epoxy unidirectional tape were taken from limited data made
available from Lockheed Missiles and Space Company and adapted for use in
Calac's "HYBRID" laminate characterization program. Where T300/934 test data
were not available, the necessary information was estimated from data for
AS/3002 graphite/epoxy in Reference [5]. These data are summarized in
Table 1.

7

TABLE 1.  TYPICAL INPUT MATERIAL PROPERTIES FOR HYBRID COMPUTER PROGRAM

| | Direction, Type of Property | Symbol | Units | Material T300/934 GR/EP[a] Average Properties at RT, $\Delta T = 111°C$ (200°F) |
|---|---|---|---|---|
| Extensional Moduli | L, Initial Tensile<br>L, Initial Compres.<br>L, Second Tensile<br>L, Second Compres. | EAl(m,1,1)<br>EAl(m,1,2)<br>EAl(m,2,1)<br>EAl(m,2,2) | GPa(psi x $10^6$) | 150.3 (21.8)<br>151.0 (21.9)<br>150.3 (21.8)<br>68.0 (9.87) |
| Extensional Moduli | T, Initial Tensile<br>T, Initial Compres.<br>T, Second Tensile<br>T, Second Compres. | EBl(m,1,1)<br>EBl(m,1,2)<br>EBl(m,2,1)<br>EBl(m,2,2) | GPa(psi x $10^6$) | 9.65 (1.40)<br>10.96 (1.59)<br>9.65 (1.40)<br>8.67 (1.285) |
| Shear Mod. | LT, Initial Shear<br>LT, Second Shear | Gl(m,1)<br>Gl(m,2) | GPa(psi x $10^6$) | 5.17 (0.750)[b]<br>2.21 (0.320)[b] |
| | LT, Major Poisson's | MUAB(m) | | .21[b] |
| Therm. Exp. | L, Coef. of Exp.<br>T, Coef. of Exp. | ALA(m,1)<br>ALA(m,2) | mm/mm/°C (in./in./°F) x$10^6$ | 0.97 (0.54)<br>30.4 (16.9) |
| Strains — Tensile | L, Yield Tensile<br>T, Yield Tensile<br>L, Ultimate Tensile<br>T, Ultimate Tensile | EPT(m,1,1)<br>EPT(m,1,2)<br>EPT(m,2,1)<br>EPT(m,2,2) | $10^{-3}$mm/mm | 10.7<br>4.5<br>10.7<br>4.5 |
| Strains — Compr. | L, Yield Compr.<br>T, Yield Compr.<br>L, Ultimate Compr.<br>T, Ultimate Compr. | EPC(m,1,1)<br>EPC(m,1,2)<br>EPC(m,2,1)<br>EPC(m,2,2) | $10^{-3}$mm/mm | 7.0<br>11.0<br>9.3<br>17.0 |
| Strains — Shear | LT, Yield Shear<br>LT, Ultimate Shear | EPS(m,1)<br>EPS(m,2) | $10^{-3}$mm/mm | 10.0[b]<br>18.0[b] |
| Auxiliary Data | Fiber Volume<br>Density<br>Ply Thickness | | kg/m$^3$(lbs/in.$^3$)<br>mm(in.) | 65%<br>157.2 (0.057)<br>0.142(.0056) |

a - Based on Average of Data from Lockheed Missiles & Space Co. Normalized at 65%

b - Est. from AS/3002 Data

From "HYBRID" the respective Y direction stresses for the $0°$, $\pm 45°$, and $90°$ plies of the quasi-isotropic laminate were determined at $\sigma_x = 84.1$ MPa (12.2 ksi). These stresses were used in the "SIGMZ" computer program to calculate free edge stresses. The "SIGMZ" program simply calculated the $\sigma_z$ and $\tau_{zy}$ stresses by the approximation method of Pagano and Pipes [6]. The laminates investigated included:

$$(0/45/90/-45/-45/90/45/0)_s$$
$$(45/90/-45/90/-45/0/45/0)_s$$
$$(0/45/90/-45/90/-45/0/45)_s$$
$$(90/45/-45/0/-45/90/45/0)_s$$
$$(90/45/-45/90/-45/45/0/0)_s$$
$$(0/45/90/-45/90/-45/45/0)_s$$

Of these, the first two had the lowest normal tension and shear stresses and were chosen as primary and alternate quasi-isotropic laminates. Results are summarized in Table 2. Figure 2 shows a diagram of the stresses.

An examination of the maximum interlaminar and normal shear stresses demonstrated the fact that separating the $+45°$ ply from the $-45°$ ply by a $90°$ ply always reduced the interlaminar normal stresses compared to laminates that had the $+45°$ and $-45°$ plies adjacent. This was due to the fact that the $\sigma_y$ in the $90°$ ply was almost balanced by the sum of the $\sigma_y$ stresses in the $+45°$ and $-45°$ plies analogous to a beam with multiple supports and multiple loads. The minimum bending moment in the beam was obtained by locating the reactions as close as possible to the applied loads. The interlaminar shear strength was greater between plies that were $45°$ apart than between plies that were $90°$ apart. This fact together with reduced interlaminar normal stresses justified the separation of $+45°$ and $-45°$ plies by a $90°$ ply.

The laminates used in this program were, of course, stressed beyond the point of transverse cracking during cyclic loading. This altered the stress distribution, and another stacking sequence than that chosen may in fact be optimum. However, based on linear behavior to $\sigma_x = 84.1$ MPa (12.2 ksi), the laminate

9

TABLE 2. FREE-EDGE STRESSES IN QUASI-ISOTROPIC TEST COUPONS

| | Primary Specimen (0/45/90/-45/-45/90/45/0)s | | | | Alternate Specimen (45/90/-45/90/-45/0/45/0)s | | | |
|---|---|---|---|---|---|---|---|---|
| | Tension | | Compression | | Tension | | Compression | |
| $\sigma_x{}^a$ MPa(ksi) | 84.1(12.2) | | -84.1(12.2) | | -84.1(12.2) | | -84.1(12.2) | |
| $\Delta T$, °C (°F) | 0 (0) | 111 (200) | 0 (0) | 111 (200) | 0 (0) | 111 (200) | 0 (0) | 111 (200) |
| $\sigma_y{}^0$, MPa(psi) | 1.43 (-208) | 27.3 (3960) | 1.33 (193) | 9.94 (1442) | 1.43 (-208) | 27.3 (3960) | 1.33 (193) | 9.94 (1442) |
| $\sigma_y{}^{45}$, MPa(psi) | 32.3 (4985) | 34.4 (4985) | -32.2 (-4669) | -32.8 (-4754) | 32.3 (4686) | 34.4 (4985) | -32.2 (-4669) | -32.8 (-4754) |
| $\sigma_y{}^{90}$, MPa(psi) | -63.2 (-9174) | -94.4 (-13700) | 63.1 (9150) | 53.7 (7794) | -63.2 (-9174) | -94.4 (-13700) | 63.1 (9150) | 53.7 (7794) |
| $\sigma_z{}^{max}$, MPa(psi) | .32 (46) | 1.70 (246) | .006 (9) | .38 (55) | .38 (55) | .39 (56) | 2.67 (387) | .89 (129) |
| $\sigma_z{}^{min}$, MPa(psi) | -.069 (-10) | .28 (41) | -.32 (-46) | -.34 (-49) | -2.66 (-386) | -7.58 (-1100) | -.37 (-54) | -.50 (-73) |

a - $\sigma$ = 84.1 MPa(12.2 ksi) is the limiting stress for first ply failure, $\sigma_{90}{}^{tu}$, when $\Delta T$ is assumed to be 111°C (200°F)

10
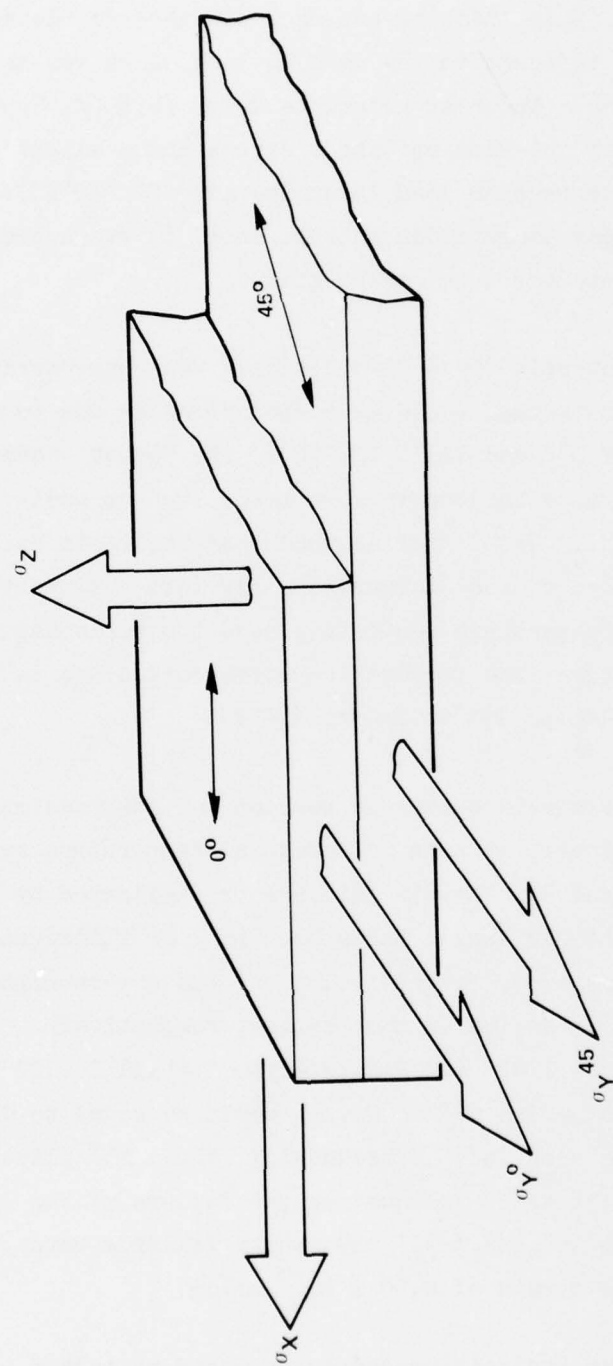
Figure 2. Diagram of Interlaminar and Normal Stresses

with the lowest $\sigma_z$, $(0/45/90/-45/-45/90/45/0)_s$, was selected as the quasi-isotropic laminate. This stacking sequence had the additional advantage of having the 0° plies adjacent to the loading tabs which was assumed to aid in reducing tab failures. The best alternate layup $(45/90/-45/90/-45/0/45/0)_s$ had a predicted lower interlaminar shear stress and a slightly higher normal stress during the compression load (assuming $\Delta T = 0°C$ (0°F)). Note that the interlaminar shear computation in Reference [6] was approximate and does not accurately reflect the true stress state.

The chosen quasi-isotropic $(0/\pm45/90)$ laminate was characterized in tension and compression with thermal residual curing stresses due to differential temperatures, $\Delta T$, of 0°C and 111°C (200°F). The former assumed that the residual stress was ammeliorated by some means such as post-curing, and represented an upper bound. The latter assumed that the resin hardens near 149°C (300°F) and was cooled to room temperature for test. Since the computations were based on room temperature properties, and the resin has reduced properties at elevated temperature, the temperature differential was taken as 111°C (200°F) instead of 146 to 173°C (230 to 280°F).

The resultant stress-strain curves in tension and compression for the selected quasi-isotropic laminate, at both differential temperature extremes, are shown in Figures 3 and 4. The ply failures are indicated by symbols. The numeral indicates the ply angle; the subscript L or T indicates fiber direction, longitudinal or transverse, respectively; and the superscripts, tu or cu, indicate failure modes, tension or compression, respectively. The 90° ply was expected to fail at 84.1 MPa (12.2 ksi) with $\Delta T = 111°C$ (200°F). Note that if $\Delta T$ was assumed to be 156°C (280°F), $\sigma_x$ would be equal to 14.1 MPa (2.04 ksi) when 90° ply failure occurred. Subsequently, the $\pm 45°$ plies were expected to fail at 221 MPa (32 ksi), followed by the failure of the laminate at 536 MPa (77.7 ksi). The 90° and $\pm 45°$ ply matrix failures were predicted on an allowable transverse strain of $4.50 \times 10^{-6}$ mm/mm.

Essentially, the same analysis procedure was used to select the 67% 0° fiber laminate. Figure 5 shows the predicted axial strength of the 67% 0° fiber
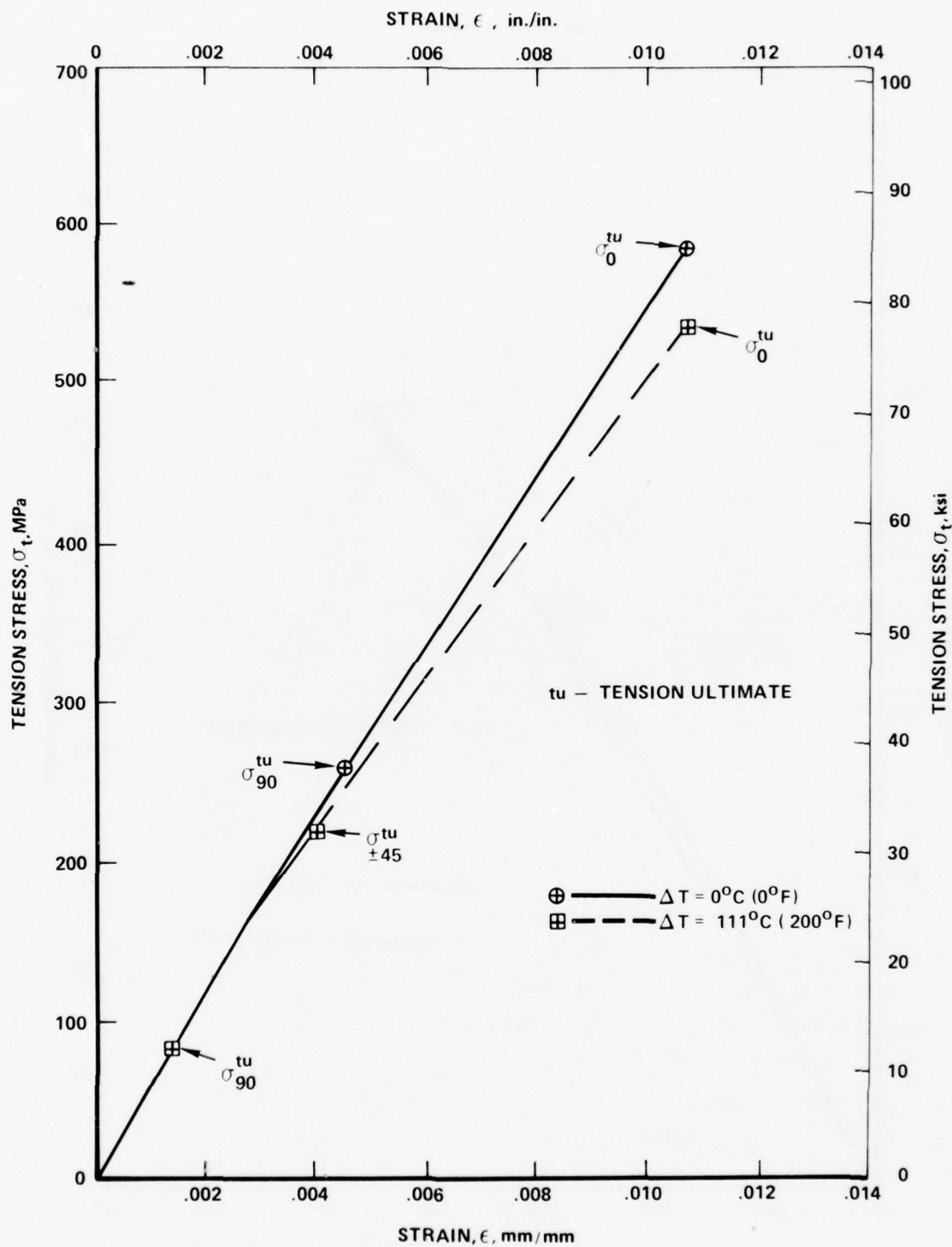
Figure 3.   Predicted Tension Stress-Strain Curves for
            Laminate 1, T300/934, $(0/45/90/-45/-45/90/45/0)_s$
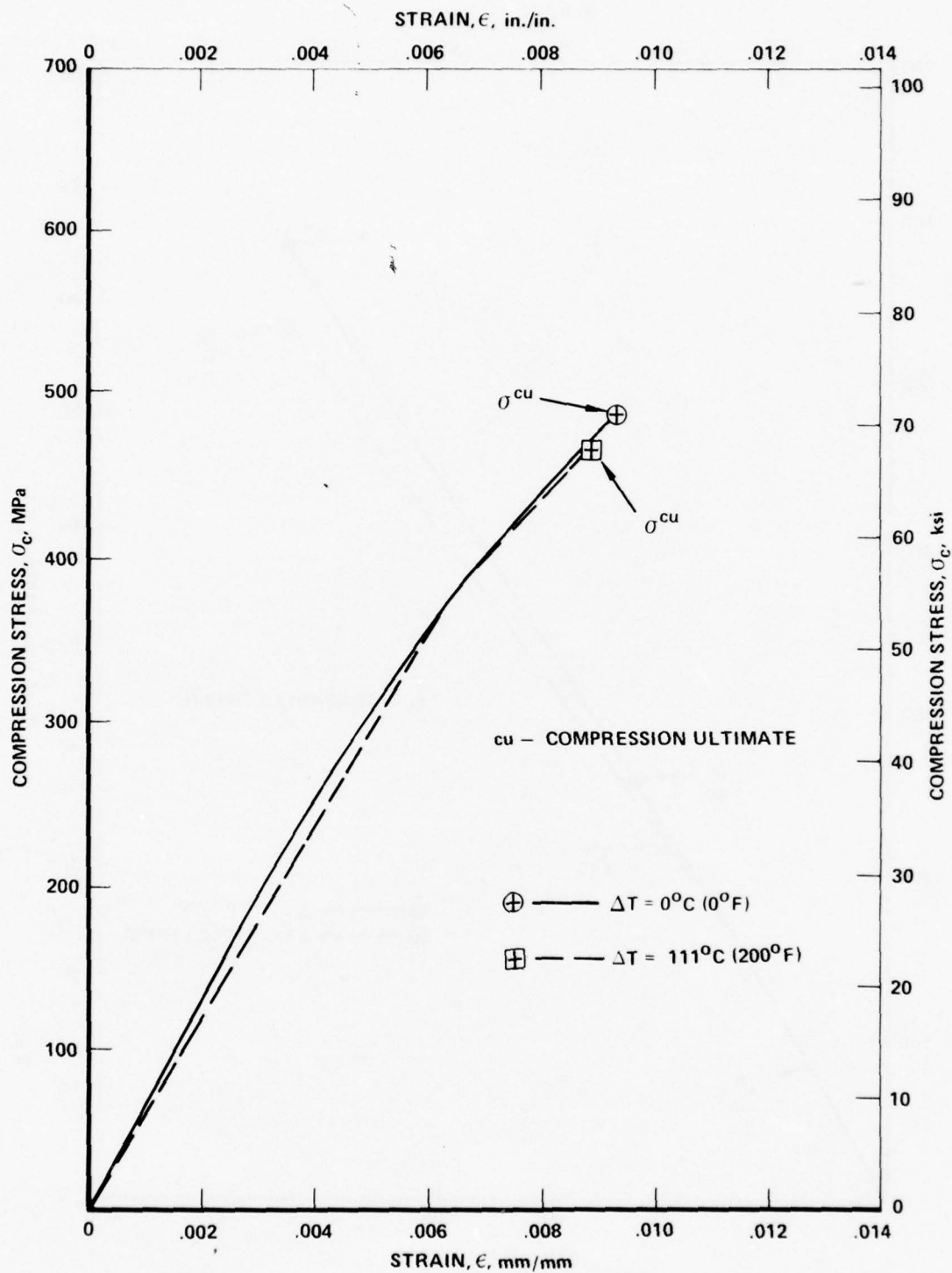
Figure 4. Predicted Compression Stress-Strain Curves for
Laminate 1, T300/934, (0/45/90/-45/-45/90/45/0)$_s$

14
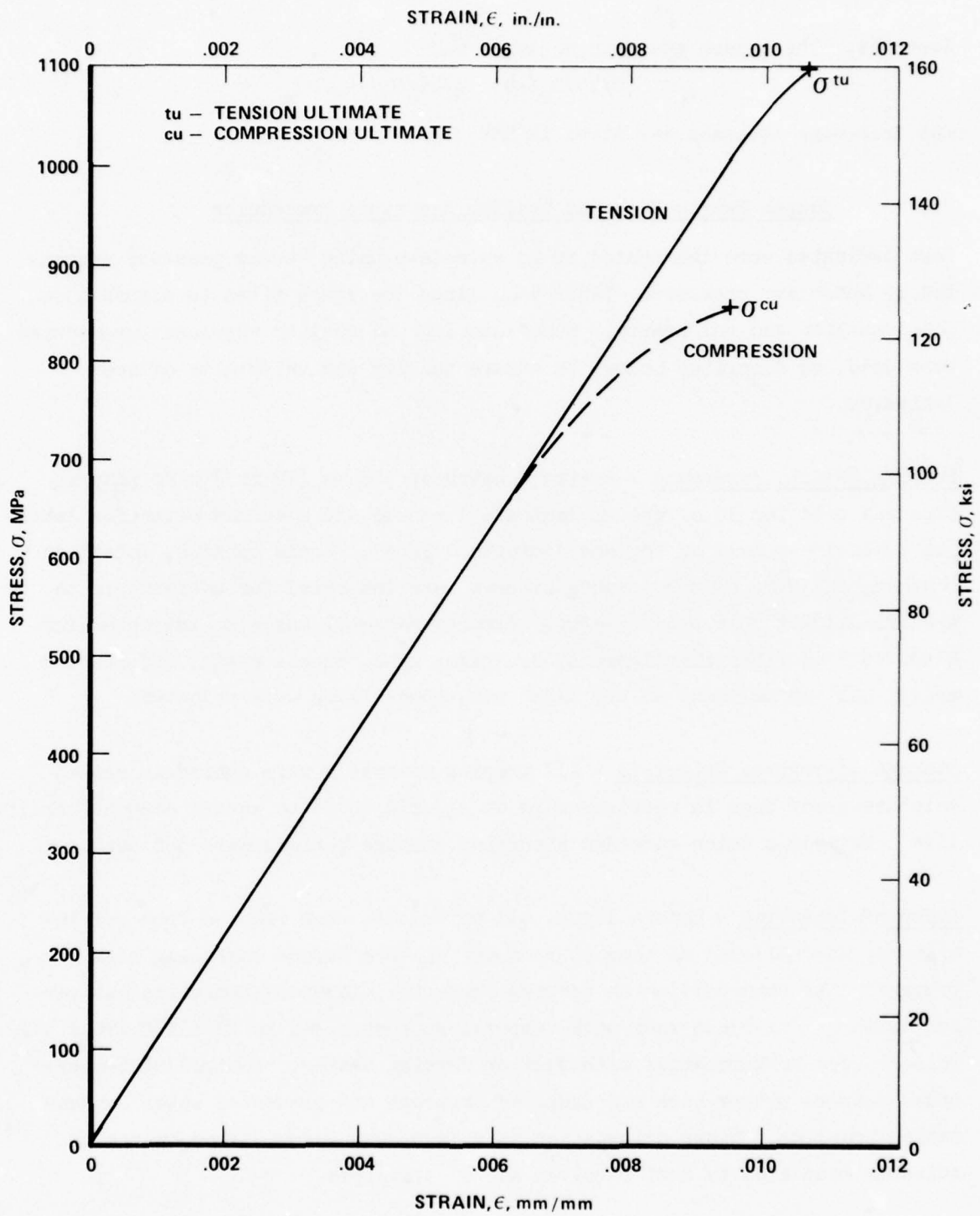
Figure 5. Predicted Axial Strength for Laminate 2,
T300/934, $(0/45/0_2/-45/0_2/45/0_2/-45/0)_s$

laminate. The chosen stacking sequence was:

$$(0/45/0_2/-45/0_2/45/0_2/-45/0)_s$$

and free-edge stresses are given in Table 3.

### 2.3 Coupon Fabrication and Quality Assurance Procedures

Test laminates were fabricated in an autoclave using vacuum pressure augmented by autoclave pressure. Table 4 outlines the steps taken to assure test panel quality and uniformity. Manufacturing and quality assurance procedures were used, as described below, to ensure quality and uniformity of test laminates.

Prepreg Quality Assurance - A single batch of 305 mm (12 in.) wide prepreg tape was used for 10 of the 11 laminate 1 panels and a second batch for laminate 2 panels as well as for one laminate 1 panel. Resin content, volatiles content, and flow of the prepreg batches were inspected for conformance to specified tolerances upon receipt. Prepreg material was also inspected for flaws such as fiber misalignment, breakage, gaps, excess resin, and starved areas, and any portions of the batch with these flaws were rejected.

Storage of Prepreg Materials - All prepreg materials were stored in sealed moisture-proof bags in refrigerators at $-17.8°C$ ($0°F$) to assure adequate shelf-life. Materials which exceeded specified storage periods were not used.

Layup of Laminates - Before layup, all materials, when removed from refrigerators, were allowed to come to room temperature before unsealing bags to prevent water condensation on prepreg surfaces. Layup of laminates was performed in a semi-clean room with temperature controlled to $21 \pm 2°C$ ($70 \pm 5°F$). This reduced contamination with dust or foreign matter. Controlled temperature assured proper tack and drape of prepregs and prevented water condensation problems. Fiber orientation in a layup was accomplished by use of suitable templates to meet required angle tolerances.

Curing of Laminates - The use of autoclave curing techniques permitted close control of pressure and temperature parameters. The autoclave incorporated

16

TABLE 3

FREE-EDGE STRESSES IN SELECTED 67% $0^{\circ}$ FIBER LAMINATE

| | Specimen B $(0/45/0_2/-45/0_2/45/0_2/-45/0)_s$ | | | |
|---|---|---|---|---|
| | Tension | | Compression | |
| [a] $\sigma_x$,MPa(ksi) | 538 (78) | | -538 (-78) | |
| $\Delta T,^{\circ}C\ (^{\circ}F)$ | 0   (0) | 111 (200) | 0   (0) | 111 (200) |
| $\sigma_y^{\ o}$, MPa(psi) | -32.1 (-4660) | -6.55(-950) | 22.2(3220) | 33.0(4790) |
| $\sigma_y^{45}$,MPa(psi) | 64.2 (9320) | 13.2 (1910) | -44.4(-6440) | -66.0(-9580) |
| $\sigma_z^{min}$,MPa(psi) | -0.34(-50) | -0.07 (-10) | 0 | 0 |
| $\sigma_x^{max}$,MPa(psi) | 0 | 0 | .28(40) | .34(50) |

a - $\sigma_x$ is 2/3 of Ultimate Strength

17

TABLE 4. QUALITY ASSURANCE TESTING OUTLINE

| Material Form | Test |
|---|---|
| Prepreg (receiving inspection) | - Visual examination (fiber uniformity, fiber alignment<br>- Volatiles content<br>- Uncured resin content<br>- Control of shelf life |
| Layup (prior to cure) | - Visual examination of excess section for proper orientation of each ply |
| Curing | - Automated autoclave programming for control of cure parameters<br>- Permanent records of cure temperature and pressure maintained for each autoclave run |
| Cured Laminates | - Visual examination (resin starvation, fiber wash-out, pinholes, etc.)<br>- Thickness per ply<br>- Cured resin content<br>- Density<br>- Void content (calculated)<br>- Examination of cross-section under magnification<br>- Nondestructive inspection of each test laminate by ultrasonic "C" scan |

automatic programming instrumentation to control heating rates and dwell times. In the autoclave, pressure was not dependent upon tool or platen quality. These factors minimized the variations between separate cure operations. Test laminate fabrication required more than one autoclave cycle, but close controls reduced the possibility of significant test panel variations.

Bleeding was accomplished by use of a perforated releasable membrane placed in contact with the laminates and backed up with an absorbent material. This permitted escape of air and volatiles as well as bleeding of resin to reduce resin content of the laminates to specified levels. Pressure bags of suitable heat resistant plastic film were sealed in place over the layup.

An optimum cure cycle was developed prior to test laminate fabrication, see Appendix A. The proper combination of factors such as heat-up rate, dwell, venting, and time of pressure application were determined. This helped to ensure proper release of volatiles, resin flow, and wetting to minimize voids and porosity and provide maximum resin compaction and adhesion to fibers.

Prior to cure, an excess section of the layup was examined to ensure proper filament orientation in each ply. During the cure cycle, a complete permanent record was maintained of temperature, vacuum pressure, and autoclave pressure. This record included heat-up rates and times of pressure application and release.

Two throw-away panels of laminate 1 were fabricated and used to ensure the uniformity of the autoclave temperature cycle. Nine thermocouples were distributed at various places in the laminate, on the caul plates, and in the bleeder papers. Laminate temperatures varied $\pm 1.7°C$ ($\pm 3°F$) during heat-up and cool-down cycles and $\pm 1/2°C$ ($\pm 1°F$) during cure cycles.

Test laminates were visually examined for defects such as resin starvation, fiber wash-out, pinholes, voids, etc. Thickness per ply, cured resin content, and density were determined. These properties were used to estimate the void content from 25.4 mm (1.0 in.) wide strip in the middle of each panel,

19

perpendicular to the 0° fiber direction. Void content was determined according to ASTM D2734-70. This procedure requires accurate values for the density of fiber and neat resin. Unfortunately these values are not usually known accurately. An excess section of each laminate was sectioned and examined under magnification for voids and other defects on the surface and cut edges. All panels were fabricated such that a 25.4 mm (1.0 in.) wide edge could be trimmed off on all sides.

Each test laminate panel was nondestructively inspected by ultrasonic "C" scan procedure for voids, delaminations and other defects. One NDI standard reference panel for laminate 1 panels was fabricated identical to panels to be used in the test program except that 0.05 mm (0.002 in.) thick Teflon film pads of 3.2 to 12.7 mm (1/8 to 1/2 in.) diameter were placed at eight locations in the upper and lower halves of the standard panel. This panel was used as a standard for the NDI-C scan inspection of the laminate 1 test panels. For laminate 2 panels, three Teflon 0.05 mm (0.002 in.) thick film pads 3.2 to 12.7 mm (1/8 to 1/2 in.) diameter were placed in the corner of each fabricated test panel.

The panel and coupon fabrication procedure used in this program is attached to this report as Appendix A. For laminate 1, ten panels were fabricated of approximate dimensions, 610 x 660 mm (24 x 26 in.) and one panel of approximately 965 x 1372 mm (38 x 54 in.) dimensions. For laminate 2, four panels were fabricated of approximate dimensions, 965 x 1372 mm (38 x 54 in.). Coupon dimensions are shown in Figure 6 for laminate 1. Coupons for laminate 2 were identical except that the tabs were 40.8 mm (2 in.) long. For all tests, coupons were fabricated and machined identically so that any scatter in test results could not be attributed to variations in coupon fabrication procedures or geometry.

After fabrication and prior to testing, the thickness of all coupons was measured in eight places and the width in four places (see Figure 7 for these locations). The width of any one coupon varied at most ± 0.0127 mm (± 0.0005 in.) (± 0.06%) within the gage length. The width of all coupons varied by less than ± 0.10 mm (± 0.004 in.) within the gage lengths. The area of any one coupon was found to vary by less than ± 1.5% and that of all coupons by less than ± 4% within the gage length.

20

1.6 (0.06)

139.7 ± 2.5 (5.50 ± 0.1)

215.9 ± 2.5 (8.50 ± 0.1)

292.1 ± 2.5 (11.50 ± 0.1)

76.0 ± 2.0 (3.0 ± 0.1)

22.225 (0.875) ±0.07 (±0.003)

ALL DIMENSIONS IN mm (in.)
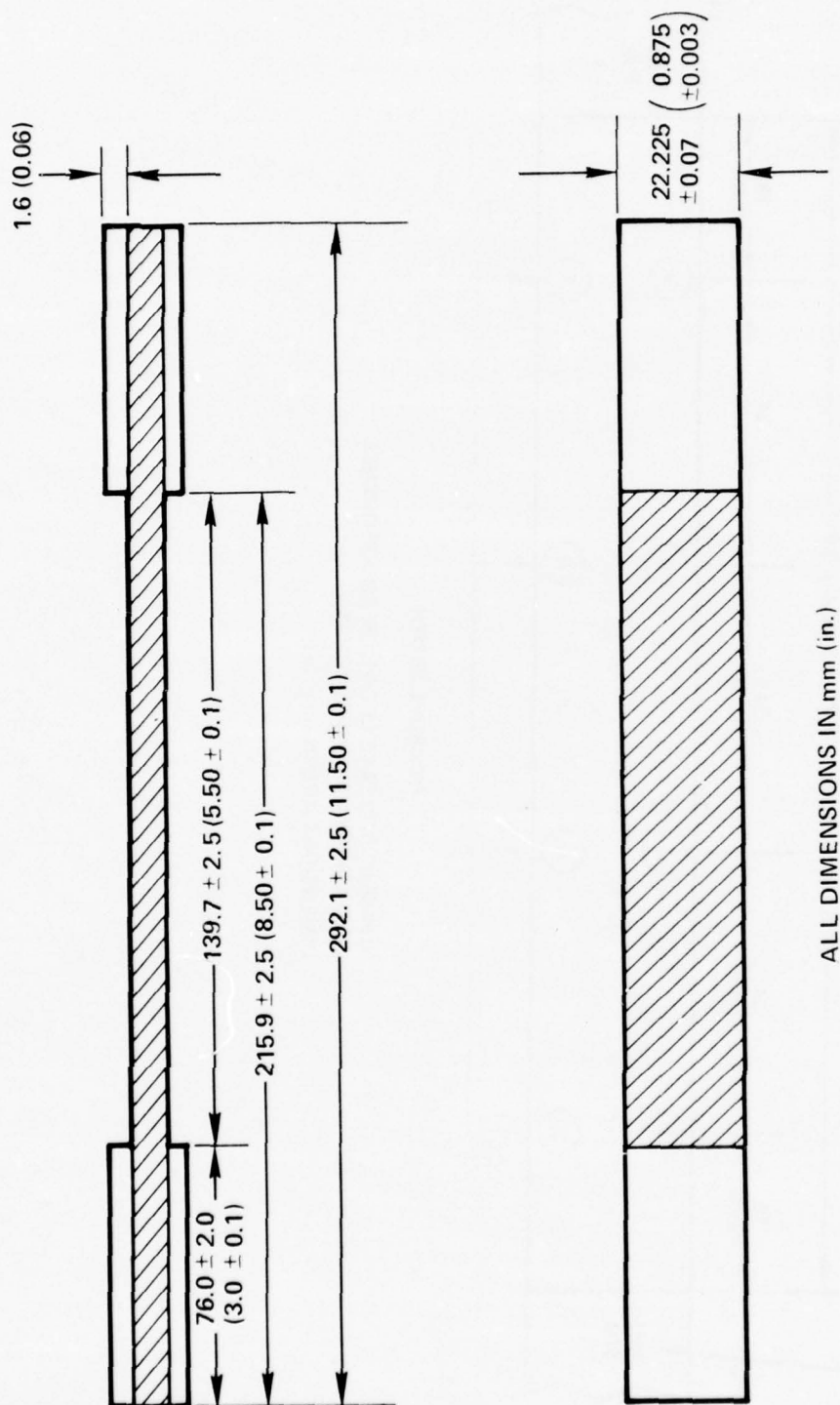
Figure 6. Coupon Geometry

21
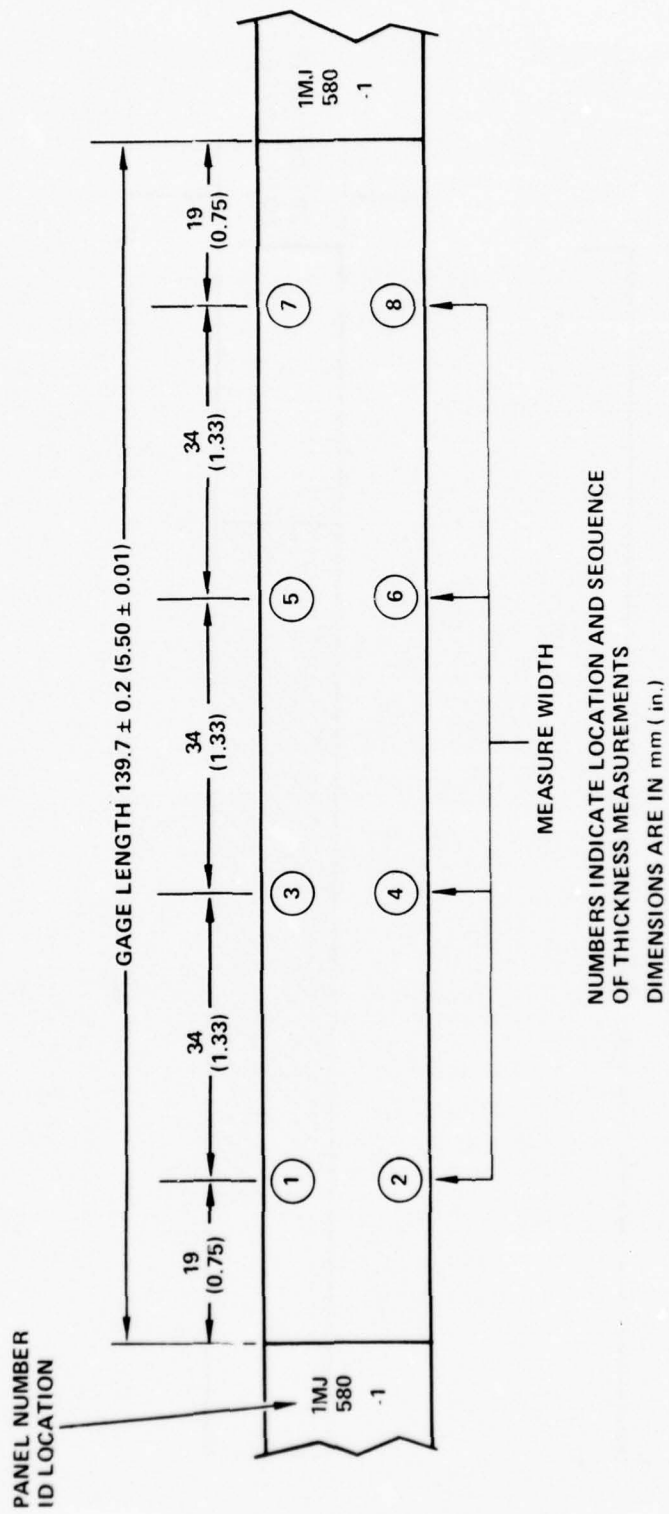
Figure 7. Location of Thickness and Width Measurements

All coupons were identified by the following system.

Autoclave
Series No.  1NH 728  -  17B ——Sub-Panel No.
                Panel No.        Coupon No.

Autoclave and panel numbers are consecutive at Lockheed and are an internal
reference number unique to each panel. The test panels were cut into 3 or 5
sub-panels, depending on whether the panel was laminate 1 or 2, and numbered
from the top as A, B, C, D, or E. This system of coupon identification
allowed for traceability of each coupon to previous panel location and
of each panel to fabrication history.

## 2.4    Program Test Matrix

The test program matrix is given in Table 5. Tests were divided into three
groups: static tension and compression tests, fatigue tests, and residual
strength tests. For each testing condition (combination of load level or
test type and laminate configuration), 25 specimens were originally intended
to be tested. However, this was subsequently reduced to 20 coupons per test
condition. All three types of testing included both laminate orientations.

All coupons were conditioned for at least 72 hours at $22 \pm 1°C$ $(72 \pm 2°F)$
and $40 \pm 10\%$ RH in an environmental chamber prior to testing. All coupons
were tested at $22 \pm 1°C$ $(72 \pm 2°F)$ and $40 \pm 10\%$ RH and remained in the environ-
mental chamber up until testing and returned to the chamber after testing.

Since a primary objective of this study was to establish a firm statistical
basis for all test results, a random sampling procedure was written and
encoded into computer software. Essentially, this program chose the order in
which each sample was to be tested in a double-blind random manner.

The number of randomly selected coupons to be tested per condition was chosen
to adequately insure a large enough data set for obtaining statistically
meaningful and reliable distributions of fatigue life and static residual

23

TABLE 5.  PROGRAM TEST MATRIX

| Testing Category | Test Type | No. of Laminate Orientations | Minimum No. of Load Levels | | Minimum No. of Coupons per Test Condition | | Total No. of Data Points |
|---|---|---|---|---|---|---|---|
| | | | Lam 1 | Lam 2 | Lam 1 | Lam 2 | |
| Static | T | 2 | - | - | 25 | 20 | 45 |
| | C | 2 | - | - | 25 | 40[a] | 65 |
| Fatigue | | | | | | | |
| T-T | S-N Curve | 2 | 6 | 4 | 3 | 3 | 30 |
| | Fatigue Scatter | 2 | 5 | 2 | 20 | 20 | 107 |
| C-T | S-N Curve | 2 | 12 | 4 | 3 | 3 | 48 |
| | Fatigue Scatter | 2 | 4 | 1 | 20 | 20 | 125 |
| Residual Strength | | | | | | | |
| T-T | T | 2 | 4 | 1 | 20 | 20 | 60 |
| | C | 2 | 2 | 1 | 20 | 20 | 60 |
| C-T | T | 2 | 2 | 1 | 20 | 20 | 60 |
| | C | 2 | 2 | 1 | 20 | 20 | 60 |

a- laminate 2 tests repeated

strength. The number of test points at any particular condition needed to insure adequate statistical confidence (at least 90% and preferably 95% or better) depends upon the dispersion of the data. The particular distribution function, binomial, Poisson, multinomial, normal, Weibull or other chosen to represent data dispersion also affects the confidence that can be applied to the same data set. The two most common distributions in fatigue are normal [7] $Y = \dfrac{1}{\sigma\sqrt{2\pi}}\, e^{-\frac{1}{2}(x - \mu)^2/\sigma^2}$, where $\mu$ is the mean and $\sigma$ the standard deviation, and Weibull [8], $P(x) = \exp[-((x-e)/(v-e))^k]$, where e, v, and k are constants. With these thoughts in mind, the number of test specimens at each test condition required for acceptable confidence of the data dispersion and probability of survival of any one coupon was considered.

In essence, this problem of coupon sampling size is more a question of the probability of survival for each coupon under the test conditions specified than one of setting the confidence levels for the data dispersion. This conclusion results from the fact that one wants to be able to state the probability of survival of the test coupon or structural component before testing or vehicle use. Essentially, there are only few options [9] available for obtaining probability of survival and, hence, specimen sample size:

(1) Have available sufficient data for the particular material and test condition of concern.

(2) Adopt, in the case of a Weibull distribution assumption, the Weibull parameters obtained from a similar material where test results are available.

(3) Assume e = 0, or arbitrarily use the median S-N curve or median value of a strength distribution of a similar material as a characteristic value curve or value, assign a shape factor k and calculate:

$$x = v\left[-\log_e P(x)\right]^{1/k}$$

(4) Arbitrate a specific percent probability of survival curve or value by means of a factor such as $x_{.99}/x_{.50} \approx 0.3$.

25

A combination of procedures 2 and 3, the most applicable in this case, led to the selection of a minimum sample size of 20.

The static tension and compression stress-strain curves, ultimate strength, and apparent modulus of elasticity were determined for each of the two laminate orientations. For constant amplitude fatigue (at 10 Hz), approximate tension-tension and tension-compression S-N curves were obtained for both laminates using three specimens at each of several load levels. Coupons were cycled to failure or to $10^6$ cycles, defined as run-out, although many coupons were cycled longer. Based on the results of the approximate S-N curves, load levels were chosen from each S-N curve for study of data scatter under tension-tension and tension-compression fatigue testing. At each of the load levels, at least 20 specimens were cycled either to failure or to at least $10^6$ cycles. This data supplied the necessary basis needed for a sound statistical analysis of the data.

The tension and compression residual strengths of specimens tested in tension-tension and tension-compression fatigue were determined. For each of the load levels selected, the number of cycles to be applied prior to residual strength testing was selected so that the chance of failing the specimens at the applied stress level was not large and yet the group of specimens was fatigue cycled long enough such that any significant change in strength and/or stiffness could be detected. For laminate 1, the number of cycles was selected equivalent to the life where 90% of the coupons could be expected to have survived as estimated from the prior data obtained to develop the fatigue life behavior. For laminate 2, the number of cycles was chosen as $10^6$ cycles of fatigue loading. For each group of specimens, half were static tested in tension and the other half in compression. Stress-strain curves, ultimate strength, and apparent modulus of elasticity were recorded.

## 2.5  Testing Procedures

For both static tension and compression tests, load and deflection were con-
tinuously read out on an X-Y recorder so that stress-strain curves could be
constructed. Ultimate strength, strain to failure, and the apparent modulus
of elasticity were calculated. For laminate 1 coupons, stress was calculated
using the minimum area because a previous Lockheed internally funded program
indicated that the failure location might be the minimum area point. However,
these coupons varied less than $\pm$ 1.5% in area within a coupon and no signifi-
cant correlation of failure location to minimum area was observed. If the
average area had been used for laminate 1 coupons, the calculated stress would
have decreased by, at most, 1.5%. For laminate 2, the average area based on
four locations equally spaced within the gage length was used to calculate
stress.

## 2.5.1  Static Tension Test Procedures

Static tension tests were conducted in a 534 kN (120 kip) Baldwin static test
machine. All testing was conducted similar to the procedures of ASTM D3039-
74. Tests of laminate 1 coupons were conducted using modified fatigue grips
while in tests of laminate 2 coupons, MTS hydraulic self-aligning grips were
used. Alignment in the modified fatigue grips was ensured by a precise fix-
ture, mounted within the grip, against which coupons were placed. For hydrau-
lic grips, a special alignment fixture was constructed exterior to the grip
assembly. Because coupon width varied only within $\pm$ 0.025 mm ($\pm$ 0.001 in.),
the alignment procedure assured end-to-end coupon alignment within $\pm$ 0.076 mm
($\pm$ 0.003 in.). A 50.8 mm (2 in.) extensometer was used to record deflection.
Testing was conducted at standard rates between 0.001 and 0.002 mm/mm/min.

## 2.5.2  Static Compression Test Procedures

Because, at present, there are no generally accepted testing standards for
obtaining the ultimate compression strength of a composite laminate, the
rationale and procedures used in this program will be discussed in detail.
An advanced composite design guide document [10] prepared by Rockwell Inter-
national Corporation discussed recommended test procedures for applications
of the United States Air Force. Other test procedures have been proposed

and are presently used by various corporations and United States Government agencies [11-16]. Recently, a test method was issued by ASTM [17].

Essentially, there are two types of compression testing procedures that have been developed for composites, end loaded [11-13] and sandwich beams [14-16]. These two different types of procedures have been developed because of the numerous possible compression failure modes which exist for composites. Each mode may have a different ultimate strength. With any particular procedure, failure will occur at the lowest possible strength and in the corresponding failure mode. The range of possible failure strengths implies that the ultimate compressive strength of a composite laminate is not a precise term, but, is primarily one of definition.

For end loaded specimens, the two primary modes of failure are column buckling and shear crippling [10]. In filamentary composites, basic material failures are defined as filament fracture, failure of matrix stabilization, matrix failure, or dominant layer instability. Normally, failure loads corresponding to these failure modes are high and thus in practical design applications, column buckling may be the most important failure mode [10].

Results of compression tests using end loaded coupons may be affected by end buckling, brooming, or splitting [10]. To obtain valid results, precise alignment was required. Since the test specimen beared on a plate, concern arose as to the extent of lateral restraining stresses acting on the coupon end due to Poisson's effect. This problem of end restraint due to Poisson's effect is, of course, not unique to composites, but is also a problem in compression testing of metallic specimens where, for example, the phenomenon of "barreling" occurs for cylindrical coupons.

In the region between the coupon end and the section where the unrestrained width is no longer affected, lateral compressive and shear loads are induced [10]. In this region, edge filaments can assume a curved shape causing a reduction in load carrying capacity. This region can be somewhat stabilized

by adding end guides or casting the ends in a suitable end block. Such procedures also help end brooming or splitting [10] . However, even if careful precautions against this problem are employed, the restraint problem and corresponding failure zone would most likely shift to a region further from the coupon end. Failure zones would then occur closer to the center of the gage section resulting in a supposedly more "valid" test, but, failure loads would not necessarily be higher and test validity would not necessarily be enhanced.

A final problem to consider in end loading of composites is termed progressive crushing failure [10] . This problem is due to the slight uneven length of the fiber ends caused by machining practice. These uneven lengths may cause only a few fibers to be loaded at first resulting in their local fracture succeeded by continuing local fracture of subsequently loaded fibers.

For this research study, an end loading test procedure for obtaining the ultimate compressive strength of large gage length graphite/epoxy composite coupons was used. The procedure employed a fully side supporting fixture, inspired by a fixture shown in Reference [18], and was designed to prevent coupon end brooming, splitting and column buckling. The large gage length was employed to ensure, as much as possible, a geometric similarity between fatigue, static tension and static compression test coupons.

Figure 8 shows both the compression testing fixture (exploded view) and a failed test specimen. Geometric details of the fixture are given in Figure 9. The testing apparatus was a fully side supporting fixture machined from medium strength steel. The fixture was designed such that the column length was slightly shorter ($\sim$ 3 mm or 1/8 in.) than the coupon gage length to allow for compression of the coupon. Width of the apparatus was the same as the coupon width although this was not a critical criterion. The testing fixture was designed to prevent buckling of the coupon and brooming of the ends. Teflon tape, 0.076mm (.003 in.) thick, was used on the inside surfaces of the
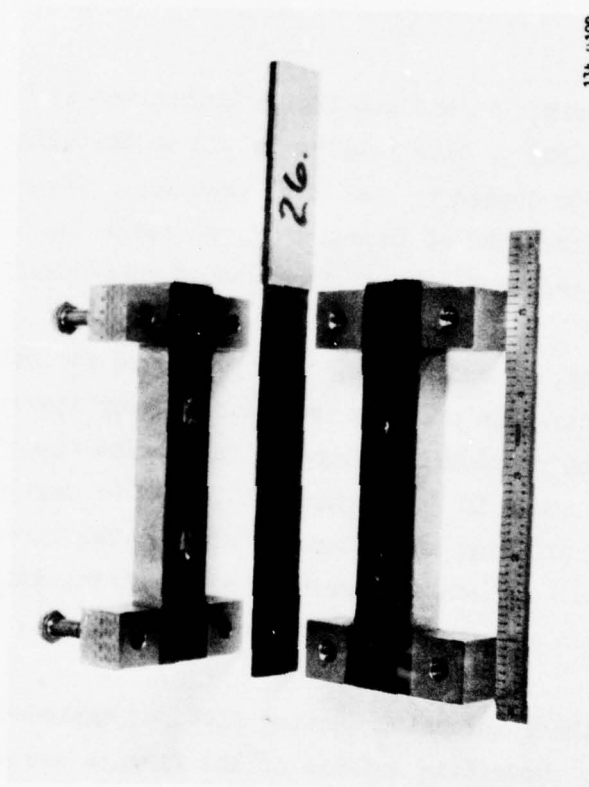
Figure 8.   Disassembled View of Compression Testing
Fixture with Example Test Coupon
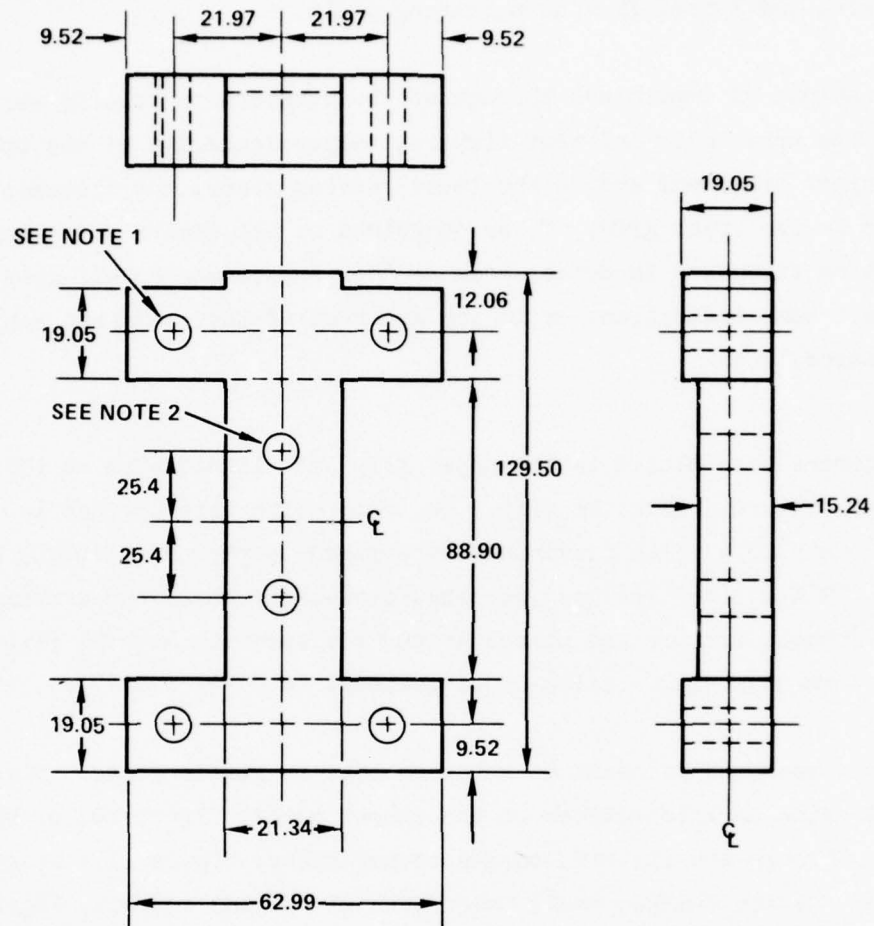
NOTE: 1. Two Required: -1 Assembly Drilled
and Tapped 1/4'' -20 4 Places,
-2 Assembly Drilled Only.

2. Hole Diameter as required for
Extensometer and/or Strain Gages.

3. Material 1100-1240 MPa Steel.

4. All Dimensions in Millimeters.

Figure 9. Geometry of Compression Testing Fixture

31

fixture to reduce surface friction. In the testing procedure described below, specimens were end tabbed on one end. The other end was untabbed, cut square, and butted flat on a bearing plate.

Considerations of importance throughout the compression testing were: alignment of the upper grip and test fixture, perpendicularity of the upper grip to the upper crosshead and to the lower bearing plate, and alignment of the specimen in the upper grip. These questions of alignment, while important, will not be discussed in detail because they are common to all good testing practice. Some indications as to the accuracy of the alignment achieved will be discussed later.

The specimens were placed in the upper grip and aligned with an integral alignment fixture within the grip. The grip bolts were torqued in a criss-cross pattern to a value previously determined to prevent slipping of the coupon, 113 N·m (1000 in.·lbs), but insufficient to cause end crushing. The lateral support fixture was placed around the specimen and the fixture bolts lightly torqued, using a criss-cross pattern, to 0.339 N·m (3 in.·lbs).

Strain was measured by means of extensometers or strain gages. Strain was measured using an extensometer on the coupon edges, Figure 10, or by means of holes through the fixture, on the coupon sides, Figure 11. To study the effect of surface damage, small tabs were put on some coupons, Figure 12. The side tab material used in this study was of the same material as the coupons and attached with epoxy glue. Strain gages for specific coupons were placed on the coupon sides and centered beneath a fixture hole. Lead wires were brought through the side hole, Figure 13.

After extensometer attachment or strain gage lead wire hookup, the compression tests were run while recording both load and strain. Testing was conducted at constant crosshead speed although constant strain rate would, in general, be preferable. Standard testing strain rates between 0.001 and 0.002 mm/mm/min were used throughout the testing program.
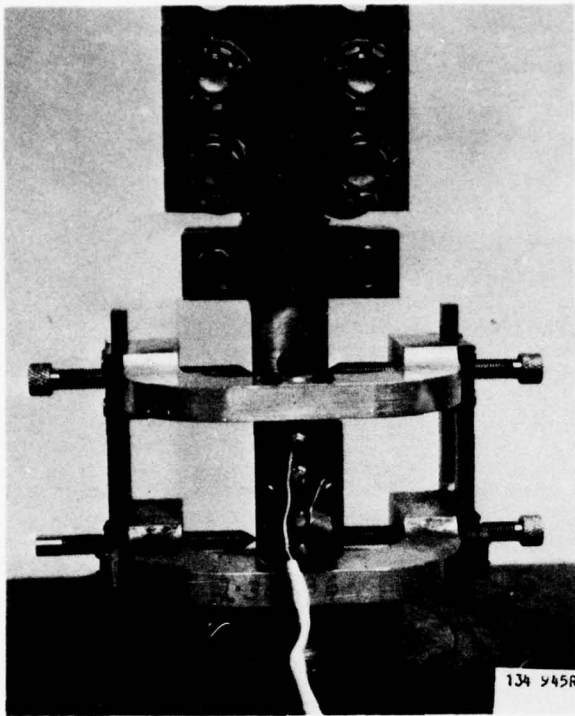
Figure 10.  Extensometer Attached
            to Specimen Edges



Figure 11.  Extensometer Attached to
            Specimen Sides
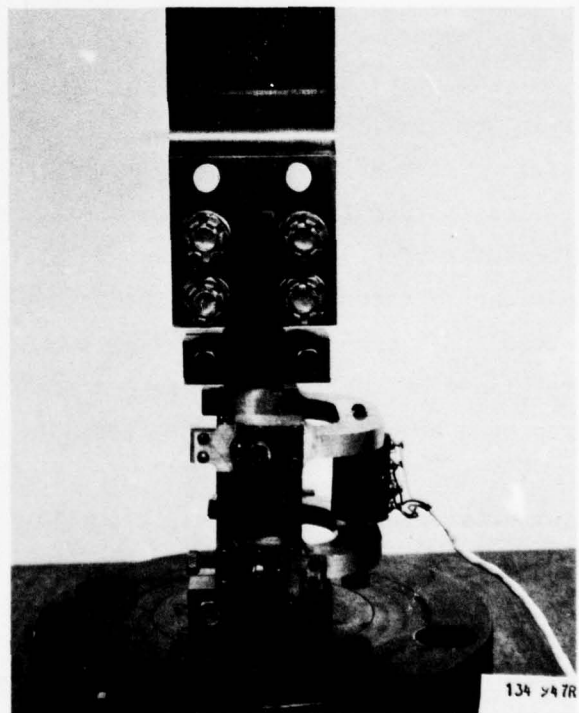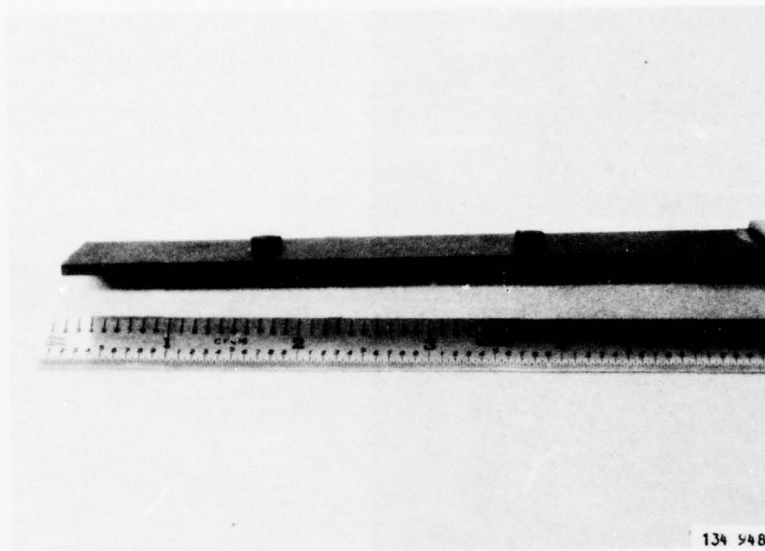
Figure 12.   Test Coupon with Side Tabs
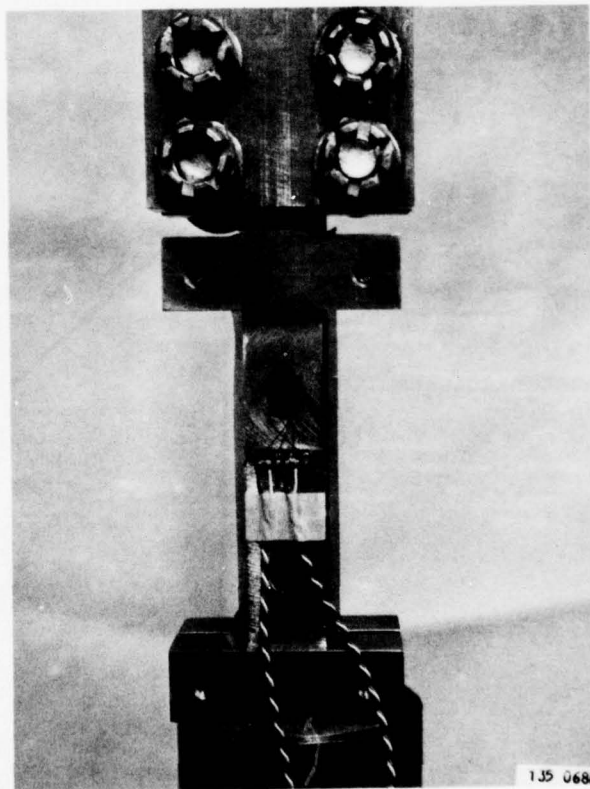


Figure 13.   Compression Fixture and Test
             Coupon with Strain Gages

34

This compression testing procedure was by no means fully satisfactory. Sig-nigicant improvements have been made at Lockheed expense and will be reported in the future. However, the procedure was internally valid for this program since the procedure was used to determine if any degradation in static com-pression properties had occurred due to fatigue.

### 2.5.3 Fatigue Test Procedures

Fatigue testing was accomplished using closed-loop electro-hydraulic servo controlled testing machines of various capacities from 89 to 220 kN (20 to 50 kips) maximum allowable load. Each machine was equipped with a peak and valley load monitoring system which allowed continuous monitoring of the load signal maximum peak, maximum valley, and minimum peak and minimum valley such that load accuracy was maintained within ± 1.0% of full-scale reading. Fatigue grips were of the friction bolt type with integral internal alignment fixtures, see Figure 14. Coupon alignment was maintained within ± 0.0762 mm (± 0.003 in.) in any direction. All tests were conducted at 10 Hz. Figure 15 shows a typical tension-tension fatigue test.

Tension-compression (T-C) fatigue tests were conducted using one or two buckl-ing guide fixtures for stiffness, see Figure 16. The two guide fixtures used for most T-C tests were spaced 50.8 mm (2 in.) apart; had teflon tape on the faces towards the coupons; and had tie-down nuts which were torqued to approx-imately 0.224 N·m (2 in.·lbs). The maximum compression load for T-C tests was chosen as that compression stress at which the maximum coupon deflection within the gage length exceeded 0.0254 mm (0.001 in.) with stiffeners attached. Min-imum load in tension-tension (T-T) fatigue tests was approximately 220 N (50 lbs).

A chosen minimum load was held constant during the tension-compression fatigue test program of each laminate while the effect on coupon life of different maximum stresses was evaluated. Other alternatives to holding the minimum load constant, such as constant mean stress or stress ratio, were discarded because the maximum load in tension would have been related to the maximum obtainable compression load. Thus, as the maximum load was reduced, the amount of compression would also be reduced. Holding the minimum load constant

35
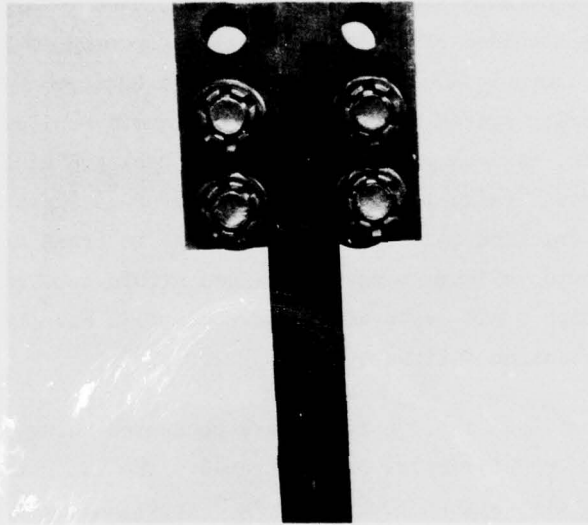
Figure 14. Fatigue Grip
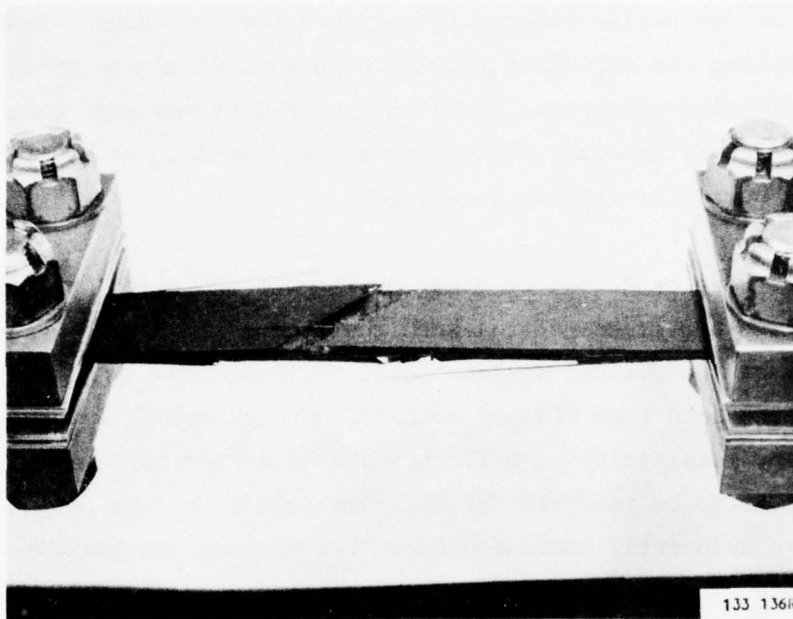
Figure 15.  Tension-Tension Fatigue Test Showing
Failed Laminate 1 Coupon
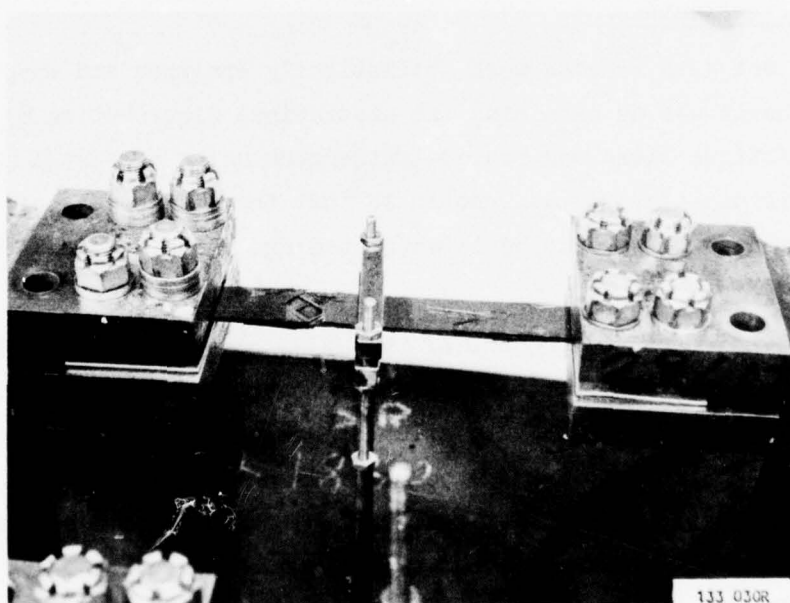


Figure 16.  Tension-Compression Fatigue Test Showing
Single Buckling Guide

37

appeared to be the better alternative because the compression load that could be obtained was maximized within the practical limits of the test. The action of using additional buckling constraints was also examined but rejected because of the possibility of masking the fatigue behavior due to an excessive number of lateral constraints.

Fatigue tests were conducted by first dialing to the calculated mean load and setting the amplitude control such that the maximum load was approximately equal to 95% of the desired maximum load. Five or less cycles were then applied and the load time history recorded on high speed visicorders. This eliminated any possibility of a first cycle load overshoot and allowed the load at failure to be recorded for any first cycle failure coupon. The span control was subsequently increased such that minimum and maximum load were those desired. The peak and valley controls shutdown the fatigue loading and returned the load to the mean value if any load deviations beyond 1/2% were detected.

## 2.6    Data Analysis

All of the test data results were statistically analyzed and compared. Primary emphasis was on examining the statistical distribution of static strengths, fatigue lives and residual strengths using a Weibull [8] distribution. This distribution was chosen so that the correctness of present "wear-out" models [19] could be investigated and further models developed.

For fatigue resistant design, one of the major questions concerning application of damage tolerance concepts is specification of percent levels of probability of survival. This question arises because of the need to translate reliability and confidence measures of data to parallel ones for design requirements [9]. In fatigue, reliability can often be successfully defined in terms of the Weibull survivorship function. The following discussion of Weibull analysis is taken from Reference [9] and was primarily inspired by Dr. G. E. Bowie.

In Weibull's representation of the statistics of fatigue, there are two random variates at each stress test condition. The first of these variates is the ordered sequence of the numbers of cycles to failure for each test result, $n_i$.

$$n_i: (n_1, n_2, n_3 \ldots \ldots n_N)$$

The second random variate, $x$, is continuous and is the argument of the Weibull survivorship function, or probability of survival, expressed as

$$P(x) = \exp \left[ - ((x-e)/(v-e))^k \right], \tag{1}$$

where $\quad x \geq e, \; v \geq e, \; k > 0, \; P(e) = 1, \; P(v) = 1/\exp(1).$

The connection between the random variates, $n_i$ and $x$, is entirely empirical. In practice, numerical procedures are used to derive the three Weibull parameters $k$, $e$, and $v$ by means of the approximation

$$P(x) = 1 - i/N \quad \text{when } x = n_i. \tag{2}$$

For example, when $N = 20$ and the values $n_i$ are distinct, $(N-1)$ relations can be used in deriving $k$, $e$, and $v$:

$$P(n_1) = 1 - 1/20 = \exp \; ((n_1-e)/(v-e))^k$$
$$P(n_2) = 1 - 2/20 = \exp \; ((n_2-e)/(v-e))^k$$
$$\vdots \qquad\qquad \vdots$$
$$P(n_{19}) = 1 - 19/20 = \exp \; ((n_{19}-e)/(v-e))^k$$

The twentieth relation, $P(n_{20}) = 0$, is not used in deriving the three parameters. The solution of the above equations is by least square analysis where either, $R$, the correlation coefficient, or FIT, sum of squares of the deviations, can be used to optimize the results [9].

For equation (1), the mean of the sample set is given by [8]:

$$\bar{x} = e + (v-e) \, \Gamma \, (1 + 1/k) \tag{3}$$

the median by:

$$\overset{\cup}{x} = e + (v-e) \, (\log_e 2)^{1/k} \tag{4}$$

and the mode by:

$$\widetilde{x} = e + (v-e) \, (1 - 1/k)^{1/k} \tag{5}$$

where $\Gamma$ indicates the Gamma function.

During the past twenty-five years, a number of names have been applied to the parameters. In general, parameters $e$ and $v$ are scale parameters or factors while the exponent $k$ is a shape parameter. Some confusion has resulted in the literature by referring to scale parameter $e$ as the minimum life estimate. With this choice of words, $e$ is often suggested on physical grounds to be $e \geq 0$. Many authors have reasoned further that since $e \ll n_i$, $i = 1, 2, 3, \ldots N$, the Weibull survivorship function can be appropriately reduced to dependence on two parameters, $k$ and $v$, with $e = 0$ arbitrarily. An argument against this practice is given in Reference [8]. Often, the term threshold parameter is applied to parameter $e$ and the term characteristic value to $v$. In analysis of composite data, $k$ is often denoted by $\alpha$ and $v$ by $\overset{\wedge}{F}$.

The influence of the shape parameter $k$ can be explained as follows. Define a reduced variate $Z$ as

$$Z = (x-e)/(v-e), \, Z \geq 0, \text{ dimensionless}, \tag{6}$$

and express the probability of survival function as

$$P(x) = \exp \left[ -Z^k \right], \, k > 0, \tag{7}$$

where    $P(Z) = 1/\exp(1)$   when $Z = 1$,

and       $P(Z) = 1$        when $Z = 0$, for all $k$.

If k < 1, this implies the test specimen material develops resistance to fatigue as the number of load cycles is increased. If k = 1, the Weibull survivorship function reduces to the constant failure rate relation commonly used in reliability studies. If k > 1, one can inquire whether the test specimen material experiences progressive damage as numbers of load cycles are increased.

Figure 17 illustrates the manner in which $P(Z)$ is dependent on the shape parameter k for the range of the reduced variate Z from zero to two. Empirical evidence does not support the interpretation that k might be a smoothly increasing function of stress amplitude. For practical purposes, in the case of structural alloy fatigue, the region of Figure 17 of most interest to designers is bounded as follows:

      (a)   Above by the limit $P(Z) = 1.0$

      (b)   Below by the median $P(Z) = 0.5$

      (c)   On the left by the curve $P(Z) = \exp\left[-Z\right]$

      (d)   On the right by the curve $P(Z) = \exp\left[-Z^{10}\right]$
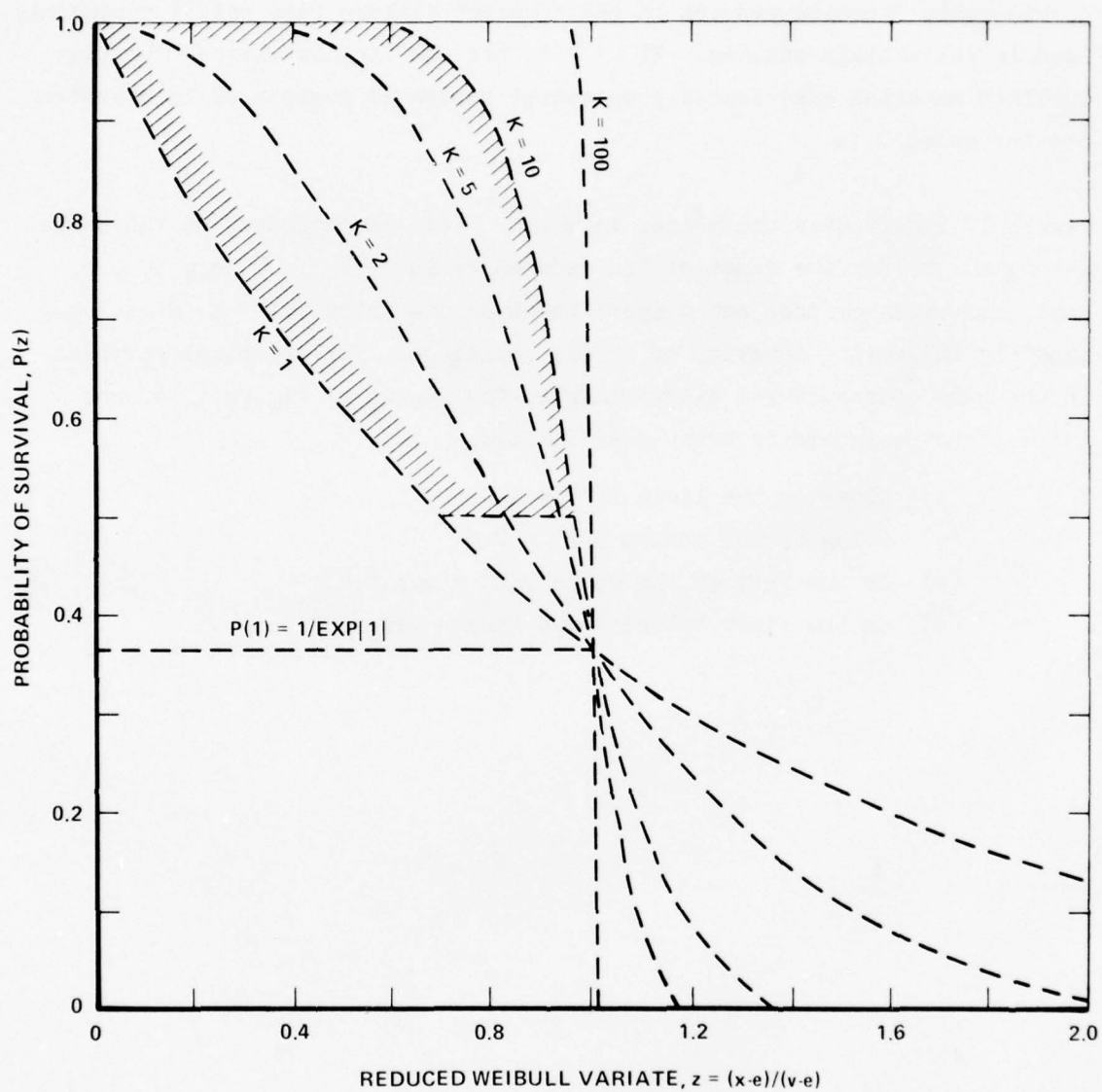
Figure 17.  Influence of Shape Parameter k on
Probability of Survival

42

# SECTION III

## MATERIAL CHARACTERIZATION

The 11 panels of laminate 1 and the four panels of laminate 2 were all fabri-
cated using the procedure of Appendix A and met all of the quality assurance
procedures discussed in Section 2.3. Resin, fiber, and void analysis results
of laminate 1 panels are given in Table 6 and those of laminate 2 in Table 7.

The fabrication procedure was intended to result in a fiber volume range from
60 to 65%. Notice in Tables 6 and 7 that all but one of the 15 panels fabri-
cated met this specification. Void contents were obtained by standard chemical
analysis procedures which unfortunately result in an error of ± 1.6% in void
content; i.e., a result of 2% voids can be between 0.4 and 3.6% voids. The
error is due to uncertainty in original fiber and matrix density properties
and in the amount of absorbed moisture which also affects density. This level
of inherent error can, of course, result in physically impossible negative
void content determinations. To alleviate this problem, void content deter-
minations were made of three panels using a 1000X light microscope. These
results also indicated that void content was extremely low.

In accordance with the fabrication procedure, each panel was non-destructively
inspected using an ultrasonic C-scan technique. Results of the C-scan NDI study
are shown in Figures 18 to 32. In Figures 18, 19, 21-27, the teflon disks
imbedded in the reference panel are clearly visible (see Appendix A for teflon
disk sizes and locations within the plies). No significant anomalies were
revealed by C-scan of the 10 panels of laminate 1 except for panel 1MJ601
(see Figure 24) where a small surface depression was observed. The coupons
from this region of panel 1MJ601 were eliminated from the test program.
Similarly, examination of C-scans of the three of the four panels of laminate
2 (Figures 29, 31 and 32) and the last panel of laminate 1 (Figure 28) revealed
no significant anomalies. However, Figure 30 shows that numerous indications
were observed for panel 1H7699 which were acoustically equivalent to the

43

TABLE 6

RESIN, FIBER, AND VOID ANALYSIS RESULTS OF LAMINATE 1 PANELS

| Panel No. | Resin Content wt. % | Fiber Content wt. % | Resin Content vol. % | Fiber Content vol. % | Void[a] Content $V_C$ % | Void[b] Content $V_M$ % |
|---|---|---|---|---|---|---|
| 1HJ 578 | 31.9 | 68.1 | 39.0 | 61.0 | +0.3[c] | <0.1 |
| 580 | 32.5 | 67.5 | 39.7 | 60.3 | -0.6 | |
| 582 | 29.9 | 70.1 | 36.8 | 63.2 | +0.3[c] | <0.1 |
| 583 | 31.9 | 68.1 | 39.0 | 61.0 | -0.1 | |
| 594 | 28.5 | 71.5 | 35.2 | 64.8 | +0.3 | |
| 596 | 29.3 | 70.7 | 36.1 | 63.9 | +0.3 | |
| 601 | 27.0 | 73.0 | 33.6 | 66.4 | +0.1 | |
| 603 | 28.7 | 71.3 | 35.5 | 64.5 | +0.5 | <0.1 |
| 604 | 31.3 | 68.7 | 38.4 | 61.6 | +0.1 | |
| 606 | 31.3 | 68.7 | 38.4 | 61.6 | +0.3 | |
| 1NH 693[d] | 32.2 | 67.8 | 39.2 | 60.8 | +0.1 | |

a - $V_C$, Void content determined by standard chemical analysis procedures

b - $V_M$, Void content determined by light microscope examination at 1000X

c - Artifact of chemical analysis procedure for void content determination

d - Panel 1NH693 was produced from the same batch of material as that used for laminate 2.

TABLE 7

RESIN, FIBER, AND VOID ANALYSIS RESULTS OF LAMINATE 2 PANELS

| Panel No. | Resin Content wt.% | Fiber Content wt.% | Resin Content Vol.% | Fiber Content Vol.% | Void[a] Content $V_c$ % |
|-----------|--------------------|--------------------|---------------------|---------------------|---------------------|
| 1NH 696 | 31.7 | 68.3 | 38.6 | 61.4 | 0.0 |
| 1NH 699 | 33.0 | 67.0 | 40.0 | 60.0 | -0.2[b] |
| 1NH 727 | 30.1 | 69.9 | 36.9 | 63.1 | 0.0 |
| 1NH 728 | 30.7 | 69.3 | 37.5 | 62.5 | +0.3 |

a - $V_c$, Void content determined by standard chemical analysis procedure

b - Artifact of chemical analysis procedure for void content determination.

45
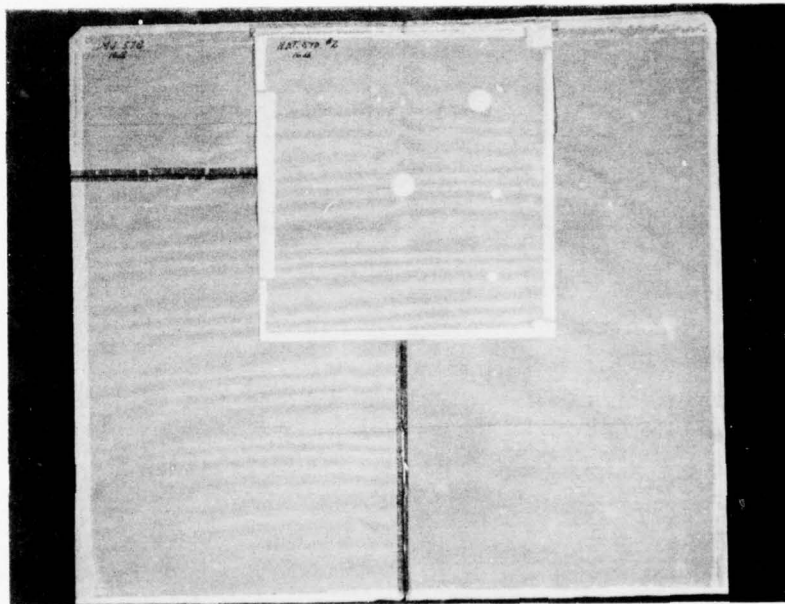
Figure 18. Ultrasonic C-Scan of Laminate 1
Panel 1MJ578

46
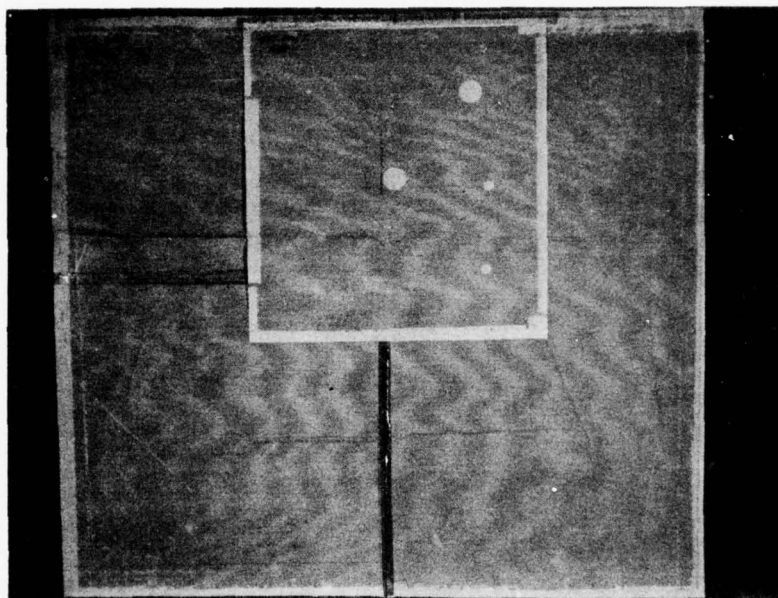
Figure 19. Ultrasonic C-Scan of Laminate 1
Panel 1MJ580
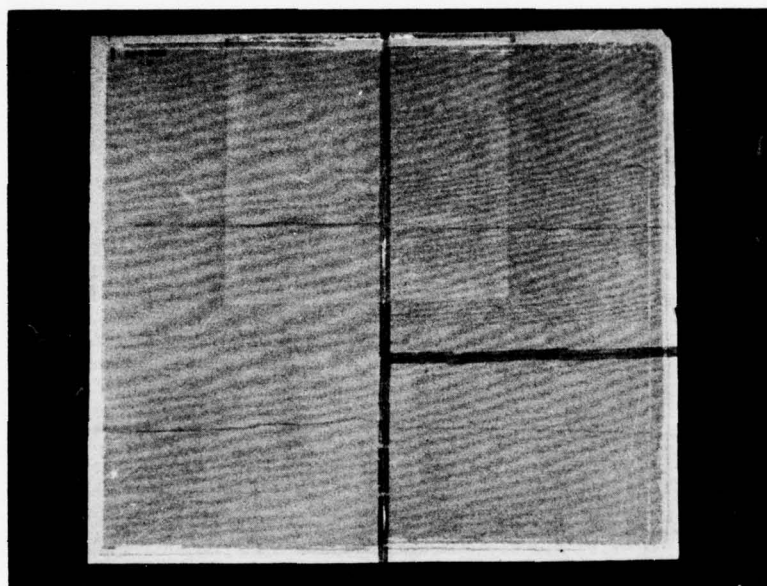
Figure 20. Ultrasonic C-Scan of Laminate 1
Panel 1MJ582
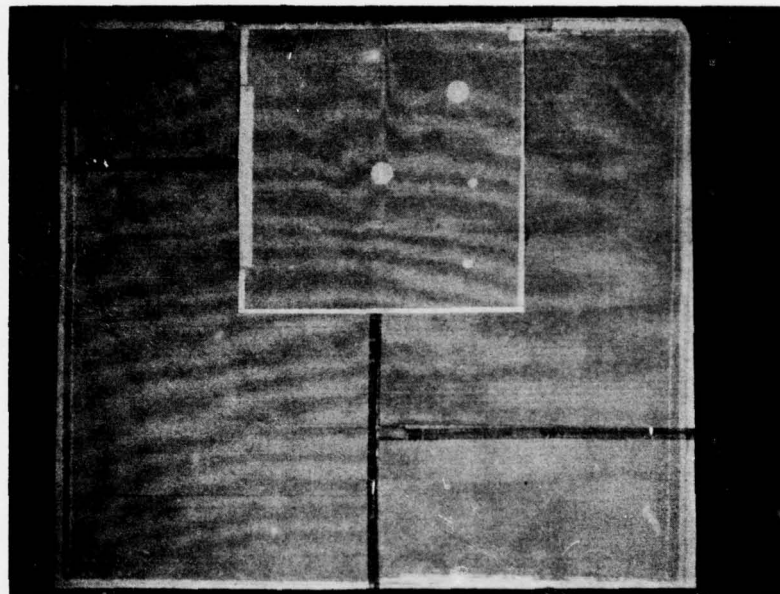
Figure 21.   Ultrasonic C-Scan of Laminate 1
              Panel 1MJ583
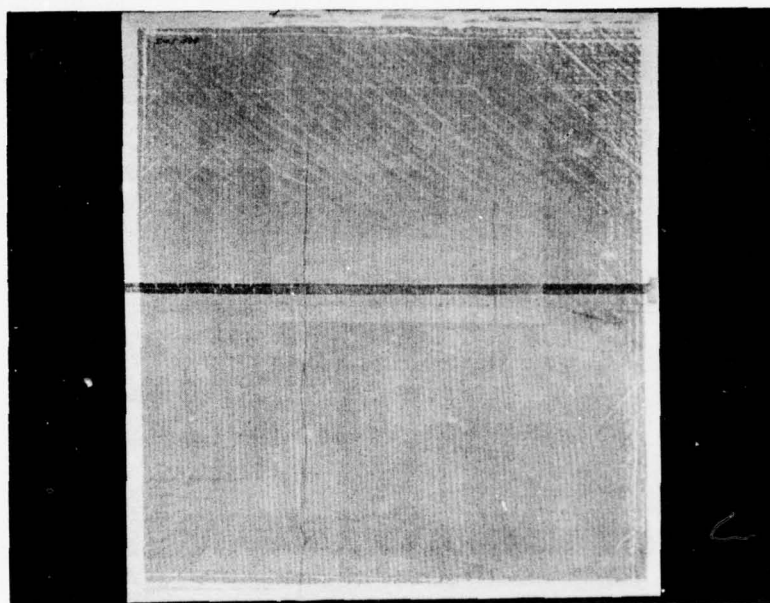
Figure 22.   Ultrasonic C-Scan of Laminate 1
Panel 1MJ594
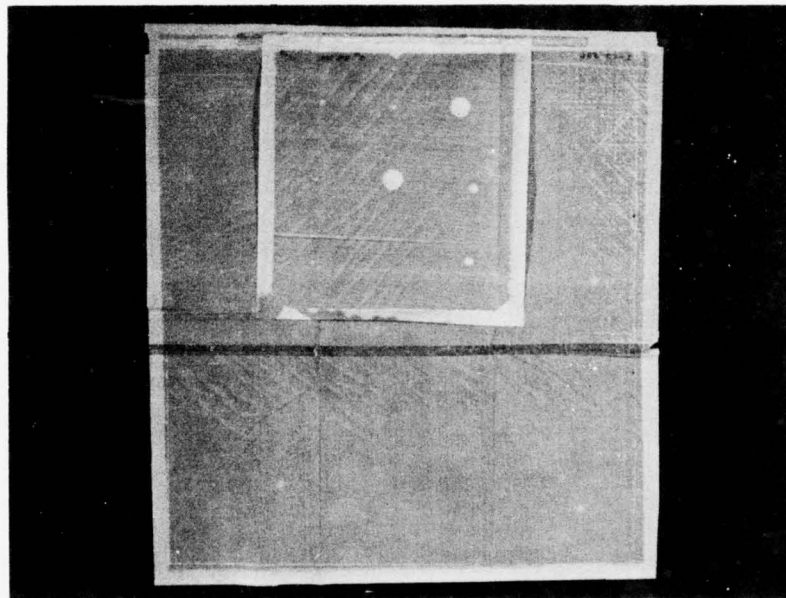
Figure 23.   Ultrasonic C-Scan of Laminate 1
Panel 1MJ596
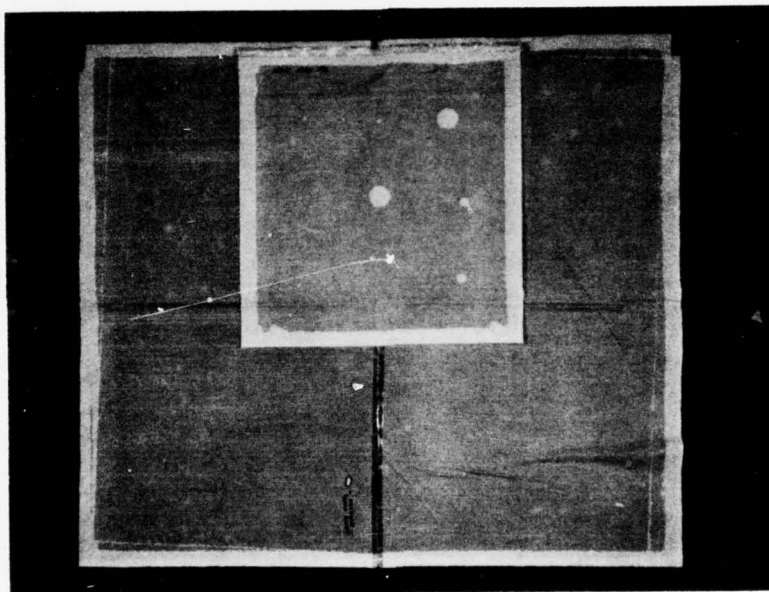
Figure 24. Ultrasonic C-Scan of Laminate 1
Panel IMJ601
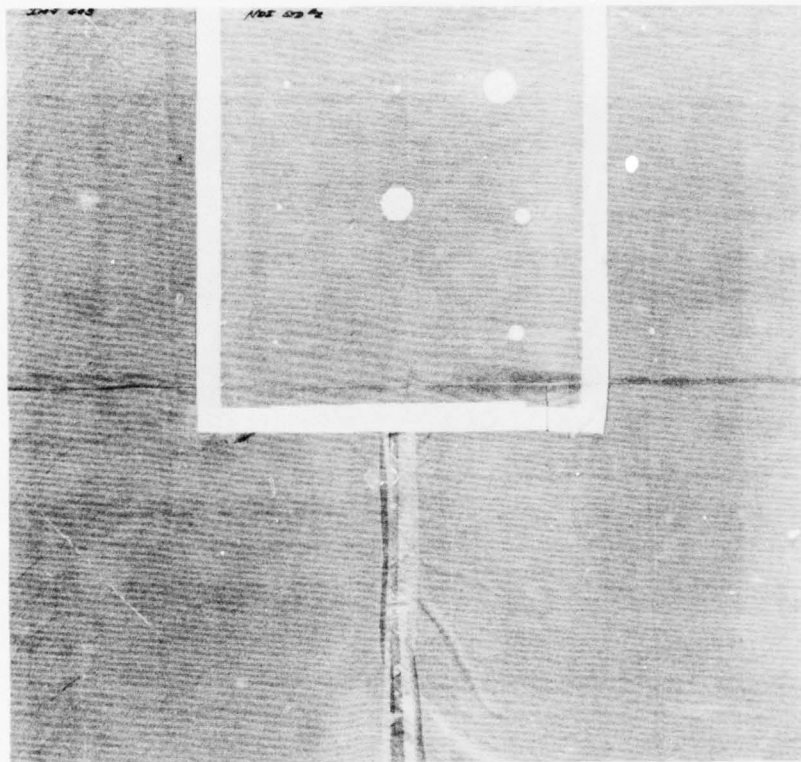
Figure 25.   Ultrasonic C-Scan of Laminate 1
Panel 1MJ603
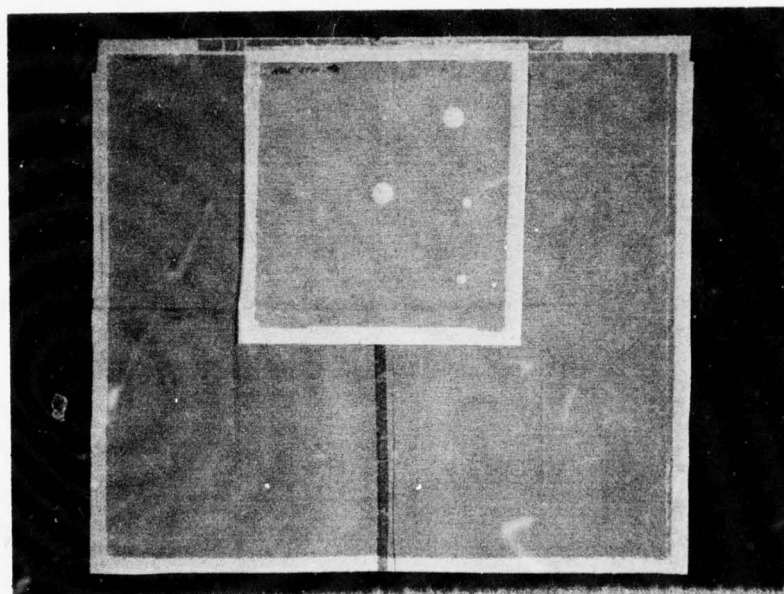
Figure 26. Ultrasonic C-Scan of Laminate 1
Panel 1MJ604
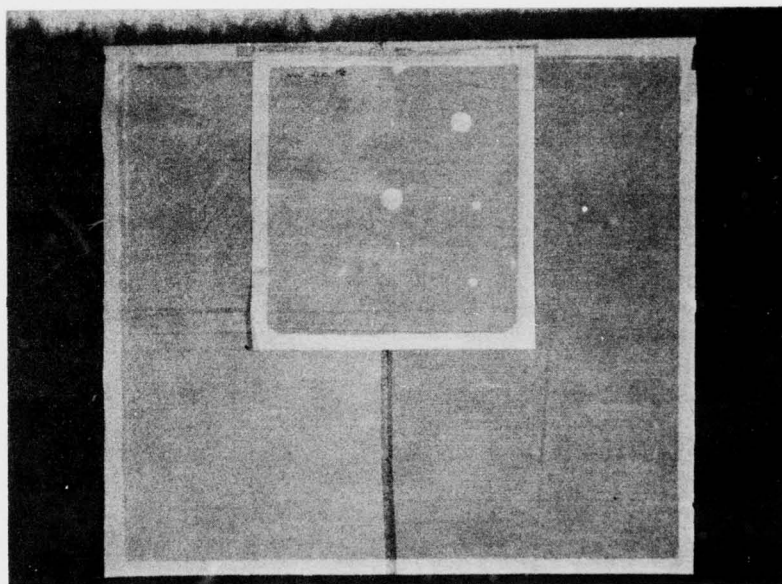
Figure 27.   Ultrasonic C-Scan of Laminate 1
Panel 1MJ606
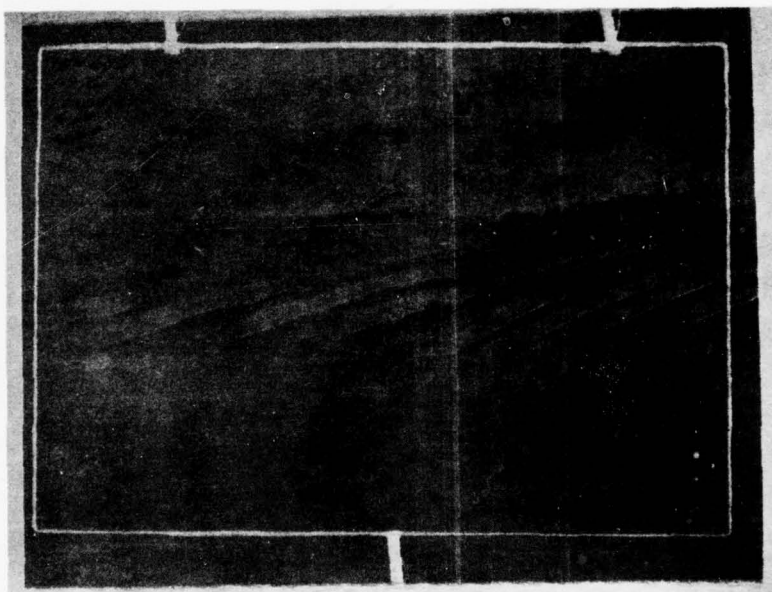
Figure 28.  Ultrasonic C-Scan of Laminate 1
            Panel 1MJ693
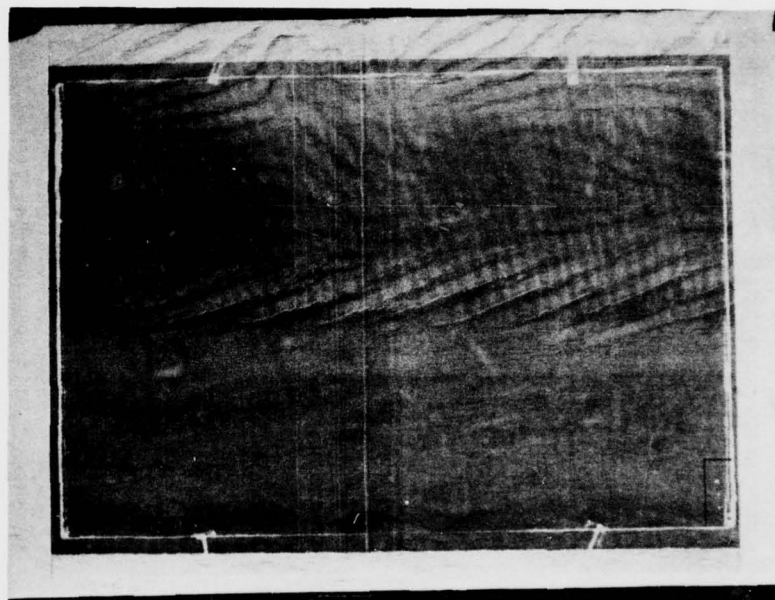
Figure 29. Ultrasonic C-Scan of Laminate 2
Panel 1NH696
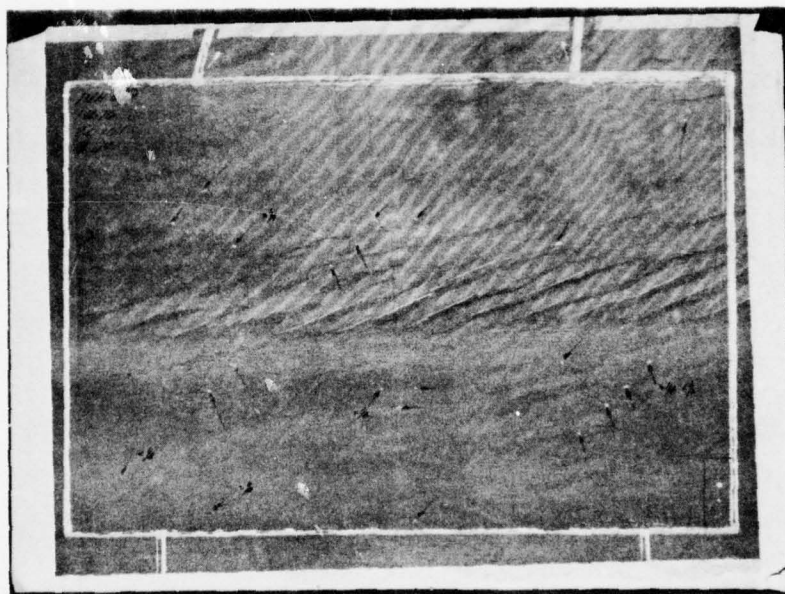
Figure 30.   Ultrasonic C-Scan of Laminate 2
Panel 1NH699
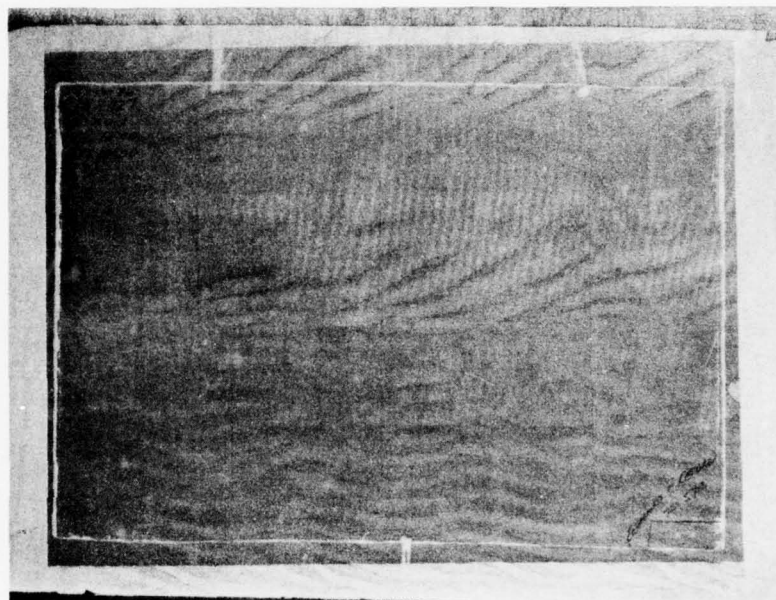
Figure 31.  Ultrasonic C-Scan of Laminate 2
            Panel 1NH727

Figure 32.    Ultrasonic C-Scan of Laminate 2
             Panel 1NH728

teflon disk control standards. The meaning of these indications is not known since later coupon post-failure correlation to these positions indicated no apparent abnormal damage.

SECTION IV

STATIC TENSION AND COMPRESSION RESULTS

## 4.1     Static Tension Test Results

Typical stress-strain curves for static tension tests are shown in Figures
33 and 34 for laminates 1 and 2, respectively.  For both laminates all
failures were brittle-like without any discernable plastic-like flow at the
end of the stress-strain curve.  As Figure 33 shows, stress-strain curves of
laminate 1 tensile coupons exhibited an initial straight portion with an
apparent modulus of elasticity designated as $E_{1a}$.  This straight portion was
followed by a short, but not abrupt, change to a straight curve to failure
with an apparent modulus designated $E_{1b}$.  In contrast, stress-strain curves
of laminate 2 coupons exhibited a nearly linear behavior to failure with an
apparent modulus designated $E_2$.

Figure 35 shows two laminate 1 coupons which failed in static tension and whose
failure modes were representative of all laminate 1 coupons.  All failures of
laminate 1 coupons were within the gage length.  Those which failed near the
end did not differ in their failure strengths.  Figure 36 shows two laminate
2 coupons which failed in static tension in a manner typical of most laminate
2 coupons.  However, as shown in Figure 37, despite the large number of $0^\circ$
plies, two laminate 2 coupons failed along the $45^\circ$ angle of the $45^\circ$ plies
unlike other coupons which failed in a more haphazard manner at more or less
of a $90^\circ$ angle to the load line.  These $45^\circ$ angle failures indicated that de-
spite the nominally lower failure strength of the $45^\circ$ plies, they could still
dominate the failure mode.  In general, failed laminate 1 static tension cou-
pons were observed to have more extensive delamination than laminate 2 coupons.

Static tension test results for the 25 coupons tested from laminate 1 are
shown in Table 8 and those for the 20 coupons tested from laminate 2 are
shown in Table 9.  The two laminate 2 coupons which failed along a $45^\circ$ angle
(699-2A, 699-3B) can be seen from Table 2 to have had two of the highest four

63
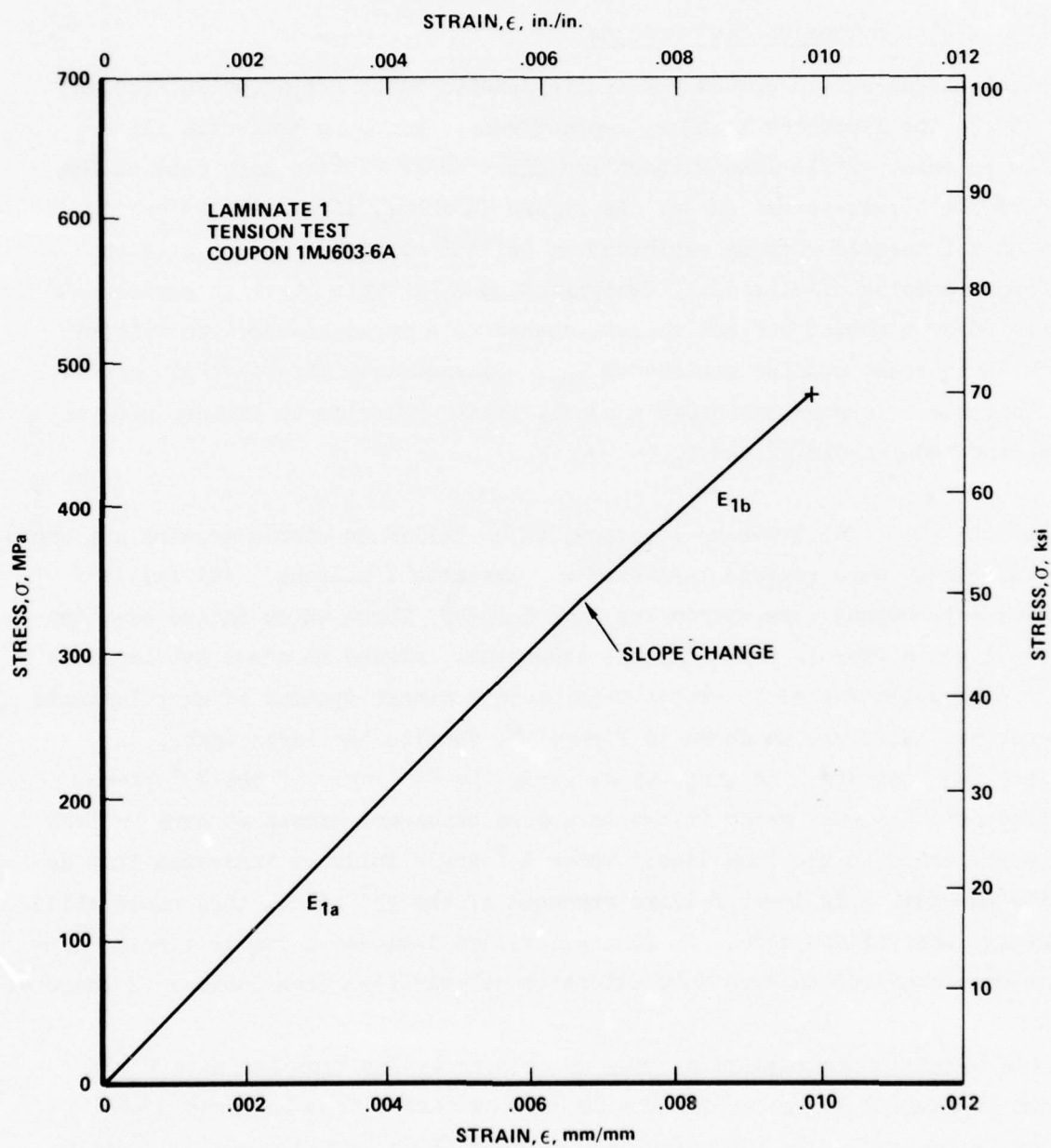
Figure 33. Tension Stress-Strain Curve for
Laminate 1 Coupon 1MJ603-6A

64
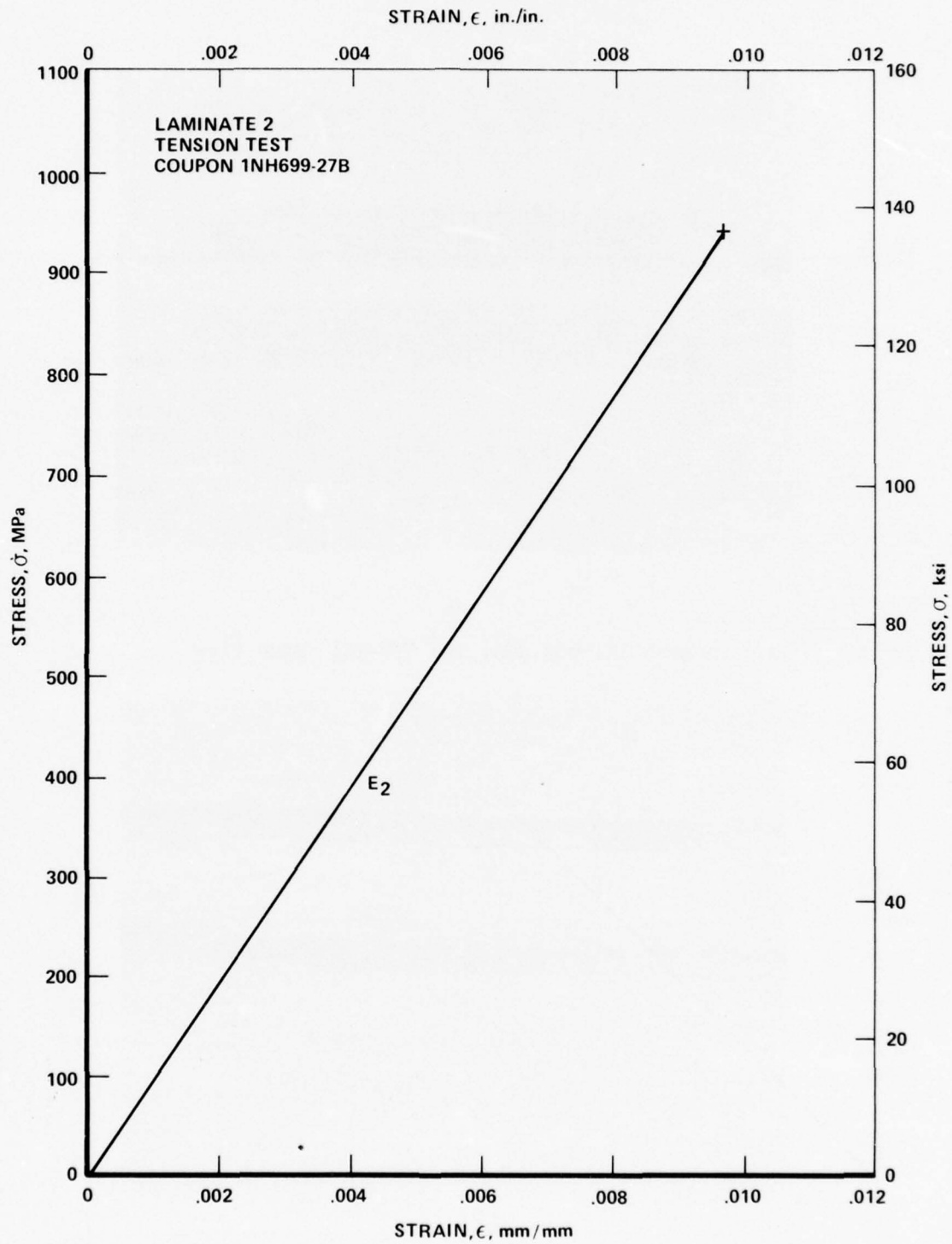
Figure 34.   Tension Stress-Strain Curve for
Laminate 2 Coupon 1NH699-27B

136 372R

a. Coupons 1MJ 603-25A, 1MJ 578-2A;  Side View



136 296R
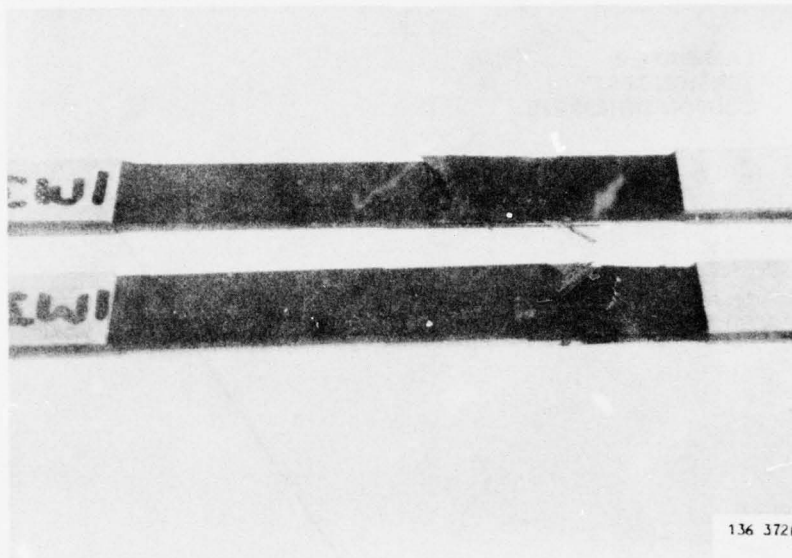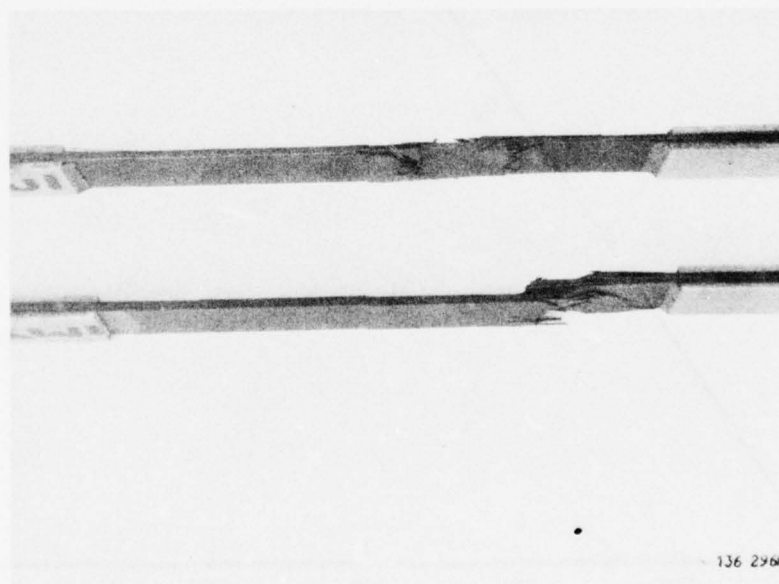
b. Coupons 1MJ 603-25A, 1MJ 578-2A;  Edge View

Figure 35.  Representative Static Tension Failure Modes
of Laminate 1 Coupons

66

136 30yR
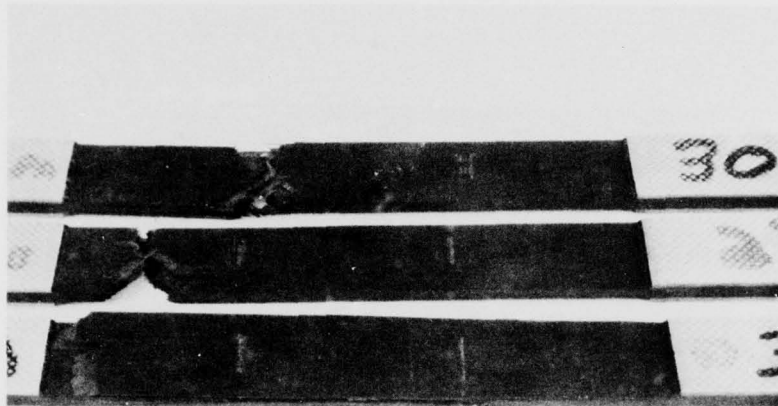
a.   Coupons 1NH 728-30A, 1NH 699-27B, 1NH 696-31A; Side View



136 29JR
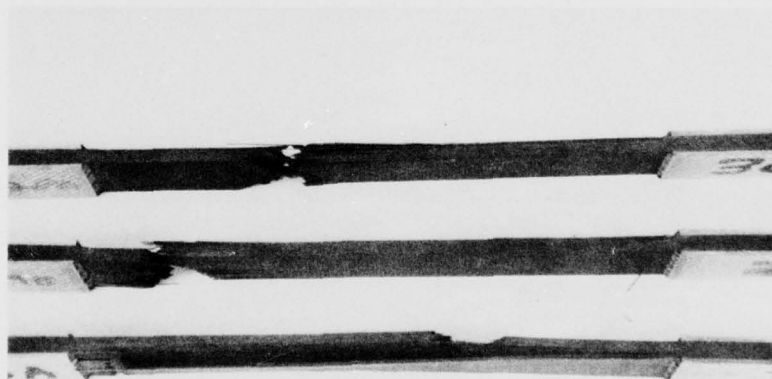
b.   Coupons 1NH 728-30A, 1NH 699-27B, 1NH 696-31A; Edge View

Figure 36.   Representative Static Tension Failure Modes
of Laminate 2 Coupons

67

136 310R

a.  Coupons 1NH 699-3B, 1NH 699-2A;  Side View



136 292R
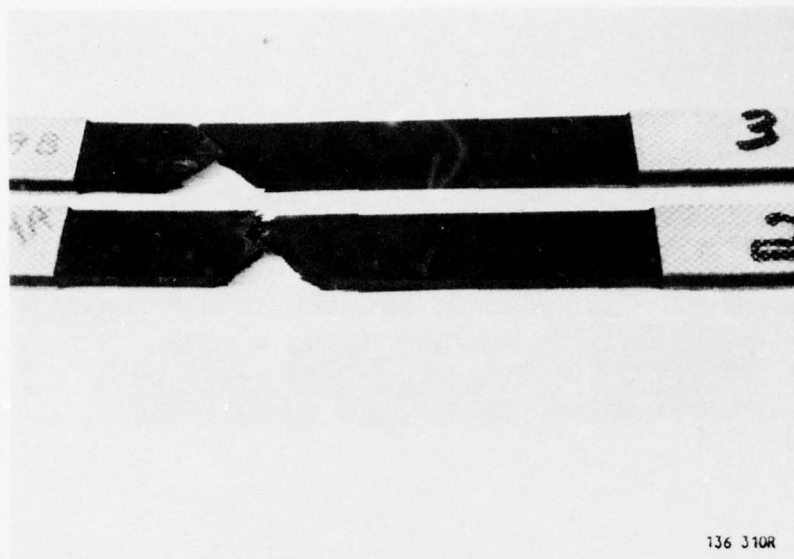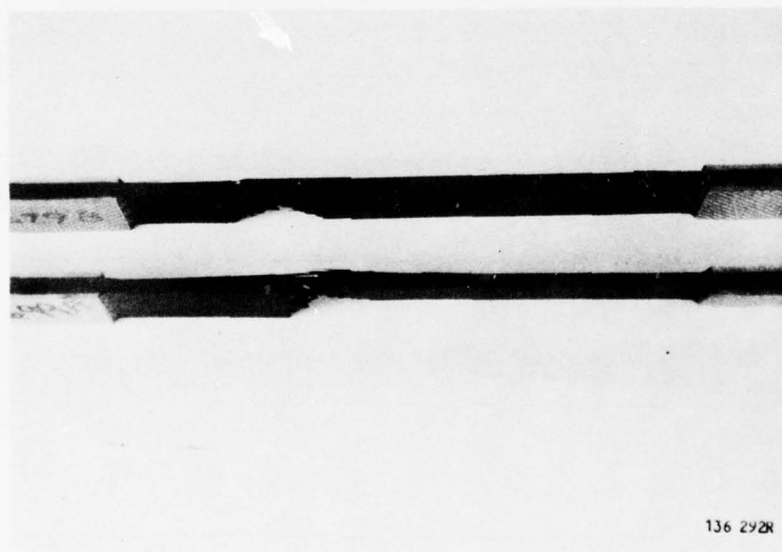
b.  Coupons 1NH 699-3B, 1NH 699-2A;  Edge View

Figure 37.  Laminate 2 Coupons Which Failed in  Static
Tension with Failure Modes Dominated by 45° Plies

68

TABLE 8A

TENSION TEST RESULTS OF LAMINATE 1 COUPONS (SAMPLE SIZE = 25)

| Sample ID | Min. Area, in.2 | Ultimate Load, $P_{ult}$, lbs | Ultimate Stress, $\sigma_{ult}$, ksi | Ultimate Strain, $\varepsilon_{ult}$, in./in. in 2 in. | Slope Deviation Load, $P_y$, lbs | Slope Deviation Stress, $\sigma_y$, ksi | Slope Deviation Strain, $\varepsilon_y$, in./in. in 2 in. | Initial Apparent Modulus of Elasticity, $E_{1a}$, psi x $10^6$ | Final Apparent Modulus of Elasticity, $E_{1b}$, psi x $10^6$ |
|---|---|---|---|---|---|---|---|---|---|
| 578-23B | .0835 | 6100 | 73.0 | .0099 | 4000 | 47.9 | .0062 | 7.73 | 6.65 |
| 2A | .0837 | 5800 | 69.3 | .0102 | 4150 | 49.6 | .0069 | 7.18 | 5.97 |
| 15A | .0857 | 5940 | 69.3 | .0107 | 3750 | 43.8 | .0063 | 6.95 | 5.98 |
| 580-19B | .0833 | 5980 | 71.8 | .0097 | 3780 | 45.4 | .0056 | 8.10 | 7.06 |
| 18A | .0820 | 6080 | 74.2 | .0090 | 3690 | 45.0 | .0055 | 8.18 | 7.17 |
| 9A | .0827 | 6240 | 75.4 | .0103 | 3960 | 47.9 | .0059 | 8.12 | 6.72 |
| 582-15A | .0840 | 5680 | 67.6 | .0090 | 4090 | 48.7 | .0062 | 7.85 | 6.61 |
| 8B | .0831 | 5350 | 64.4 | .0088 | 3640 | 43.8 | .0056 | 7.82 | 6.69 |
| 20B | .0815 | 5380 | 66.0 | .0088 | 3800 | 46.6 | .0059 | 7.90 | 6.82 |
| 583-24B | .0805 | 5800 | 72.0 | .0103 | 3390 | 42.1 | .0054 | 7.80 | 6.54 |
| 25B | .0821 | 5960 | 72.6 | .0101 | 3570 | 43.5 | .0056 | 7.76 | 6.41 |
| 8A | .0836 | 5900 | 70.6 | .0099 | 3950 | 47.2 | .0063 | 7.50 | 5.98 |
| 594-11A | .0822 | 5100 | 62.0 | .0086 | 4100 | 49.9 | .0066 | 7.56 | 5.79 |
| 10B | .0819 | 5850 | 71.4 | .0088 | 4170 | 50.2 | .0064 | 7.96 | 6.10 |
| 596-4A | .0820 | 5790 | 70.6 | .0095 | 3780 | 46.1 | .0061 | 7.56 | 6.78 |
| 12B | .0827 | 5780 | 69.9 | .0100 | 3650 | 44.1 | .0058 | 7.61 | 5.90 |
| 601-11B | .0820 | 5300 | 64.6 | .0093 | 3800 | 46.3 | .0064 | 7.24 | 6.10 |
| 6B | .0815 | 5700 | 69.9 | .0091 | 4250 | 52.2 | .0066 | 7.90 | 6.46 |
| 603-25A | .0819 | 5340 | 65.2 | .0098 | 3620 | 44.2 | .0058 | 7.62 | 6.43 |
| 6A | .0821 | 5740 | 69.9 | .0099 | 4200 | 51.2 | .0069 | 7.41 | 6.77 |
| 604-8B | .0835 | 5820 | 69.7 | .0100 | 3150 | 37.7 | .0051 | 7.40 | 6.65 |
| 22A | .0824 | 5600 | 68.0 | .0090 | 3100 | 37.6 | .0051 | 7.38 | 6.74 |
| 24A | .0817 | 5280 | 64.6 | .0090 | 2830 | 34.6 | .0047 | 7.37 | 6.80 |
| 606-24B | .0804 | 5300 | 66.0 | .0090 | 3340 | 41.5 | .0055 | 7.55 | 6.56 |
| 14A | .0841 | 6000 | 71.3 | .0101 | 3800 | 45.2 | .0061 | 7.41 | 6.26 |
| Average | | | 69.2 +6.2 -7.2 | .0096 +.0011 -.0010 | | 45.3 + 6.9 -10.7 | .0059 +.0010 -.0012 | 7.64 +0.54 -0.69 | 6.48 +0.70 -0.68 |

69

TABLE 8B

TENSION TEST RESULTS OF LAMINATE 1 COUPONS (SAMPLE SIZE = 25)

| Sample ID | Min. Area, mm² | Ultimate Load P_ult, kN | Ultimate Stress σ_ult, MPa | Ultimate Strain ε_ult, mm/mm in 50.8 mm | Slope Deviation Load P_y, kN | Slope Deviation Stress σ_y, MPa | Slope Deviation Strain ε_y, mm/mm in 50.8 mm | Initial Appar. Modulus of Elasticity E_1a, GPa | Final Appar. Modulus of Elasticity E_1b, GPa |
|---|---|---|---|---|---|---|---|---|---|
| 578-23B | 53.9 | 27.1 | 503 | .0099 | 17.8 | 330 | .0062 | 53.3 | 45.8 |
| -2A | 54.0 | 25.8 | 478 | .0102 | 18.5 | 342 | .0069 | 49.5 | 41.2 |
| -15A | 55.3 | 26.4 | 478 | .0107 | 16.7 | 302 | .0063 | 47.9 | 41.2 |
| 580-19B | 53.7 | 26.6 | 495 | .0097 | 16.8 | 313 | .0056 | 55.8 | 48.7 |
| -18A | 52.9 | 27.0 | 512 | .0090 | 16.4 | 310 | .0055 | 56.4 | 49.4 |
| -9A | 53.4 | 27.8 | 520 | .0103 | 17.6 | 330 | .0059 | 56.0 | 46.3 |
| 582-15A | 54.2 | 25.3 | 466 | .0090 | 18.2 | 336 | .0062 | 54.1 | 45.6 |
| -8B | 53.6 | 23.8 | 444 | .0080 | 16.2 | 302 | .0056 | 53.9 | 46.1 |
| -20B | 52.6 | 23.9 | 455 | .0088 | 16.9 | 321 | .0059 | 54.5 | 47.0 |
| 583-24B | 51.9 | 25.8 | 496 | .0103 | 15.1 | 290 | .0054 | 53.8 | 45.1 |
| -25B | 53.0 | 26.5 | 501 | .0101 | 15.9 | 300 | .0056 | 53.5 | 44.2 |
| -8A | 53.9 | 26.2 | 487 | .0099 | 17.6 | 325 | .0063 | 51.7 | 41.2 |
| 594-11A | 53.0 | 22.7 | 427 | .0086 | 18.2 | 344 | .0066 | 52.1 | 39.9 |
| -10B | 52.8 | 26.0 | 492 | .0088 | 18.5 | 340 | .0064 | 54.9 | 42.0 |
| 596-4A | 52.9 | 25.8 | 487 | .0095 | 16.8 | 318 | .0061 | 52.1 | 46.7 |
| -12B | 53.4 | 25.7 | 482 | .0100 | 16.2 | 304 | .0058 | 52.5 | 40.7 |
| 601-11B | 52.9 | 23.6 | 445 | .0093 | 16.9 | 319 | .0064 | 49.9 | 42.0 |
| -6B | 52.6 | 25.4 | 482 | .0093 | 18.9 | 360 | .0066 | 54.5 | 44.5 |
| 603-25A | 52.8 | 23.8 | 450 | .0091 | 16.1 | 305 | .0058 | 52.5 | 44.3 |
| -6A | 53.6 | 25.5 | 482 | .0098 | 18.7 | 352 | .0069 | 51.1 | 46.7 |
| 604-8B | 53.9 | 25.9 | 481 | .0099 | 14.0 | 260 | .0051 | 51.0 | 45.8 |
| -22A | 53.2 | 24.9 | 469 | .0100 | 13.8 | 259 | .0051 | 50.9 | 46.5 |
| -24A | 52.7 | 23.5 | 445 | .0090 | 12.6 | 239 | .0047 | 50.8 | 46.9 |
| 606-24B | 51.9 | 23.6 | 455 | .0090 | 14.9 | 286 | .0055 | 52.1 | 45.2 |
| -14A | 54.3 | 26.7 | 492 | .0101 | 16.9 | 312 | .0061 | 51.1 | 43.2 |
| Average | | | 477 +43 -49 | .0096 +.0011 -.0010 | | 312 +48 -74 | .0059 +.0010 -.0012 | 52.7 +3.7 -4.8 | 44.7 +4.8 -4.7 |

TABLE 9A

TENSION TEST RESULTS
OF LAMINATE 2 COUPONS

(Sample Size = 20)

| Sample ID | Average Area, in.$^2$ | Ultimate Load, $P_{ult}$, lbs | Ultimate Stress $\sigma_{ult}$, ksi | Ultimate Strain $\epsilon_{ult}$, in./in. in 2.0 in. | Apparent Modulus of Elasticity, $E_2$, psi x 10$^6$ |
|---|---|---|---|---|---|
| 727-29A | .1268 | 18670 | 147.2 | .0095 | 15.5 |
| 8B | .1280 | 18760 | 146.6 | .0099 | 14.8 |
| 10B | .1303 | 17800 | 136.6 | .0086 | 15.9 |
| 32B | .1282 | 19300 | 150.5 | .0092 | 16.4 |
| 12C | .1264 | 16860 | 133.4 | .0088 | 15.2 |
| 728-30A | .1294 | 16790 | 129.8 | .0081 | 16.0 |
| 21B | .1310 | 17620 | 134.5 | .0082 | 16.4 |
| 35B | .1308 | 18360 | 140.4 | .0093 | 15.1 |
| 29C | .1282 | 19060 | 148.7 | .0098 | 15.2 |
| 36C | .1301 | 18320 | 140.8 | .0090 | 15.6 |
| 696-14A | .1252 | 17680 | 141.2 | .0095 | 14.9 |
| 15A | .1278 | 17830 | 139.5 | .0098 | 14.4 |
| 31A | .1281 | 15200 | 118.7 | .0065 | 18.3 |
| 24B | .1264 | 17200 | 136.1 | .0101 | 13.5 |
| 25C | .1259 | 18300 | 145.4 | .0094 | 15.5 |
| 699- 2A a | .1257 | 18700 | 148.8 | .0097 | 15.3 |
| 3B a | .1258 | 20360 | 161.8 | .0098 | 16.5 |
| 27B | .1270 | 17320 | 136.4 | .0097 | 14.1 |
| 15C | .1260 | 18600 | 147.6 | .0099 | 14.9 |
| 30C | .1278 | 19190 | 150.2 | .0101 | 14.5 |
| Average | | | 141.7 +20.1 -23.0 | .0092 +.0009 -.0027 | 15.4 +2.9 -1.9 |

a - Coupon failed along a 45° angle

71

TABLE 9B

TENSION TEST RESULTS

OF LAMINATE 2 COUPONS

(Sample Size = 20)

| Sample ID | Average Area, mm$^2$ | Ultimate Load, $P_{ult}$, kN | Ultimate Stress $\sigma_{ult}$, MPa | Ultimate Strain $\varepsilon_{ult}$, mm/mm in 50.8 mm | Apparent Modulus of Elasticity, $E_2$, GPa |
|---|---|---|---|---|---|
| 727-29A | 81.8 | 83.0 | 1015 | .0095 | 107 |
| 8B | 82.6 | 83.4 | 1011 | .0099 | 102 |
| 10B | 84.1 | 79.2 | 942 | .0086 | 110 |
| 32B | 82.7 | 85.8 | 1038 | .0092 | 113 |
| 12C | 81.5 | 75.0 | 920 | .0088 | 105 |
| 728-30A | 83.5 | 74.7 | 895 | .0081 | 110 |
| 21B | 84.5 | 78.4 | 927 | .0082 | 113 |
| 35B | 84.4 | 81.7 | 968 | .0093 | 104 |
| 29C | 82.7 | 84.8 | 1025 | .0098 | 105 |
| 36C | 83.9 | 81.5 | 971 | .0090 | 108 |
| 696-14A | 80.8 | 78.6 | 974 | .0095 | 103 |
| 15A | 82.4 | 79.3 | 962 | .0098 | 99.3 |
| 31A | 82.6 | 67.6 | 818 | .0065 | 126 |
| 24B | 81.5 | 76.5 | 938 | .0101 | 93.1 |
| 25C | 81.2 | 81.4 | 1002 | .0094 | 107 |
| 699- 2A$^a$ | 81.1 | 83.2 | 1026 | .0097 | 105 |
| 3B$^a$ | 81.2 | 90.6 | 1116 | .0098 | 114 |
| 27B | 81.9 | 77.0 | 940 | .0097 | 97.2 |
| 15C | 81.3 | 82.7 | 1018 | .0099 | 103 |
| 30C | 82.4 | 85.4 | 1036 | .0101 | 100 |
| Average | | | 977 +139 -159 | .0092 +.0009 -.0027 | 106 20 -13 |

a - Coupon failed along a 45° angle

failure strengths. The laminate 2 coupon which had the lowest failure strength, 696-31A, was observed to have the largest amount of delamination. A summary of the static tension results comparing the two laminates is shown in Table 10. Data scatter was larger for laminate 2 coupons than for laminate 1 which was anticipated because of the large number of $0^\circ$ fibers in laminate 2. Notice in Table 10 that the strain to failure of the two laminates differed by less than 5%.

Figures 38 and 39 show comparisons of the predicted versus experimental average stress-strain curves for the two laminates. Predicted moduli of elasticity for laminate 1 were close to the experimental values, however, the $45^\circ$ ply failure strain was underestimated and the strain to failure overestimated, see Figure 38. For laminate 2, the modulus of elasticity was also accurately predicted and the strain to failure over esimated, see Figure 39. The comparison results were not surprising in view of the derth of ply data on this material available prior to the research program.

Table 11 summarizes the analytically derived Weibull parameters for the static tension test data of the two laminates. Notice that for this static data, the difference between a two or three parameter Weibull function was negligible although as the fit terms indicate, the three parameter function was slightly better. For both laminates, R was quite high and Fit low. In Table 12 the relationship between probability of survival and expected ultimate tensile strength is tabulated for the two laminates while Figures 40 and 41 show the relationship in a plotted format. Those two figures show the accuracy of the three parameter Weibull fit to the data.

An eleventh laminate 1 panel was manufactured from the same batch of material used for and at the same time as laminate 2 panels. Coupons from this panel, in addition to those from the other panels, were used to evaluate the long life fatigue characteristics of laminate 1 under tension-compression fatigue loading. Table 13 shows results of the tension test evaluation of the panel. The average of the five tests was virtually the same as that for the previous

TABLE 10

SUMMARY OF STATIC TENSION TEST RESULTS

| | Avg. Ultimate Stress, $\sigma_{ult}$, MPa (ksi) | Avg. Ultimate Strain, $\varepsilon_{ult}$, mm/mm in 50.8 mm | Avg. Initial Apparent Modulus of Elasticity, $E_A$, GPa (psi x $10^6$) |
|---|---|---|---|
| LAMINATE 1 | 477 (69.2)[a] <br> + 43 (6.2), 9% <br> - 50 (7.2), 10% | 0.0096 <br> +0.0011, 11% <br> -0.0010, 10% | 52.7 (7.64) <br> + 3.7 (0.54), 7% <br> - 4.8 (0.69), 9% |
| LAMINATE 2 | 977 (141.7) <br> +139 (20.1), 14% <br> -140 (20.3), 14% | 0.0092 <br> +0.0009, 10% <br> -0.0027, 29% | 106 (15.4) <br> + 20 (2.9), 19% <br> - 13 (1.9), 12% |

a - Based on minimum area

74
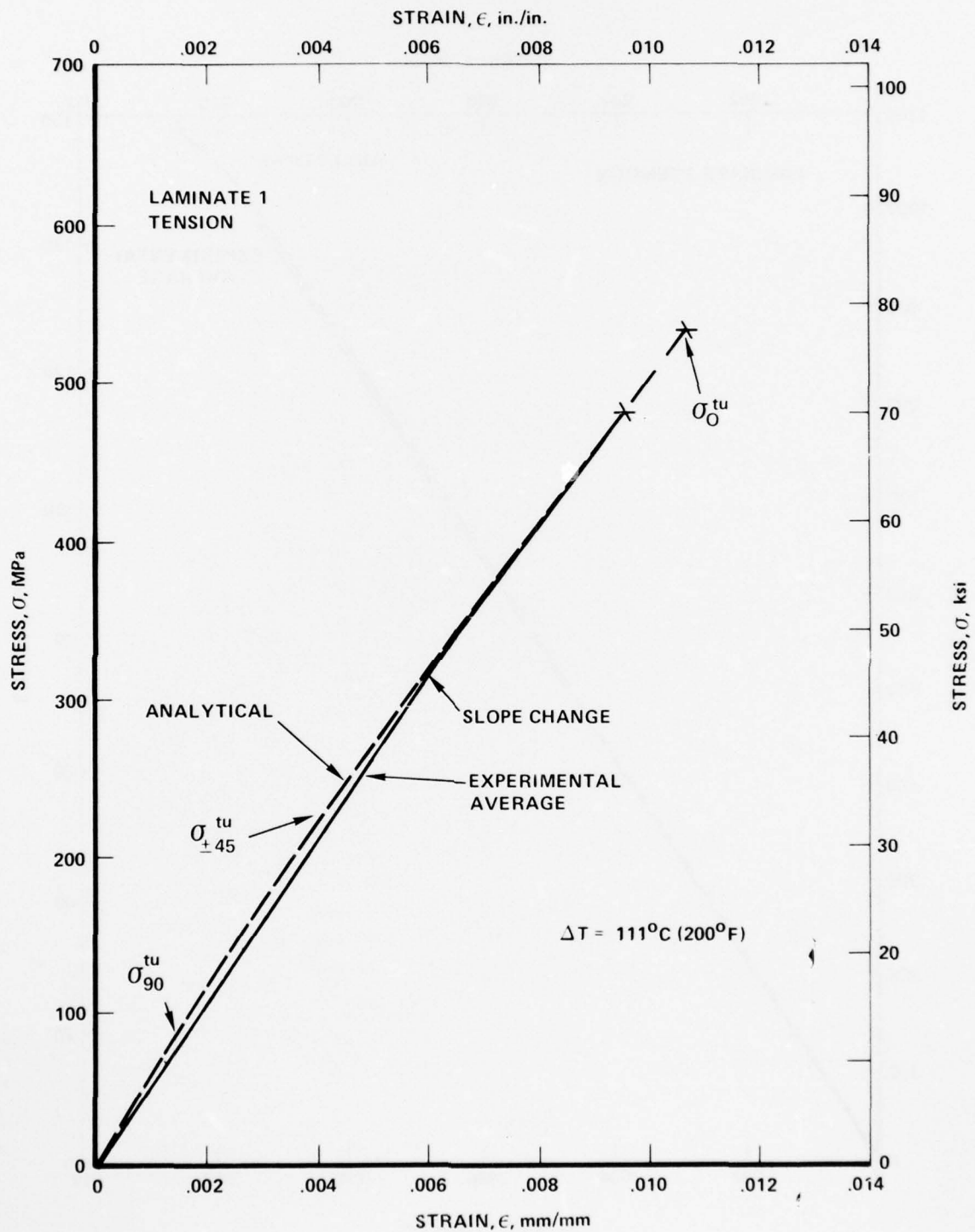
Figure 38. Comparison Between Predicted and Experimental Average
Tension Stress-Strain Curves for Laminate 1

75
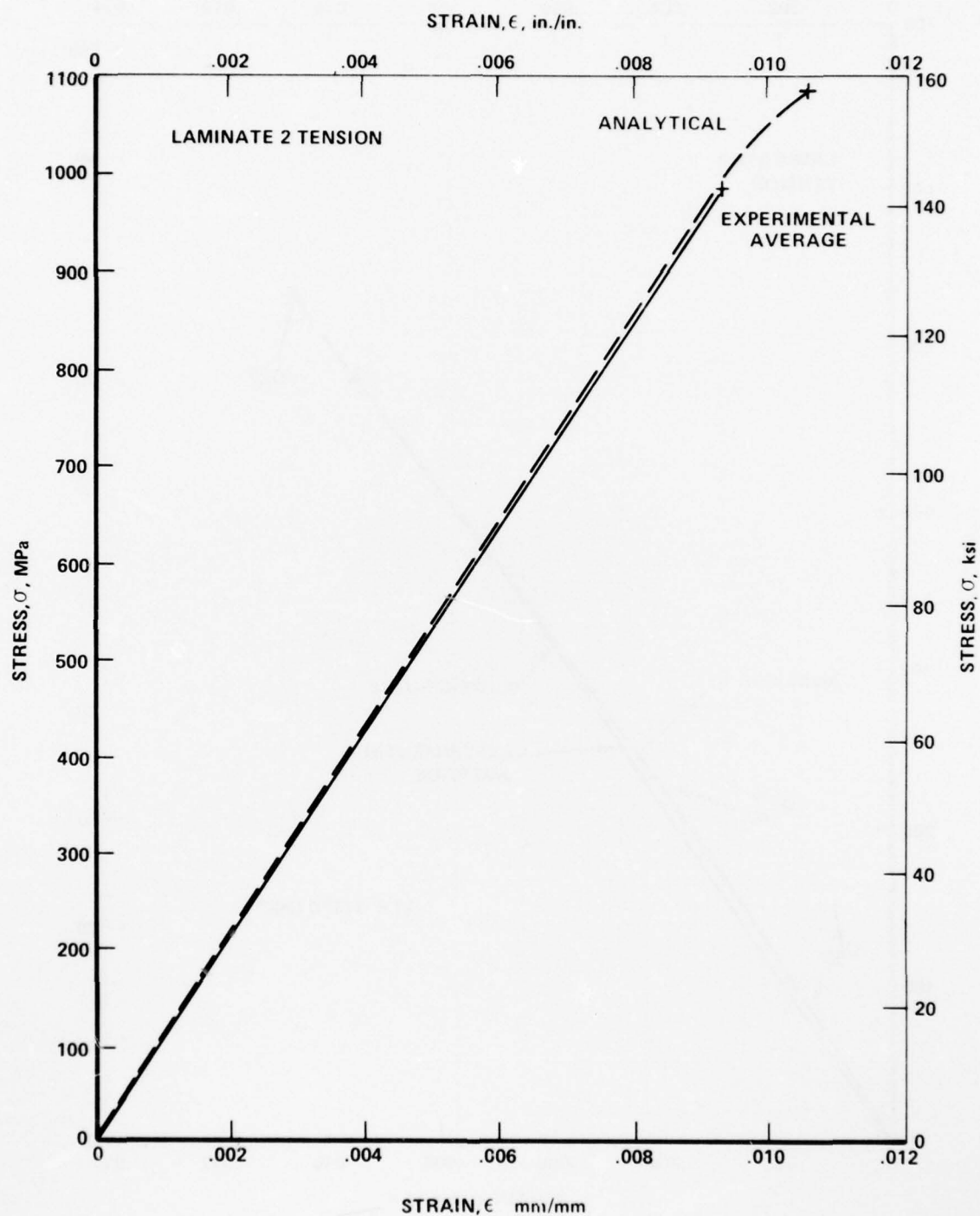
Figure 39.   Comparison Between Predicted and Experimental Average
Tension Stress-Strain Curves for Laminate 2

## TABLE 11

### SUMMARY OF STATIC TENSION TEST PARAMETERS

| | Number of Weibull Parameters | Weibull Coefficients | | | Correlation Coefficient, R | Fitting Coefficient, FIT |
|---|---|---|---|---|---|---|
| | | k | e | v | | |
| LAMINATE 1 | 3 | 24.750 | -0.075323 | 70.500 | 0.99947 | 0.00101 |
| | 2 | 24.1227 | 0 | 70.571 | 0.99947 | 0.00104 |
| LAMINATE 2 | 3 | 18.8662 | -0.430439 | 144.407 | 0.99868 | 0.00253 |
| | 2 | 18.680 | 0 | 144.811 | 0.99867 | 0.00268 |

$$P(x) = \exp\left[-\left(\frac{x-e}{v-e}\right)^k\right]$$

FOR 2 PARAMETERS, $\alpha = k$, $\hat{F} = v$

77

TABLE 12

RELATIONSHIP[a] BETWEEN

PROBABILITY OF SURVIVAL

AND ULTIMATE TENSION STRENGTH

| Probability of Survival P(i) | Ultimate Tensile Strength, $\sigma_{ult}$, MPa(ksi) | |
|---|---|---|
| | Laminate 1 | Laminate 2 |
| .99 | 402 (58.3) | 780(113.1) |
| .95 | 430 (62.3) | 850(123.3) |
| .9 | 443 (64.2) | 883(128.1) |
| .8 | 457 (66.3) | 919(133.3) |
| .7 | 466 (67.6) | 942(136.7) |
| .6 | 473 (68.6) | 960(139.3) |
| .5 | 478 (69.4) | 976(141.6) |
| .4 | 484 (70.2) | 991(143.7) |
| .3 | 489 (71.0) | 1005(145.8) |
| .2 | 496 (71.9) | 1021(148.1) |
| .1 | 503 (73.0) | 1040(150.9) |
| .05 | 509 (73.8) | 1056(153.1) |
| .01 | 518 (75.1) | 1080(156.6) |

a - Strength values were calculated based on a
    3-parameter Weibull Fit to the Data.

78
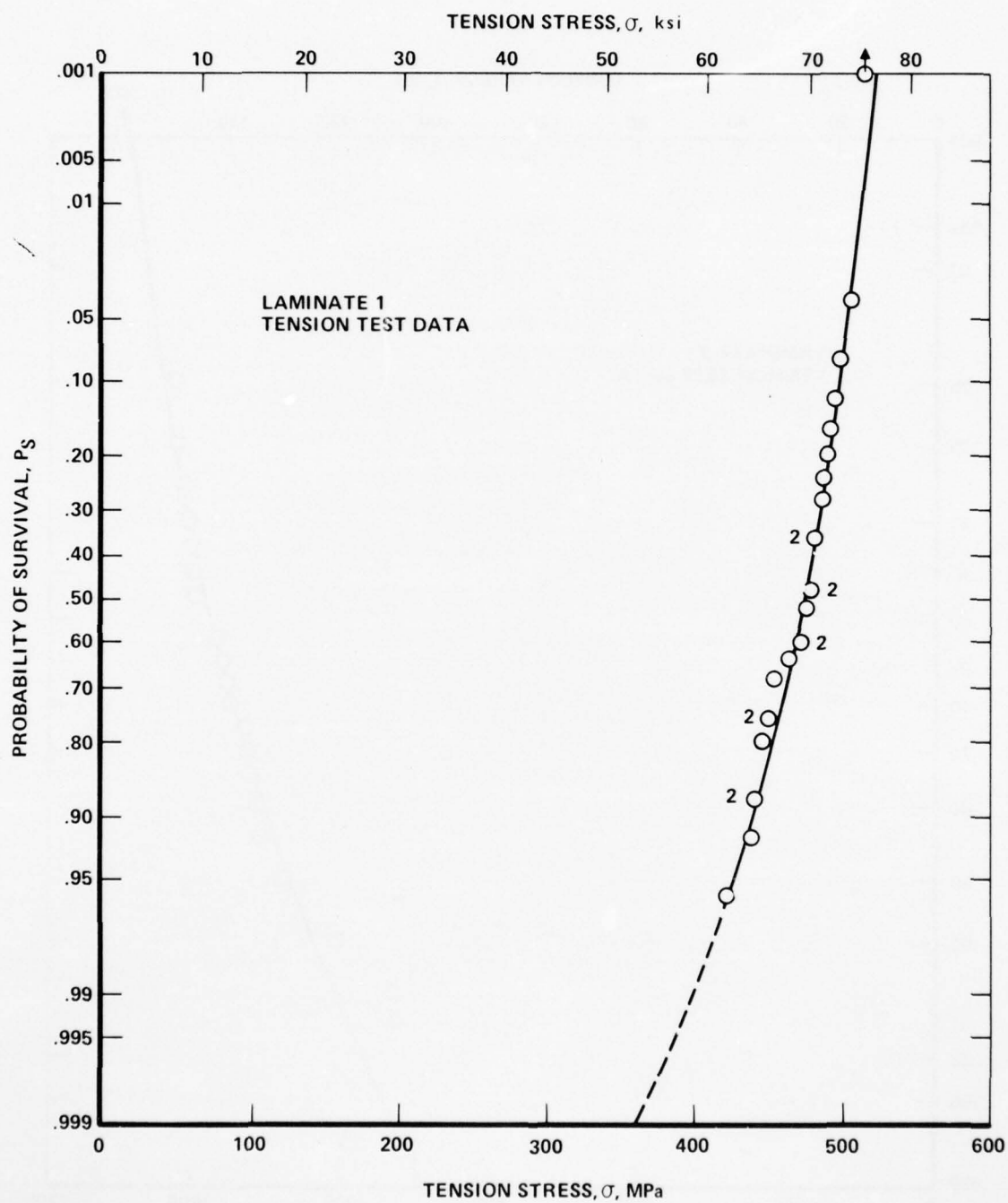
Figure 40. Probability of Survival Versus Ultimate Tension Strength for Laminate 1 Coupons
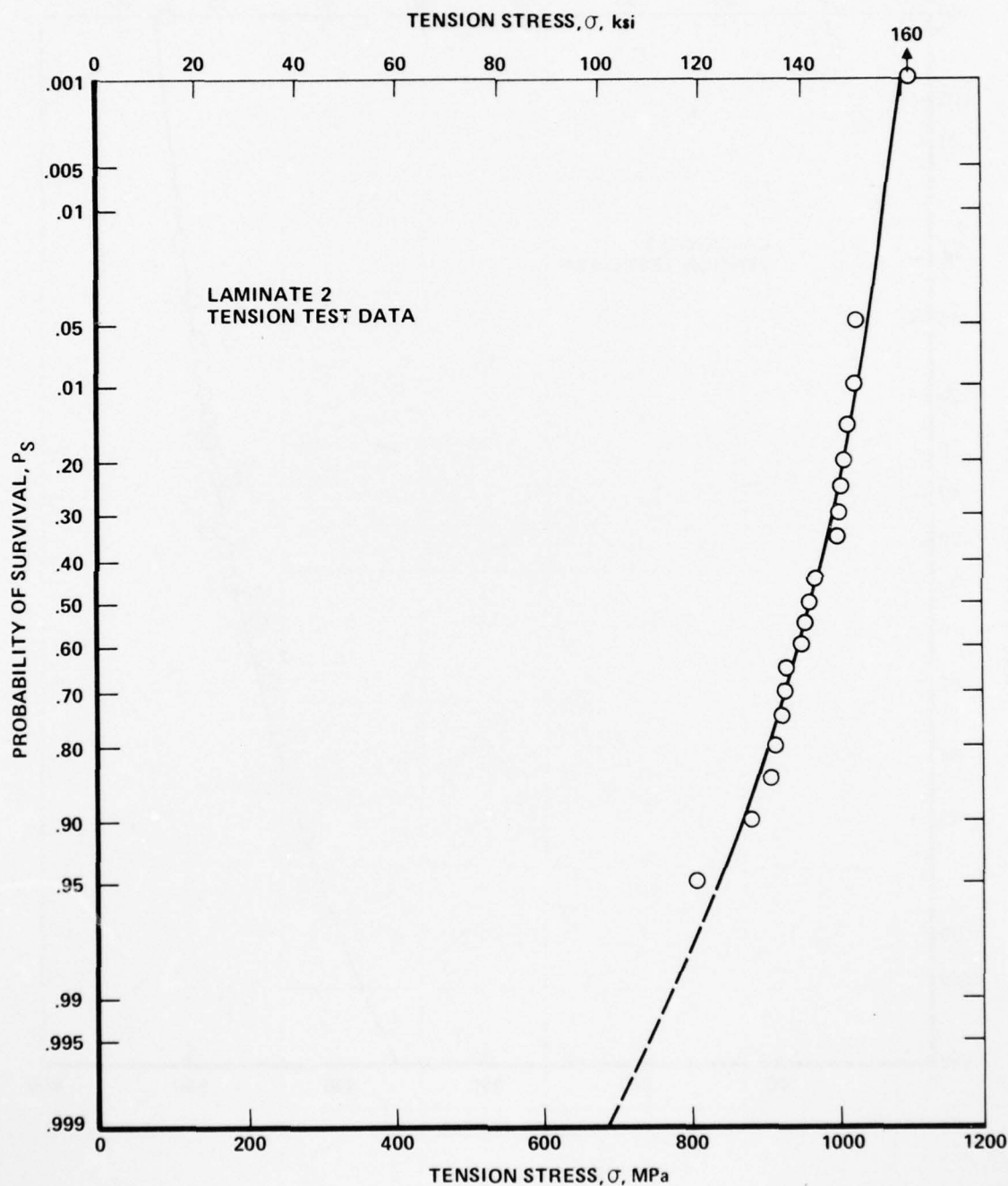
Figure 41. Probability of Survival Versus Ultimate
Tension Strength for Laminate 2 Coupons

## TABLE 13A

### TENSILE TEST RESULTS FOR PANEL 1NH 693, LAMINATE 1

| Sample ID | Min. Area in.$^2$ | Ultimate Load, $P_{ult}$, lbs | Ultimate Stress $\sigma_{ult}$, ksi | Ultimate Strain, $\varepsilon_{ult}$, in./in. in 2.0 in. | Slope Deviation Load, $P_y$, lbs | Slope Deviation Stress, $\sigma_y$, ksi | Slope Deviation Strain, $\varepsilon_y$, in./in. in 2.0 in. | Initial Appar. Modulus of Elasticity, $E_{1a}$, psi x 10$^6$ | Final Appar. Modulus of Elasticity, $E_{1b}$, psi x 10$^6$ |
|---|---|---|---|---|---|---|---|---|---|
| 693- 4A | .0852 | 6740 | 79.1 | .0104 | 4300 | 50.5 | .0062 | 7.82 | 6.18 |
| -11B | .0853 | 5640 | 66.1 | .0091 | 3800 | 45.1 | .0056 | 7.82 | 6.51 |
| -17B | .0876 | 5620 | 64.2 | .0089 | 4500 | 51.4 | .0068 | 7.61 | 6.34 |
| - 8C | .0853 | 5920 | 69.4 | .0090 | 4300 | 50.4 | .0062 | 7.33 | 6.51 |
| -19C | .0861 | 6100 | 70.8 | .0101 | 3800 | 44.1 | .0058 | 7.26 | 6.11 |
| Average Panel 693 | | | 69.9 | .0095 | | 48.3 | .0061 | 7.57 | 6.33 |
| | | | + 9.2 | +.0009 | | + 2.2 | +.0007 | +0.44 | +0.18 |
| | | | - 5.7 | -.0006 | | - 3.1 | -.0003 | -0.31 | -0.22 |
| Average Panels 578 to 606 | | | 69.2 | .0096 | | 45.3 | .0059 | 7.64 | 6.48 |
| | | | + 6.2 | +.0011 | | + 6.9 | +.0010 | +0.54 | +0.70 |
| | | | - 7.2 | -.0010 | | -10.7 | -.0012 | -0.69 | -0.68 |

TABLE 13B

TENSILE TEST RESULTS FOR PANEL 1NH 693, LAMINATE 1

| Sample ID | Min. Area mm² | Ultimate Load Pult, kN | Ultimate Stress, σult MPa | Ultimate Strain εult, mm/mm in 50.8 mm | Slope Deviation Load, Py, kN | Slope Deviation Stress, σy, MPa | Slope Deviation Strain, εy, mm/mm in 50.8 mm | Initial Appar. Modulus of Elasticity, E1a, GPa | Final Appar. Modulus of Elasticity, E1b, GPa |
|---|---|---|---|---|---|---|---|---|---|
| 693- 4A | 55.0 | 30.0 | 545 | .0104 | 19.1 | 348 | .0062 | 53.9 | 42.6 |
| -11B | 55.0 | 25.1 | 456 | .0091 | 17.3 | 311 | .0056 | 53.9 | 44.9 |
| -17B | 56.5 | 25.0 | 443 | .0089 | 20.0 | 354 | .0068 | 52.5 | 43.7 |
| - 8C | 55.0 | 26.3 | 478 | .0090 | 19.1 | 347 | .0062 | 50.5 | 44.9 |
| -19C | 55.5 | 27.1 | 488 | .0101 | 16.9 | 304 | .0058 | 50.0 | 42.1 |
| Average Panel 693 | | | 482 | .0095 | | 333 | .0061 | 52.2 | 43.6 |
| | | | + 63 | +.0009 | | + 15 | +.0007 | + 3.0 | + 1.2 |
| | | | - 39 | -.0006 | | - 21 | -.0003 | - 2.1 | - 1.5 |
| Average Panels 578 to 606 | | | 477 | .0096 | | 312 | .0059 | 52.7 | 44.7 |
| | | | + 43 | +.0011 | | + 48 | +.0010 | + 3.7 | + 4.8 |
| | | | - 50 | -.0010 | | - 74 | -.0012 | - 4.8 | - 4.7 |

MICROCOPY RESOLUTION TEST CHART

NATIONAL BUREAU OF STANDARDS-1963-A

10 panels. This good agreement gave some indication of a possible low variability in static tension results from batch-to-batch of prepreg provided panels are manufactured soon after batch receipt.

Eight tension tests were conducted using coupons of both laminates 1 and 2, but with "T" type longitudinal and transverse strain gages. Table 14 lists test results. Note that the apparent moduli of elasticity were the same using the strain gages as those determined previously using an extensometer. However, the strains to failure as recorded by the extensometer did not have precise agreement with the longitudinal strain gages for two of the three coupons tested. The last two columns of Table 14 show that essentially no hysteresis was observed when the coupons were subjected to five repeated load cycles. These results indicated that if the apparent elastic modulus changes during fatigue such a change must be due to a gradual and progressive form of damage throughout the fatigue loading.

## 4.2    Static Compression Test Results

Figures 42 to 44 show static compression stress-strain curves for particular coupons, but which are representative of the types of curves seen for all test coupons. For laminate 1, stress-strain curves exhibited an initial straight portion of the curve, designated $E_{1c}$ in Figure 42, followed by a continuously curved portion with an average slope approximately 10 percent less than $E_{1c}$. Just prior to failure of laminate 1 coupons, distinct popping sounds were heard each accompanied by small but noticeable horizontal jumps in the stress-strain curve not observable at the scale of Figure 42. Failure was sudden and "brittle-like", called failure mode 1, for approximately half of the coupons, Figure 42, and "flat topped" followed by brittle failure, called failure mode 2, for the other coupons, Figure 43. Post failure examinations of coupons showed no observable difference between those which failed as in Figure 42, compared to those which failed as in Figure 43. Coupons appeared to fail as soon as some small instability occurred provided some critical load had been reached. The practical differences between the two apparently different failure modes, indicated by their stress-strain diagrams, were considered at this point to be insignificant.

83

TABLE 14

TENSION TEST RESULTS
USING STRAIN GAGES

| Sample ID | Area, mm² (in.²) | Ultimate Load P$_{ult}$,kN(lbs) | Ultimate Stress σ$_{ult}$, MPa(ksi) | Longitudinal Ultimate Strain ε$_L$, mm/mm | Extensometer Ultimate Long. Strain ε$_L$, mm/mm in 50.8 mm | Transverse Ultimate Strain ε$_T$, mm/mm | Apparent Longitudinal Modulus of Elasticity, E$_{AL}$, GPa(psi x 10⁶) | Number of Hysteresis Loops | Maximum Stress of Hysteresis Loop MPa(ksi) |
|---|---|---|---|---|---|---|---|---|---|
| 582-24A [a] | 53.2 (.0825) | 24.4 (5480) | 458 (66.4) | .0092 | .0087 | -.0028 | 52.0 (7.55)[b] | None | - |
| 594-15A [a] | 53.2 (.0826) | 25.6 (5760) | 480 (69.7) | .0098 | - | -.0031 | 51.1 (7.41)[b] | 5 | 451 (65.4)[d] |
| 596-11B [a] | 54.1 (.0838) | 24.3 (5460) | 450 (65.2) | .0086 | - | -.0024 | 54.0 (7.84)[b] | 5 | 352 (51.1)[e] |
| 606-1A [a] | 52.5 (.0814) | 24.1 (5420) | 459 (66.6) | .0088 | - | -.0022 | 53.9 (7.82)[b] | 5 | 433 (62.8)[e] |
| 696-34B | 81.5 (.1264) | 64.8 (14580) | 795 (115.3) | .0075 | .0075 | -.0049 | 106 (15.4)[c] | None | - |
| 699-17C | 83.7 (.1297) | 84.2 (18940) | 1007 (146.0) | .0098 | .0090 | -.0063 | 103 (14.9)[c] | None | - |
| 727-13B | 81.6 (.1265) | 88.5 (19900) | 1084 (157.3) | .0104 | - | -.0068 | 104 (15.1)[c] | 5 | 787 (114.2)[e] |
| 728-7A | 83.4 (.1292) | 86.2 (19380) | 1034 (150.0) | .0102 | - | -.0064 | 101 (14.7)[c] | 5 | 785 (113.9)[e] |

Notes:

a - The ultimate stress for these coupons was based on average area

b - Initial Slope for Laminate 1; Previous average of 52.7 GPa(7.64 psi x 10⁶), this average 52.7 GPa (7.65 psi x 10⁶)

c - Average Slope for Laminate 2; Previous average of 106 GPa (15.4 psi x 10⁶), this average 103 GPa (15.0 psi x 10⁶)

d - Small amount of apparent hysteresis

e - No apparent hysteresis
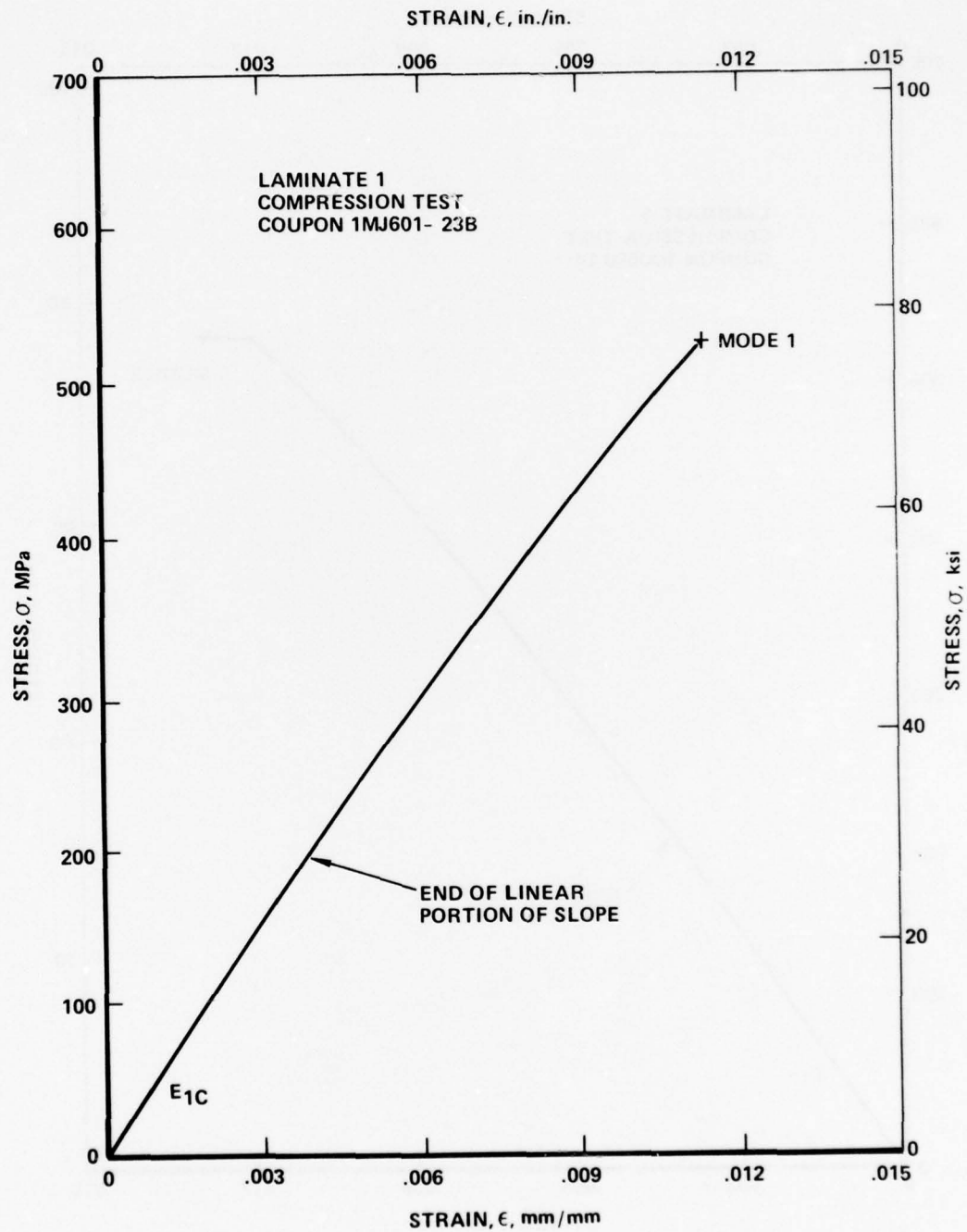
Figure 42.   Compression Stress-Strain Curve for Laminate 1
Coupon 1MJ601-23B

85
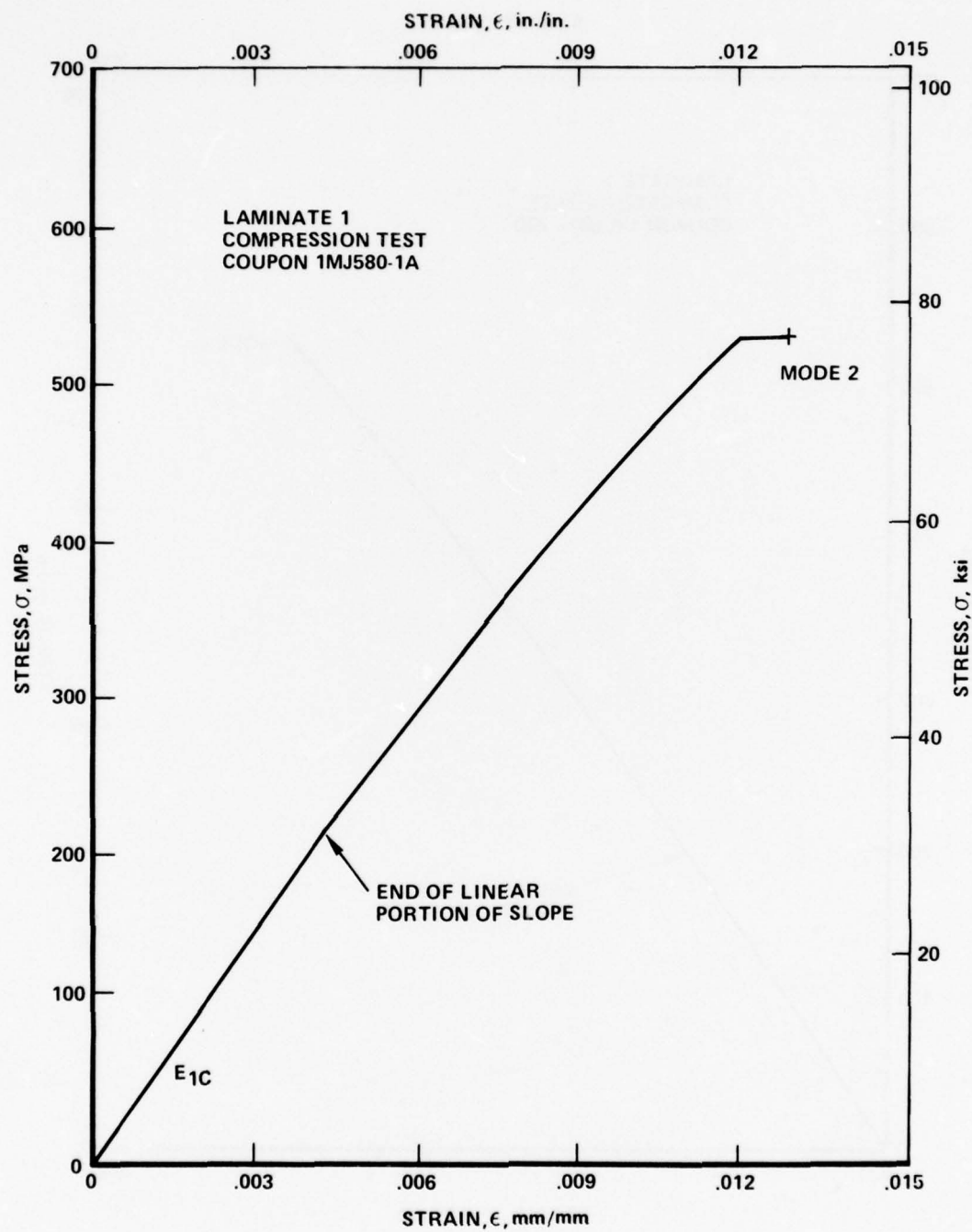
Figure 43.   Compression Stress-Strain Curve for Laminate 1
            Coupon 1MJ580-1A
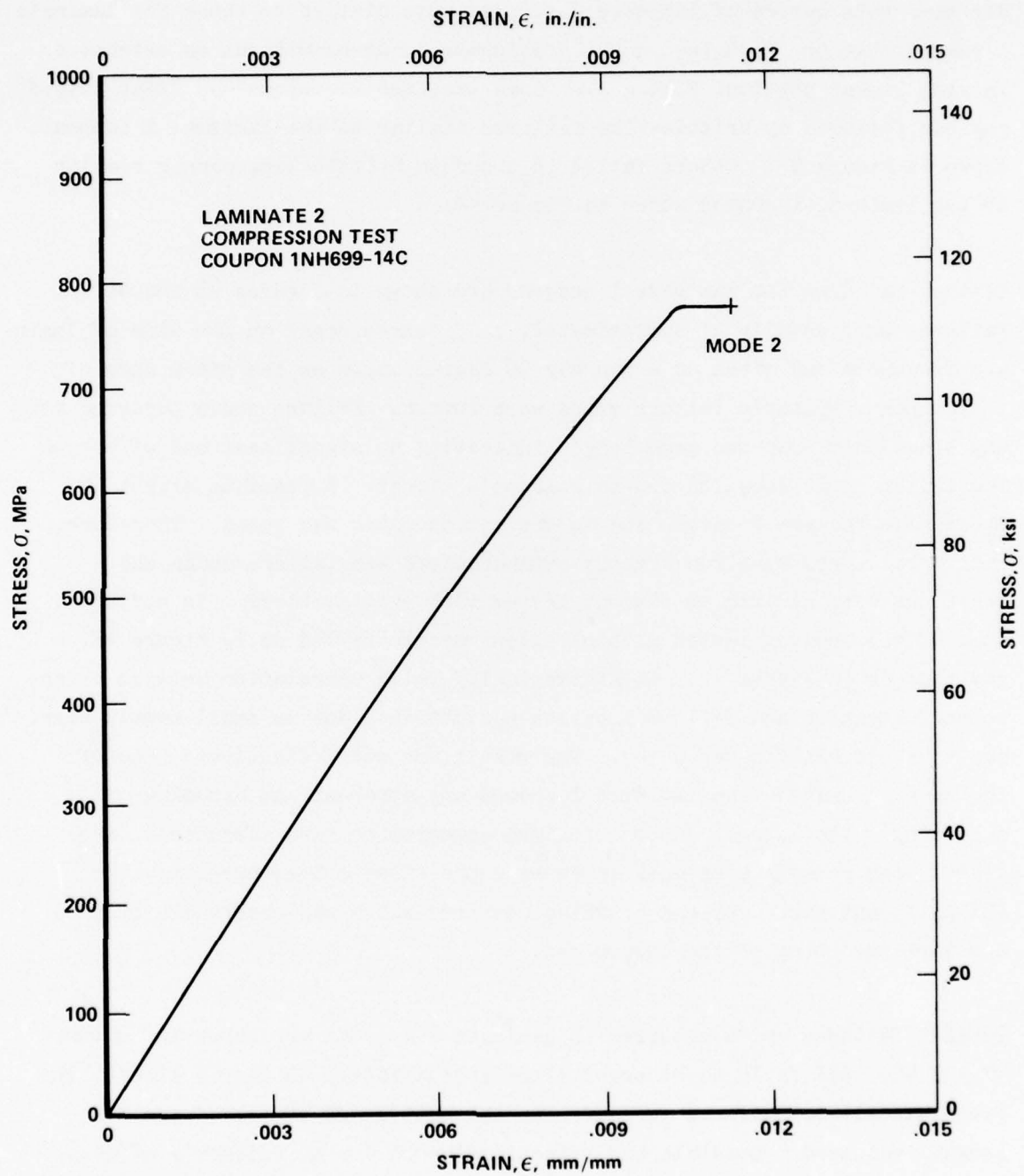
Figure 44. Compression Stress-Strain Curve for Laminate 2
Coupon 1NH699-14C

Stress-strain curves of laminate 2 coupons were similar to those for laminate 1 except that the test record was continuously curved without an extensive initial linear portion, Figure 44. Some laminate 2 coupons had "flat topped" regions followed by brittle-like failures similar to the laminate 1 coupon shown in Figure 43. Others failed in a sudden brittle-like manner similar to the laminate 1 coupon shown in Figure 42.

Typical failures for laminate 1 coupons are shown in Figures 45 and 46. Failures were usually at approximately a 45 degree angle on one side of laminate 1 coupons and often at a roughly 90 degree angle on the other side of the coupon. Multiple failure zones were common. Failure zones occurred at any location within the gage length indicating no significant end effect on the failure zone location due to Poisson's effect. A possible slight influence on failure location due to the extensometer was noted. Therefore, additional tests were run without extensometers and failure modes and locations were similar to coupons tested with extensometers. In addition, some of the coupons tested without extensometers failed as in Figure 42, and some as in Figure 43. No statistically valid correlation between extensometer location and failure location was obtained due to small sample size, but some correlation was noted. The result was not definitive. None of the coupons tested from laminate 1 showed any apparent end brooming or splitting. The lateral support fixture appeared to have adequately prevented such phenomena as well as to have prevented column buckling. An insignificant amount of end crushing occurred which was observable only as a slight smoothing of the coupon end.

Typical failures which occurred in laminate 2 coupons are shown in Figures 47 and 48. All failures occurred along approximately 45 degree lines. The fact that all failures occurred within the bottom 1/2 of the coupon gage length indicated a possible end effect influence due to Poisson's effects. Figure 49, a magnified photo of the end of a typically failed laminate 2 coupon, illustrates that despite a possible Poisson's end effect on failure location, no end brooming or splitting was observed for any coupons.
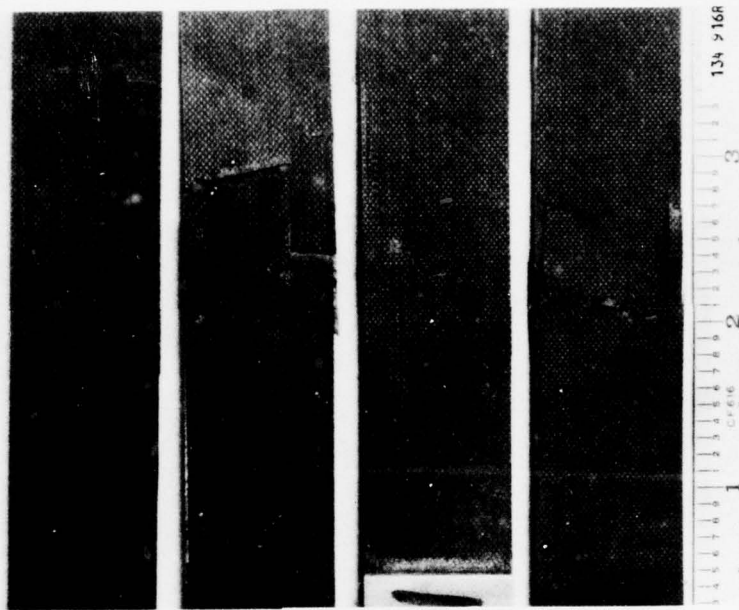
Figure 45.  Laminate 1 Failed Coupons; Specimens, Numbered
Left to Right, are:  603-26A, 596-2B, 601-17B,
601-5A
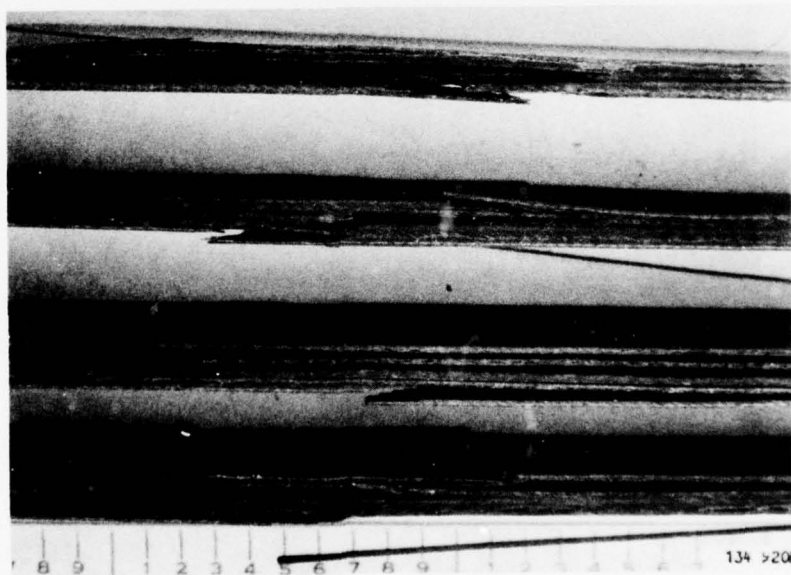


Figure 46.  Laminate 1 Failed Coupons; Specimens Numbered
Top to Bottom, are:  601-5A, 601-17B, 596-2B,
603-26A
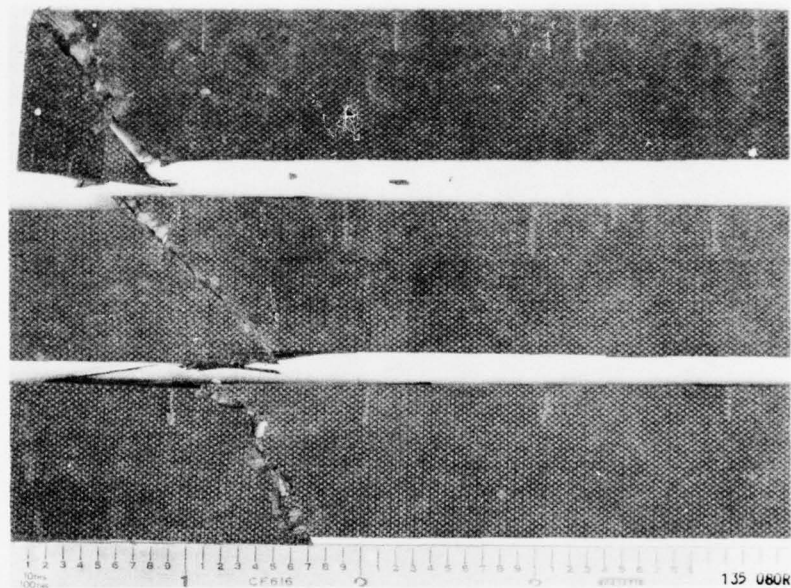
Figure 47. Laminate 2 Failed Coupons; Specimens, Numbered
Top to Bottom, are: 727-34A, 699-29C, 728-12B
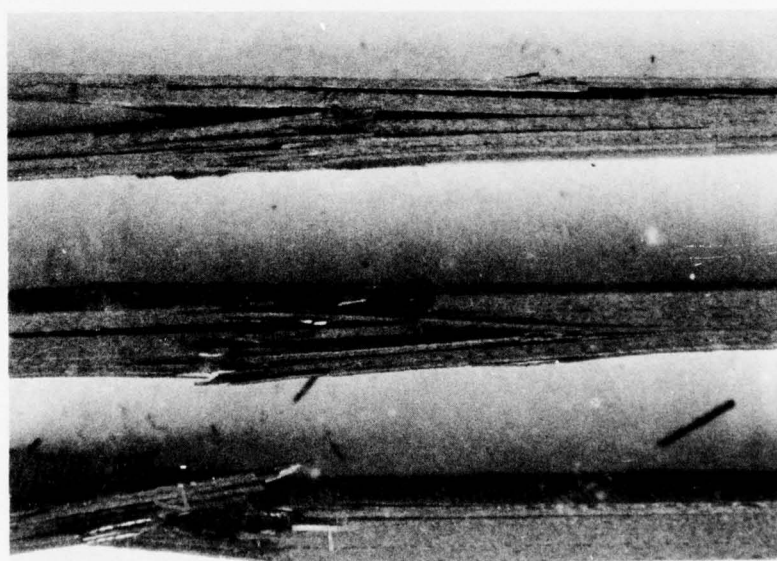


Figure 48. Laminate 2 Failed Coupons; Specimens, Numbered
Top to Bottom, are: 728-12B, 699-29C, 727-34A
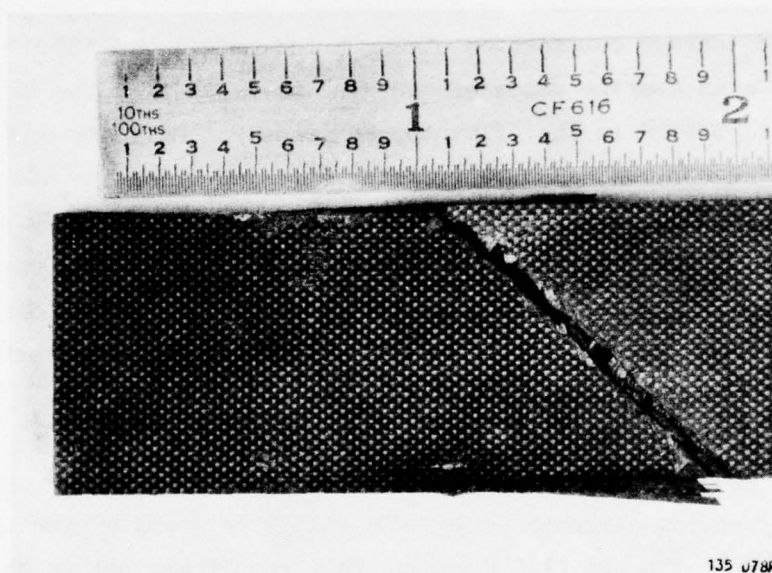
Figure 49.  Laminate 2 Failed Coupon; Specimen
728-10B

Tabulated static compression test results. Tables 15 and 16, showed, as expected, a higher compression strength for laminate 2. In Table 15 the stress and strain values for laminate 1 coupons at which the slope deviated from a straight line were somewhat subjective and should not be construed as precise measurements since a best fit-by-eye technique was used. For laminate 2, the slope, being an average value, was again somewhat subjective. The ultimate strains listed are the strain values either to failure (curves without a "flat topped" region) or to the point where the curve became flat.

For laminate 1, failure mode 1 was observed in eleven of the 26 coupons tested. The average compression strength for mode 1 was 505 MPa (73.2 ksi) as opposed to an average value of 463 MPa (67.1 ksi) for the fifteen coupons which failed in the "flat topped" mode 2. Only one of the eleven mode 1 failure coupons had a compression strength below the 481 MPa (69.7 ksi) average value for all 26 coupons. These results strongly suggested that for laminate 1, the compression strength for mode 2 failures was less than that for mode 1. This result indicated a possible physical difference between the failure modes which was not observable in post fracture examination of the coupons.

Nine of the 20 laminate 2 coupons listed in Table 16 failed in mode 1 at an average compression strength of 799 MPa (115.9 ksi) and eleven in mode 2 at an average of 778 MPa (112.8 ksi). This result was not as significant as the result for laminate 1, but again suggested an apparent difference between the two failure modes. Interestingly, 10 of the 20 coupons failed away from the bottom within the gage length and of these 9 failed in mode 2.

The compression test results of the two laminates are compared in Table 17. As expected, laminate 2 coupons were stronger, however, the ultimate stresses and strains may be lower than theoretical because of the test method (see Section 2.4). Comparison of Tables 10 and 17 shows that for laminate 1, scatter in the tension data was less than for the compression data while the reverse was true for laminate 2 data. Figures 50 and 51 show comparisons

92

TABLE 15A

STATIC COMPRESSION TEST RESULTS OF LAMINATE 1 COUPONS

(Sample Size = 26)

| Sample ID | Min. Area, in.² | Ultimate Load, $P_{ult}$, lbs | Ultimate Stress, $\sigma_{ult}$, ksi | Ultimate Strain $\varepsilon_{ult}$, in./in. in 2.0 in. | Load at Initial Curve Deviation, $P_{CD}$, lbs | Stress at Initial Curve Deviation, $\sigma_{CD}$, ksi | Strain at Initial Curve Deviation, $\varepsilon_{CD}$, in./in. in 2.0 in. | Initial Apparent Modulus of Elasticity, $E_{1c}$, psi x $10^6$ | Amount of Strain at Ultimate Load, $\varepsilon$, in./in. in 2.0 in. |
|---|---|---|---|---|---|---|---|---|---|
| 578-10B | .0828 | 6750 | 81.5 | .0128 | 3260 | 39.4 | .0056 | 7.09 | 0[a] |
| 18A | .0856 | 6650 | 77.7 | .0130 | 2870 | 33.5 | .0048 | 6.98 | .0006 |
| 9A | .0840 | 6180 | 73.6 | .0120 | 3000 | 35.7 | .0051 | 7.00 | 0 |
| 580-25A | .0824 | 5180 | 62.9 | .0099 | 2660 | 32.3 | .0048 | 6.73 | .00045 |
| 1A | .0828 | 6360 | 76.8 | .0118 | 2460 | 29.7 | .0042 | 7.07 | .0006 |
| 582-19B | .0823 | 6410 | 77.9 | .0132 | 3010 | 36.6 | .0056 | 6.59 | 0 |
| 10A | .0824 | 6340 | 76.9 | .0123 | $\sigma$-$\varepsilon$ record continuous curve | | | | |
| 583-5A | .0824 | 5360 | 65.0 | .0098 | 3330 | 40.4 | .0057 | 7.09 | .0006 |
| 4A | .0824 | 6070 | 73.7 | .0113 | 2420 | 29.4 | .0048 | 6.12 | .0018 |
| 18A | .0860 | 6230 | 72.4 | .0117 | 3130 | 36.4 | .0052 | 6.93 | .0006 |
| 16B | .0849 | 6560 | 77.3 | .0128 | 3250 | 38.3 | .0056 | 6.90 | 0 |
| 594-21B | .0813 | 5790 | 71.1 | .0108 | 2800 | 34.4 | .0050 | 6.96 | 0 |
| 14B | .0830 | 5660 | 68.2 | .0108 | 1630 | 31.7 | .0045 | 7.04 | .0006 |
| 596-19A | .0809 | 5260 | 65.0 | .0112 | 2760 | 34.1 | .0050 | 6.82 | .00045 |
| 25B | .0813 | 4890 | 60.2 | .0106 | 2520 | 31.0 | .0044 | 6.81 | .0006 |
| 3B | .0820 | 5370 | 65.5 | .0100 | 2670 | 32.6 | .0045 | 7.24 | .0012 |
| 601-23B | .0811 | 6280 | 77.4 | .0114 | 3080 | 38.0 | .0052 | 7.23 | .00045 |
| 6A | .0819 | 5720 | 69.8 | .0106 | 3150 | 38.5 | .0057 | 6.75 | 0 |
| 603-5A | .0822 | 6000 | 73.0 | .0116 | 2520 | 30.7 | .0045 | 6.81 | 0 |
| 14B | .0828 | 5380 | 65.0 | .0100 | 2540 | 30.9 | .0044 | 7.10 | 0 |
| 13B | .0819 | 5720 | 69.8 | .0106 | 3150 | 38.5 | .0057 | 6.75 | .0003 |
| 604-20B | .0832 | 5300 | 63.7 | .0102 | 2380 | 28.6 | .0042 | 6.81 | 0 |
| 26B | .0816 | 4700 | 57.6 | .0086 | 3180 | 39.0 | .0054 | 7.22 | 0 |
| 19B | .0833 | 4820 | 57.9 | .0085 | 3360 | 40.3 | .0057 | 7.08 | .0006 |
| 606-20A | .0829 | 5260 | 63.4 | .0099 | 2780 | 33.5 | .0046 | 7.21 | .0003 |
| 23A | .0806 | 5580 | 69.2 | .0102 | 3090 | 38.3 | .0052 | 7.37 | .0003 |
| Average | | | 69.7 +11.8 -12.1 | .0110 +.0022 -.0025 | | 34.9 +5.5 -8.5 | .0050 +.0007 -.0008 | 6.95 +0.42 -0.83 | |

a - A zero denotes that the coupon failed without a flat topped region prior to failure, see Figure 43.

93

TABLE 15B

STATIC COMPRESSION TEST RESULTS OF LAMINATE 1 COUPONS

(Sample Size = 26)

| Sample ID | Minimum Area, mm² | Ultimate Stress σ_ult, MPa | Ultimate Strain ε_ult, mm/mm in 50.8 mm | Stress at Initial Curve Deviation, σ_CD, MPa | Strain at Initial Curve Deviation ε_CD, mm/mm in 50.8 mm | Initial Apparent Modulus of Elasticity E_1C, GPA | Amount of Strain at Ultimate Load ε, mm/mm in 50.8 mm |
|---|---|---|---|---|---|---|---|
| 578-10B | 53.4 | 561.9 | .0128 | 271.6 | .0056 | 48.9 | 0 [a] |
| 18A | 56.0 | 535.7 | .0130 | 231.0 | .0048 | 48.1 | .0006 |
| 9A | 54.9 | 507.4 | .0120 | 246.1 | .0051 | 48.3 | 0 |
| 580-25A | 53.9 | 433.7 | .0099 | 222.7 | .0048 | 46.4 | .00045 |
| 1A | 54.2 | 529.5 | .0118 | 204.8 | .0042 | 48.7 | .0006 |
| 582-19B | 53.8 | 537.1 | .0132 | 252.3 | .0056 | 45.4 | 0 |
| 10A | 53.9 | 530.2 | .0123 | σ - ε record continuous curve | | 48.9 | .006 |
| 583-5A | 53.9 | 448.2 | .0098 | 278.5 | .0057 | 42.2 | .0018 |
| 4A | 53.9 | 508.1 | .0113 | 202.7 | .0048 | 47.8 | .0006 |
| 18A | 56.2 | 499.2 | .0117 | 251.0 | .0052 | 47.6 | 0 |
| 16B | 55.5 | 533.0 | .0128 | 264.1 | .0056 | 48.0 | .0006 |
| 594-21B | 53.2 | 490.2 | .0108 | 237.2 | .0050 | 48.5 | .00045 |
| 14B | 54.3 | 470.2 | .0108 | 218.6 | .0045 | 47.0 | .0006 |
| 596-19A | 52.9 | 448.2 | .0112 | 235.1 | .0050 | 47.0 | .0012 |
| 25B | 53.2 | 415.1 | .0106 | 213.7 | .0044 | 49.9 | .00045 |
| 3B | 53.6 | 451.6 | .0100 | 224.8 | .0045 | 49.8 | 0 |
| 601-23B | 53.0 | 533.6 | .0114 | 262.6 | .0052 | 46.5 | 0 |
| 6A | 53.6 | 481.2 | .0106 | 265.4 | .0057 | 47.0 | .0003 |
| 603-5A | 53.8 | 503.3 | .0116 | 211.7 | .0045 | 49.0 | 0 |
| 14B | 54.2 | 448.2 | .0100 | 213.0 | .0044 | 46.5 | 0 |
| 13B | 53.6 | 481.2 | .0106 | 265.4 | .0057 | 47.0 | .0003 |
| 604-20B | 54.4 | 439.2 | .0102 | 197.2 | .0042 | 49.8 | 0 |
| 26B | 53.3 | 397.1 | .0086 | 268.9 | .0054 | 48.8 | .0006 |
| 19B | 54.5 | 399.2 | .0085 | 277.8 | .0057 | 49.7 | .0003 |
| 606-20A | 54.3 | 437.1 | .0099 | 231.0 | .0046 | 50.8 | .0006 |
| 23A | 52.7 | 477.2 | .0102 | 264.1 | .0052 | | 0 |
| Average | | 480.6 +81.3 -83.5 | .0110 +.0022 -.0025 | 240.6 +37.9 -43.4 | .0050 +.0007 -.0008 | 47.9 +2.9 -5.7 | |

a--0 denotes that the coupon failed without a flat topped region prior to failure, see Figure 43.

TABLE 16A

STATIC COMPRESSION TEST RESULTS OF LAMINATE 2 COUPONS
(Sample Size = 20)

| Sample ID | Average Area, in.$^2$ | Ultimate Load, $P_{ult}$, lbs | Ultimate Stress, $\sigma_{ult}$, ksi | Ultimate Strain, $\epsilon_{ult}$, in./in. in 2.0 in. | Apparent Modulus of Elasticity, $E_A$, psi x 10$^6$ | Amount of Strain at Ultimate load, $\epsilon$, in./in. in 2.0 in. |
|---|---|---|---|---|---|---|
| 696-20A | .1295 | 13950 | 107.7 | .0096 | 11.0 | .0003 |
| 21A | .1303 | 14100 | 108.2 | .0091 | 11.7 | 0$^a$ |
| 28A | .1283 | 14300 | 111.4 | .0088 | 12.3 | .0011 |
| 11B | .1276 | 15125 | 118.5 | .0101 | 11.6 | 0 |
| 14C | .1281 | 15050 | 117.5 | .0102 | 11.0 | .0008 |
| 699-7A | .1303 | 13550 | 104.0 | .0087 | 11.6 | 0 |
| 18A | .1286 | 15100 | 118.2 | .0105 | 11.4 | 0 |
| 19B | .1277 | 15150 | 118.6 | .0102 | 11.1 | 0 |
| 14C | .1281 | 15050 | 117.5 | .0106 | 11.2 | .0009 |
| 29C | .1273 | 14000 | 110.0 | .0089 | 12.2 | .0008 |
| 727-12A | .1262 | 14250 | 112.9 | .0099 | 11.2 | 0 |
| 27A | .1234 | 14000 | 113.4 | .0095 | 11.4 | .0009 |
| 20B | .1281 | 14500 | 113.2 | .0093 | 12.2 | .0009 |
| 7C | .1277 | 15100 | 118.2 | .0101 | 11.6 | .0006 |
| 15C | .1290 | 15000 | 116.3 | .0101 | 11.5 | 0 |
| 728-23A | .1322 | 15550 | 117.6 | .0102 | 11.6 | 0 |
| 10B | .1322 | 15750 | 119.1 | .0102 | 11.5 | .0009 |
| 12B | .1294 | 13850 | 107.0 | .0096 | 11.1 | .0011 |
| 3C | .1289 | 16650 | 129.2 | .0112 | 11.4 | 0 |
| 20C | .1319 | 14000 | 106.1 | .0087 | 11.8 | .0011 |
| Average | | | 114.2 +15.0 -10.2 | .0098 +.0014 -.0011 | 11.5 +0.8 -0.5 | |

a - A 0 denotes that the coupon failed with a flat topped region prior to failure, see Figure 44.

95

TABLE 16B

STATIC COMPRESSION TEST RESULTS OF LAMINATE 2 COUPONS

(Sample Size = 20)

| Sample ID | Average Area, mm$^2$ | Ultimate Stress, $\sigma_{ult}$, MPa | Ultimate Strain $\varepsilon_{ult}$, mm/mm in 50.8 mm | Appar. Modulus of Elasticity $E_A$, GPa | Amount of Strain at Ultimate Load $\varepsilon$, mm/mm, in 50.8 mm |
|---|---|---|---|---|---|
| 696-20A | 84.7 | 742.6 | .0096 | 75.8 | .0003 |
| 21A | 85.3 | 746.0 | .0091 | 80.7 | 0[a] |
| 28A | 83.9 | 768.1 | .0088 | 84.8 | .0011 |
| 11B | 83.5 | 817.0 | .0101 | 80.0 | 0 |
| 14C | 83.8 | 810.0 | .0102 | 75.8 | .0008 |
| 699- 7A | 85.2 | 717.0 | .0087 | 80.0 | 0 |
| 18A | 84.1 | 815.0 | .0105 | 78.6 | 0 |
| 19B | 83.5 | 817.7 | .0102 | 76.5 | 0 |
| 14C | 83.8 | 810.1 | .0106 | 77.2 | .0009 |
| 29C | 83.3 | 758.4 | .0089 | 84.1 | .0008 |
| 727-12A | 82.6 | 778.4 | .0099 | 77.2 | 0 |
| 27A | 80.7 | 781.9 | .0095 | 78.6 | .0009 |
| 20B | 83.8 | 780.5 | .0093 | 84.1 | .0009 |
| 7C | 83.5 | 815.0 | .0101 | 80.0 | .0006 |
| 15C | 84.4 | 801.9 | .0101 | 79.3 | 0 |
| 728-23A | 86.5 | 810.8 | .0102 | 80.0 | 0 |
| 10B | 86.5 | 821.2 | .0102 | 79.3 | .0009 |
| 12B | 84.6 | 737.7 | .0096 | 76.5 | .0011 |
| 3C | 84.3 | 890.8 | .0112 | 78.6 | 0 |
| 20C | 86.3 | 731.5 | .0087 | 81.4 | .0011 |
| Average | | 787.4 +103.4 -70.4 | .0098 +.0014 -.0011 | 79.3 +5.5 -3.5 | |

a - A 0 denotes that the coupon failed without a flat topped region prior to failure, see Figure 44.

TABLE 17

COMPARISON OF

STATIC COMPRESSION TEST RESULTS

|  | AVERAGE ULTIMATE STRESS, $\sigma_{ult}$, MPa (ksi) | AVERAGE ULTIMATE STRAIN, $\epsilon_{ult}$, mm/mm in 50.8 mm | AVERAGE APPARENT MODULUS OF ELASTICITY, $E_{avg}$, GPa (psi x $10^6$) |
|---|---|---|---|
| LAMINATE 1 | 481 (69.7)[a]<br>+81 (11.8), 17%<br>-82 (12.1), 17% | 0.0110<br>+0.0022, 20%<br>-0.0025, 23% | 47.9 (6.95)[b]<br>+2.0 (0.29), 4%<br>-5.7 (0.83), 12% |
| LAMINATE 2 | 787 (114.2)<br>+103 (15.0), 13%<br>-70 (10.2), 9% | 0.0098<br>+0.0014, 14%<br>-0.0011, 11% | 79.3 (11.5)<br>+5.5 (0.8), 7%<br>-3.4 (0.5), 4% |

a - Based on minimum area

b - Average Initial Apparent Modulus of Elasticity

97
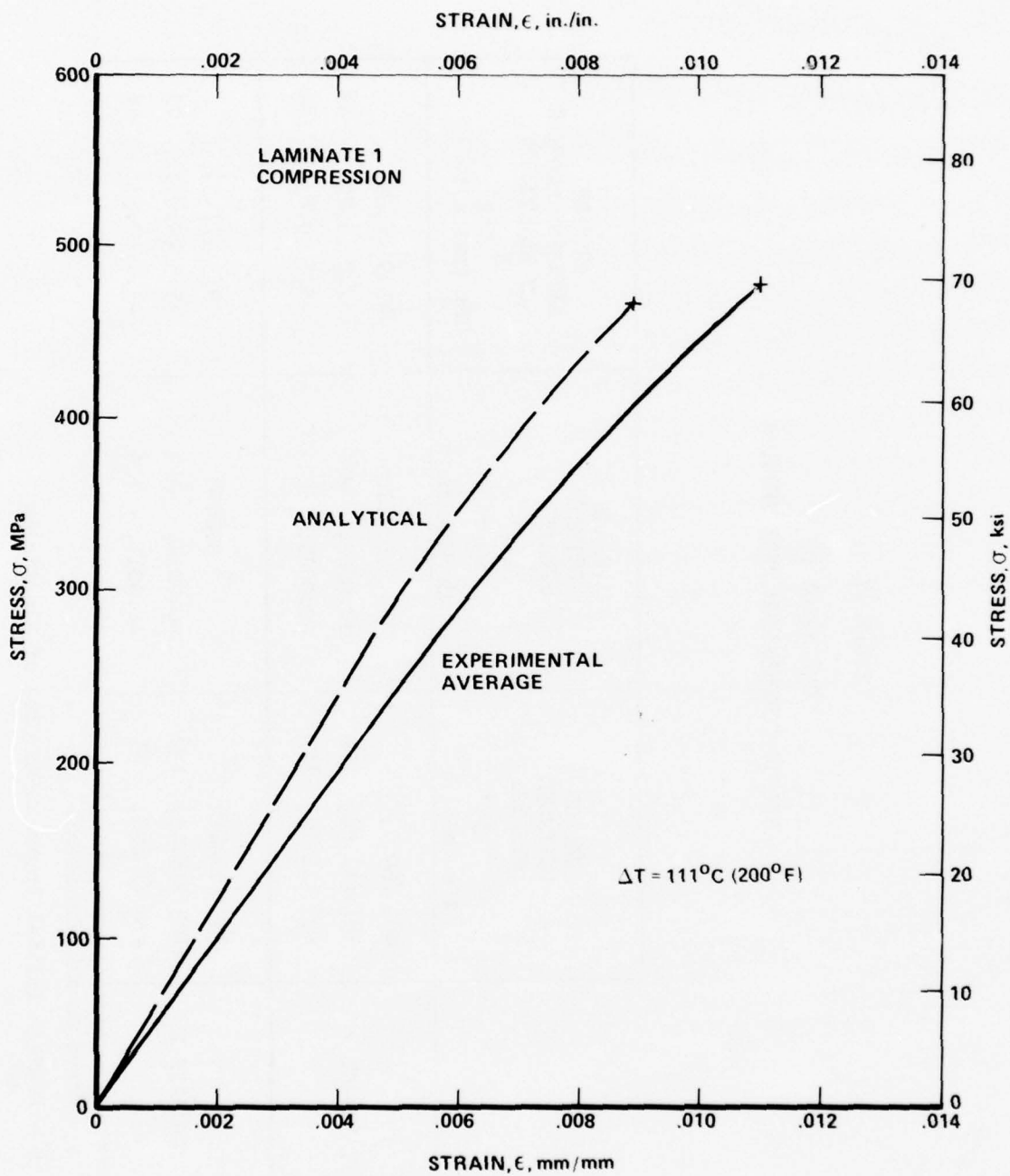
Figure 50.   Comparison Between Predicted and Experimental Average
Compression Stress-Strain Curves for Laminate 1
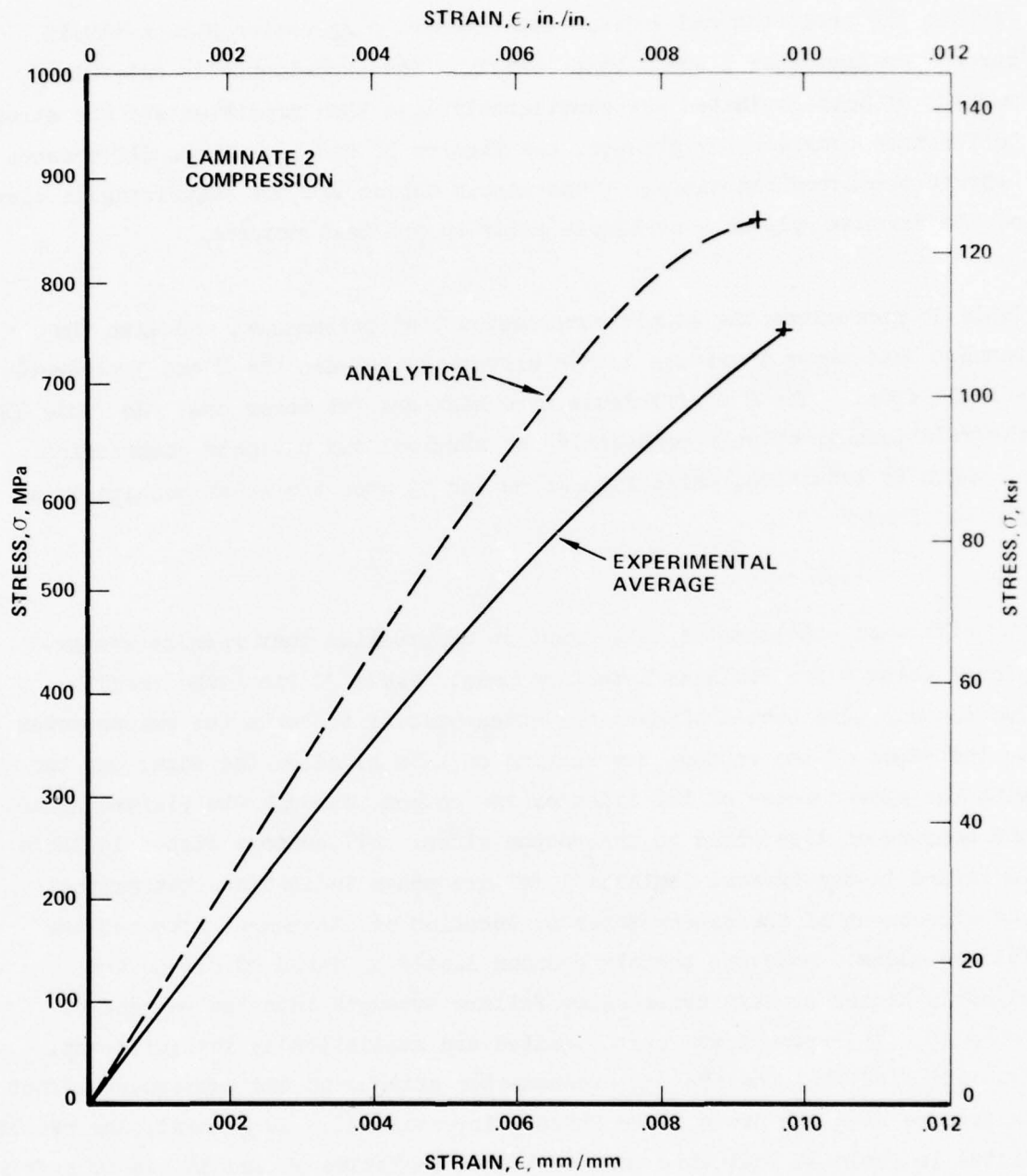
Figure 51. Comparison Between Predicted and Experimental Average
Compression Stress-Strain Curves for Laminate 2

between the predicted and average experimental compression stress-strain curves for laminates 1 and 2 respectively. The experimentally determined modulus of both laminates was considerably less than predicted and the strain to fracture considerably greater, see Figures 50 and 51. These differences between predicted and actual stress-strain curves are not surprising in view of the derth of ply data available prior to the test program.

Table 18 summarizes the static compression test parameters, and like the tension data shows there was little difference between the 2 and 3 parameter Weibull fits. The R coefficients were high and Fit terms low. In Table 19 the relationship between probability of survival and ultimate compression strength is tabulated, while Figures 52 and 53 show the relationships in a plotted format.

The effect of extensometer attachment on compression test results was explored using a few laminate 1 test coupons. Table 20 lists the results. Two coupons were tested without the extensometer; two with the extensometer on the edges of the coupon, but bearing on tabs glued on the edge; and two with the extensometer on the sides of the coupon, through the fixture holes, and bearing on tabs glued to the coupon sides. All coupons listed in Table 20 failed in the typical laminate 1 failure modes indicating that neither the attachment of the extensometer or location of attachment affected the failure modes. However, the six coupons listed in Table 20 did have a slightly higher average compression failure strength than the coupons of Table 15. This result was quite limited and statistically insignificant, but indicated that the type of extensometer attachment and subsequent effect on failure strength needs to be further investigated. In general, the results listed in Table 20 indicated that test data in Tables 15 and 16 can be safely compared because test procedures were identical, but precise comparisons to other test results using different strain measuring devices must be made with caution.

100

## TABLE 18

### SUMMARY OF STATIC COMPRESSION TEST PARAMETERS

| | NUMBER OF WEIBULL PARAMETERS | WEIBULL COEFFICIENTS | | | CORRELATION COEFFICIENT, R | FITTING COEFFICIENT, FIT |
|---|---|---|---|---|---|---|
| | | k | e | v | | |
| LAMINATE 1 | 3 | 12.089 | -0.457164 | 72.194 | 0.99730 | 0.00578 |
| | 2 | 11.940 | 0 | 72.534 | 0.99727 | 0.00632 |
| LAMINATE 2 | 3 | 25.018 | -0.259155 | 115.821 | 0.99888 | 0.00211 |
| | 2 | 24.905 | 0 | 116.074 | 0.99888 | 0.00220 |

$$P(x) = \exp\left[ -\left(\frac{x-e}{v-e}\right)^k \right]$$

FOR 2 PARAMETERS, $\alpha = k$, $\hat{A} = v$

101

## TABLE 19

### RELATIONSHIP BETWEEN PROBABILITY OF SURVIVAL
### AND ULTIMATE COMPRESSION STRENGTH[a]

| Probability of Survival P(i) | Ultimate Compressive Strength, $\sigma_{ult}$, MPa (ksi) | |
|:---:|:---:|:---:|
| | Laminate 1 | Laminate 2 |
| .999 | 280  (40.6) | 605  (87.8) |
| .995 | 320  (46.4) | 646  (93.7) |
| .99 | 339  (49.2) | 664  (96.3) |
| .95 | 389  (56.4) | 709 (102.8) |
| .90 | 412  (59.8) | 729 (105.8) |
| .80 | 439  (63.7) | 752 (109.1) |
| .70 | 457  (66.3) | 766 (111.1) |
| .60 | 471  (68.3) | 777 (112.7) |
| .50 | 483  (70.0) | 787 (114.1) |
| .40 | 494  (71.7) | 796 (115.4) |
| .30 | 505  (73.3) | 805 (116.7) |
| .20 | 518  (75.1) | 814 (118.0) |
| .10 | 534  (77.4) | 826 (119.8) |
| .05 | 545  (79.1) | 834 (121.0) |
| .01 | 565  (82.0) | 849 (123.1) |
| .005 | 578  (83.9) | 854 (123.8) |
| .001 | 585  (84.8) | 863 (125.1) |

a - Strength values were calculated based on a 3-parameter Weibull fit to the data.
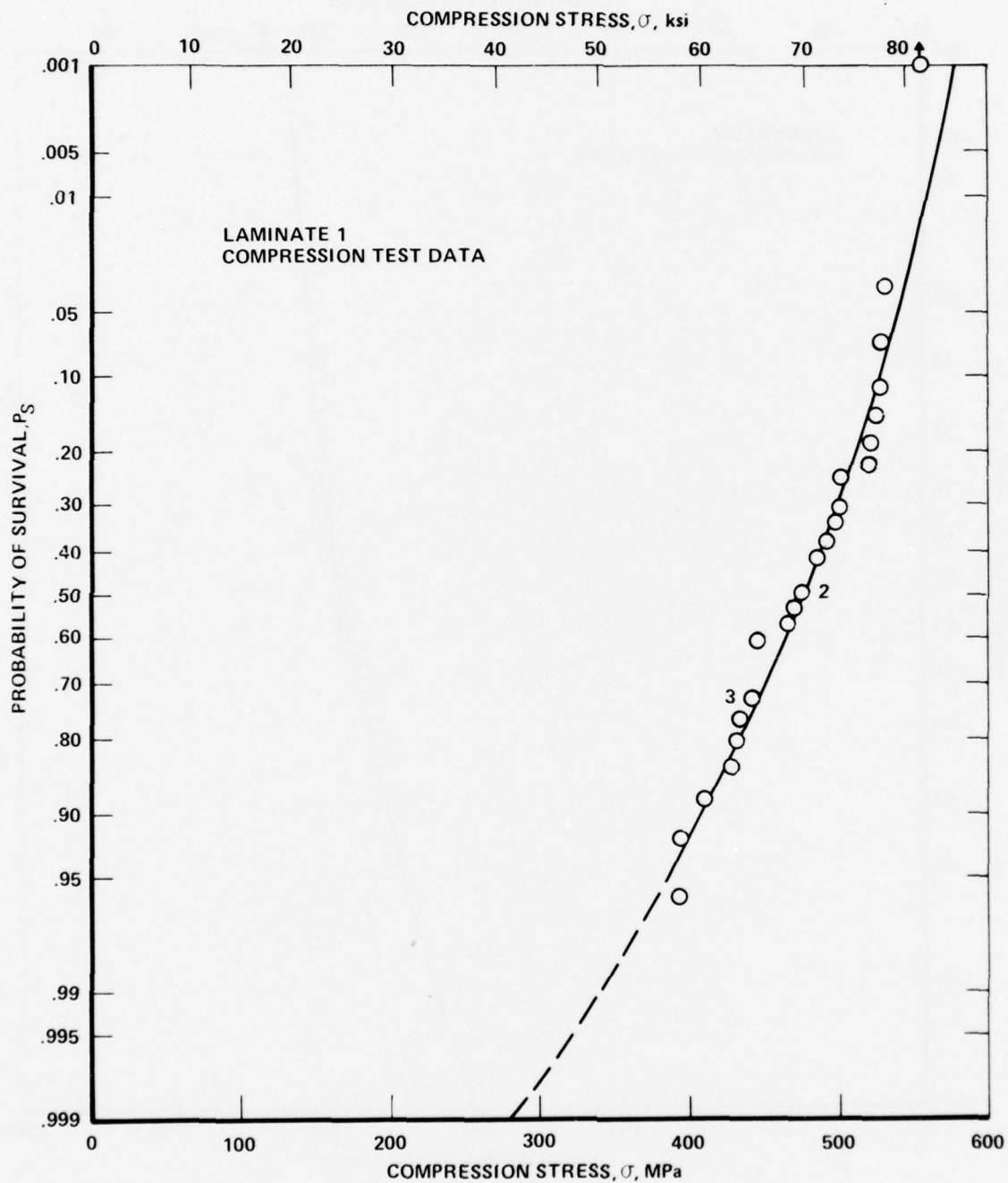
Figure 52.  Relationship Between Probability of Survival and
Ultimate Compression Strength for Laminate 1 Coupons

103
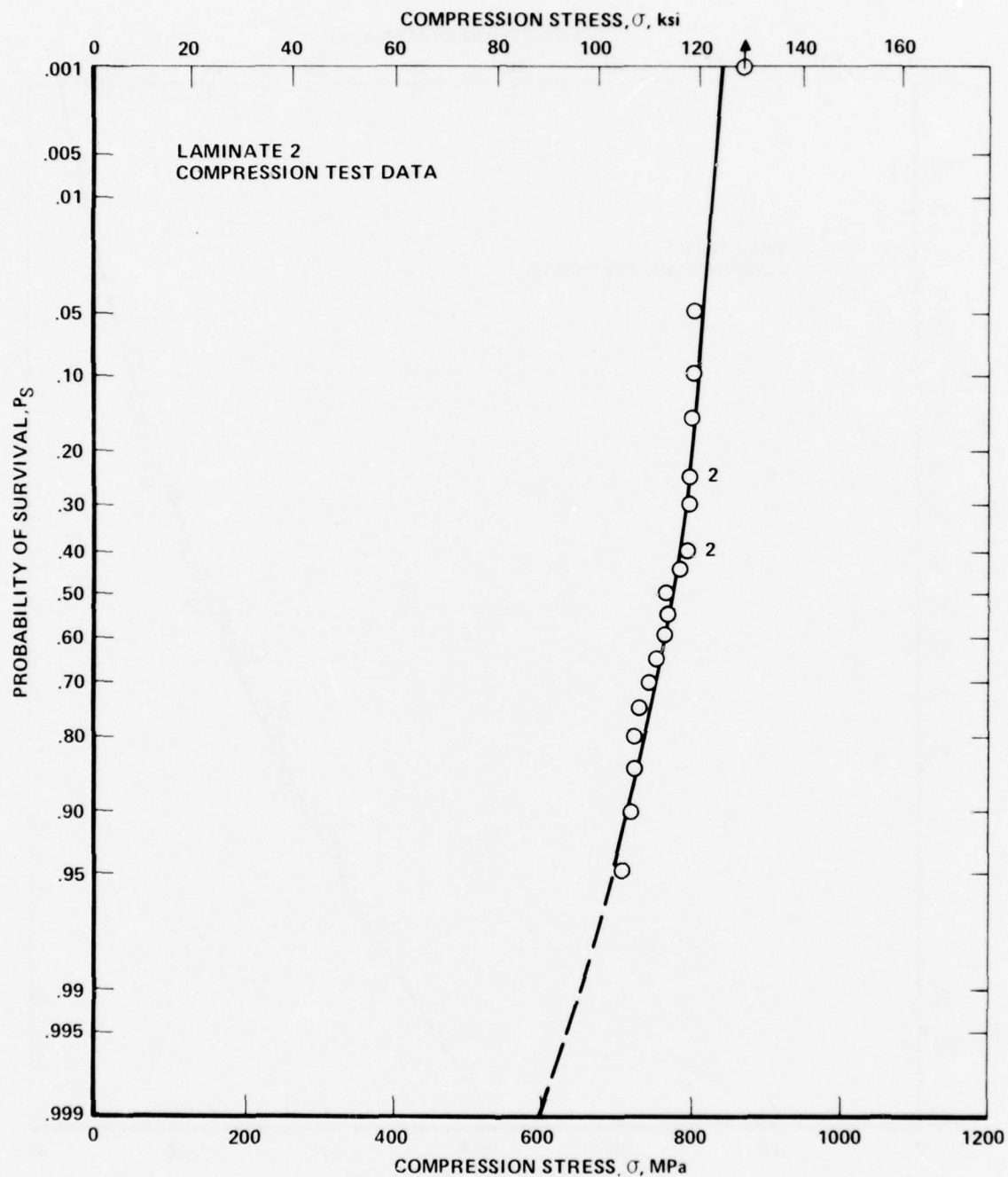
Figure 53.  Relationship Between Probability of Survival and
Ultimate Compression Strength for Laminate 2 Coupons

TABLE 20A

EFFECT OF TEST DETAIL

ON

COMPRESSION RESULTS OF LAMINATE 1 COUPONS

| Sample ID | Min. Area, in.² | Ultimate Load, $P_{ult}$, lbs | Ultimate Stress, $\sigma_{ult}$, ksi | Ultimate Strain, $\epsilon_{ult}$, in./in. in 2.0 in. | Load at Initial Curve Deviation, $P_{CD}$, lbs | Stress at Initial Curve Deviation, $\sigma_{CD}$, ksi | Strain at Initial Curve Deviation, $\epsilon_{CD}$, in./in. in 2.0 in. | Apparent Modulus of Elasticity, $E_{1C}$, psi $\times 10^6$ | Amount of Strain at Ultimate Load, $\epsilon$, in./in. in 2.0 in. |
|---|---|---|---|---|---|---|---|---|---|
| 582-12A[a] | .0819 | 6330 | 77.3 | Curve Not Recorded | | | | 7.51 | 0[d] |
| 594-12A[a] | .0826 | 5290 | 64.0 | .0093 | 3100 | 37.5 | .0050 | 7.00 | .0009 |
| 582-20A[b] | .0822 | 6230 | 75.8 | .0111 | 3800 | 46.2 | .0066 | 6.56 | - |
| 603-15B[b] | .0824 | 5800 | 70.4 | - | 3400 | 41.3 | .0063 | 7.31 | .0012 |
| 580-6A[c] | .0823 | 6680 | 81.2 | .0132 | 3550 | 43.1 | .0059 | 7.00 | .0015 |
| 583-26B[c] | .0816 | 5940 | 72.8 | .0120 | 3200 | 39.2 | .0056 | 7.00 | .0015 |
| Average | | | 73.6 +7.6 -9.6 | .0114 +.0018 -.0021 | | 41.5 +4.7 -4.0 | .0059 +.0007 -.0003 | 7.08 +0.43 -0.52 | |
| Previous Average | | | 69.7 +11.8 -12.1 | .0110 +.0022 -.0025 | | 34.9 +5.5 -8.5 | .0050 +.0007 -.0008 | 6.95 +0.42 -0.83 | |

a - Tests run with graphite tabs glued on coupon edges, extensometer on coupon edges.

b - Tests run with extensometer on coupon faces.

c - Tests run with extensometer on coupon faces with tabs glued on coupon.

d - A 0 denotes that the coupon failed without a flat topped region prior to failure, see Figure 43.

TABLE 20B

EFFECT OF TEST DETAIL

ON COMPRESSION RESULTS OF LAMINATE 1 COUPONS

| Sample ID | Min. Area, mm² | Ultimate Stress, $\sigma_{ult}$, MPa | Ultimate Strain, $\epsilon_{ult}$, mm/mm in 50.8 mm | Stress at Initial Curve Deviation, $\sigma_{CD}$, MPa | Strain at Initial Curve Deviation, $\epsilon_{CD}$, mm/mm in 50.8 mm | Apparent Modulus of Elasticity, $E_{1c}$, GPa | Amount of Strain at Ultimate Load, $\epsilon$, mm/mm in 50.8 mm |
|---|---|---|---|---|---|---|---|
| 582-12A[a] | 52.8 | 533.0 | Curve Not Recorded | | | | 0[d] |
| 594-12A[a] | 53.3 | 441.3 | .0093 | 258.6 | .0050 | 51.8 | .0009 |
| 582-20A[b] | 53.0 | 522.6 | .0111 | 318.5 | .0066 | 48.3 | - |
| 603-15B[b] | 53.2 | 485.4 | - | 284.8 | .0063 | 45.2 | .0012 |
| 580- 6A[c] | 53.1 | 559.9 | .0132 | 297.2 | .0059 | 50.4 | .0015 |
| 583-26B[c] | 52.6 | 501.9 | .0120 | 270.3 | .0056 | 48.3 | |
| Average | | 507.4 +52.5 -66.1 | .0114 +.0018 -.0021 | 286.1 +32.4 -27.7 | .0059 +.0007 -.0003 | 48.5 +3.0 -3.6 | |
| Previous Average | | 480.6 +81.3 -83.5 | .0110 +.0022 -.0025 | 290.6 +37.9 -43.4 | .0050 +.0007 -.0008 | 47.9 +2.9 -5.7 | |

a - Tests run with graphite tabs glued on coupon edges, extensometer on coupon edges.

b - Tests run with extensometer on coupon faces.

c - Tests run with extensometer on coupon faces with tabs glued on coupon.

d - A 0 denotes that the coupon failed without a flat topped region prior to failure, see Figure 43.

Table 21 lists four coupons, two of each laminate, which were tested using strain gages to record strain. All gages were placed on each specimen at the same location; under the top fixture holes, see Figure 13. One coupon of each laminate had strain gages on both sides of the coupon at the same location to allow specimen misalignment to be studied. Two of the coupons also had an extensometer attached to the coupon sides as indicated in Table 21. All gages were "T" type and thus both longitudinal and transverse strains were recorded. Experimentation conducted for a Lockheed-California Company funded test program indicated that strain gages must be attached to areas where the outer layer of epoxy has been carefully removed if reliable readings are to be obtained. All gages used in this limited study were attached using this procedure.

Table 21 shows that, for either laminate, this testing procedure provided near perfect alignment, as indicated by the ultimate longitudinal strain readings of the two coupons with two "T" type gages. The two longitudinal and transverse strain gages of these coupons had nearly identical values throughout the tests. In addition, Table 21 shows that extensometer strain and longitudinal strain gage readings agreed within 1-1/2 percent, which gave confidence in the extensometer strain results of Tables 15 and 16. The possible effect of the extensometer on the ultimate failure strength is also indicated in Table 21 and shows that, for both laminates, the coupon with attached extensometer and strain gage had a lower compression ultimate strength than the coupon with strain gages only. This result was suggestive only, with no statistical significance, and needs to be further investigated. However, the test result cautions against comparison between test results unless all testing procedures are identical.

Table 22 shows the results of the experimental determination of Poisson's ratio based on a limited number of strain gaged tension and compression coupons. For each laminate, Poisson's ratio was determined to be the same in tension and compression. The average Poisson's ratio for laminate 2 was approximately 0.63 as opposed to that for laminate 1 which was approximately

TABLE 21

COMPRESSION TEST RESULTS

USING STRAIN GAGES

| Sample ID | Area, mm² (in.²) | Ultimate Load, $P_{ult}$, kN(lbs) | Ultimate Stress, $\sigma_{ult}$, MPa(ksi) | Longitudinal Ultimate Strain, $\varepsilon_L$, mm/mm | Extensometer Ultimate Longitudinal Strain, $\varepsilon$, mm/mm in 50.8 mm | Transverse Ultimate Strain $\varepsilon_T$, mm/mm | Average Apparent Longitudinal Modulus of Elasticity, $E_A$, GPa (psi x 10⁶) | Remarks |
|---|---|---|---|---|---|---|---|---|
| 596-19B[a] | 53.5 (.0830) | 24.1(5420) | 450 (65.3) | .0098 | .0099 | .0024 | - | - |
| 603- 7B[a] | 54.0 (.0837) | 32.0(7200) | 593 (86.0) | .0129[c] .0133 | - | .0036[b] .0035 | - | 2 "T" Gages |
| 696-17c[b] | 83.5 (.1295) | 65.3(14700) | 783 (113.5) | .0090 | .0089 | .0055 | 85.5(12.4) | - |
| 727- 6c[b] | 80.9 (.1254) | 72.1(16200) | 891 (129.2) | .0106[c] .0106 | - | .0065[b] .0068 | 85.5(12.4) | 2 "T" Gages |

a - The ultimate stress for these coupons (Laminate 1) was based on average area.

b - Laminate 2

c - Gages on both sides read similar values indicating good alignment

108

TABLE 22

TEST RESULTS FOR

DETERMINATION OF POISSON'S RATIO

| Laminate | Tension or Compression (T,C) | Poisson's Ratio | Number of Coupons |
|---|---|---|---|
| 1 | T | 0.29 | 4 |
| | C | 0.26 | 2 |
| | | Average 0.28 | |
| 2 | T | 0.64 | 4 |
| | C | 0.62 | 2 |
| | | Average 0.63 | |

0.28. Therefore, if the end effect influenced failure location, the effect would be expected to be more important for the laminate with the higher Poisson's ratio. This assumption was supported by the large variation in failure location for laminate 1; hence, there was no apparent end effect due to Poisson induced restraint. However, for laminate 2 the end effect was apparently large enough that, if the end was not sufficiently stabilized, failure occurred at the end. If sufficient end stabilization existed, the failure zone shifted towards the center of the gage length, for reasons explained in Section 2.5.2, and observed for exactly half of the laminate 2 failed coupons. Therefore, these test results appear to support the assumption that compression tests conducted with a stabilizing end guide cannot solve an inherent end effect for high Poisson ratio laminates, but would merely shift the failure location. This shift in failure location towards the center of the gage length does not necessarily imply an increase in test validity.

# SECTION V

## FATIGUE RESULTS

The fatigue study was divided into two major sub-tasks. In the first task, the general stress-life characteristics of the two laminates were developed under both tension-tension and tension-compression loading. This S-N scan was conducted by testing three coupons at each of several maximum stress levels. Subsequent to determining the general characteristics of the S-N behavior, the extent of fatigue scatter was determined by conducting 20 or more tests of several specifically chosen maximum stress levels.

A major consideration prior to the fatigue test program was which of the loading variables pertinent to fatigue should be held constant. The variables considered were: load ratio, R; maximum stress, $\sigma_{max}$; stress range $\Delta\sigma$; and minimum stress, $\sigma_{min}$. Any one of these variables could have been held constant and two others allowed to vary while the effect of the fourth was evaluated.

Coupled with the considerations of loading variables was the practical problem that these laminates acted like thin columns, thus limiting the maximum compression that could be reached without buckling. A laminate 1 coupon was loaded in a fatigue test machine in compression using one central buckling restraint and a second coupon loaded using two constraints spaced 50.8 mm (2 in.) apart. A laminate 2 coupon was also loaded in compression using two restraints. For these tests buckling was defined as 0.0254 mm (0.001 in.) deflection out-of-plane anywhere within the gage length. For laminate 1 with one restraint, this criterion limited the maximum compression stress in fatigue to - 68.9 MPa (-10 ksi) and for two restraints to - 110 MPa (-16 ksi). Laminate 2 with two restraints was limited to - 207 MPa (-30 ksi). Based on the practical test restraint of buckling, fatigue tests conducted at constant R values were considered impractical because stress ranges would be severely restricted. All fatigue tests were thus conducted at a constant minimum stress (0, -68.9, -110 MPa (0, -10, -16 ksi) for laminate 1 and 0 and -207 MPa

(O and -30 ksi) for laminate 2) and the maximum stress was allowed to vary. This procedure permitted direct comparison of results based on $\sigma_{max}$ or $\Delta\sigma$ as well as a limited study of the effect of R.

For tension-tension tests, failure was defined as breakage of the coupon; for tension-compression tests, failure was defined as coupon breakage or inability to sustain compression load due to severe delamination. Investigation showed that if the latter failure definition was used, breakage of the specimen could be forced by the addition of a few more cycles. Only four tension-compression specimens of laminate 1 and none of laminate 2 failed due to inability to sustain compression load.

A primary observation was that significant visible delamination often did not occur in tension-tension testing prior to failure, but when such delamination did occur, the remaining cycles to failure could be either small or large. However, for tension-compression testing when delamination was noted prior to failure, normally 90% or more of the coupon life was exceeded. Therefore, in the future delamination may possibly be a more useful definition of failure in tension-compression fatigue while coupon breakage may be more useful for tension-tension fatigue.

Another problem of major concern was the possibility of an increase in coupon temperature during fatigue cycling. Both laminates were studied by measuring coupon temperature at the tab midpoint; on the coupon surface near each tab; and on the coupon surface at the center of the gage length. For laminate 1, the temperature of tension-tension fatigue coupons remained constant at the laboratory air temperature until a cycle count was reached approximately equal to when delamination was noted. At this point, temperature quickly increased approximately 4° to 8°C (8° to 15°F) and remained constant to failure. The tension-compression coupons of laminate 1 exhibited a temperature rise of 4° to 8°C (8° to 15°F) immediately after test commencement, but afterwards the temperature remained constant until failure. In contrast, laminate 2 coupons tested under both conditions exhibited a

small temperature rise ($3°$ to $8°C$ ($5°$ to $15°F$)) within the gage length, but a large rise (up to $39°C$ ($70°F$)) within the tabs. The rise of tab temperature was due to the large strains induced in the adhesive and resulted in creep of the tab relative to the coupon and tab pull-off. Therefore, grip ends of laminate 2 coupons were cooled with forced room temperature, shop air to keep the grip temperature near room air temperature.

Fatigue failure modes of the two laminates appeared to differ from each other as well as from static tension and compression failure modes. Laminate 1 coupons tested in tension-tension fatigue failed due to extensive delamination which started between the two $-45°$ layers at the free edge and progressed inwards. Figure 54 shows typical failures. Laminate 1 coupons tested in tension-compression fatigue failed similarly to those tested in tension-tension, but large out-of-plane buckling of the outer four plies also occurred reducing fatigue life after the onset of delamination. Typical failures are shown in Figure 55. Laminate 2 coupons sustained no early delamination during fatigue under either tension-tension or tension-compression loading. Fatigue damage in laminate 2 coupons was characterized by outer $0°$ fiber shredding eventually followed by sudden failure which sometimes resulted in massive delamination, see Figure 56, but not always, see Figure 57. Some laminate 2 fatigue failures were dominated by the $45°$ plies, see Figure 58. Tension-compression fatigue failures of laminate 2 coupons also exhibited plies with sharp breaks due to the accompanying buckling, see Figure 59. All laminate 1 and 2 coupons tested in tension-compression fatigue failed during the compression load excursions. Laminate 1 coupons and most laminate 2 coupons displayed fatigue failure modes which appeared quite different from static tension or compression failure modes.

## 5.1 Stress-Life Scan Results

The results of the stress-life study used to determine the general form of the fatigue behavior of the two laminates are shown in Figures 60 - 62 for laminate 1 and in Figure 63 for laminate 2. The data shown for the tension-

113
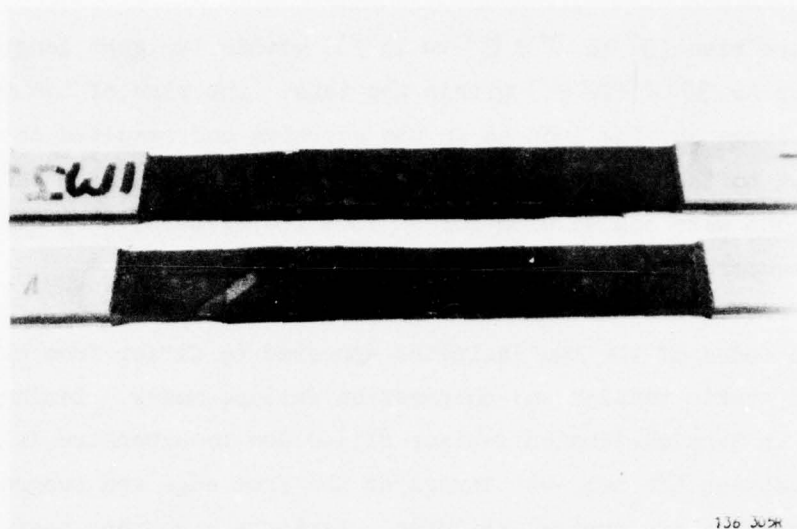
a. Coupons 1MJ 599-21A, 1MJ 601-19A;  Side View
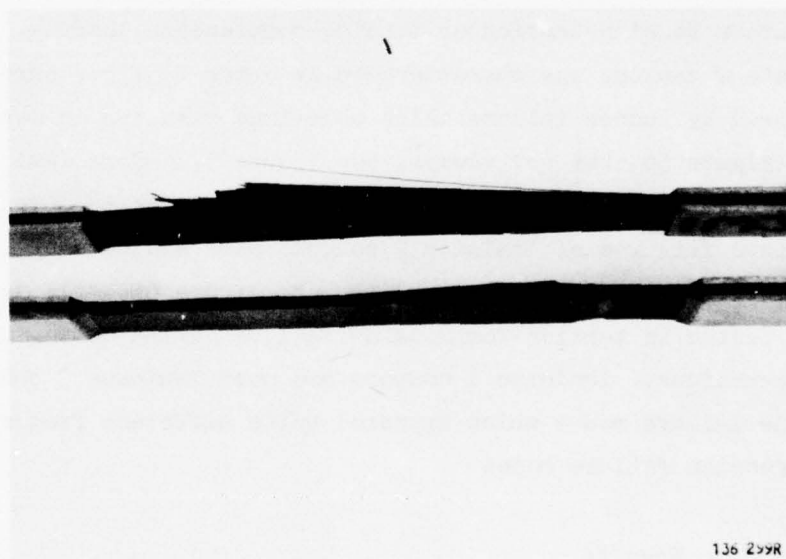


b. Coupons 1MJ 599-21A, 1MJ 601-19A;  Edge View

Figure 54.    Typical Tension-Tension Laminate 1 Fatigue Failures

114
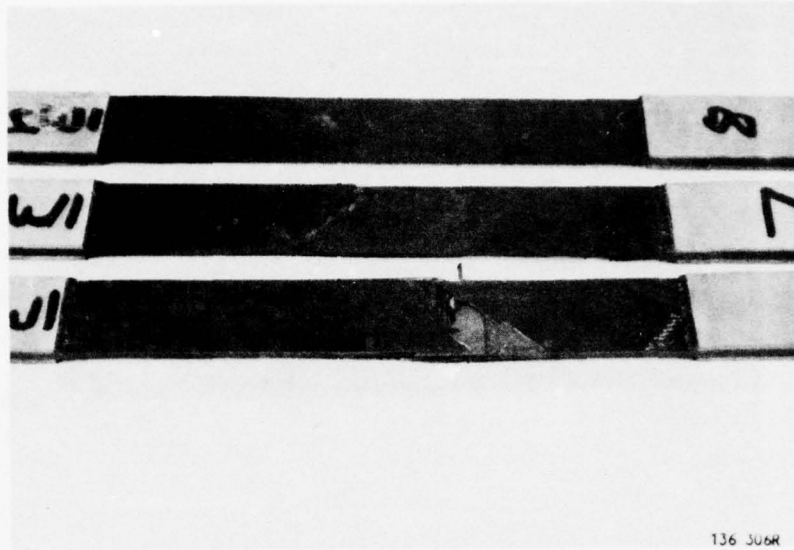
a.  Coupons 1MJ 578-8A, 1MJ 604-7A, 1MJ 580-24B;  Side View
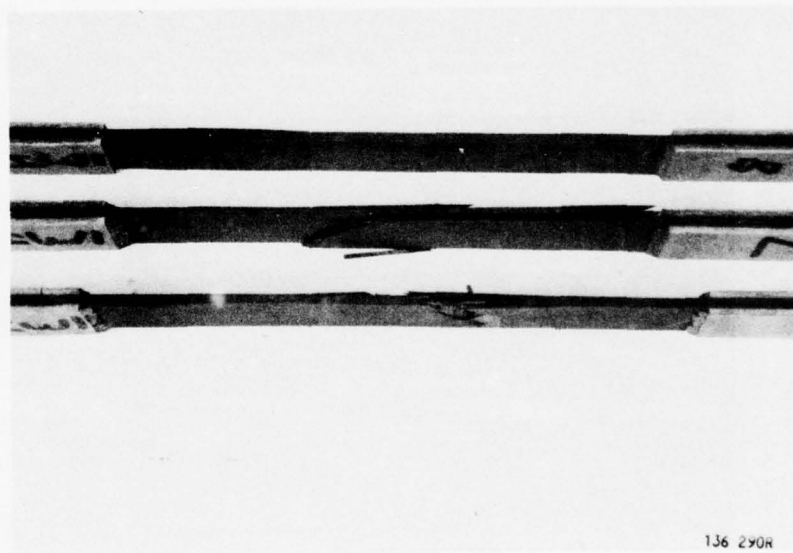


b.  Coupons 1MJ 578-8A, 1MJ 604-7A, 1MJ 580-24B;  Edge View

Figure 55.  Typical Tension-Compression Laminate 1 Fatigue Failures
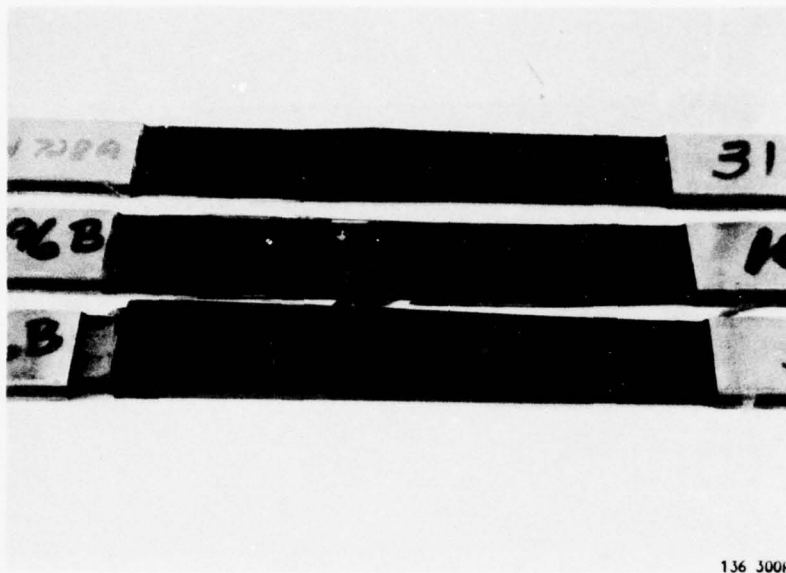
115

136 300R

a. Coupons 1NH 728-31A, 1NH 696-10B, 1NH 696-5B;  Side View



136 291R
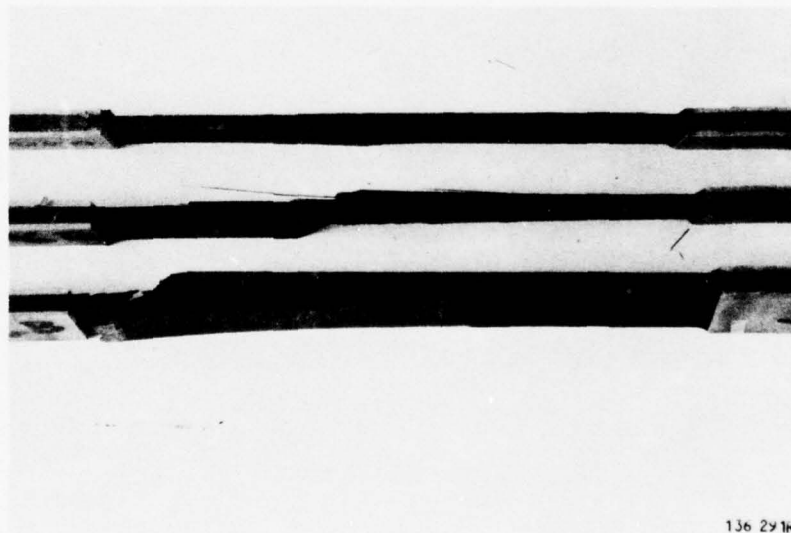
b. Coupons 1NH 728-31A, 1NH 696-10B, 1NH 696-5B;  Edge View

Figure 56.   Typical Delaminated Laminate 2 Coupons Which Failed
Under Tension-Tension Fatigue Loading.

116

136 301R
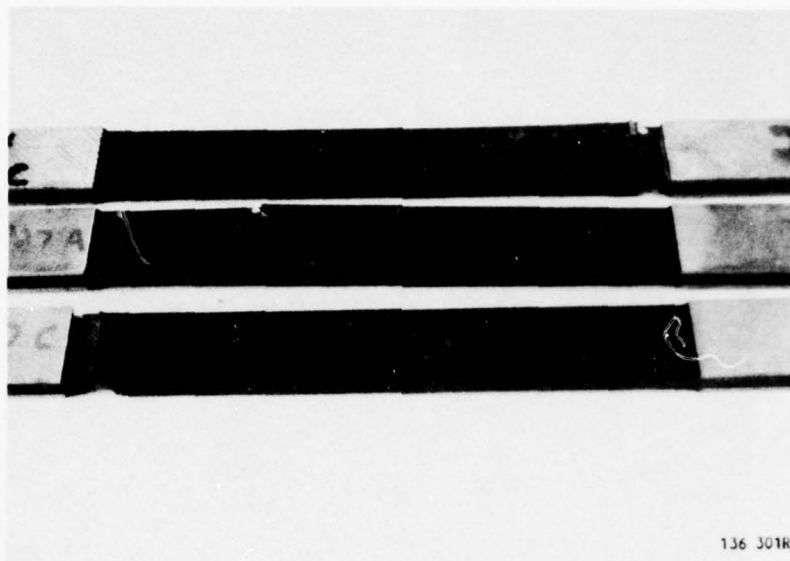
a. Coupons 1NH 728-27C, 1NH 727-15A, 1NH 727-36C; Side View



136 295R
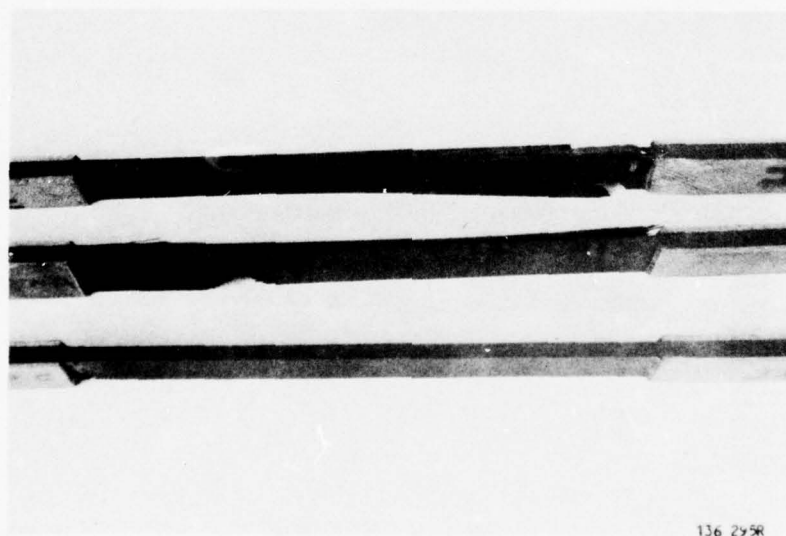
b. Coupons 1NH 728-27C, 1NH 727-15A, 1NH 727-36C; Edge View

Figure 57. Typical Laminate 2 Coupons Which Failed Under
Tension-Tension Fatigue Loading Without Signi-
ficant Delamination.

117

136 303R
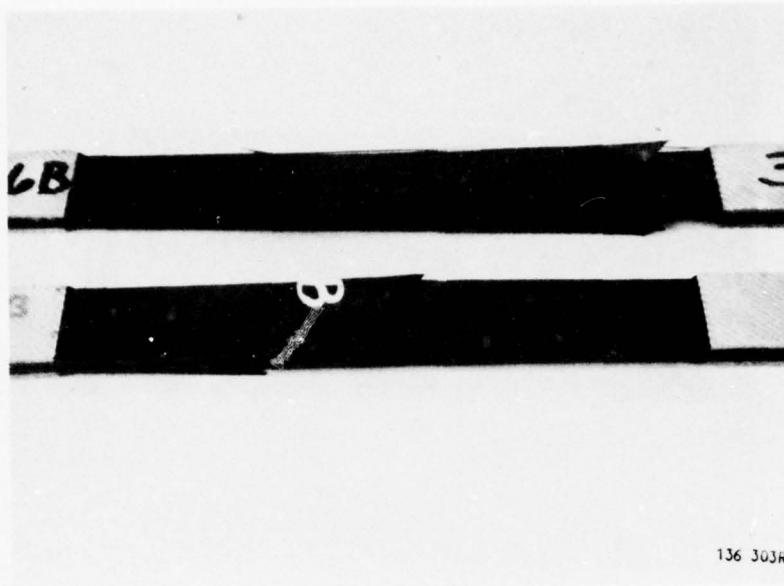
a.  Coupons 1NH 696-31B, 1NH 727-35B;  Side View



136 297R
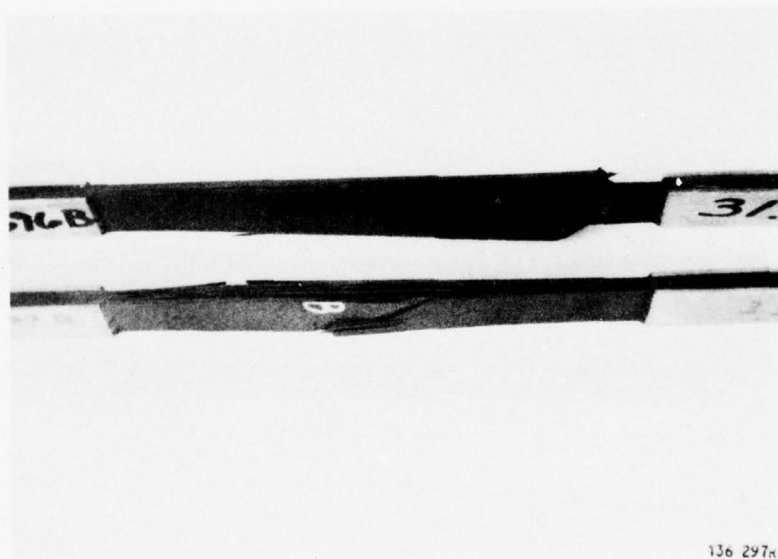
b.  Coupons 1NH 696-31B, 1NH 727-35B;  Edge View

Figure 58.   Laminate 2 Tension-Tension Fatigue Failures
Dominated by 45° Plies

118

136 302R
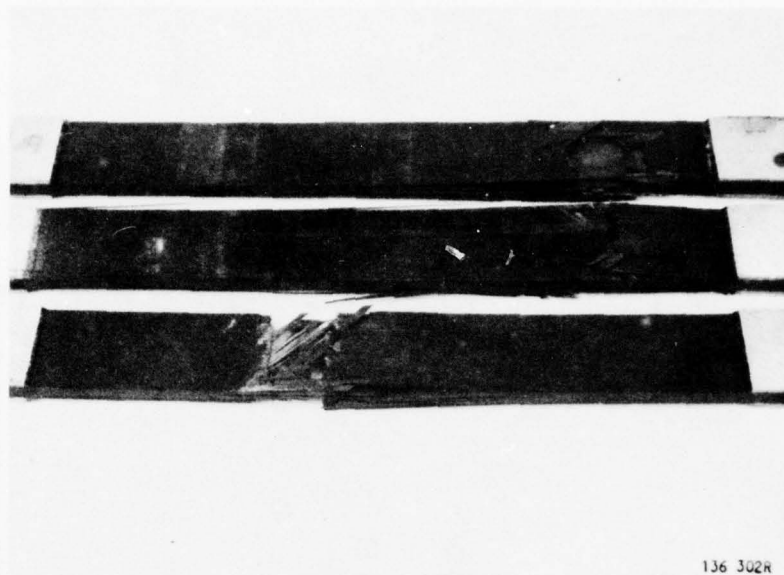
a. Coupons 1NH 728-24A, 1NH 727-16C, 1NH 728-20A; Side View



136 278R
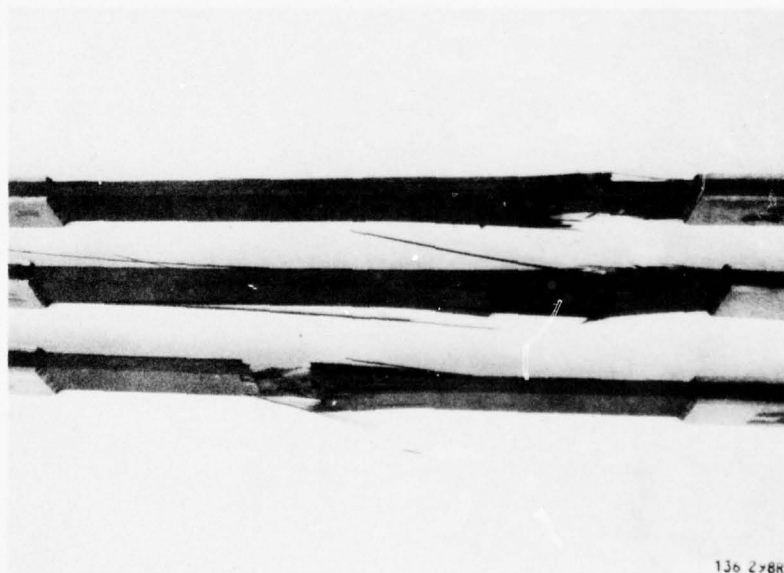
b. Coupons 1NH 728-24A, 1NH 727-16C, 1NH 728-20A; Edge View

Figure 59. Laminate 2 Tension-Compression Fatigue Failures

119
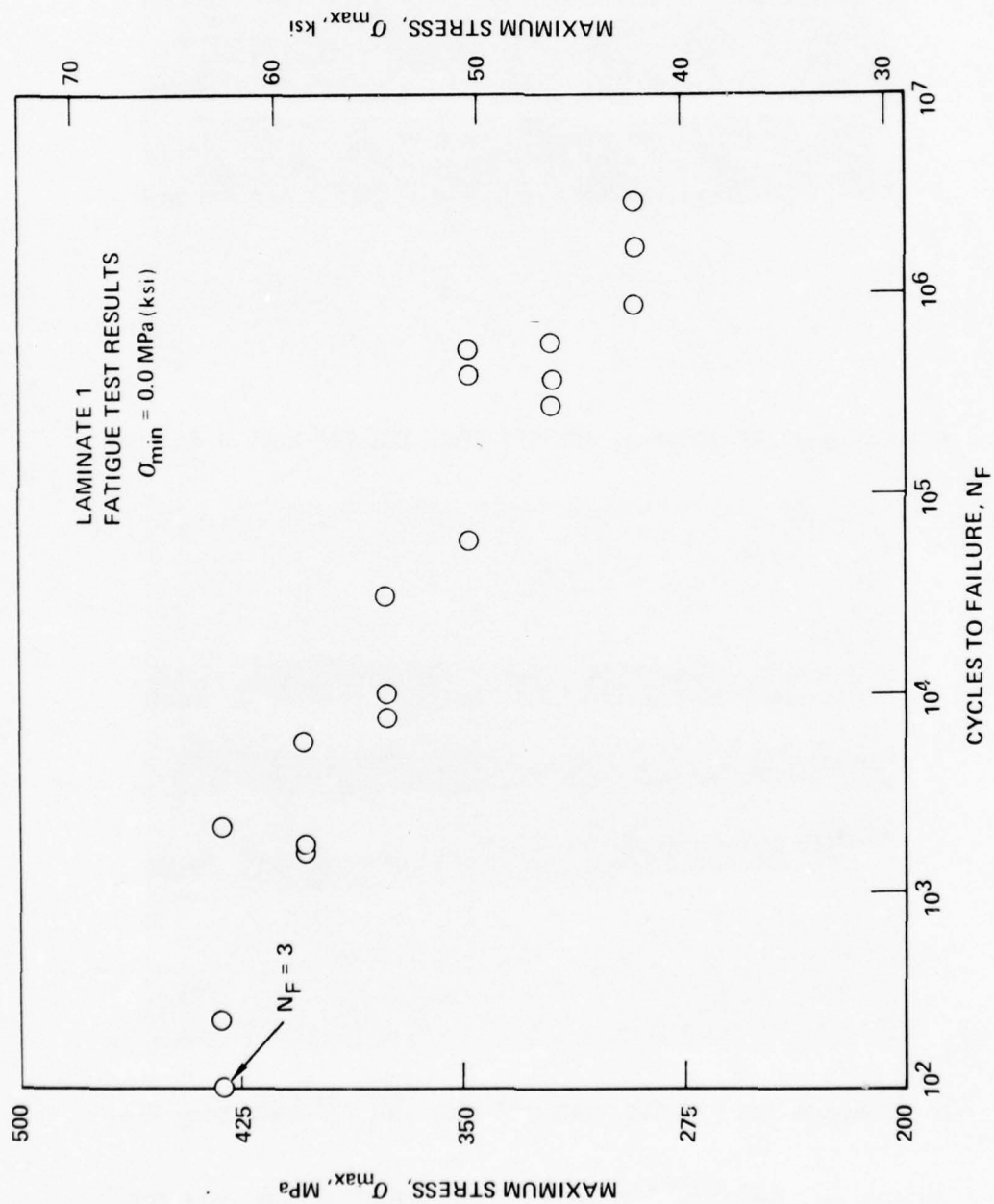
Figure 60. Laminate 1 Tension-Tension Fatigue Stress-life Scan Results at $\sigma_{min}$ = 0.0 MPa (ksi)
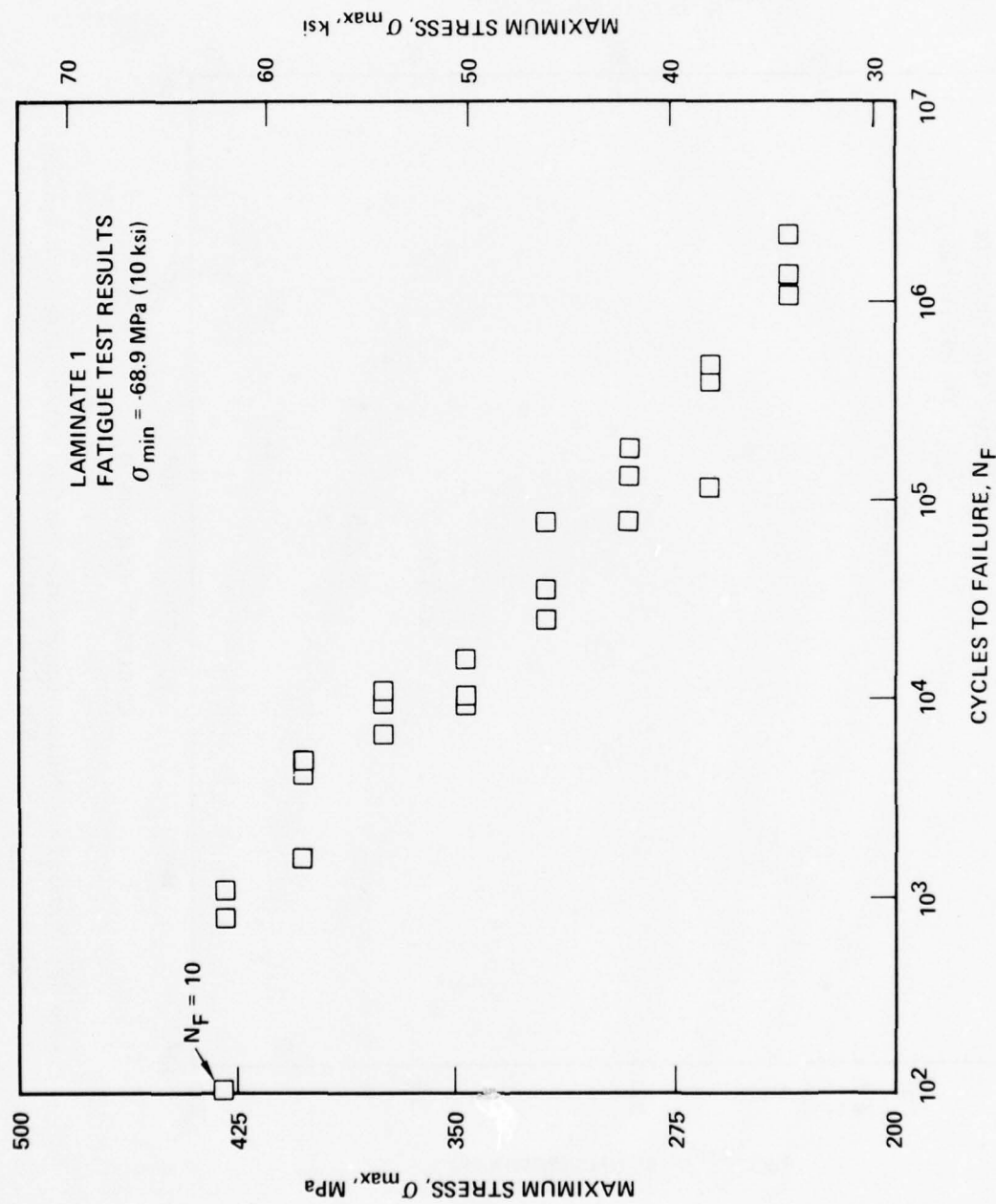
Figure 61. Laminate 1 Tension-Compression Fatigue Stress-Life Scan Results
at $\sigma_{min}$ = -69 MPa (10.0 ksi)

121
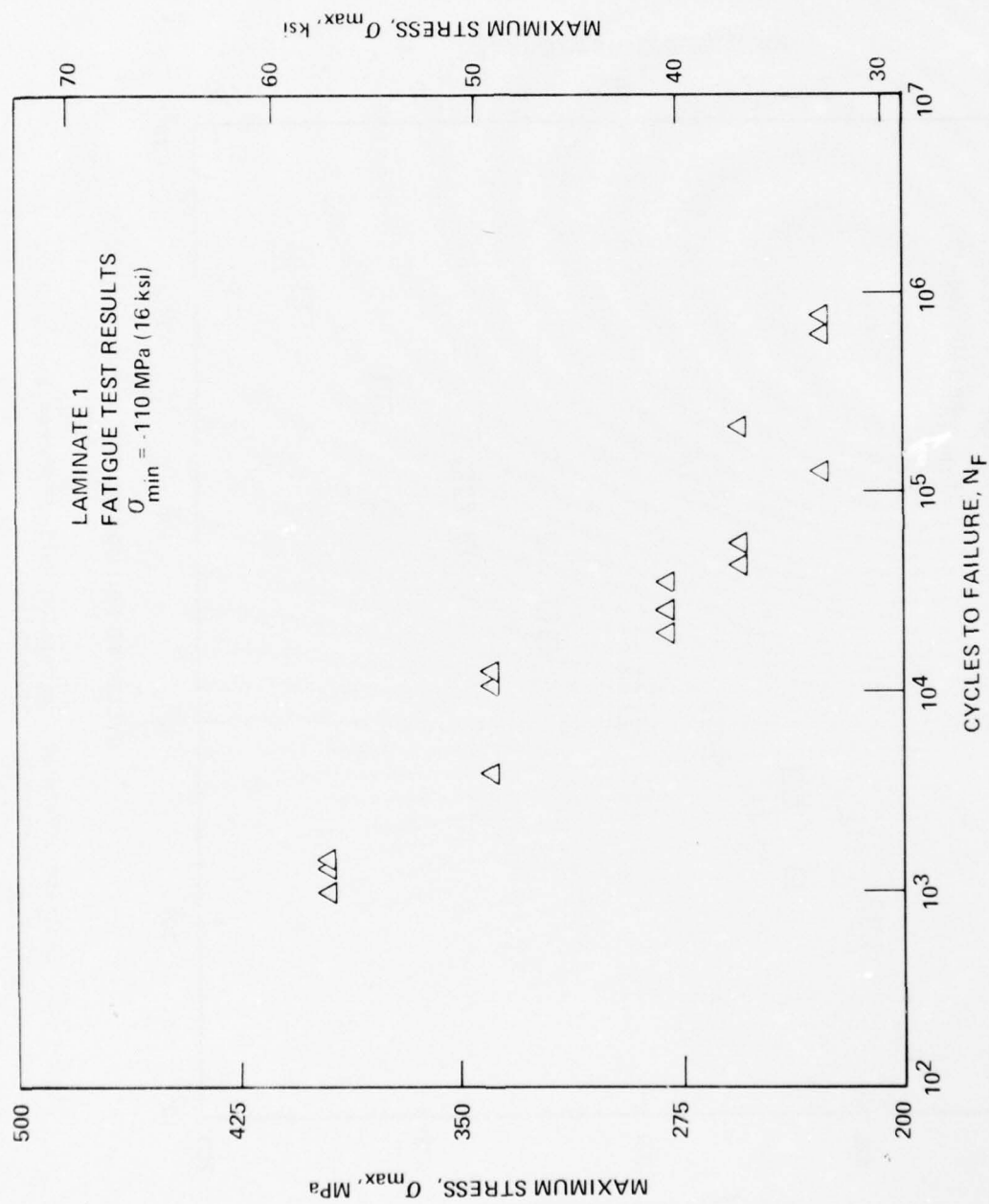
Figure 62. Laminate 1 Tension-Compression Fatigue Stress-Life Scan Results at $\sigma_{min}$ = -110 MPa (16.0 ksi)
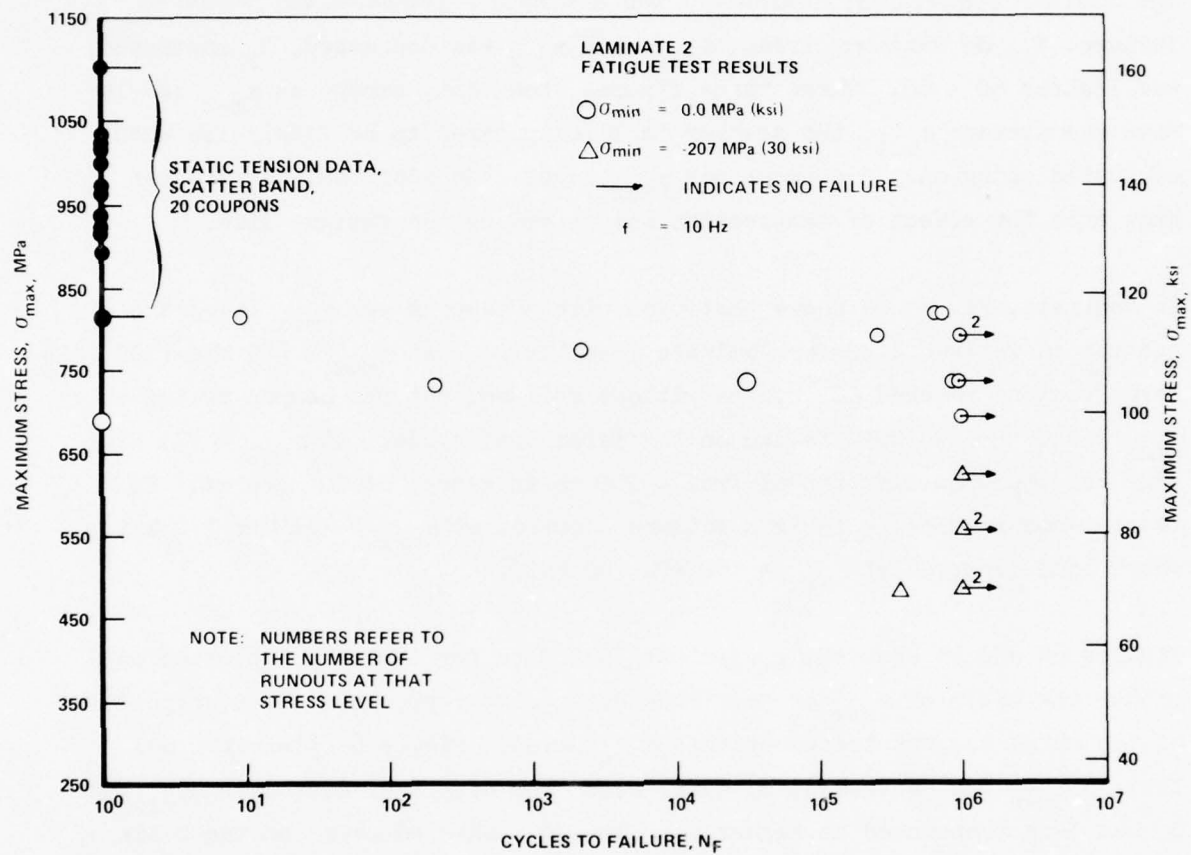
Figure 63. Laminate 2 Fatigue Stress-Life Scan Results

123

compression results for laminate 2 were limited because all but one coupon tested above 620 MPa (90 ksi) maximum stress failed due to tab adhesive failure. The data used in Figures 60-63 are given in Appendix B.

The fatigue behavior of laminate 1 was a simple dependence of cycles to failure, $N_F$, on maximum stress, $\sigma_{max}$. As $\sigma_{max}$ was decreased, $N_F$ increased, see Figures 60 - 62. These three figures show that, except at $\sigma_{max}$ levels near the average $\sigma_{ult}$, the scatter in life appeared to be fairly low when evaluated using only 3 coupons per $\sigma_{max}$ level. In addition, the figures show that the effect of compression was to reduce the fatigue life.

In contrast, Figure 63 shows that even with 3 coupons per $\sigma_{max}$ level the scatter in fatigue life for laminate 2 was large. At $\sigma_{max}$ = 689 MPa (100 ksi), three coupons reached $10^6$ cycles without failure, but the coupon tested at $\sigma_{max}$ = 648 MPa (94 ksi) failed on the first load cycle. At $\sigma_{max}$ = 731 MPa (106 ksi), coupon life ranged from ∼ 200 to in excess of $10^6$ cycles. In tension-compression, a fatigue failure occurred at $\sigma_{max}$ = 483 MPa (70 ksi) where none occurred at $\sigma_{max}$ = 552 MPa (80 ksi).

Figures 64 and 65 show the preliminary S-N data for laminate 1 plotted on either the basis of $\sigma_{max}$ or $\Delta\sigma$. Each data point represents the average life of the three coupons tested at that $\sigma_{max}$ level. Figure 64 clearly shows that as $\sigma_{min}$ was decreased, $N_F$ decreased. The effect of decreasing $\sigma_{min}$ on $N_F$ was less pronounced at higher $\sigma_{max}$ levels. When compared on the basis of $\Delta\sigma$, Figure 65, the effect of $\sigma_{min}$ on $N_F$ decreased at lower $\Delta\sigma$ levels. Therefore, a tentative conclusion was made that for laminate 1, $N_F$ was dominated by the effect of $\sigma_{max}$ at high $\sigma_{max}$ levels (above ∼ 345 MPa (50 ksi)) and by $\Delta\sigma$ at low $\sigma_{max}$ levels.

## 5.2   Extent of Fatigue Scatter

Based on the S-N results, specific $\sigma_{max}$ stress levels were chosen to determine the extent of fatigue life scatter.

124
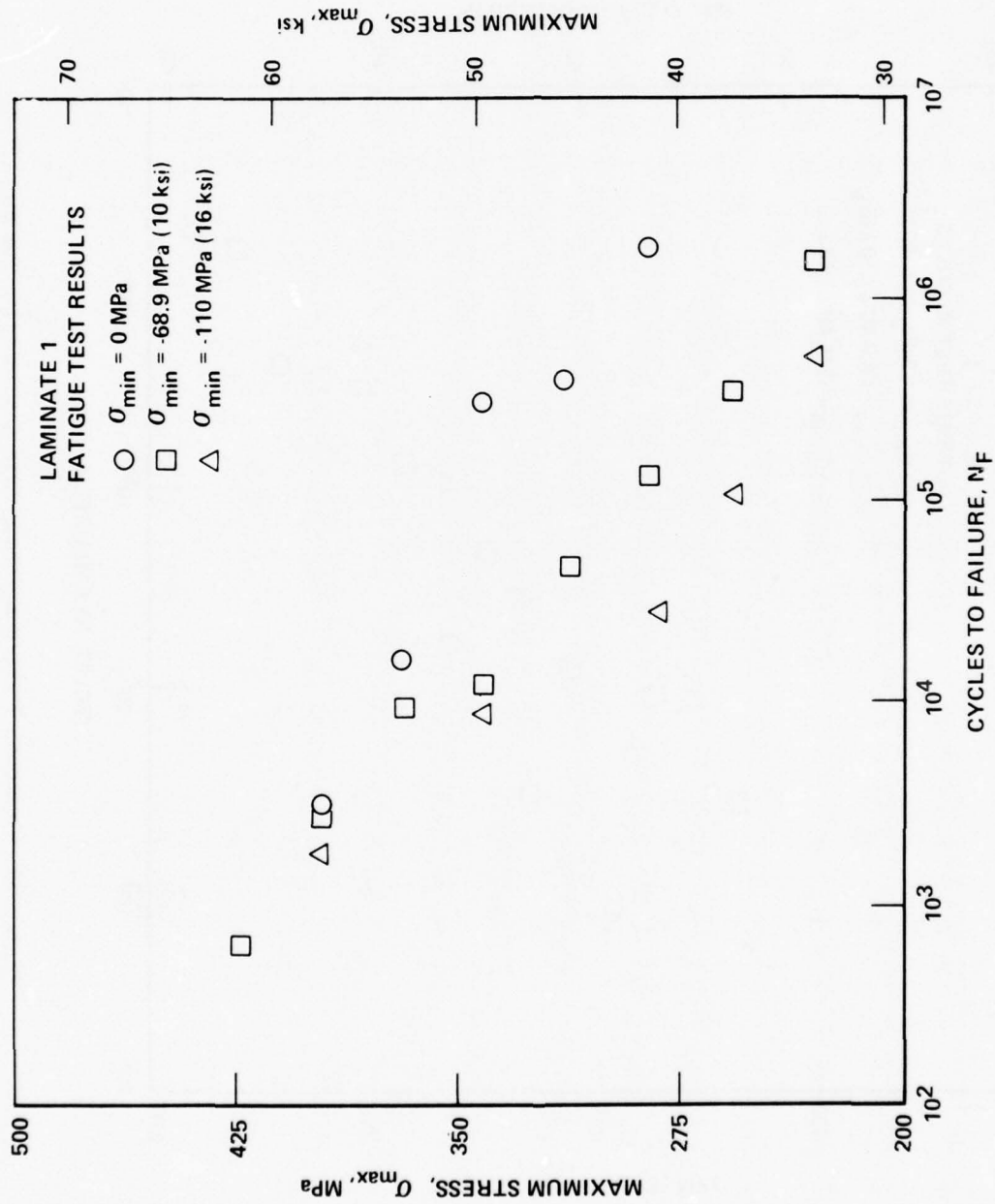
Figure 64. Laminate 1 Fatigue Stress-Life Scan Results for $\sigma_{max}$
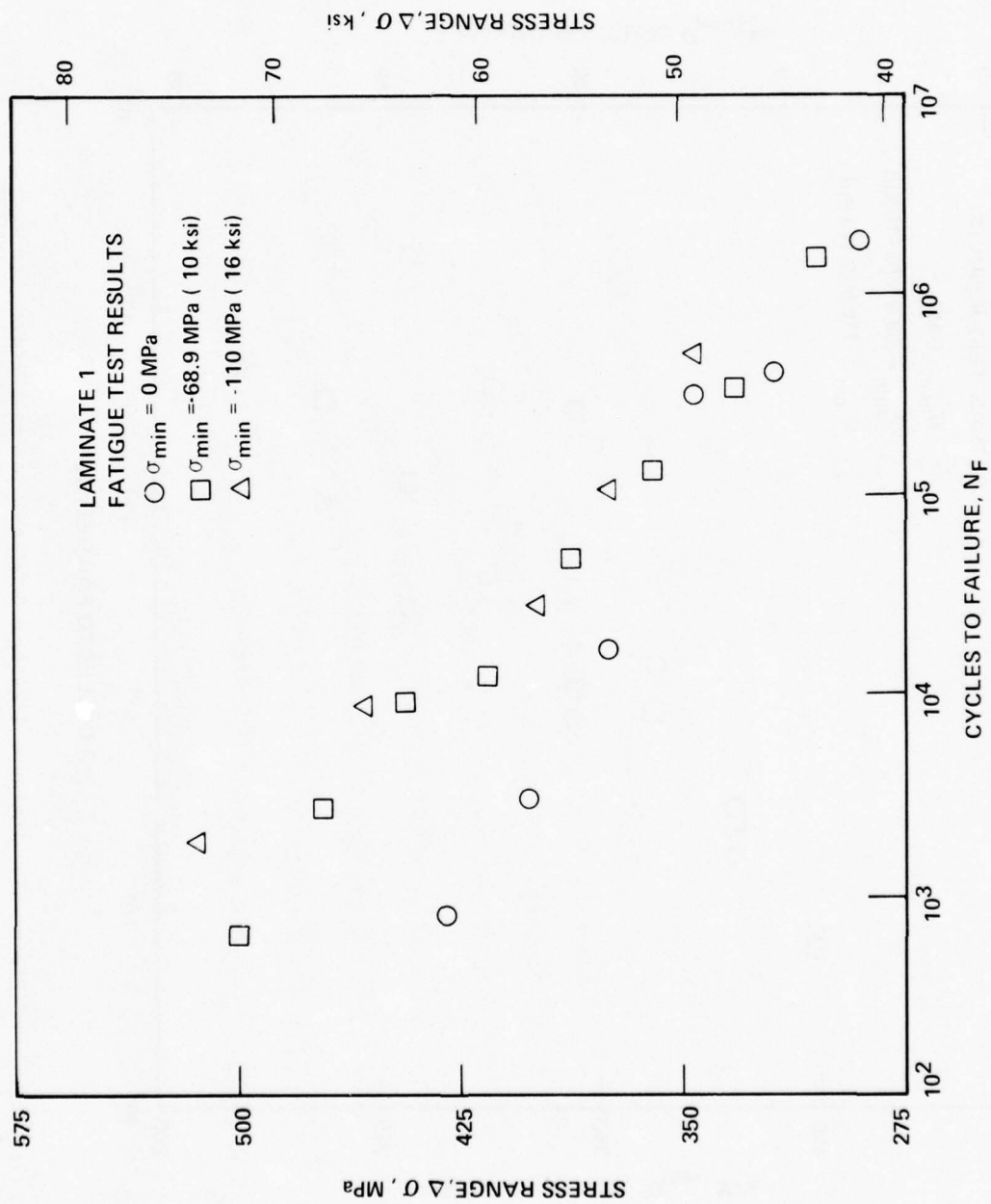
Figure 65.  Laminate 1 Fatigue Stress-Life Scan Results for $\Delta\sigma$

## 5.2.1    Fatigue Behavior - Laminate 1

For laminate 1, three stress levels, 400, 345 and 290 MPa (58, 50 and 42 ksi),
were chosen to define the scatter of the tension-tension and tension-compres-
sion fatigue curves.  The highest stress level was chosen as representative
of the life region where the maximum stress dominated the fatigue curve while
the lowest stress level was chosen as representative of the life region where
stress range was more predominant.  A stress level of 345 MPa (50 ksi) appeared
to be about the life at which maximum stress and stress range were equally
important.  At each of these three stress levels, twenty coupons were fatigue
cycled, including the original three, to failure under tension-tension load-
ing and twenty under tension-compression loading.

For laminate 1, the extent of fatigue scatter can be clearly seen in Figures
66 and 67.  Each data point represents a single test point while the dashed
lines indicate 95% and 5% probability of survival ($P_{.95}$ and $P_{.05}$) limits
based on the 20 point data sets.  The vertical lines in Figures 66 and 67
indicate the limits of the data at each stress level.  Question marks indicate
that the shape of an extrapolated curve was unknown as was the exact position
of the $P_{.95}$ and $P_{.05}$ curves at all stress levels.  The data used in Figures 66
and 67 are given in Appendix B.

In general, the data for a sample size of 20 scattered over approximately two
orders of magnitude in life at any $\sigma_{max}$ level.  The data appeared to indicate
that a type of endurance limit may exist at lower $\sigma_{max}$ levels.  This was
especially indicated for the tension-tension data when none of the coupons
tested at $\sigma_{max}$ = 179 or 231 MPa (26 or 33.5 ksi) failed up to the maximum life
tested.  The possibility of a practical endurance limit was also supported
when the data were replotted on a linear life scale as shown in Figures 68
and 69.  These two figures show that no coupons under either tension-tension
or tension-compression loading survived $10^6$ cycles until $\sigma_{max}$ was reduced to
345 MPa (42 ksi) (tension-tension) or 179 MPa (26 ksi) (tension-compression).
Below $\sigma_{max}$ = 290 MPa (42 ksi), tension-tension fatigue lives appeared to
dramatically increase.  The possibility of a practical endurance limit fatigue
life for this laminate must be investigated in a future study.
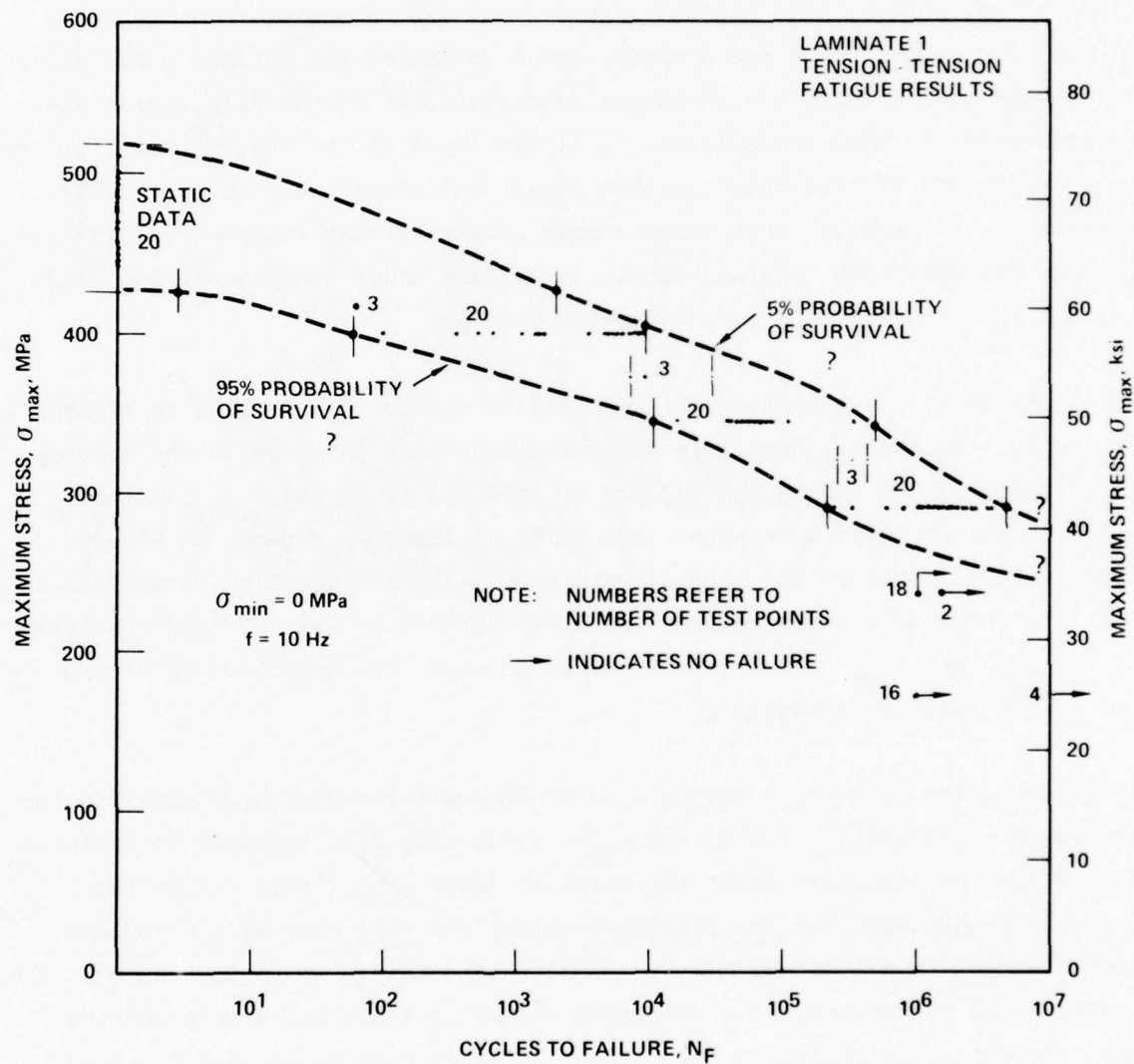
Figure 66.  Laminate 1 Tension-Tension Fatigue Results at
$\sigma_{min}$ = 0.0 MPa (ksi)

128

Figure 67.  Laminate 1 Tension-Compression Fatigue Test Results
at $\sigma_{min}$ = -110 MPa (16.0 ksi)
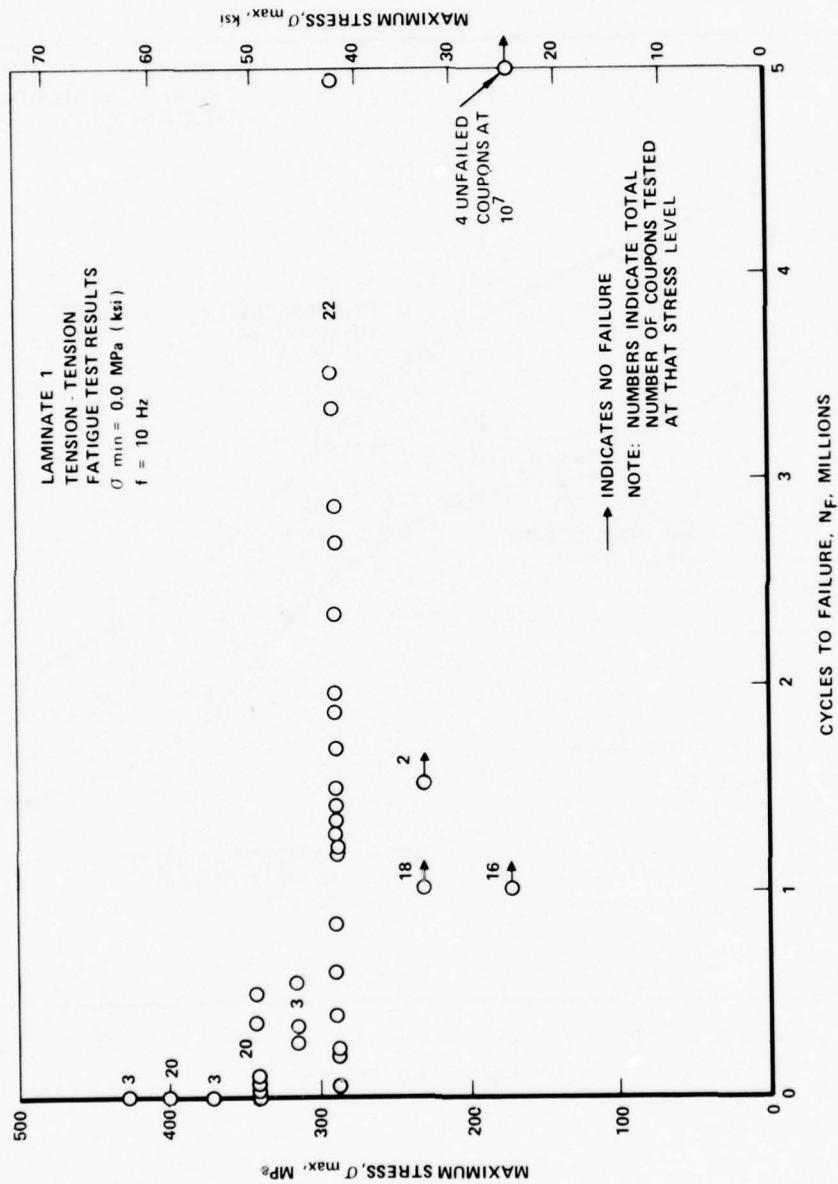
Figure 68. Linear Plot of Laminate 1 Tension-Tension Fatigue Results at $\sigma_{min}$ = 0.0 MPa (ksi)
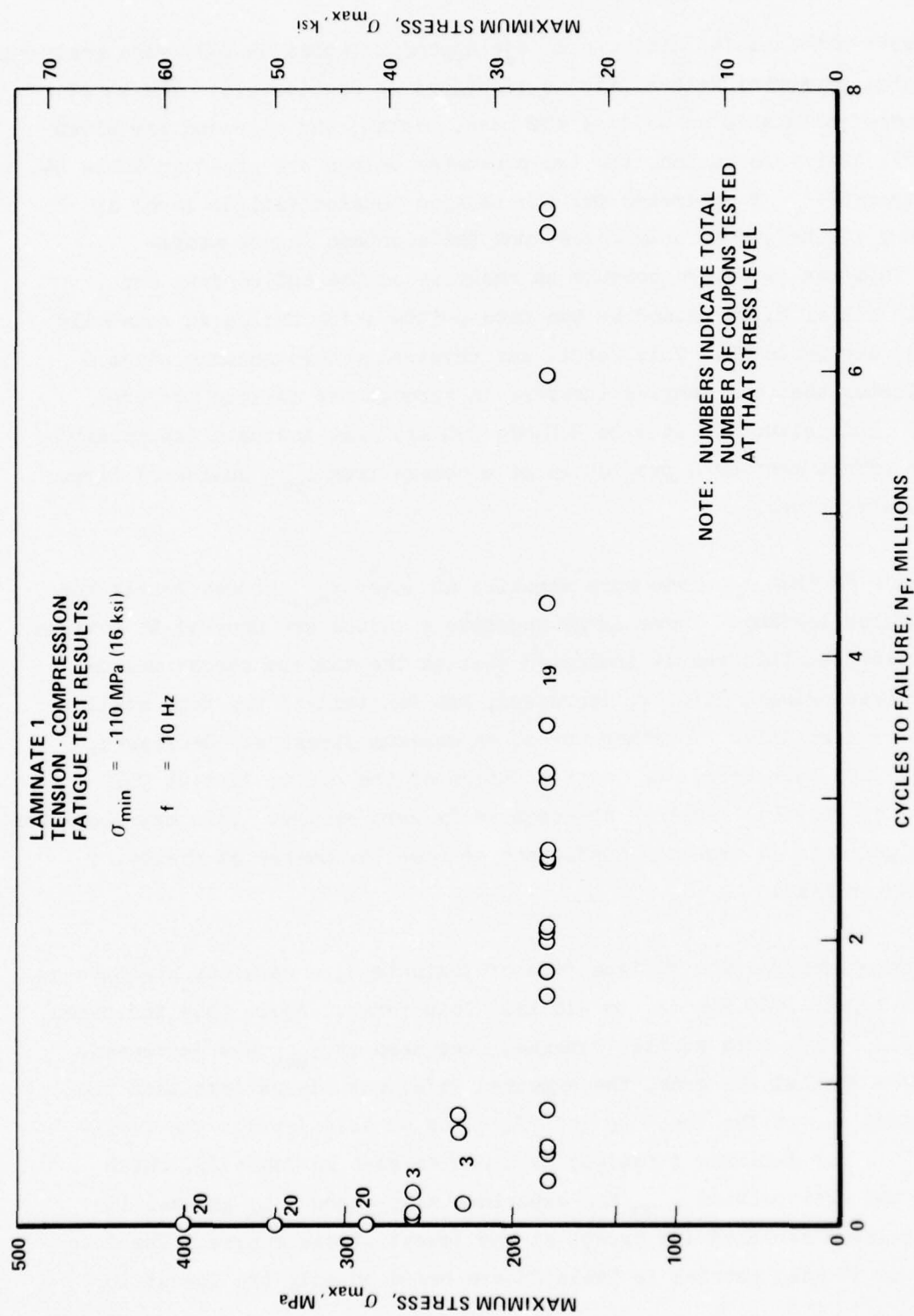
Figure 69. Linear Plot of Laminate 1 Tension-Compression Fatigue Results at $\sigma_{min} = -110$ MPa (16.0 ksi)

The data sets obtained for laminate 1 (see Appendix Tables 5B-13B) were analyzed using a three parameter Weibull fit as disucssed in Section 2.6. The k, e, v values were calculated as well as the mean, median, and mode and are given in Table 23. For information, the two parameter values are given in Table 24. Weibull parameters and estimates for the tension-tension fatigue level of 0 to 345 MPa (50 ksi) were only based upon the eighteen lowest sample entries. This was necessary because an analysis of the entire data set resulted in a k of 0.195 caused by two data points which failed at unusually long lives, see Table 6B. This result was physically unreasonable since a k < 1 indicates that the samples increase in strength as fatigue cycling continues. This situation at 0 to 345 MPa (50 ksi) may indicate the possible transition effect mentioned previously of a change from $\sigma_{max}$ dominated lives to $\Delta\sigma$ dominated lives.

Note in Table 23 that e became more negative at lower $\sigma_{max}$ stress levels for tension-tension loading. These large negative e values are unusual in fatigue data. In essence, this result indicated that as the maximum stress was decreased, characteristic life, v, increased, but the tail of the data still extended near zero life. In other words, as maximum stress was decreased, the average life increased, but extrapolation of the cyclic life at 99% probability of survival remained at essentially zero cycles. This extrapolation of the fatigue data is probably inadequate at some low number of cycles, a few thousand or less.

For the tension-compression fatigue data of laminate 1, e remained negative except at the 179 to -110 MPa (26 to -16 ksi) load range. Again this indicated that the tail of the data scatter remained near zero as $\sigma_{max}$ was decreased. Note in Table 23 that the mode, the expected life, was always less than the mean or median except for the 0 to 345 MPa (0 to 50 ksi) level. The implication of this for laminate 1 fatigue data can be seen in Table 25, which shows that the extrapolated $P_{.99}$ and experimentally based $P_{.95}$ probability of survival lives remained low except at the lowest stress ranges. The 0 to 345 MPa (0 to 50 ksi) entries in Table 25 are based on only the lowest 18

132

TABLE 23

WEIBULL PARAMETERS AND ESTIMATES FOR LAMINATE 1 FATIGUE DATA

(20 Coupons/Stress Level)

| Stress MPa (ksi) | | Weibull Coefficients | | | | Estimated Cycles to Failure | | | |
|---|---|---|---|---|---|---|---|---|---|
| max | min | k | e | | v | Mean | Median | Mode |
| 400(58) | 0 | 1.988 | − 2,030 | | 4,899 | 4,007 | 3,660 | 2,868 |
| 345(50) | 0 | 4.564 | − 20,711 | | 64,621 | 57,224 | 58,036 | 60,119 |
| 290(42) | 0 | 1.846 | −280,781 | 1,900,898 | | 1,657,169 | 1,508,046 | 1,148,930 |
| 400(58) | −110(−16) | 2.409 | − 1,015 | | 1,979 | 1,639 | 1,556 | 1,381 |
| 345(50) | −110(−16) | 2.796 | − 4,973 | | 10,964 | 9,217 | 9,006 | 8,630 |
| 290(42) | −110(−16) | 2.915 | − 3,040 | | 33,806 | 29,822 | 29,452 | 28,860 |
| 179(26) | −110(−16) | 1.214 | + 74,246 | 2,892,580 | | 2,717,625 | 2,138,043 | 748,300 |

133

TABLE 24.

WEIBULL PARAMETERS FOR TWO PARAMETER FIT
TO FATIGUE DATA OF LAMINATE 1 COUPONS

| Stress MPa (ksi) | | Weibull Coefficients | |
|---|---|---|---|
| max | min | k | v |
| 400(58) | 0 | 1.523 | 5,910 |
| 345(50) | 0 | 3.159 | 71,374 |
| 290(42) | 0 | 1.639 | 1,992,588 |
| 460(58) | -110(-16) | 1.684 | 2,300 |
| 345(50) | -110(-16) | 1.936 | 12,380 |
| 290(42) | -110(-16) | 2.536 | 33,880 |
| 179(26) | -110(-16) | 1,234 | 2,861,394 |

TABLE 25

FATIGUE LIVES AT VARIOUS PROBABILITIES

OF SURVIVAL FOR LAMINATE 1

| Stress MPa (ksi) | | Probability of Survival | | | | | |
|---|---|---|---|---|---|---|---|
| max | min | 0.99 | 0.95 | 0.90 | 0.50 | 0.1 | 0.01 |
| | | | | Cycles N | | | |
| 400 (58) | 0 | ~ 0[a] | ~ 0 | ~ 0 | 3,661 | 8,575 | 12,986 |
| 345 (50) | 0 | 10,430 | 23,800 | 31,404 | 58,036 | 81,731 | 98,535 |
| 290 (42) | 0 | ~ 0 | 155,784 | 364,000 | 1,508,000 | 3,147,000 | 4,709,000 |
| 231 (33.5) | -110 (-16) | -[b] | >1,000,000 | - | - | - | - |
| 179 (26) | -110 (-16) | - | >1,000,000 | - | - | - | - |
| 460 (58) | -110 (-16) | ~ 0 | ~ 0 | 162 | 1,557 | 3,218 | 4,629 |
| 345 (50) | -110 (-16) | ~ 0 | 536 | 2,153 | 9,006 | 16,503 | 22,546 |
| 290 (42) | -110 (-16) | 4,564 | 10,261 | 13,986 | 29,452 | 46,011 | 59,179 |
| 179 (26) | -110 (-16) | 137,937 | 318,177 | 515,633 | 2,138,043 | 5,677,060 | 9,991,962 |

a - 0 indicates that the number of cycles to failure at that $P(x)$ was essentially zero.

b - Indicates no entry.

sample lives of Table 6B. Even for tension-tension fatigue testing at 0 to 290 MPa (0 to 42 ksi) the $P_{.99}$ probability of survival cycles remained near zero. This result is, from a design viewpoint, clearly unacceptable. However, at 0 to 231 MPa (0 to 33.5 ksi) the $P_{.95}$ life dramatically increased as did the $P_{.95}$ life at 179 to -110 MPa (26 to -16 ksi). This result again indicated the possibility of a fatigue endurance limit for laminate 1.

The average lives of all of the fatigue data obtained for laminate 1 are plotted in Figure 70. Although the tail of data scatter is of more importance, these average values show that stress range was, at best, a poor parameter for relating fatigue life under tension-tension and tension-compression fatigue testing. In Figure 70, the fatigue behavior below $\Delta\sigma = 290$ MPa (42 ksi) is clearly shown to be unknown. An endurance limit was only one of two possibilities the other being a continual linear extrapolation of $\Delta\sigma$ versus $N_F$. If this latter possibility is true, the implications for using composites like laminate 1 in certain helicopter design applications are adverse.

### 5.2.2   Fatigue Behavior - Laminate 2

Because of the distinctly different fatigue response of laminate 2, the same procedure for choosing $\sigma_{max}$ levels to define the fatigue life scatter could not be used as was used for laminate 1. Therefore, for tension-tension loading 20 coupons (including the original three) were fatigue cycled to failure at $\sigma_{max} = 772$ MPa (112 ksi) while at $\sigma_{max} = 689$ MPa (100 ksi), coupons were fatigue cycled until at least 40 unfailed coupons were obtained which had been subjected to $10^6$ load cycles. Tension-compression tests were conducted only at a maximum stress of 483 MPa (70 ksi) due to the temperature induced adhesive breakdown problem discussed previously. Testing of coupons was continued until 40 coupons were obtained which had survived $10^6$ cycles.

Results of the fatigue tests of laminate 2 coupons are tabulated in Appendix B and are plotted as $\sigma_{max}$ versus log ($N_F$) in Figure 71. The data are also plotted as $\sigma_{max}$ versus linear $N_F$ in Figure 72. The main conclusion that can

136
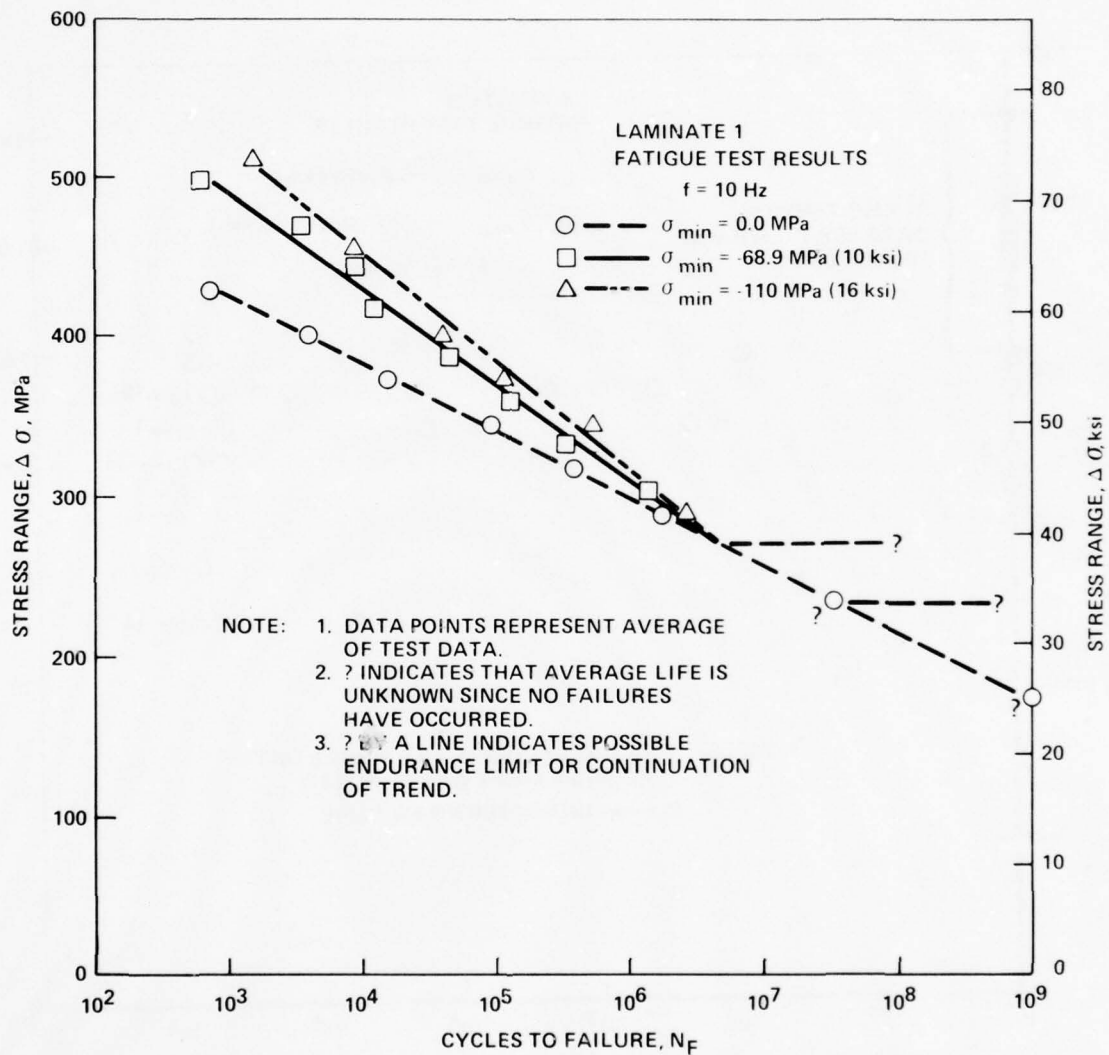
Figure 70.  Combined Plot of Laminate 1 Fatigue Results

137

Figure 71.  Laminate 2 Fatigue Results

138
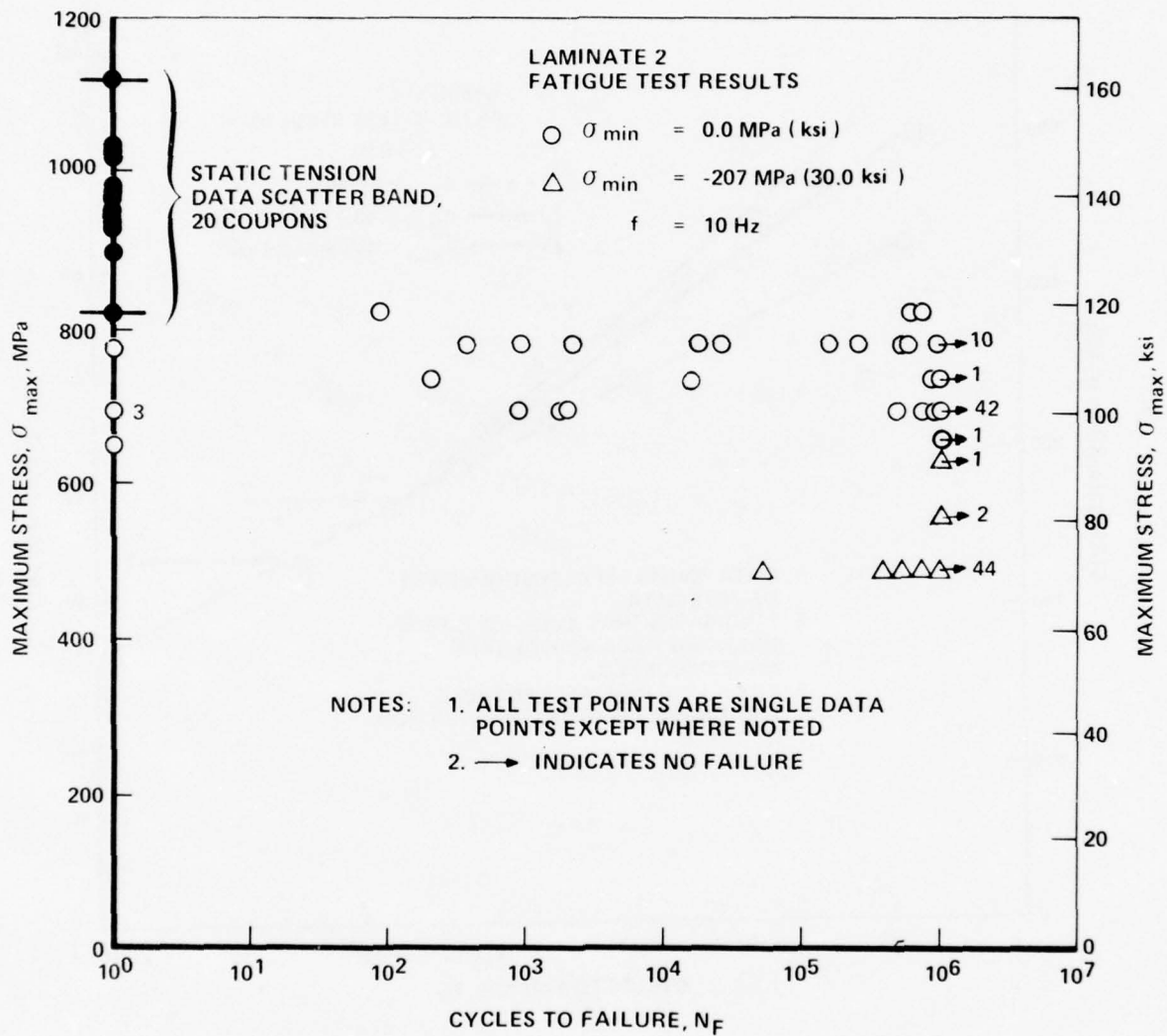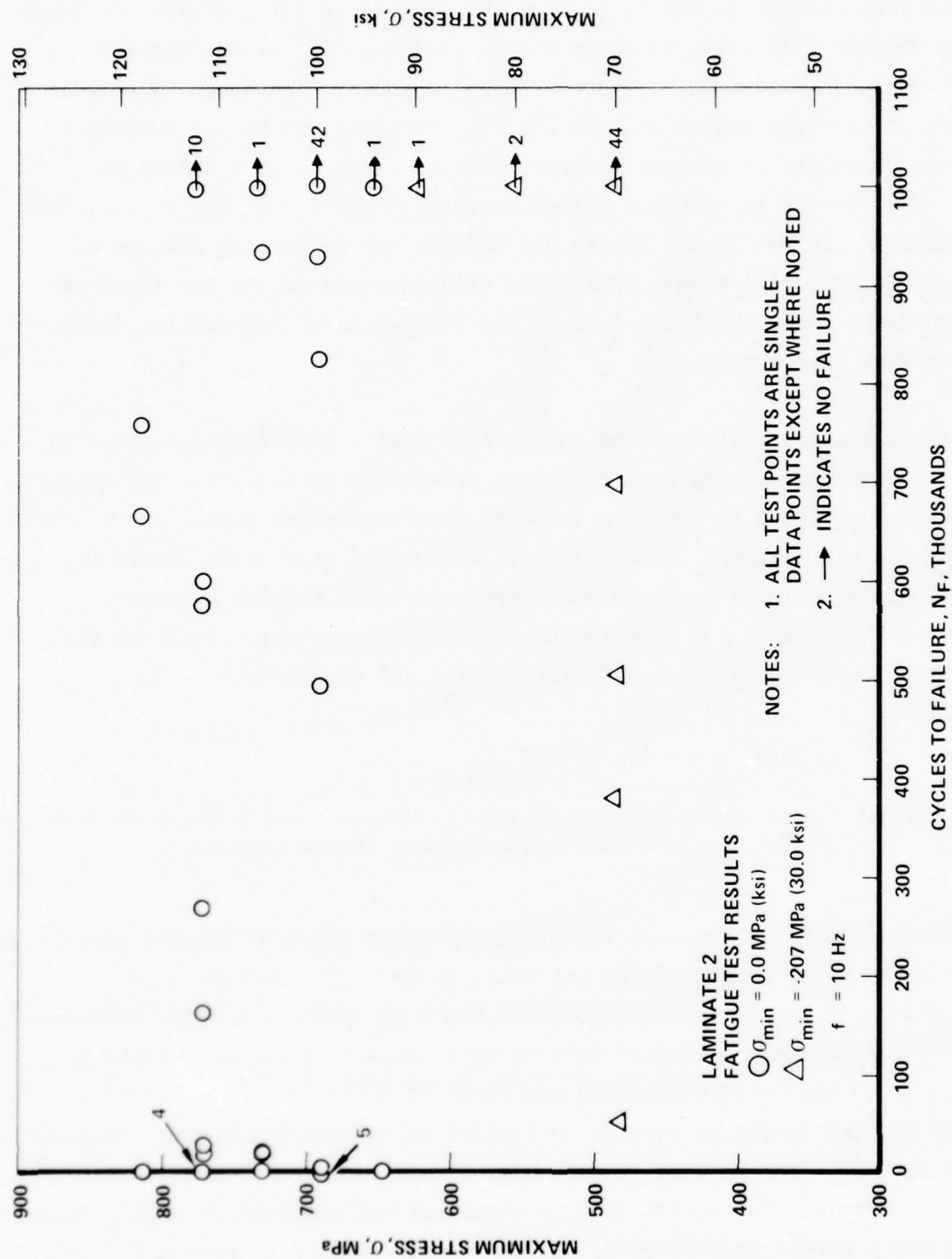
Figure 72. Linear Plot of Laminate 2 Fatigue Results

be drawn from Figures 71 and 72 is that the scatter in fatigue life was large. At 0 to 772 MPa (112 ksi), 10 coupons were cycled to $10^6$ cycles without failure while 10 failed between 1 and 599,330 cycles.  Although 43 coupons survived $10^6$ fatigue cycles at 0 to 689 MPa (100 ksi), 10 failed between 1 and 930,000 cycles, an extremely large scatter.  Four coupons tested at 483 to -207 MPa (70 to -30 ksi) failed between 58,090 to 696,420 cycles.  The data shown in Figures 71 and 72 did not provide any indication whether an endurance fatigue life stress exists for this laminate or whether there is a stress level below which the tail of the fatigue life distribution under-goes a marked improvement.

The fatigue results indicated the possibility that a much larger scatter in static tensile strength existed than that previously considered.  The question was especially raised by the five laminate 2 coupons which failed on the first cycle of fatigue loading.  Since all fatigue coupons were first loaded in tension, these failures could be considered as static tension failures. Therefore, the probability of survival of these coupons was calculated as-suming they were static tension failures using the equation:

$$P(x) = 1 - \frac{1}{n}$$

where    $n$ = the number of static or fatigue coupons whose
         maximum first cycle tension stress equaled or
         exceeded $x$

The value of failure stress, $x$, was precisely known for 4 of the 5 early failure coupons and within 5% for the other coupon.  The failure load was determined using the permanent records of the high speed visicorder recorded for the first few load cycles of each fatigue coupon.  Based on the above procedure, the $P(x)$ values obtained are shown in Table 26.  Also listed in Table 26 are the estimated strains to failure based upon the average apparent tensile modulus.  The modulus at such high strain rates may have been slightly different, however, the lowest failure stress of the original 20 static failure coupons had a strain to failure of 0.0065 mm/mm; the same as coupon 728-19B

TABLE 26

SUMMARY OF FIRST CYCLE FATIGUE FAILURES
OF LAMINATE 2

| Coupon ID | Ultimate Stress at $\sigma_{ult}$, MPa (ksi) | Estimated[a] Strain to Failure, $\epsilon_{ult}$, mm/mm | Probability of Survival, P(x) |
|---|---|---|---|
| 728-19B | 687 (99.7) | .0065 | .989 |
| 727-1C | 633 (91.8) | .0060 | .99 |
| 699-1B | 543 (78.8) | .0051 | .9906 |
| 699-28C | 540 (78.3) | .0051 | .99065 |
| 699-34B | 483 (70)[b] | .0045 | .994 |

a - Based on the average apparent tensile modulus of
    106 GPa ($15.4 \times 10^6$ psi)

b - Estimated at 483 MPa (70 ksi) within 5%

which failed on the first load cycle. Three of the five coupons of Table 26 were from panel 1NH699 which may be significant considering the C-scan record for that panel.

Figure 73 shows the estimated distribution of static tensile strength data for laminate 2. The distribution indicates the possibility of an extended tail in the static strength data. The low static strength data could have been caused by any of four possibilities; (1) a strain rate effect, (2) a material defect, (3) a geometric variation in the coupon, (4) an error in testing.

1) The strain rate during static tensile testing was approximately 0.0015 mm/mm/min. while that during the first cycle of a fatigue test was approximately 6.0 mm/mm/min. or $\sim$ a $10^3$ faster rate. This high strain rate may have caused a coupon to be more sensitive to any small local defect. However, as will be shown in Section 6 by the static residual tension strength data, this effect is unlikely because no degradation in residual strength of the unfailed coupons was observed. 2) Possibly rare, but not unique unobserved defects in the coupons caused the five first cycle fatigue failures particularly in the case of those from panel 699. If this was true, such defects were not larger than the coupon gage length area because coupons which were situated in the panels above or below or on either side of the failed coupons had long fatigue lives or high static tension strengths. 3) Extremely small variations in the tab geometry ($\pm$ 0.0254 mm (0.001 in.)) may have caused load introduction problems and resultant early failure. 4) One possibility for an error in testing was an excessive torque on the grip bolts. Although this could have occurred, bolts on each laminate 2 coupon were uniformly tightened to 181 N·m (1600 in.·lbs) thus any variation would have to have been due to the specific load transfer caused by the particular geometry of each bolt. The possibility of an inadvertent coupon overload was prevented by maximum and minimum peak and valley detectors used on all tests which would have tripped if the load exceeded the preset maximum fatigue load. Additionally, visicorder records revealed no load overshoots.

Figure 73. Distribution of Laminate 2 Static Tension Strength Data

To determine the cause of these laminate 2 first cycle fatigue failures, a large number of static coupons must be tested at different strain rates using uniformly loading hydraulic grips.  Regardless of the final cause (most likely items 1, 2, and 3, in that order), no such failures occurred within laminate 1 coupons again revealing the difference in response of the two laminates.

SECTION VI

RESIDUAL STRENGTH RESULTS

Due to the different fatigue life scatter behaviors of the two laminates, the residual strength degradation study was designed differently for each laminate. For laminate 1, coupons were fatigue cycled to a life chosen equivalent to a probability of survival equal to $P_{.90}$ at each $\sigma_{max}$ level. Coupons were fatigue cycled until 40 unfailed samples were obtained. Coupons which failed during fatigue were replaced. For laminate 2, coupons were fatigue cycled at 0 to 689 MPa (100 ksi) and at 483 to -207 MPa (70 to -30 ksi) until at least 40 unfailed coupons after $10^6$ cycles were obtained at each maximum stress level. Half of all unfailed coupons of both laminates were subsequently tested in static tension and half in static compression.

## 6.1    Laminate 1 Residual Strength Results

Table 27 shows the number of cycles equivalent to $P_{.90}$ at each $\sigma_{max}$ level to which 40 coupons were fatigue cycled for the residual strength study of laminate 1 coupons. The cycles listed in Table 27 are equal to a probability of survival of $P_{.90}$ based on a 3-parameter fit at the tabulated fatigue stress levels. Appendix C contains the static tension and compression residual strength data for the coupons fatigue tested to the cycles shown in Table 27. Included in Appendix C are the coupons which failed during fatigue cycling together with their respective cycles to failure.

Table 28 lists a summary of all of the residual strength data for laminate 1. The essential equivalence of the two and three parameter Weibull fits to the static data is clearly evident in Table 28. The average ultimate stress, ultimate strain and apparent initial modulus of the tension or compression residual strength coupons increased with the severity of the fatigue stress range. This result implied that fatigue cycling at more severe stress ranges screened more coupons by early failure and that the nature of the obvious strength degradation was not simple.

145

TABLE 27

NUMBER OF FATIGUE CYCLES TO WHICH LAMINATE 1
RESIDUAL STRENGTH COUPONS WERE SUBJECTED
(The number of cycles is equivalent to a
Probability of Survival of $P_{.90}$)

| Fatigue Stress Level MPa (ksi) | Number of Fatigue Loading Cycles |
|---|---|
| 290 to 0 (42 to 0) | 364,000 |
| 345 to 0 (50 to 0) | 31,400 |
| 290 to-110 (42 to -16) | 14,400 |
| 345 to-110 (50 to -16) | 2,150 |

TABLE 28

SUMMARY OF RESIDUAL STRENGTH TESTS FOR LAMINATE 1

(20 Coupons/Test Condition)

| Fatigue Stress Levels, MPa (ksi) | Weibull Parameters | | | Correlation Coefficient, R | Average Ultimate Stress, $\sigma$ avg, MPa (ksi) | Average Ultimate Strain, $\epsilon$ avg, mm/mm in 50.8 mm | Average Apparent Modulus, E avg, GPa (psi x 10^6) |
|---|---|---|---|---|---|---|---|
| | k | e | v | | | | |
| **Tension Test Results** | | | | | | | |
| Before Fatigue | 24.18 | -0.0753 | 70.50 | 0.9995 | 477(69.2) | 0.0096 | 52.7(7.64) |
| | 24.12 | 0 | 70.57 | 0.9995 | | | |
| 290 to 0 (42 to 0) | 12.12 | -0.6276 | 64.52 | 0.9958 | 430(62.4) | 0.0090 | 47.2(6.84) |
| | 11.88 | 0 | 65.04 | 0.9957 | | | |
| 345 to 0 (50 to 0) | 12.85 | -0.1688 | 67.31 | 0.9987 | 449(65.1) | 0.0093 | 48.3(7.01) |
| | 12.78 | 0 | 64.45 | 0.9987 | | | |
| 290 to -110 (42 to -16) | 18.51 | -0.0608 | 68.43 | 0.9995 | 463(67.2) | 0.0094 | 49.4(7.17) |
| | 18.48 | 0 | 68.49 | 0.9995 | | | |
| 345 to -110 (50 to -16) | 18.34 | -0.1326 | 69.26 | 0.9992 | 467(67.7) | 0.0095 | 49.2(7.13) |
| | 18.27 | 0 | 69.38 | 0.9992 | | | |
| **Compression Test Results** | | | | | | | |
| Before Fatigue | 12.09 | -0.4572 | 72.19 | 0.9973 | 480(69.7) | 0.0110 | 47.9(6.95) |
| | 11.94 | 0 | 72.53 | 0.9973 | | | |
| 290 to 0 (42 to 0) | 7.22 | -0.6574 | 60.15 | 0.9962 | 394(57.2) | 0.0098 | 43.9(6.37) |
| | 7.07 | 0 | 60.52 | 0.9961 | | | |
| 345 to 0 (50 to 0) | 13.02 | -0.2053 | 65.62 | 0.9988 | 439(63.7) | 0.0111 | 45.8(6.64) |
| | 12.94 | 0 | 65.79 | 0.9988 | | | |
| 290 to -110 (42 to -16) | 12.54 | -0.2387 | 67.26 | 0.9982 | 450(65.3) | 0.0108 | 45.9(6.66) |
| | 12.46 | 0 | 67.45 | 0.9982 | | | |
| 345 to -110 (50 to -16) | 14.74 | -0.5418 | 70.34 | 0.9969 | 473(68.6) | 0.0110 | 45.9(6.66) |
| | 14.52 | 0 | 70.82 | 0.9969 | | | |

Throughout the residual strength analysis for laminate 1 results, coupons which failed during fatigue were not included in the static data analysis. The procedure and associated implications will be discussed further in Section 7.4. They were excluded because of the apparent difference in failure modes between static and fatigue failures and because the static residual strength distributions did not appear to directly relate to coupons which failed during fatigue. The latter point is illustrated in Table 29 which shows that for the tension results, the strength of the weakest tensile coupon was significantly above the maximum fatigue stress. Figures 74 and 75 show typical failure modes for tension and compression residual strength coupons, respectively. These failure modes were similar to previous static failure modes and less similar to fatigue failure modes.

6.2    Laminate 2 Residual Strength Results

For laminate 2, residual strength tests were conducted on coupons cycled to $10^6$ cycles either under tension-tension loading from 0 to 689 MPa (100 ksi) or from 483 to -207 MPa (70 to -30 ksi) under tension-compression loading. Forty unfailed coupons at each $\sigma_{max}$ level were tested, half in tension and half in compression. The detailed results of these tests are given in Appendix C.

The only difference in failure modes between the original tensile tests and the tensile residual strength tests was that most of the static tensile residual strength stress-strain curves had a short "flat-topped" region prior to fracture. Figure 76 shows similar tension failure modes as those noted previously on the initial tensile tests. Compression residual strength stress-strain curves and failure modes, see Figure 77, were also similar to the initial unfatigued static compression data.

Table 30 summarizes the results of the laminate 2 residual strength study. The tension residual strength results were virtually identical in all properties to the original tension results even though 9 of 52 coupons tested in fatigue at 0 to 689 MPa (100 ksi) failed. In contrast to laminate 1 data, there was no tension residual strength degradation after $10^6$ cycles at the stress levels

148

TABLE 29

RESIDUAL STRENGTH STUDY FOR LAMINATE 1

| Type of Test T-Tension, C-Compression | Fatigue Stress Level, MPa (ksi) | Lowest Tension or Compression Failure Stress, MPa (ksi) | Average Tension or Compression Strength, MPa (ksi) |
|---|---|---|---|
| T | 290 to 0 (42 to 0) | 339 (49.2) | 430 (62.4) |
| | 345 to 0 (50 to 0) | 376 (54.6) | 449 (65.1) |
| | 290 to -110 (42 to -16) | 407 (59.0) | 463 (67.2) |
| | 345 to -110 (50 to -16) | 402 (58.3) | 467 (67.7) |
| | Static Tension | 427 (62.0) | 477 (69.2) |
| C | 290 to 0 (42 to 0) | 285 (41.4) | 394 (57.2) |
| | 345 to 0 (50 to 0) | 356 (51.6) | 439 (63.7) |
| | 290 to -110 (42 to -16) | 362 (52.5) | 450 (65.3) |
| | 345 to -110 (50 to -16) | 390 (56.5) | 473 (68.6) |
| | Static Compression | 397 (57.6) | 481 (69.7) |
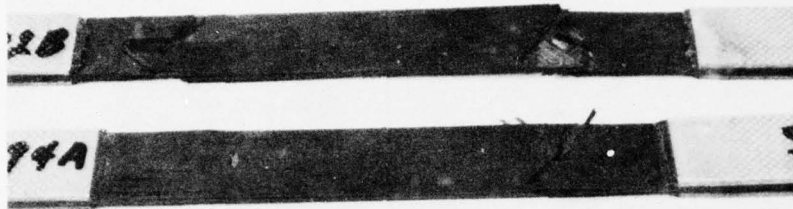
136 313R

a. Coupon 1MJ 582-6B, 1MJ 594-10A;  Side View
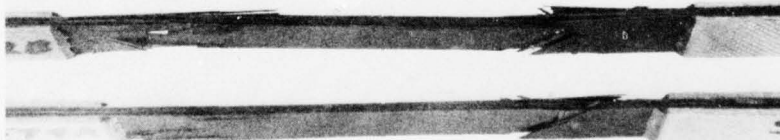


136 294R

b. Coupon 1MJ 582-6B, 1MJ 594-10A;  Edge View

Figure 74.  Typical Laminate 1 Static Tension Residual
Strength Failure Modes

136 314R
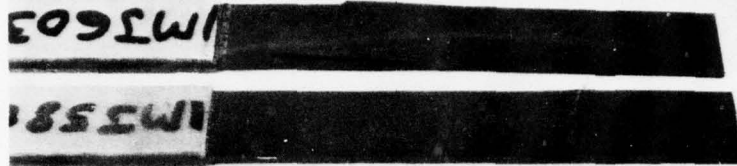
a.  Coupons 1MJ 603-5A, 1MJ 580-1A;  Side View



136 287R

b.  Coupons 1MJ 603-5A, 1MJ 580-1A;  Edge View

Figure 75.  Typical Laminate 1 Static Compression Residual
Strength Failure Modes
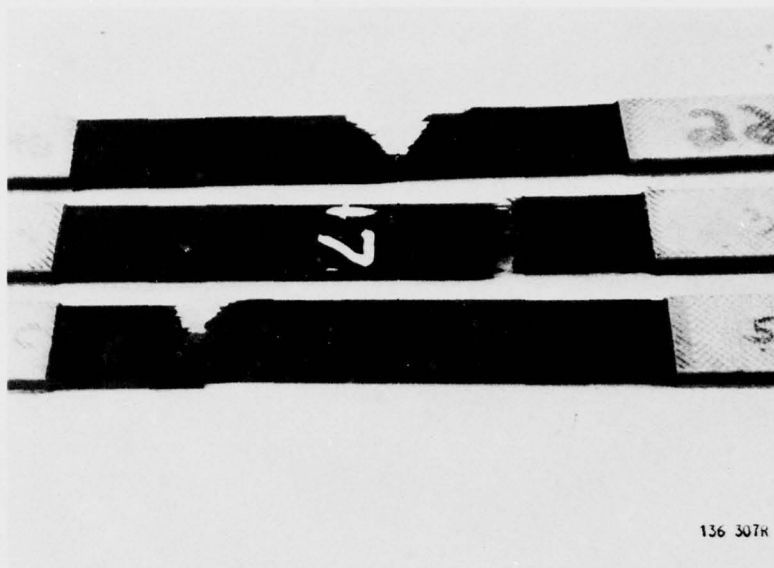
a. Coupons 1NH 699-22B, 1NH 728-37A, 1NH 727-5C; Side View
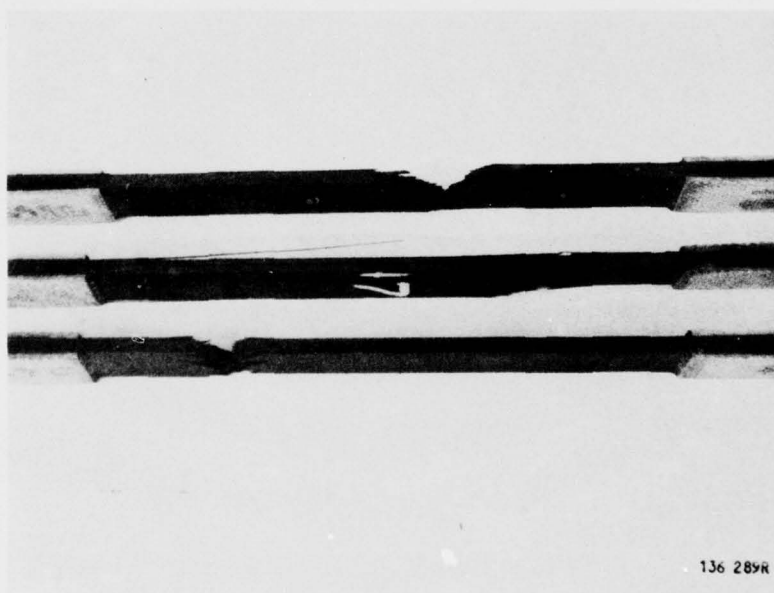


b. Coupons 1NH 699-22B, 1NH 728-37A, 1NH 727-5C; Edge View

Figure 76. Typical Laminate 2 Static Tension Residual Strength Failure Modes

136 308R
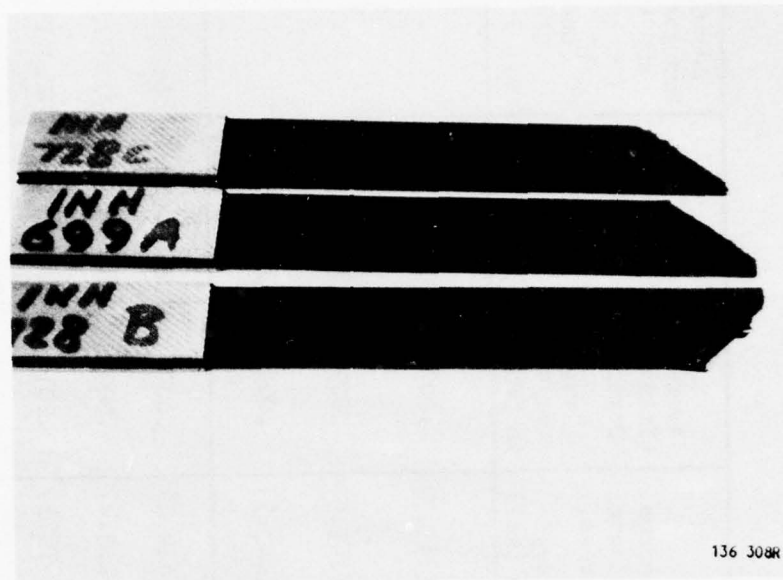
a. Coupons 1NH 728-31C, 1NH 699-27A, 1NH 728-35B; Side View



136 288R
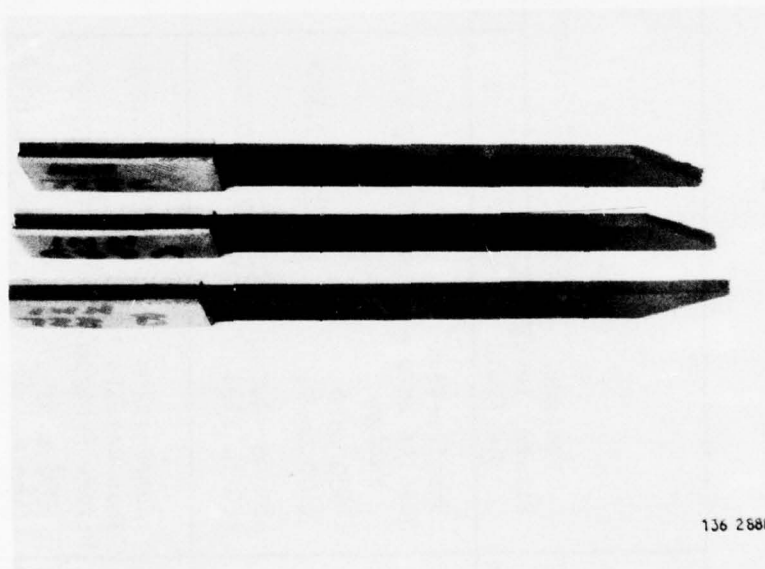
b. Coupons 1NH 728-31C, 1NH 699-27A, 1NH 728-35B, Edge View

Figure 77. Typical Laminate 2 Static Compression Residual
Strength Failure Modes

153

TABLE 30

SUMMARY OF RESIDUAL STRENGTH TESTS FOR LAMINATE 2

(20 Coupons/Test Condition)

| Type of Static Test, T-Tension C-Compression | Fatigue Stress Level, MPa (ksi) | Weibull Parameters | | | Average Ultimate Stress, $\sigma_{avg}$, MPa (ksi) | Average Ultimate Strain, $\varepsilon_{avg}$, mm/mm in 50.8 mm | Average Apparent Modulus, $E_{avg}$, GPa (psi x 10⁶) | Secant Modulus at 483 MPa (70 ksi) $E_{sec}$, GPa (psi x 10⁶) |
|---|---|---|---|---|---|---|---|---|
| | | k | e | v | | | | |
| T | Tensile Test Results Before Fatigue | 18.87 | -0.4304 | 144.41 | 977(141.7) | .0092 | 106 (15.4) | - |
| | 689 to 0 (100 to 0) | 17.19 | -0.3926 | 146.81 | 989(143.5) | .0092 | 108 (15.7) | - |
| | 483 to -207 (70 to -30) | 21.57 | -0.1409 | 146.42 | 991(143.7) | .0094 | 105 (15.3) | - |
| C | Compression Test Results Before Fatigue | 25.02[a] | -0.2592 | 115.82 | 787(114.2) | .0098 | 79.3 (11.5) | 86.2(12.50) |
| | 689 to 0 (100 to 0) | 19.79[b] | -0.4902 | 115.97 | 782(113.4) | .0093 | 83.4 (12.1) | 91.0(13.21) |
| | 483 to -207 (70 to -30) | 9.30 | -1.6398 | 103.07 | 665( 99.3) | .0078 | 87.6 (12.7) | 92.9(13.46) |
| | | 9.32 | -4.8439 | 102.60 | 681( 98.8) | .0079 | 86.7 (12.6) | 92.9(13.50) |

a - Tested 3-76

b - Tested 10-76

investigated. However, this was not true for the compression residual strength tests. Table 30 shows the degradation which occurred in $\sigma_{ult}$ and in $\varepsilon_{avg}$. The degraded compression residual strength results were virtually identical to each other, but drastically different from the original compression data. Note the large decrease in the exponent k for the residual compression results.

Because the average apparent modulus increased for the compression residual strength coupons and because the residual strength results resembled each other more than the initial distribution of unfatigued static coupons, the initial tests of unfatigued compression coupons were duplicated using 20 new coupons. In addition, due to the subjective nature of the apparent modulus the secant modulus from 0 to 483 MPa (70 ksi) was measured for all 80 coupons. The results of the new compression tests of unfatigued coupons are also summarized in Table 30 and tabulated in Table 13C of Appendix C. Table 30 clearly shows that $\sigma_{avg}$ was unchanged, but that $\varepsilon_{avg}$ decreased and $E_{avg}$ and $E_{sec}$ increased. This result gave confidence in the original tests as well as supported the observed increase in $E_{avg}$ for the residual strength coupons. The conclusion was that $E_{avg}$ actually increased for the compression residual strength coupons as supported by the four sets of test results for $E_{avg}$ and the non-subjective $E_{sec}$. Additionally, the compression residual strength properties did degrade, but the effects of the T-T and T-C load ranges were identical.

The cause of the increase in apparent modulus of the compression residual strength coupons was hypothesized to be due to two effects. First, an increase in moisture due to longer shelf storage prior to testing could decrease strain to failure and increase the modulus as supported by the observations for the two sets of unfatigued coupons (see Table 30) and predicted theoretically for this layup as shown in Figure 78. This figure also shows that the same effect, though less observable, should occur in a different matrix. Second, fatigue cycling may redistribute residual stresses by inducing matrix cracking and thus allow the modulus to increase.
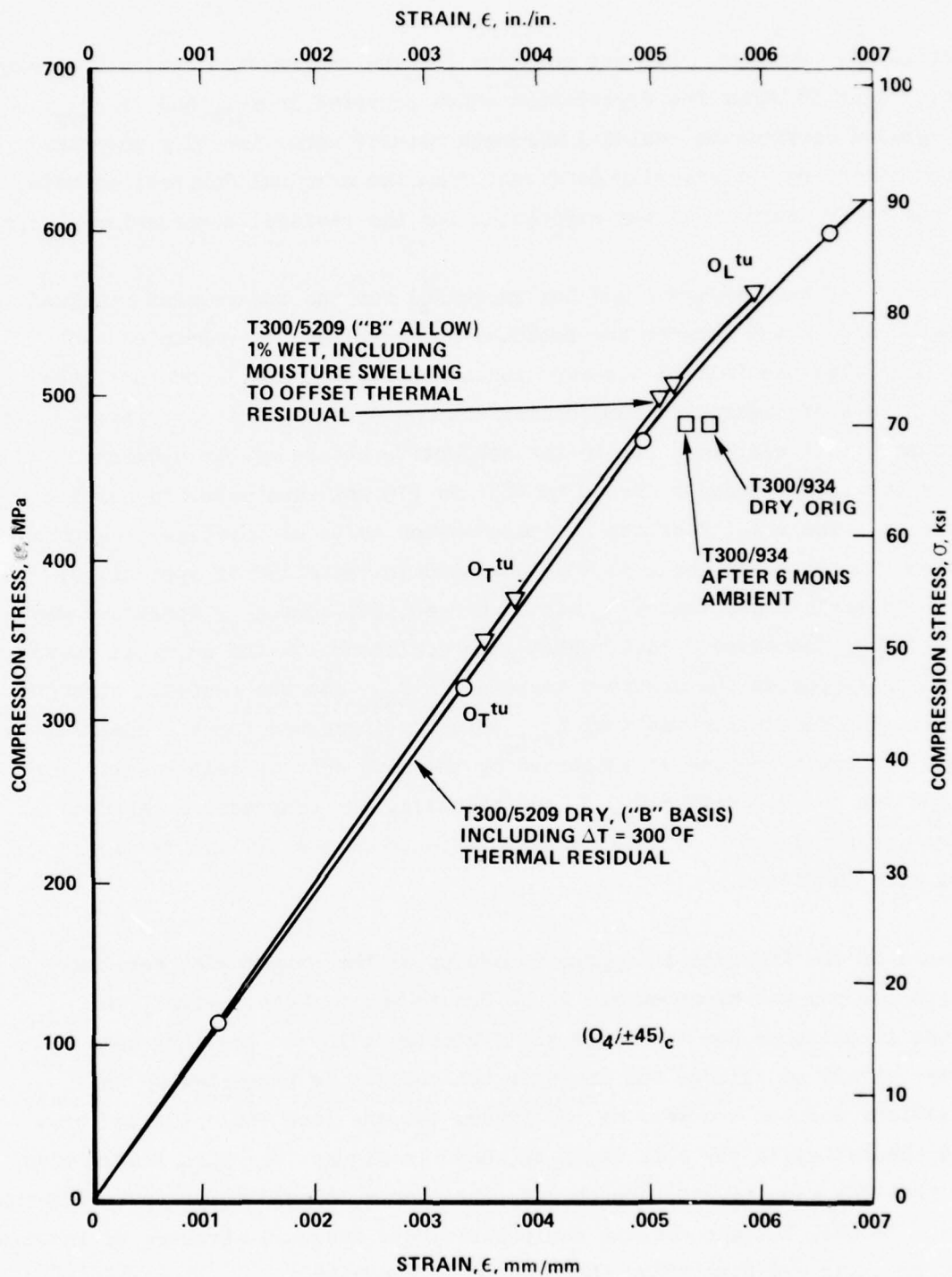
Figure 78. Theoretical Prediction of the Effect of Moisture on the Compression Strength of Laminate 2

SECTION VII

DISCUSSION

In this section differences and comparisons between the test results of the
two laminates will be drawn. In addition, the effects on data analysis and
modeling of a data sample set due to using either a 3- or 2- parameter
Weibull fit will be discussed as well as the minimum sample size needed to
extrapolate predictions. Finally, the applicability of one commonly used
formulation of the "wear-out" type analytical model for predicting residual
strength degradation will be discussed.

## 7.1     Comparison of Laminate Results

### 7.1.1    Tension and Compression Results

Although the static tension ultimate strengths and apparent moduli of elasticity
of the two laminates were greatly different, their strains to failure were quite
similar and, in fact, similar to that of the 0° fibers alone. Thus, the par-
ticular layup essentially only affected the apparent modulus of elasticity
while the change in ultimate strength appeared to be a reflection of this
modulus change. The layup also affected Poisson's ratio: laminate $1 \sim 0.28$,
laminate $2 \sim 0.63$.

Static compression moduli for both laminates were lower than their respective
tension moduli and the strains to failure did not agree as well as the tension
strains to failure. The scatter in the compression data was greater than in
the tension data for laminate 1, but this situation was reversed for laminate
2.

### 7.1.2    Fatigue Results

The primary difference between the two laminates in their fatigue properties,
besides the difference due to relative strength, was the apparent larger
scatter of the laminate 2 data. The tension-tension fatigue response of the

two laminates is compared in Figure 79 which shows the large difference
observed. For equivalent fatigue lives, $\sigma_{max}$ was higher for laminate 2 than
for laminate 1, however, this was primarily a reflection of the higher static
strength of laminate 2. The scatter in fatigue lives was noted to be less
for laminate 1 than that for laminate 2. A more pronounced slope, i.e., de-
pendence of $N_F$ on $\sigma_{max}$ of the laminate 1 data compared to laminate 2 data
appeared possible. However, Figure 80 shows the tension-tension fatigue
data replotted as $\sigma_{max}/\sigma_{ult}$ versus $\log N_F$ and indicates that the shape of the
laminate 2 curve may be similar to that of laminate 1, but was possibly
masked by the large laminate 2 data scatter. To settle the question of the
S-N curve shape for laminate 2, more data would be needed at $\sigma_{max}$ levels
below 689 MPa (100 ksi). Note in Figure 80 that the first cycle laminate 2
fatigue failures were not plotted because of lack of knowledge as to the
true cause of their failure.

Laminate 2 also appeared to respond to fatigue loading differently from
laminate 1 as supported by the first cycle failures of some laminate 2 coupons.
The cause of these early failures is unknown, however, the fact remains that
no laminate 1 coupons experienced such a phenomenon.

The tension-tension fatigue response of the two laminates shown in Figure 80
is essentially plotted on the basis of average failure strain because strains
at failure were similar. Perhaps in the future, strain should be used as a
common variable instead of stress.

### 7.1.3   Residual Strength Results

The static tension and compression residual strengths and moduli of laminate
1 coupons degraded with application of fatigue loading. In contrast, only
the static compression residual strength of laminate 2 degraded. Because
the amount of observed degradation in the laminate 1 residual strength proper-
ties appeared to decrease with an increase in severity of the fatigue loading,
the degradation was probably not as simple as the "wear-out" type of
degradation normally assumed.

158
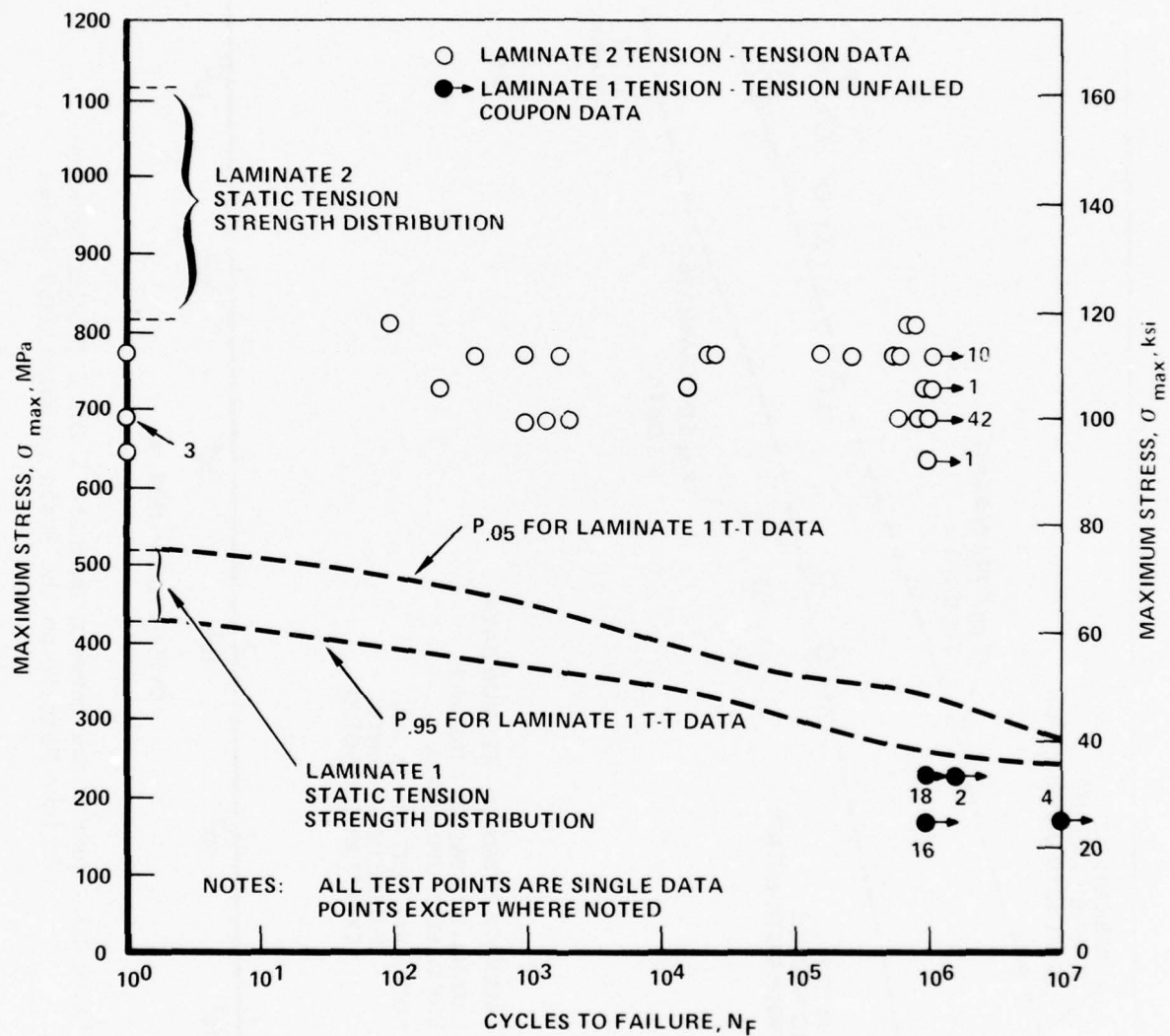
Figure 79. Comparison between Laminate 1 and 2 Tension-Tension Fatigue Results
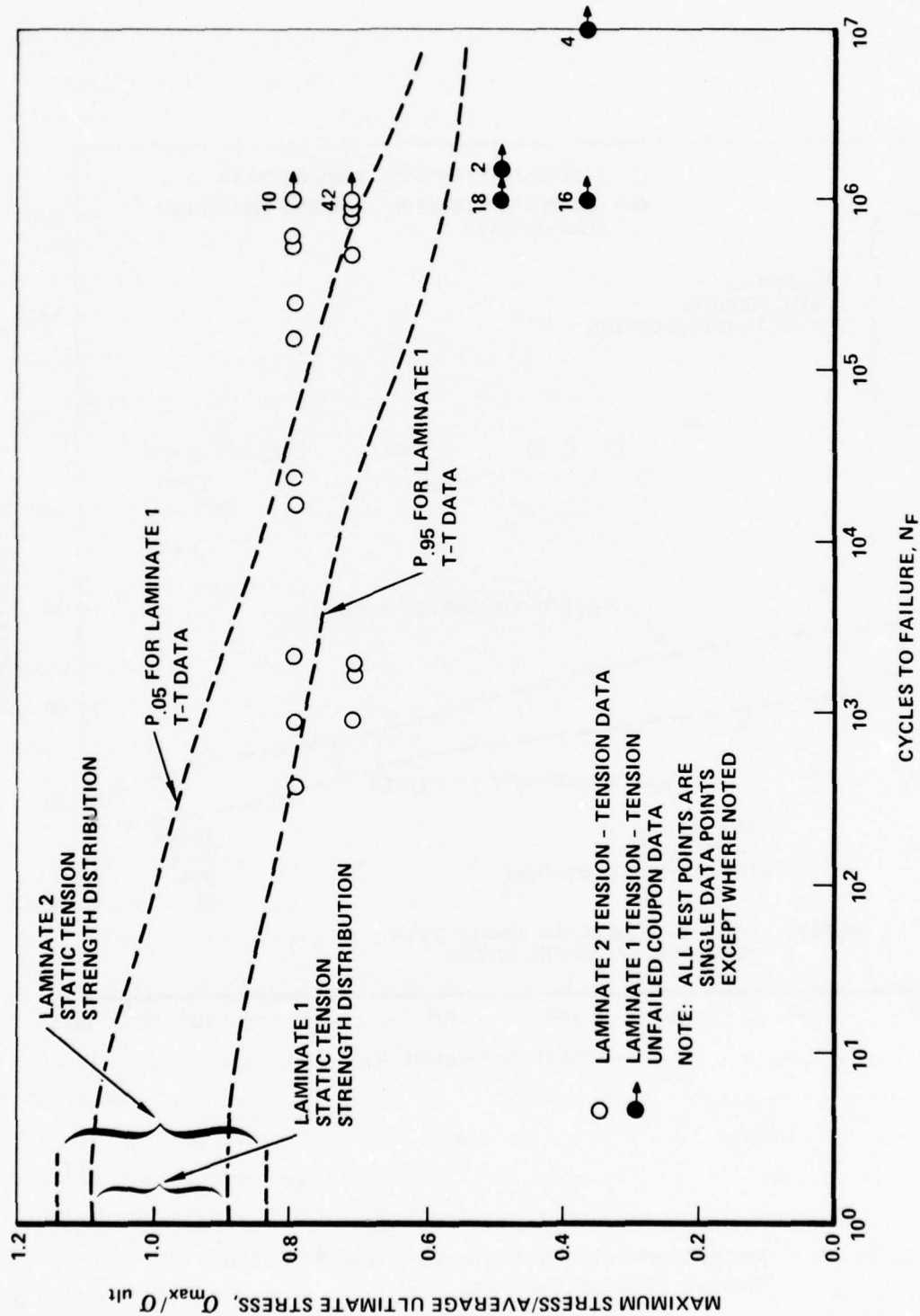
Figure 80. Comparison Between Laminate 1 and 2 Tension-Tension Fatigue Results on the Basis of Normalized Stress

160

## 7.1.4  Summary

The mechanical behavior test results of the two laminates were, in general, strikingly different. A major conclusion appears to be that a significant number of different stacking sequences and/or layups may have to be fully and independently evaluated for response to mechanical testing prior to drawing any general conclusions. This appears to be true in spite of the fact that different layups are made of the same material. Without such an evaluation, prediction of laminate properties, especially fatigue and residual strength, will require considerable test data on laminates of interest until greater experience in the use of composite materials is developed. Perhaps relating properties of different layups on the basis of strain will prove fruitful. The scatter in fatigue properties was especially disturbing, particularly the existence of a long tail in the data. The cause of this scatter needs to be determined and reduced.

At first glance, the conclusion regarding the large differences in mechanical response of the two laminates and the extent of their data scatter appears to present a formidable challenge to future structural use of composites. Though the challenge is real, the situation for all metal alloys was no different in the past, and for many alloys still is today, than the situation for graphite/ epoxy composites.

The large differences in mechanical response of these two laminates made of the same material are similar to those found for different heat treatments of the same metal alloy. Possibly, different layups of the same material are as different as two different heat treatments of the same metal alloy while the effect of different stacking sequences of the same laminate may be like the more subtle effects of small differences in some heat treatments of one metal alloy. In metals, as the strength of an alloy is increased, the scatter in properties increases like that of laminate 2 data compared to laminate 1. Carrying the analogy further, metals, especially titanium, often have fatigue scatter in the range of two orders of magnitude in life if special care is not given to alloy manufacture and extreme care to preventing cold work and surface degradation during machining. The scatter in composites may possibly

161

be reduced by attention to the same type of details. For metals, special care must be given to furnace cool-down rate to minimize microcracking, a situation undoubtedly analogous in composites concerning autoclave cool-down rates. However, in metals slow cool-down rates, though at first glance, advantageous, can result in other problems; also a likely possibility in composites.

In summary, though the difference in mechanical response between different layups of the same composite material was large, the situation is analogous to metal alloys. The physical principles appear to be the same although the details of their application differ due to the nature of fibrous directionally reinforced materials. Difficulties in applying the details of physical and mechanical principles to composites appear to be no greater than applying them to metals. The problem of data scatter for composites appears to be formidable and yet the same problem of a similar magnitude has been solved for many metal alloys. The problem of wide scatter may, of course, be far less severe for notched coupons. The development of better understanding of property trends and quality control of composites may prove to be difficult and costly, but most likely is no worse than that already accomplished for many metal alloys. Similar analogies can also be made for the special problems that may exist in the testing of composite materials.

7.2     Comparison of 3- and 2- Parameter Weibull Analysis Results

To investigate differences between the accuracy of fitting fatigue data with a 2- or 3- parameter Weibull equation, the data of laminate 1 was more extensively analyzed. Based on the original fatigue sample size at each fatigue level, an extrapolation was made for each stress level based on a 3-parameter Weibull fit. This extrapolation was compared to the actual large sample sets at each stress level which consisted of the original 20 coupons plus the first fatigue coupons used for static residual strength testing before any failures were replaced. This procedure allowed for a comparison between predicted and actual fatigue failure rates for a large sample size (60) based on the analysis of a smaller sample size (20). In addition, the same procedure was used based on a 2-parameter Weibull equation so that direct comparisons could be drawn

between 2- and 3- parameter Weibull fits.  This was especially important in
light of the observed large scatter in fatigue data since the 3-parameter
fit would be expected to predict the extrapolated short life tail better than
the 2-parameter fit.  Results of this life prediction study are shown in
Tables 31 and 32.

To explain the significance of the results listed in Tables 31 and 32, con-
sider the results for the fatigue stress level, 0 to 290 MPa (42 ksi).  Accord-
ing to Table 31 and based on a 3-parameter fit to the original 20 coupon
sample set of Section 5.2.1, the life equal to that at which 90% of the coupons
would survive, $P_{.90}$, was calculated as 364,000 cycles compared to 504,860
cycles calculated at $P_{.90}$ for a 2-parameter fit, see column (2) of Table 31.

Two of the original 20 coupons should have failed at a cycle life equal to
or less than the number of cycles equivalent to a 90% probability of survival,
$P_{.90}$, regardless of whether the calculated cycles were based on a 2- or 3-
parameter fit.  As can be seen in column 5 of Table 31, 3 coupons of the 20
actually failed below the predicted life of 364,000 cycles (3-parameter fit)
as did 3 at less than 504,860 cycles (2-parameter fit).  Column (6) shows
that 40 coupons were fatigue cycled before failed coupons were replaced for
the residual strength study while column (7) shows that at $P_{.90}$, 4 would, of
course, be expected to fail.  Column (8) shows that actually 5 of the 40
coupons of column (7) failed below the life corresponding to $P_{.90}$ based on a
3-parameter fit.  The accuracy of the 2-parameter fit could not be evaluated
in column (8) because coupons were not cycled beyond a life equivalent to $P_{.90}$
predicted by the 3-parameter fit (364,000 cycles).  Columns (9 and 10) show
that the total sample size was 60 with 6 expected to fail below $P_{.90}$, and
column (11) shows that 8 failed below the calculated life at $P_{.90}$ based on a
3-parameter fit.

The sample size at any one stress level in Table 31 was not large enough to
judge the accuracy of the 2- or 3-parameter Weibull fits.  Therefore, in the
bottom row results were summed, since the accuracy of the fits to their re-
spective data sets were essentially equivalent.  The total row shows that

163

TABLE 31

SUMMARY OF EXPECTED AND OBSERVED FAILURE RATES AT P.90

FOR LAMINATE 1

(BASED ON WEIBULL ANALYSIS)

| (1) Fatigue Stress Range, MPa (ksi) | (2) Number of Cycles to Failure at P.90[a] | | (3) Initial Sample Size [b] | (4) Number of Expected Failures Below P.90 | (5) Number of Failed Coupons Below P.90 | | (6) Sample Size Fatigue Tested Prior to Residual Strength Tests | (7) Number of Expected Failures Below P.90 | (8) Number of Failed Coupons Below P.90 [c] | (9) Total Sample Size | (10) Total Number of Expected Failures Below P.90 | (11) Total Number of Failed Coupons Below P.90 |
|---|---|---|---|---|---|---|---|---|---|---|---|---|
| | 3 Parameter | 2 Parameter | | | 3 Parameter | 2 Parameter | | | 3 Parameter | | | 3 Parameter |
| 0 to 290 (0 to 42) | 364,000 | 504,860 | 20 | 2 | 3 | 3 | 40 | 4 | 5 | 60 | 6 | 8 |
| 0 to 345 (0 to 50) | 31,400 | 35,000 | 20 | 2 | 2 | 2 | 40 | 4 | 4 | 60 | 6 | 6 |
| 290 to -110 (42 to -16) | 14,000 | 13,950 | 20 | 2 | 1 | 1 | 40 | 4 | 4 | 60 | 6 | 5 |
| 345 to -110 (50 to -16) | 2,150 | 3,870 | 20 | 2 | 3 | 4 | 40 | 4 | 1 | 60 | 6 | 4 |
| TOTAL | | | 80 | 8 | 9 | 10 | 160 | 16 | 14 d | 240 | 24 | 23 d |

a - P.90 means that 90% of the samples are expected to survive the number of equivalent fatigue cycles and 10% to fail

b - These were the sample sets which were fitted by Weibull analysis used to estimate the cycles at P.90

c - These coupons were replaced for the residual strength study

d - 2-parameter data could not be calculated because coupons were not fatigue cycled to the cycle life based on 2-parameters.

164

TABLE 32

SUMMARY OF EXPECTED AND OBSERVED FAILURE RATES AT P.95

LAMINATE 1

(BASED ON WEIBULL ANALYSIS)

| (1) Fatigue Stress Range, MPa (ksi) | (2) Number of Cycles to Failure at P.95 [a] 3 Parameter | (2) 2 Parameter | (3) Initial Sample Size [b] | (4) Number of Expected Failures Below P.95 | (5) Number of Failed Coupons Below P.95 3 Parameter | (5) 2 Parameter | (6) Sample Size Fatigue Tested Prior to Residual Strength Tests | (7) Number of Expected Failures Below P.95 | (8) Number of Failed Coupons Below P.95 3 Parameter [c] | (8) 2 Parameter | (9) Total Sample Size | (10) Total Number of Expected Failures Below P.95 | (11) Total Number of Failed Coupons Below P.95 3 Parameter | (11) 2 Parameter |
|---|---|---|---|---|---|---|---|---|---|---|---|---|---|---|
| 0 to 290 (0 to 42) | 155,780 | 325,430 | 20 | 1 | 0 | 2 | 40 | 2 | 3 | 5 | 60 | 3 | 3 | 7 |
| 0 to 345 (0 to 50) | 23,800 | 27,870 | 20 | 1 | 2 | 2 | 40 | 2 | 3 | 3 | 60 | 3 | 5 | 5 |
| 290 to -110 (42 to -16) | 10,260 | 10,500 | 20 | 1 | 1 | 1 | 40 | 2 | 2 | 2 | 60 | 3 | 3 | 3 |
| 345 to -110 (50 to -15) | 540 | 2,670 | 20 | 1 | 1 | 3 | 40 | 2 | 0 | 1 | 60 | 3 | 1 | 4 |
| TOTAL | | | 80 | 4 | 4 | 8 | 160 | 8 | 8 | 11 | 240 | 12 | 12 | 19 |

a - P.95 means that 95% of the samples are expected to survive the number of equivalent fatigue cycles and 5% to fail.

b - These were the sample sets which were fitted by Weibull analysis used to estimate the cycles at P.95

c - These coupons were replaced for the residual strength study

80 coupons were in the initial sample set (column 3), 8 were expected to fail below the cycles equal to $P_{.90}$ and that 9 failed below the calculated life based on the 3-parameter fit while 10 failed below the calculated life based on 2-parameter fit, see column (5). This limited result indicated a possible preference for the 3-parameter fit for extrapolation of the tail of the fatigue lives. Continuing on in the total row of Table 31, 160 coupons were tested for residual strength of which 16 should fail below $P_{.90}$ while according to a 3-parameter fit, 14 failed below the $P_{.90}$ calculated life, see column (8). The total sample size was 240, column (9), the total expected failures was 24, column (10); and the number of failures below the calculated cycles equivalent to $P_{.90}$, based on a 3-parameter fit, was 23, column (11). This result showed the apparent accuracy of the 3-parameter Weibull fit for extrapolating the tail of the fatigue data to 60 coupons based on 20 coupons.

To more fairly compare failure rate extrapolations based on a 2-parameter fit *versus a 3-parameter fit*, the exercise of Table 31 was repeated at a probability of survival of 95%, $P_{.95}$, as shown in Table 32. Considering the total row, column (3) shows the 80 coupons in the initial sample set; column (4) the expected 4 failures at $P_{.95}$; column (5) shows that 4 failures actually occurred below the calculated $P_{.95}$ life based on the 3-parameter fit while 8 failed below the calculated $P_{.95}$ life based on the 2-parameter fit. Column (6) of Table 32 lists the 160 coupons fatigue tested for the residual strength study and column (7) the 8 expected to fail of the 160 while column (8) shows that 8 coupons failed below the calculated $P_{.95}$ life based on the 3-parameter fit while eleven failed below the calculated $P_{.95}$ life based on the 2-parameter fit. Finally, column (9) shows the 240 coupons of the total sample set; column (10) the 12 expected failures; and column (11) the fact that 12 failed below the calculated $P_{.95}$ life based on the 3-parameter fit, but 19 failed below the calculated $P_{.95}$ life based on the 2-parameter fit. In summary, the 2 parameter fit was dangerously unconservative in extrapolating the initial 80 coupon set to 240 coupons for calculating the expected life at $P_{.95}$ since only 12 of 240 coupons should have failed below the calculated $P_{.95}$ life based on 2-parameter fit, but 19 actually failed.

166

In Table 33, a comparison between calculated and actual number of failures at $P_{.90}$ and $P_{.95}$ in the 160 sample size residual strength set based on the 80 sample size initial data set is summarized for the 3-parameter fit. The accuracy of the calculations is apparent.

## 7.3    Extrapolation of Fatigue Life Results

Although the previous section showed the apparent superiority of the 3-parameter Weibull fit over the 2-parameter fit for predicting the $P_{.95}$ fatigue cycle life of a fatigue data is illustrated in Figure 81 which is a plot of the probability of failure versus log cycles to failure for the given data set. If 20 fatigue test points are analyzed, prediction of $P_{.95}$ for a larger data set will be accurate using a 3-parameter Weibull fit, but how many test points are needed to predict $P_{.99}$ or $P_{.999}$. This question is of extreme importance for presently used composites if they are to be used in aerospace structural applications because of the large data scatter presently inherent in such materials. Thus, predicting the tail or low life regime of the data is of utmost concern.

The accuracy of a 3-parameter Weibull fit for predicting the tail or low cycle life of the fatigue data is illustrated in Figure 81 which is a plot of the probability of failure versus log cycles to failure for the fatigue data obtained from tension-tension testing laminate 1 coupons at $\sigma_{max}$ = 290 MPa (42 ksi). Open circles are the original baseline twenty point data set. The filled circles are failures which occurred in the first forty coupons subjected to fatigue cycling for subsequent residual strength tests. The accuracy of the 3-parameter fit to the baseline data compared to the 2-parameter fit is well illustrated in Figure 81. The dashed line is an extrapolation of the 3-parameter fit to the 98% probability of survival, $P_{.98}$, level. The accuracy of extrapolating the 3-parameter fit to $P_{.98}$ is apparent. Unfortunately, extrapolation of the data to $P_{.99}$ did not appear to be possible because of the large data scatter.

TABLE 33

SUMMARY OF EXPECTED AND OBSERVED FAILURE RATES

FOR LAMINATE 1

(BASED ON THREE PARAMETER WEIBULL FIT)

| Fatigue Stress Levels, MPA (ksi) | Calculated Number of Cycles | | Initial Sample Size [c] | Number of Expected Failures Below | | Number of Failed Coupons Below | | Sample Size Fatigue Tested Prior to Residual Strength Tests | Number of Expected Failures Below | | Number of Failed Coupons Below | |
|---|---|---|---|---|---|---|---|---|---|---|---|---|
| | P.90 [a] | P.95 [b] | | P.90 | P.95 | P.90 | P.95 | | P.90 | P.95 [d] | P.90 | P.95 |
| 0 to 290 (0 to 42) | 364,000 | 155,780 | 20 | 2 | 1 | 3 | 0 | 40 | 4 | 2 | 5 | 3 |
| 0 to 345 (0 to 50) | 31,400 | 23,800 | 20 | 2 | 1 | 2 | 2 | 40 | 4 | 2 | 4 | 3 |
| 290 to -110 (42 to -16) | 14,400 | 10,260 | 20 | 2 | 1 | 1 | 1 | 40 | 4 | 2 | 4 | 2 |
| 345 to -110 (50 to -15) | 2,150 | 540 | 20 | 2 | 1 | 3 | 1 | 40 | 4 | 2 | 1 | 0 |
| TOTAL | | | 80 | 8 | 4 | 9 | 4 | 160 | 16 | 8 | 14 | 8 |

a - P.90 means that 90% of the samples are expected to survive the number of equivalent fatigue cycles and 10% to fail.

b - P.95 means that 95% of the samples are expected to survive the number of equivalent fatigue cycles and 5% to fail.

c - This is the sample set which was fitted by Weibull analysis used to estimate the P.90 and P.95 cycles.

d - These failed coupons were replaced for the residual strength tests.
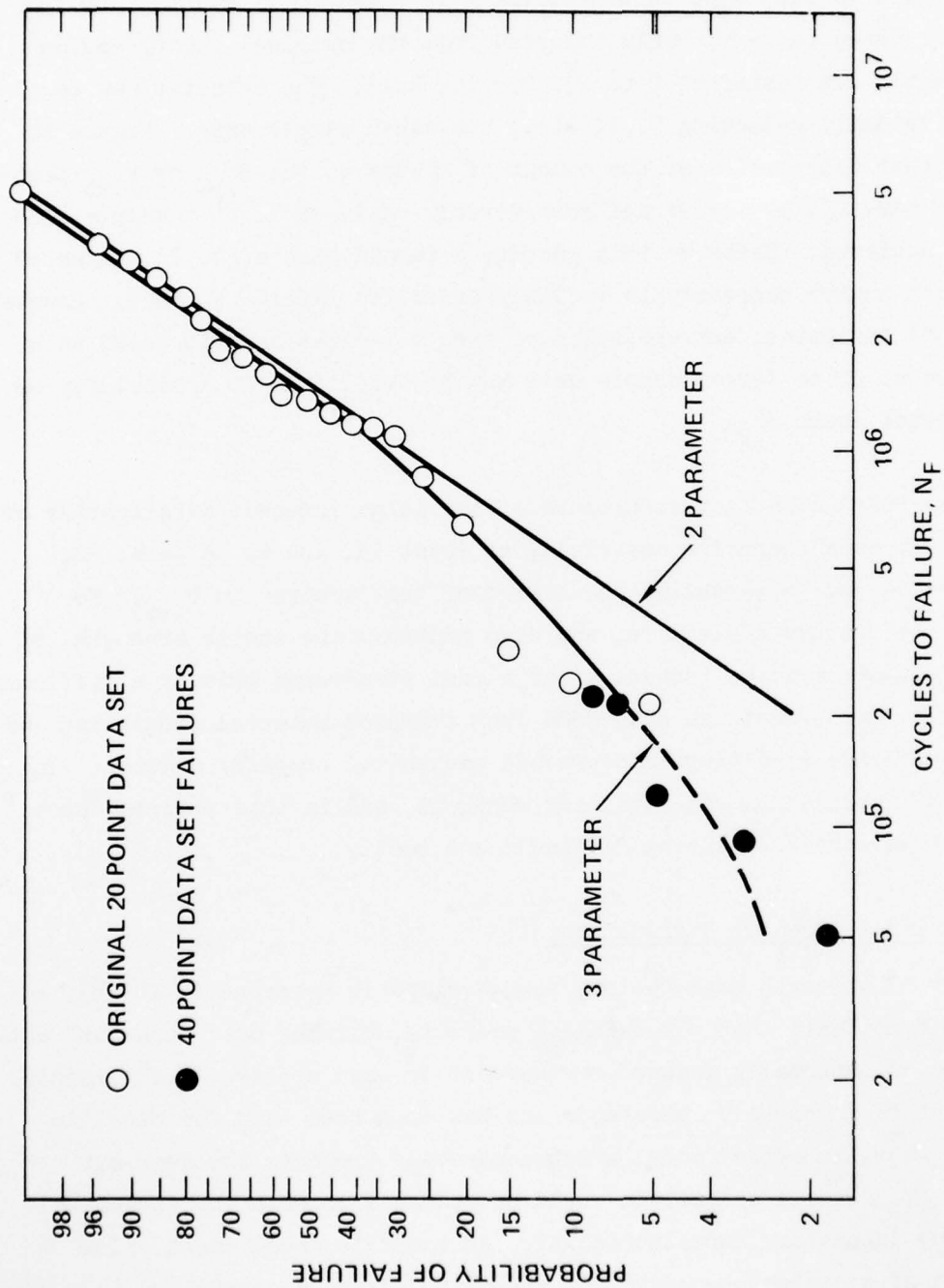
Figure 81. Probability of Failure for Laminate 1 Tension-Tension Fatigue Results at $\sigma_{max}$ = 290 MPa (42.0 ksi)

In Figure 82 the effect of sample size on probability of survival is illus-
trated. The data displayed in the figure were obtained by calculating the
results for three tests randomly selected from the original twenty coupon
fatigue sample set tested at 0 to 290 MPa (42 ksi). The exercise was re-
peated by randomly selecting 5, 7, etc., sub-sized sample sets. Figure 82
indicates that calculation of the number of cycles at the $P_{.90}$ or $P_{.95}$ prob-
ability of survival levels varied considerably until at least a sample size
of 15 was achieved. Based on this result, a sample size of 20 is suggested
as a minimum number necessary to reliably establish fatigue scatter. However,
as Figure 81 indicates, extrapolation of even a 3-parameter fit based on a
sample size of 20 to larger sample sets may be unreliable at probability of
survival rates above $P_{.98}$.

The primary conclusion is that because of the large inherent data scatter of
the presently used composite materials, at least 15, and to be safe, 20,
coupons are needed to establish the extent of that scatter to $P_{.95}$. To
establish the fatigue cycle life, and also probably the static strength, at
$P_{.99}$, 100 coupons must be tested. From a cost standpoint this is a difficult
conclusion. Improvement can only come from improved material processing and
coupon manufacture resulting in decreased mechanical property scatter. In
light of the fabrication and machining controls used in this program, such
improvement will most likely be difficult and costly.


7.4     Residual Strength Degradation

The concept of strength degradation, as described in References [24-28], re-
fers to an hypothesis that a mechanical property degrades or "wears-out" with
time due to an externally induced environment or load spectrum. In general,
this concept is physically reasonable and has long been used for metallic
materials. A mathematical model which accurately predicts the wear-out
properties of advanced composites would be valuable to both the structural
designer and laboratory experimentalist. An accurate model might allow
formulation of a design procedure for employing advanced composites in aircraft
structures similar to that outlined for metallic materials in MIL-STD 1530 [29].
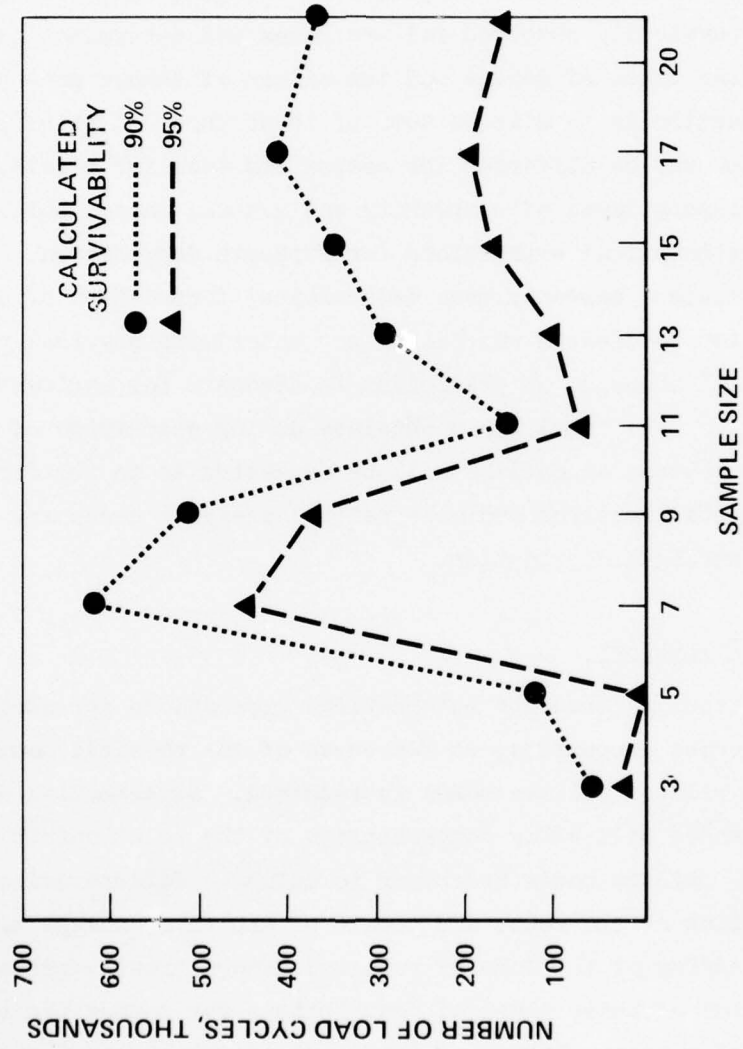
Figure 82. Effect of Sample Size on the Number of Fatigue Cycles at Specific Probability of Survivals (Laminate 1 Data at 0 to 290 MPa (42.0 ksi))

Essentially, development of a model representative of strength degradation consists of making three assumptions: 1) the nature of the degradation rate; 2) the criterion of failure; 3) the relationship between failure modes which occur under static to those resulting from dynamic loads. Fundamental to mathematically formalizing these assumptions into engineering practice is an awareness of the physically observed failure modes and determination and understanding of the types of damage and the nature of damage growth. One purpose of this section is to discuss some of these physical principles, especially how they may be different for composites than for metals, to ascertain the necessary level of complexity and general format which may be required of the mathematical expressions for strength degradation. A second purpose is to evaluate a commonly used mathematical formulation of composite strength degradation to discern whether or not underlying physical principles are satisfied and if accuracy of prediction is adequate for engineering purposes. Based upon the conclusions obtained during discussion of the above described purposes, an outline will be suggested as to the direction of future experimental research and mathematical analysis necessary to accurately predict strength degradation.

## 7.4.1    Physical Principles

In order to successfully formulate mathematical expressions for strength degradation in fibrous composites, an awareness of the physical nature of damage growth and related failure modes is required. Experimental data on observed failure modes will allow comprehension of the relationship between static and fatigue failure modes necessary to define a failure criterion. Similarly description of the cause and nature of growth of damage zones allows an understanding of the form of required damage growth expression. Lastly, a comparison of these physical descriptions for composites to those for metals will allow determination of the level of mathematical complexity required for expression of composite strength degradation.

### 7.4.1.1 Damage Growth and Failure Modes Observed in this Program

Although no obvious damage was visible to the eye prior to coupon separation, the stress-strain curves, and analysis and data results found in the liter- ature such as in Reference [30], suggest that the 90° and 45° plies of lamin- ate 1 coupons failed during static tension loading before final coupon fracture. Observation of the failed laminate 1 static tension coupons (see Figure 35) revealed only minor amounts of delamination essentially confined to the fracture region. Multiple fracture locations sometimes occurred. As expected, the 90° and 45° plies failed in the matrix while the fibers in the 0° ply were fractured. This mode of failure was observed to be essentially the same for the static tension residual strength coupons except for those which also had extensive delamination due to the prior fatigue loading (see Figure 74).

Laminate 1 static compression coupons exhibited no obvious damage prior to fracture although the stress-strain curve often was flat just prior to failure indicating internal damage. Coupons usually failed at one location with the outer plies in the fracture region buckled out of plane in a sym- metrical pattern with respect to the axis of the coupon, see Figures 45 and 46. Extensive delamination occurred, but was limited over approximately 25 to 50 mm (1 to 2 in.) of the gage length in the vicinity of the fracture region. Fractures appeared on the outer surface of the coupon along a 45° angle to the loading or along an irregular line approximately 90° to the loading direction. The static compression failure mode of coupons previously tested in fatigue was similar to that of the unfatigued coupons except that the amount of delamination was often more extensive due to the delamination which occurred during fatigue loading, see Figure 75.

In contrast to damage which occurred in the static tests, laminate 1 coupons tested in fatigue displayed damage prior to fracture in the form of extensive delamination. The amount of observed delamination was dependent on stress level, the lower stressed coupons having more extensive delamin- ation. Regardless of whether the coupon was tested in tension-tension or

173

tension-compression fatigue, delamination started at the free edge, at one or more locations, primarily between the two -45° plies and propagated towards the center of the coupon and along the free edge. Local out-of-plane buckling of the outer four plies often occurred in various localized regions of delamination. These regions did not necessarily extend to the coupon edge and occurred under both T-C and T-T loading, but were more pronounced under T-C fatigue. Delamination often developed early in the life of T-T coupons while T-C coupons usually failed soon after the delamination was observed. The final fracture of coupons tested in T-T was due to tensile overload of unbroken 0° fibers and 45° and 90° plies with the failure location usually confined to one region. The damage zone could be quite extensive, see Figures 54 and 55. Final failure of T-C coupons which only occurred during a compression load excursion was also usually confined to one region, but was caused by fracture of the plies which were buckled out of plane.

Like laminate 1 coupons, laminate 2 coupons exhibited different failure modes and damage growth depending on the type of loading. In static tension, regardless of whether coupons had experienced prior T-T or T-C fatigue loading, the failure mode was typified by one localized failure region dominated by 0° fiber breaks, 45° ply matrix failures and extensive delaminations over a large portion of the coupon usually between the outer $0_2$ and -45 plies, see Figures 36 and 76. Sometimes the failure regions were dominated by breakage of the 0° fibers along a line 45° to the load line direction, see Figure 37. In essense, the failure in these coupons was dominated by the 45 plies. The coupons which failed along a 45° line sustained much less delamination than the coupons which failed along 90° lines. Typically static compression failures of laminate 2 coupons, whether or not they had been exposed to the fatigue loading, were along a predominately 45° line to the loading direction with delamination confined primarily to the failure region and with broken plies buckled out of plane in a symmetrical fashion about the coupon centerline, see Figures 47, 48 and 77. Under either static tension or compression loading, no damage was visually observed prior to fracture.

174

Tension-tension and tension-compression fatigue coupons of laminate 2 exhibited delamination damage during the last portion of the coupon life. Unlike laminate 1 coupons, this damage did not necessarily start at free edges and was confined in extent. Delamination, during fatigue cycling which was more extensive under T-C loading, consisted of shredded and broken single fibers or small groups of fibers from the outer $0°$ plies. Damage zones appeared to grow by out-of-plane localized buckling of the delaminated plies. Failures of T-T coupons usually, but not always, showed extensive internal delamination usually between the $0°$ and $-45°$ plies, see Figures 56 and 57. The failure zones were dominated by either $0°$ fiber fractures at $90°$ to the load line and $45°$ ply matrix failures or sometimes by $0°$ fiber fractures at $45°$ to the load line which showed the large influence of the $45°$ plies, see Figure 58. The primary difference between the static tension and tension-tension fatigue failure mode appearances was in the failure region which for the static loading was much more confined and far less ragged in appearance. Failure of T-C coupons occurred only during a compression load excursion and appeared to be caused by local breakage of delaminated fibers while buckling out-of-plane, see Figure 59. Only single location fracture regions were observed for both T-T and T-C coupons.

The specific types of damage growth and failure modes observed for the two laminates and four different types of loading are summarized in Table 34. Essentially four different types of failure modes were observed. Damage growth between static and dynamic loading was quite different, but more similar between T-T and T-C fatigue loading. Damage growth during fatigue was different for each laminate layup. The most similar failure modes were those seen for laminate 2 coupons tested in static tension and in T-T fatigue, though even for these two cases differences were evident. The fact that the laminate 2 residual static tension strength was identical to the original strength after exposure to T-T fatigue levels which caused 9 failures out of 51 coupons suggests that the static and fatigue damage mechanisms were indeed significantly different.

TABLE 34

SUMMARY OF OBSERVED DAMAGE GROWTH AND FAILURE MODES

| | Test Type | Static Tension | Static Tension Residual Strength | Static Compression | Static Compression Residual Strength | T-T Fatigue | T-C Fatigue |
|---|---|---|---|---|---|---|---|
| Laminate 1 | Damage Growth During Test | None | None | None | None | Delamination between the two -45° plies starting at free edge progressing along edge and toward center. | a. Delamination between the two -45° plies starting at free edge progressing along edge and toward center. <br> b. More pronounced out-of-plane buckling of delaminated plies than in T-T. |
| | Failure Mode | a. Small amounts of Delamination confined to fracture region <br> b. 90° & 45° ply matrix fractures <br> c. 0° fiber fracture <br> d. Occasional Multiple Fracture region | a. Similar to static tension failures <br> b. Some coupons had extensive delamination due to prior fatigue loading | a. Extensive localized delamination <br> b. Fracture of outer plies due to out-of-plane buckling <br> c. Outer surface fractures along 45° line or irregular 90° line to load direction <br> d. Occasional Multiple fracture region | a. Similar to static compression failures <br> b. Some coupons had extensive delamination due to prior fatigue loading | a. One failure location often quite extensive <br> b. Large amount of delamination especially between two -45° plies <br> c. Many 0° fiber fractures, mostly matrix fractures in 45° & 90° plies. | a. One failure location often extensive <br> b. Large amount of delamination especially between two -45° plies <br> c. Many 0° fiber fractures, mostly matrix fractures in 45° and 90° plies <br> d. Fractured outer 4 plies buckled out-of plane |
| Laminate 2 | Damage Growth | None | None | None | None | Random localized delamination of fibers and fiber bundles from the outer surface 0° plies, not usually occurring at free edges, late in coupon life. | Similar to T-T coupons but with more extensive delamination |
| | Failure Mode | a. Extensive delamination usually between 0₂ and 45° plies <br> b. One failure location <br> c. 0° fiber fracture and 45° ply matrix fracture <br> d. Several coupons with 0° fibers fractured along a 45° line to load direction | a. Similar to static tension coupons | a. Localized delamination <br> b. Fracture of coupon along a 45° line to load direction <br> c. Fractured plies buckled symmetrically out-of-plane | a. Similar to static compression failures <br> b. Some coupons had extensive delamination due to prior fatigue loading | a. Usually extensive delamination regions often between 0₂ and 45° plies <br> b. Rugged fracture regions dominated by 0° fiber fractures essentially at 90° to the load line and 45° ply matrix fracture <br> c. Some coupons with 0° fiber fractures running at 45° to the load line | a. Usually extensive delamination regions often between 0₂ and -45° plies <br> b. Plies fractured out-of-plane due to buckling and fracture during compression load excursion |

## 7.4.1.2    Comparisons Between Composites and Metals

To understand the practical problems of developing a model for strength degradation in composites a short review of the nature of damage growth in metals will be discussed.  The purpose of this review is to explain the reasons for the success, albeit a limited one, of relatively simple damage growth models for metals and why this fortuitous situation should not necessarily be expected to occur in continuous fiber composites.

In metals, regardless of whether loading is static or dynamic, damage consists [31], simplifying a complex situation, of the pile up of dislocations, generation of dislocation tangles, slip, and twinning which results in inelastic deformation and the generation and propagation of cracks or crack-like defects.  In ductile materials, only large cracks affect static failure load which is primarily due to plastic or tensile instability.  Materials which are more brittle generally exhibit failure loads sensitive to the presence of cracks.

During fatigue, numerous micro-sized crack-like defects develop and propagate, (especially around holes or notches).  The dominance of these cracks, regardless of whether the metal is brittle or ductile, is dependent on stress level (or, better, strain range).  At very high stresses or strains, large plastic flow occurs leading to tensile instability and short life and unless the material contains a large sharp notch or crack, the effect of the flaw is not obviously manifested.  At lower, but still high stresses, a predominant crack (or cracks) develops early in life resulting in damage and failure due to crack growth at an intermediate life.  If the stress is still lower, fatigue life can become long, many microcracks develop and grow, but a predominant flaw does not occur until late in fatigue life.

This outline of damage growth in metals indicates that, in most cases, formulation of relatively simple expressions, which include the crack, for damage growth and the failure criterion would be quite difficult.  In fact, only for brittle materials have such simple expressions been developed, and even then only when they are subjected to fatigue loading at the intermediate stress

177

levels where a dominant flaw can develop. Even in this relatively restricted case large complications arise [32]. This is not to say that strength degradation or flaw growth does not occur in the other materials, but only that the analysis of such flaw growth is extremely onerous due to the associated extensive plasticity. Only in recent years has analysis of flaws and flaw growth in a large scale plastic field been undertaken with, to date, limited success.

In the situations where flaw growth can be analyzed, the reasons which make the analysis possible are due to the nature and scale of the metallic microstructure. In a crude sense, a metal consists of a crystallographic arrangement of the principal elements with the structure containing substitial and interstitial elements and colonies of the other constituent elements. This crystallographic structure is arranged into grains (subregions of like orientation) and often has two phases (such as in steel or titanium) within a grain. Within these grains and along their boundaries, cracks form and propagate. Although there are numerous exceptions, grain size is usually of the order of .025 to .25 mm (.001 to .01 in.) while the secondary subgrain structure (called "platelets" in titanium) is even smaller. Based on this general microstructural scheme, one can understand the reasons for the small number of situations for which relatively simple crack growth expressions can be formulated.

At the level of the grain or subgrain, crack growth is necessarily complex for as the crack grows all sorts of changes in the crystal structure, element type, and strain field are met. These changes encountered by the moving crack tip result in a rather tortuous crack path. At the microscopic level, the effects of the nucleating and growing cracks can be manifested in three essentially different, though hardly distinct ways. If the remote stress (or strain) is high, plastic flow within the grains is large and the resultant crack growth is complex and no one flaw is likely to be dominant. If stresses are lower, one or a few cracks will propagate to a length beyond that which is grossly affected by the microstructure which allows for the possibility of applying a relatively simple crack growth expression. At still lower stresses, none of the cracks nucleate or propagate quickly which restricts macrostructural damage

MICROCOPY RESOLUTION TEST CHART

NATIONAL BUREAU OF STANDARDS-1963-A
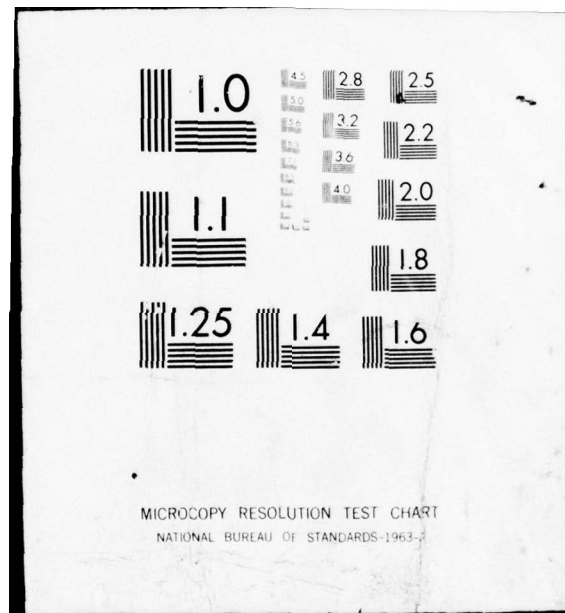
to the accumulated effect of many small cracks locked within the local grain region. In this latter case and in the first case, simple crack growth expressions are difficult to formulate.

The above described three cases are the same regardless of whether the material is "brittle" or "ductile". Of course, the distinction between the three cases and between brittle and ductile is diffuse. Only if the material is relatively brittle can the second case frequently occur in service and one or a few cracks become dominant on a macrostructural level. In all other cases, the macrostructurally observed damage is dominated by the microstructure. Even for the more brittle materials, simple growth rate expressions are not possible until the scale of the crack dominates the scale of the microstructure.

One can see that the success of the expressions is dependent upon the microstructure being such that macrostructural damage growth and failure criterion are not dominated by the microstructural discontinuities. For the restricted class of metal applications where the material is more "brittle" and stresses are such that flaws can develop of a size which dominates the microstructure, analytical expressions for crack (damage) growth and failure criterion have been derived. These expressions come under the general heading of linear elastic fracture mechanics, LEFM.

The assumption is made in LEFM that the metal alloy in static tension or fatigue will fail when the crack-like defect grows to a critical length defined by the expression (see, for example, Reference [33]):

$$K = \sigma f_g \sqrt{a} \qquad\qquad (8)$$

where

$K$ = fracture toughness

$\sigma$ = far field stress

$a$ = crack-like defect length

$f_g$ = function of geometry

Equation (8) is assumed to hold for a metal that is essentially responding in a linear-elastic fashion regardless of whether the load is applied only once as in static tension or repeatedly as in fatigue. The term $f_g$ can be and often is extremely complex. Expressions similar to Equation (8) have been developed to allow limited handling of the situation where greater plasticity occurs (see for example References [34, 35, 36]).

In order to predict the life of a metal component subject to fatigue, Equation (8) is combined with a suitable rate equation of which many have been proposed [32]. The solution to predicting cyclic life prior to failure under fatigue loading is in principle quite simple using Equation (8) and the selected rate equation: the initial flaw size prior to fatigue loading is assumed; the value of K is obtained from static tests and Equation (8); the critical crack length, $a_c$, for the part is calculated; the life is determined by integrating the selected rate equation until the crack length reaches $a_c$. The procedure is assumed to work despite the fact that the manner in which $a_c$ was reached is quite different for a static load as opposed to fatigue loads. In the static case, $a_c$ is the defect size of any notch present prior to loading. Under fatigue loading, $a_c$ is reached by propagation of an initial crack to that size. This outlined procedure is more or less accurate depending on the relative accuracy of the individual steps. The procedure has proven successful in many applications [32].

Equation (8) and the selected associated rate equation, are only valid for the restricted class of metals described above where: the fatigue failure is dominated by a crack-like defect; linear elasticity applies; the values of K obtained from a static test are applicable to the dynamic case. The last point, the major assumption which allows the failure criterion to have practical utility, does not appear to be strictly true. Calculation of K, using Equation (8), at the crack length present when failure occurred often leads to higher values than the value calculated in the static case [37]. This problem is not greatly important because normally the time between when the crack reaches the critical crack length, $a_c$, calculated using a static

toughness value and the actual value of $a_c$ which occurs in fatigue is usually short compared to previous component life. This fact is equivalent to saying that for metals the distribution of residual strengths can be expressed with the fatigue failures included without an undue amount of conservativeness.

At first glance, one might conclude that the limited number of situations meeting the restrictions described above where simple rate equations and failure criteria can be formulated for metals would be small. In fact, however, many practical problems in metal structural applications meet the restricted conditions. For this reason, simple expressions such as Equation (8) have found great utility.

Now that the reasons for the limited success of relatively simple failure criteria and damage growth expressions for metals are understood, the probable situation in composites can be analyzed. In a general sense, damage in composites consists of: fiber fractures and matrix cracks and crazing (within and between the plies). Graphite/epoxy composites have two component materials, fiber and epoxy, both of which respond to load in an essentially brittle fashion. However, as the stress-strain curves of an unnotched composite show, the response of the composite loaded to failure is non-linear and highly inelastic. The reason for this inelastic response is due to the nature of the microstructure and damage processes.

Roughly speaking, the microstructure of a composite consists of the fibers, matrix, and plies. The fibers and matrix are analogous to the two phases of a metal such as titanium except that the strength and elastic moduli of the phases are drastically different. A single ply is analogous to a metallic grain except the scale is large. Within and between the plies cracks can nucleate and propagate. The low modulus of elasticity of the brittle matrix allows a local stress field change due to the fracture of one fiber to be easily redistributed without a significant concomitant macrostructural strength loss. This property of stress redistribution which is much like plasticity allows the two brittle constituents of a graphite/epoxy composite to have metal-like inelastic response.

Keen awareness of how cracks act at the microstructural level in metals can now help in understanding their expected response in composites. A crack in a graphite/epoxy composite should propagate in a highly torturous complex fashion because of the two phase nature of the material. This form of propagation is observed and is similar to the form of propagation seen in a metal (especially a 2-phase alloy) at the microstructural level. Unlike a metal, the "grains" (plies) of a composite are macrosized and therefore we would expect that for a single flaw to dominate the failure response, flaw dimensions would have to be much larger than required in metals. This, in fact, is exactly the situation observed. Flaws in brittle metal alloys can be as small as the order of grain size before complex expressions for failure criterion or growth rate need be written. Thus successfully analyzable flaws can be quite small (.2 mm (.01 in.) or in some cases even less). For composites, the flaw must be of a magnitude similar to that of the ply ("grain") dimension before simple expressions for failure criterion would be successful. Research investigations have strongly supported this contention under both static and dynamic loading (see for example References [38 to 46]) which effectively implies damage zones must be larger than ~25 mm (1.0 in.). This does not imply that linear elastic fracture mechanics cannot be applied to composites, but only that the range of utility will be strongly restricted. In fact, much of the information given in References [38 to 46] may prove to be quite useful when more fully developed.

The above discussion by no means implies that crack (damage) growth or strength degradation concepts are not true for composites. The conclusions are simply that: 1) expressions for these concepts should not be expected to be simple; 2) failure modes under different loading should not be expected to be constant. The latter conclusion is made because different loading types will lead to quite different distributions of fiber and matrix cracks and matrix crazing whose interactional effect will be greatly influenced by the large ply (grain) size resulting in different strength distributions.

The above two conclusions are strongly supported by the data generated in this test program. For example laminate 1, T-T fatigue coupon lives were

dominated by $\sigma_{max}$ at high stress levels, but by $\Delta\sigma$ at low stress levels.
These data suggest that the rate of damage growth is determined by both strain
range and maximum strain. Laminate 2 static tension residual strength coupons
showed no loss in strength after being subjected for $10^6$ cycles to either T-T
or T-C fatigue loadings which resulted in many fatigue failures. However,
these same fatigue load levels caused a reduction in residual compression
strength. These laminate 2 data indicate that the same amount of damage
can result in quite different effects depending on the type of loading.
Finally, one should expect large scatter in the mechanical property data,
especially in the fatigue data, for composites when compared to many metals
because of the highly irregular damage growth pattern caused by the micro-
structure. The expected large scatter, especially in fatigue, was observed
in this test program.

### 7.4.1.3   Nature of Required Failure and Damage Growth Expressions for Composites

The microstructure of a metal has a great influence upon the rate of damage
growth and upon the response of the material to environmental influences
(see as one example Reference [47]). However, microstructural details in
metals are not always manifested macroscopically to the extent that a domin-
ant flaw theory is invalidated. For this reason, linear elastic fracture
mechanics has had a limited, albeit extremely valuable, success in metals.
In contrast, fibrous composites are materials in which microstructural
details are manifested directly at the macrostructural level and thereby
intimately control the defect growth process. This fact renders the develop-
ment of simple useful expressions for growth and failure criteria difficult
to develop. Similarly, the fact that the macrostructural influence and
growth of a damage zone in a composite is strongly affected by the plies
("grains"), and thus also by the layup, invalidates the practical assumption
of a constant mode of fracture or at least the easy expression of the manner
in which the fracture mode changes with loading type.

The above described, admittedly disturbing problem, naturally raises the
question as to whether or not the problem is true for notched as well as

unnotched components. The failure of a constant failure mode assumption and the loss of simple expressions for damage growth and failure criterion for unnotched composites is not necessarily of great importance if the system of assumptions and expressions can be shown to have reasonable validity for most notched components. However, limited investigations into the response of notched coupons would suggest that, at best, the hypothesis of a constant failure mode may have only limited validity for specific layups. Static tests of notched coupons strongly imply that large notches are required if a simple equation for failure criterion is needed [38-46]. Such notched data, whether or not the notch is a circular hole or thin slit, appear to be better correlated with other types of formulations [48].

The static tension failure modes of such notched coupons, regardless of layup appear to be dominated by the stress concentrations at the hole and the induced localized damage at the hole. Failure modes of notched coupons in tension-tension fatigue appear to possibly depend on the layup and/or loading direction. For example, damage growth in quasi-isotropic layups appears to consist of the extension of a damage region from the notch equal to the notch width, consisting of broken $0°$ fibers and $45°$ and $90°$ ply matrix cracking, to the end of the gage length in a plane parallel to the loading direction [49-51]. The failure mode of such a notched damaged coupon would be quite different from that observed under static loading. In layups with no $90°$ plies and a high percentage of $0°$ plies, damage appears to progress in a limited zone in an apparently through thickness plane perpendicular to the loading direction [49-51]. The problem is even more complex in that different failure modes under the same fatigue load cycle and loading direction can apparently occur in the same layup of a notched composite [52]. Even different frequencies can result in different failure modes [53]. Fatigue investigations [54,24] even indicate that residual strength can first increase before decreasing.

The general conclusion is that predicting composite residual strength degradation will require possibly quite complex expressions. At a minimum they will be of a quite different form than those used in linear elastic fracture mechanics for metals.

184

7.4.2    Evaluation of a Strength Degradation Model

Because of the conclusions reached as to the required nature of successful
mathematical formulations for strength degradation in composites, a detailed
analysis of one proposed formulation was undertaken.  This formulation was
chosen because of the relatively simple mathematical expressions and assump-
tions used.  The analysis was expected to show whether or not the conclusions
reached in the foregoing discussion were valid.  In essence, despite the
logic which led to the conclusions, can the simple model be shown to have at
least enough accuracy for engineering utility.  The particular formulation
chosen for analysis will be shown to lead to an inadequate representation
of strength degradation.

One model of strength degradation or "wear-out" for composites is well formu-
lated in References [24-28 and 55-57].  Because much of the discussion in
these references is similar as are the data presented, the following outline
of the model is based upon Reference [24] which contains a complete presen-
tation of the model.  Throughout the discussion which follows, the notation
of Reference [24] will be maintained.  This notational choice allows for easier
comparison of the equations as presented here to the manner in which they appear
in Reference [24].

In this model, the rate of damage growth is assumed to be defined as:

$$\frac{dc}{dt} = MC^r \tag{9}$$

where    $C$  =  damage zone size

             $t$  =  time

             $M \propto$  constant $\cdot W^r \simeq AD^r F_{max}^{2r}$

where    $W$  =  far field work inputted by the environment

             $r$  =  rate exponent

             $A$  =  constant

             $D$  =  effective compliance

             $F_{max}$ = maximum stress level of the external load

185

The criterion for failure is assumed to be:

$$K = F \sqrt{C} \tag{10}$$

where $K$ = toughness. Equations (9) and (10) are analogous to equations formulated in linear elastic fracture mechanics for metallic materials [58, 33]. Because Equation (10) is assumed to apply regardless of the cause of degradation or loading, the corollary assumption is made to join the two equations, namely that the mode of fracture remains constant. This is, of course, similar to the assumption made for Equation (8) for metals.

Based on these three assumptions, the strength at any time, $t$, for the $i$th member of a population can be found by integrating Equation (9) with the aid of Equation (10) which results in:

$$F_i(t)^{2(r-1)} = F_i(t_o)^{2(r-1)} - (r-1) A_4 F_{max}^{2r} (t-t_o) \tag{11}$$

where
$$A_4 = AD^r K^{2(r-1)} \tag{12}$$

Equations (9) and (10) and the associated corollary form the basis of a formulation for modeling strength degradation while Equation (11) describes the strength of a coupon or component at some future time. Equation (11) will have accurate predictive capability if the forms of the equations for rate of degradation and failure criterion were correctly assumed.

At this point, no assumption has been made as to the manner in which the initial and residual strengths, $F(t_o)$ and $F(t)$, are distributed. Their manner of distribution is not of real importance to formulation of the model. Any distribution could be used, such as Normal or Weibull, provided the data are properly described. A 2-parameter Weibull distribution was chosen because the static strength distribution of a composite material could apparently be accurately represented.

186

The 2-parameter Weibull distribution can be combined with Equation (11) and used to derive an equation which, hopefully, accurately predicts the future (residual) strength distribution. Using the 2-parameter Weibull distribution and following Reference [24], the initial static strength distribution, $F(t_o)$, is assumed to be modeled by:

$$P\left[F > F_i(t_o)\right] = \exp\left|-\left(\frac{F}{\hat{F}(t_o)}\right)^{\alpha_o}\right| \tag{13}$$

Equation (13) represents the static strength distribution at time $t_o$ where $\hat{F}(t_o)$ is the characteristic strength and $\alpha_o$ is the shape parameter.

The probability that $F(t) > F$ is just the probability that Equation (11) holds:

$$F(t_o) > \left[F(t)^{2(r-1)} + (r-1) A_4 F_{max}^{2r} (t-t_o)\right]^{\frac{1}{2(r-1)}} \tag{14}$$

By Equation (13), this probability is:

$$P\left[F(t) > F\right] = \exp\left\{-\left[\frac{F(t)^{2(r-1)}+(r-1) A_4 F_{max}^{2r} (t-t_o)}{\hat{F}(t_o)^{2(r-1)}}\right]^{\alpha_f}\right\} \tag{15}$$

where $\alpha_f$ is defined as:

$$\alpha_f = \frac{\alpha_o}{2(r-1)} \tag{16}$$

If the cause of strength degradation is fatigue, as in this investigation, the highest value of probability which can occur for the residual strength distribution is that calculated for the maximum fatigue stress, $F_{max}$. Effectively the residual strength distribution, $F(t)$, is truncated by $F_{max}$. Therefore, assuming $F_{max}$ is significantly less than $F(t_o)$, that $t_o = 0$, and that $t \to \infty$, then $F(t)^{2(r-1)} \to 0$ and:

$$P\left[F(t) > F_{max}\right] = \exp\left[-\frac{t}{\hat{t}_b}\right]^{\alpha_f} \tag{17}$$

187

where
$$\hat{t}_b \, F_{max}^{2r} = \frac{\hat{F}(t_o)^{2(r-1)}}{(r-1) \, A_4} \qquad (18)$$

and where $\hat{t}_b$ is the characteristic fatigue life for the distribution of fatigue lives obtained at $F_{max}$ and $\alpha_f$ is the fatigue life shape parameter.

Equation (17) implies [24], since a constant mode of fracture was assumed, an approximate fixed fatigue life shape parameter, $\alpha_f$, independent of load history, environment, and scale effects. The parameter $\alpha_f$ is related to $\alpha_o$ by Equation (16) and both parameters are assumed to be material variables [24]. If a constant loading rate is assumed during the static strength tests, $\alpha_o$ can be written as [24]:

$$\alpha_o = 2r + 1 \qquad (19)$$

and, thus, by Equation (16), $\alpha_f$ becomes:

$$\alpha_f = \frac{2r + 1}{2(r-1)} \qquad (20)$$

Because $t_o$ is usually taken as time zero, Equation (15) can be rewritten as:

$$P\left[F(t) > F\right] = \exp\left\{-\left[\left(\frac{F(t)}{\hat{F}(t_o)}\right)^{2(r-1)} + \frac{t}{\hat{t}_b}\right]^{\alpha_f}\right\} \qquad (21)$$

Equation (21) is the basic equation of the model with predictive capability because the equation describes the distribution of strength at a future time. The equation is based on the assumed rate equation and failure criterion as well as on a 2-parameter Weibull distribution. Expressions similar to Equation (21) could be derived, of more or less validity, if other distributions describing the static strength were assumed.

If the formulation of a model for wear-out as expressed in Equation (21) is valid, a powerful tool is available for use in engineering design. For

188

example, in theory the characteristic static strength, $\hat{F}(t_o)$, and shape parameter, $\alpha_o$, (and by Equation (16), r) for the static strength distribution of a particular composite could be determined as well as the characteristic life, $\hat{t}_b$, and shape parameter $\alpha_f$, at a particular maximum fatigue stress, $F_{max1}$. Using Equation (18), $A_4$ could be determined using $\hat{t}_{b1}$ and $F_{max1}$ and therefore, from the same equation, $\hat{t}_b$ at any other maximum fatigue stress, $F_{max2}$, could be calculated. Equation (21) could be used to calculate the distribution of static strength at any time t for any other $F_{max}$. Therefore, a limited amount of fatigue testing at a few stress levels would allow prediction of strength degradation caused by any other stress level. In theory, this procedure could be extended to complex fatigue loading and a full scale structure [24]. Because of the potential value of the model, the validity of Equations (18) and (21), and thus, by implication, the assumed growth rate and failure criterion, Equations (9) and (10), will be assessed.

To prove the applicability of this formulation of the wear-out process and the associated Equations (15) or (21), both necessary and sufficient conditions must be satisfied. The necessary conditions are actually mathematical boundary conditions while the sufficient conditions are the specific physical predictions which must be met accurately. Three boundary conditions and at least five separate, although related, sufficient conditions can be formulated. Proof that the boundary conditions are met is not adequate, contrary to the practice [24] used in the composite literature, to prove the validity of the model as formulated in Equations (9) and (10).

This question of necessary and sufficient conditions is not just esoteric. Proof that the necessary or boundary conditions are met proves that Equation (21) has been correctly derived and is internally consistent, a requirement of any mathematical formulation. Proof that the sufficient conditions are met proves that Equation (21) has value to the practicing engineer; in essence, proves that the mathematical formulation actually describes the mechanical properties of composites.

The necessary or boundary conditions consist of the restriction that Equation (21) must be internally valid. The boundary conditions are:

Boundary Condition 1 (BC1): At $t = 0$, Equation (21) must reduce to Equation (13).

This boundary condition can easily be shown to be true.

Setting $t = 0$, Equation (21) becomes:

$$P\left[F(0) > F\right] = \exp\left[-\left(\frac{F(0)}{\hat{F}(0)}\right)^{\alpha_f 2(r-1)}\right]$$

which is the same as Equation (13) since $t_o = 0$ and $\alpha_f = \alpha_o/2(r-1)$. Note that since BC1 is met, this implies that for $t \ll \hat{t}_b$, Equation (21) should fairly accurately predict the residual strength distribution since little strength degradation will have occurred.

Boundary Condition 2 (BC2): The truncated maximum level of probability of survival of the residual strength distribution, $P\left[F(t) > F\right]$, must closely approximate the correct value for the spectrum and associated $F_{max}$ level used to calculate $\alpha_f$ and $\hat{t}_b$.

BC2 is met because for $F(t) \ll \hat{F}(t_o)$:

$$\frac{t}{\hat{t}_b} \gg \left[\frac{F(t)}{\hat{F}(t_o)}\right]^{2(r-1)}$$

and thus Equation (21) reduces to:

$$P\left[F(t) > F\right] \simeq \exp\left[-\left(\frac{t}{\hat{t}_b}\right)^{\alpha_f}\right]$$

which is just the original fatigue distribution and at any time, t, will give essentially the correct, although not precise, truncated value of $P\left[F(t) > F\right]$.

190

Boundary Condition 3 (BC3): At any time, t, the probability of survival for the residual strength distribution must → 0 for F(t) >> F.

This condition can be shown by the fact that for F(t) >> F, then in Equation (21).

$$\left(\frac{F(t)}{\hat{F}(t_o)}\right)^{2(r-1)} >> \frac{t}{\hat{t}_b}$$

and therefore,

$$P\left[F(t) > F\right] \simeq \left| -\left(\frac{F(t)}{\hat{F}(t_o)}\right)^{\alpha_o} \right|$$

This equation does → 0 for F(t) >> $\hat{F}(t_o)$.

The sufficient conditions which must be satisfied to completely prove this particular formulation of the wear-out model, as expressed in Equation (21), are, listed in their order of importance: 1) prediction of probability of survival, $P\left[F(t) > F\right]$, must be correct over the entire range of P for the data obtained at the original $F_{max}$ levels; 2) prediction of both the truncated value of P and all intermediate values at any other $F_{max}$ level must be correct; 3) the residual strength distribution must be smooth when the failures which occurred during fatigue testing are included; 4) Equations (16), (19), and (20) must give essentially the same damage rate exponent, r; 5) failure modes must remain constant.

Now that the specifics of one common formulation of the wear-out model have been expressed, the data of this report and that contained in others can be used to assess the validity of the rate and failure assumptions (Equations 9 and 10). Recall that the analysis of the data should show that the three boundary conditions (necessary conditions) are satisfied and that this does

not constitute proof of the above outlined expression of the theory. Only
if the sufficient conditions are satisfied can the hypothesis be reasonably
considered to have been confirmed.

Consider the quasi-isotropic data for the T300/934 material obtained in this
program. The question arises as to how well Equation (21) models the ob-
served static tensile strength degradation. For this layup and using a
2-parameter Weibull fit and the data of Tables 10 and 11, the static tensile
data for laminate 1 is:

$$F(\hat{t}_o) = 487 \text{ MPa } (70.57 \text{ ksi})$$

$$\alpha_o = 24.1$$

and from Table 24 for the fatigue data, also using a 2-parameter fit:

| Stress Range MPa (ksi) | $t_b$ min | $\alpha_f$ | $F_{max}$ MPa (ksi) |
|---|---|---|---|
| 0 to 400 (0 to 58) | 9.58 | 1.52 | 400 (58) |
| 0 to 345 (0 to 50) | 119.0 | 3.16 | 345 (50) |
| 0 to 290 (0 to 42) | 3321 | 1.64 | 290 (42) |

Average $\overline{\alpha_f}$ =2.11

Using Equation (16), the rate exponent, r, is found to be:

$$r = 6.71$$

and, therefore $2(r-1) = 11.42$

However, based on Equation (19)

$$r = 11.55$$

and by Equation (20)

$$r = 2.35$$

Since the different methods of determining r do not agree, Equation (16) will be used and r will be taken as $r = 6.71$. Using Equation (18), the following values of $A_4$ can be obtained:

| $F_{max}$ MPa (ksi) | $A_4$ |
|---|---|
| 400 (58) | $4.965 \times 10^{-5}$ |
| 345 (50) | $3.012 \times 10^{-5}$ |
| 290 (42) | $1.120 \times 10^{-5}$ |
| Average   $\overline{A_4}$ = | $3.032 \times 10^{-5}$ |

The term $A_4$ can be seen not to be a constant contrary to the implications of Equation (18). In order to continue, $A_4$ must be considered as a constant therefore the average value of $3.032 \times 10^{-5}$ will be used.

To evaluate the formulated model, the strength distribution at the two lower stress levels as represented by Equation (21) will be compared to the actual residual strength data discussed in Section 6. The time values at probability of survival of $P_{.90}$ are:

| $F_{max}$ MPa (ksi) | t, min |
|---|---|
| 345 (50) | 52.3 |
| 290 (42) | 606.7 |

Tables 35 and 36 and Figures 83 and 84 compare the distribution given by Equation (21), to the nominal distribution based on Equation (2) of Section 2.6. In both Tables 35 and 36, only the data from the first 20 coupons fatigue tested to determine static tension residual strength were used. Failures which occurred during the fatigue tests were included as per the modeling procedure. Note in these tables and figures, that for $F_{max}$ = 345 MPa (50 ksi), the calculated values of $P_s$ determined using Equation (21) were

193

## TABLE 35

PREDICTED AND ACTUAL PROBABILITY OF SURVIVAL VALUES AT $F_{max}$ = 345 MPa (50 ksi)

| Index | Failure Stress, MPa (ksi) | Probability of Survival $P_s$ | Probability of Survival, Based on Equation (21) $P_s$ |
|-------|---------------------------|-------------------------------|-------------------------------------------------------|
| 1 | 345 (50.0)[a] | 0.95 | .824 |
| 2 | 376 (54.6) | 0.90 | .799 |
| 3 | 398 (57.7) | 0.85 | .763 |
| 4 | 399 (57.9) | 0.80 | .759 |
| 5 | 407 (59.0) | 0.75 | .739 |
| 6 | 412 (59.8) | 0.70 | .722 |
| 7 | 418 (60.6) | 0.65 | .701 |
| 8 | 425 (61.6) | 0.60 | .670 |
| 9 | 444 (64.4) | 0.55 | .548 |
| 10 | 444 (64.4) | 0.55 | .548 |
| 11 | 455 (66.0) | 0.45 | .451 |
| 12 | 456 (66.2) | 0.40 | .437 |
| 13 | 462 (67.0) | 0.35 | .381 |
| 14 | 465 (67.5) | 0.30 | .344 |
| 15 | 478 (69.3) | 0.25 | .207 |
| 16 | 482 (69.9) | 0.20 | .165 |
| 17 | 492 (71.4) | 0.15 | .076 |
| 18 | 494 (71.7) | 0.10 | .063 |
| 19 | 494 (71.7) | 0.10 | .063 |
| 20 | 501 (72.6) | 0.00 | .032 |

a - Coupon failed in Fatigue

TABLE 36

PREDICTED AND ACTUAL PROBABILITY OF SURVIVAL VALUES AT $F_{max}$ = 290 MPa (42 ksi)

| Index | Failure Stress, MPa (ksi) | Probability of Survival $P_s$ | Probability of Survival, Based on Equation (21) $P_s$ |
|---|---|---|---|
| 1 | 290 (42.0)[a] | 0.95 | .972 |
| 2 | 290 (42.0)[a] | 0.95 | .972 |
| 3 | 339 (49.2) | 0.85 | .967 |
| 4 | 367 (53.2) | 0.80 | .959 |
| 5 | 401 (58.2) | 0.75 | .928 |
| 6 | 403 (58.5) | 0.70 | .925 |
| 7 | 404 (58.6) | 0.65 | .924 |
| 8 | 409 (59.4) | 0.60 | .913 |
| 9 | 410 (59.5) | 0.55 | .912 |
| 10 | 417 (60.5) | 0.50 | .895 |
| 11 | 418 (60.7) | 0.45 | .891 |
| 12 | 427 (62.0) | 0.40 | .860 |
| 13 | 427 (62.0) | 0.40 | .860 |
| 14 | 440 (63.8) | 0.30 | .798 |
| 15 | 468 (67.9) | 0.25 | .521 |
| 16 | 474 (68.8) | 0.20 | .433 |
| 17 | 476 (69.0) | 0.15 | .413 |
| 18 | 480 (69.6) | 0.10 | .350 |
| 19 | 490 (71.1) | 0.05 | .199 |
| 20 | 499 (72.4) | 0.00 | .095 |

a - Coupon failed in Fatigue
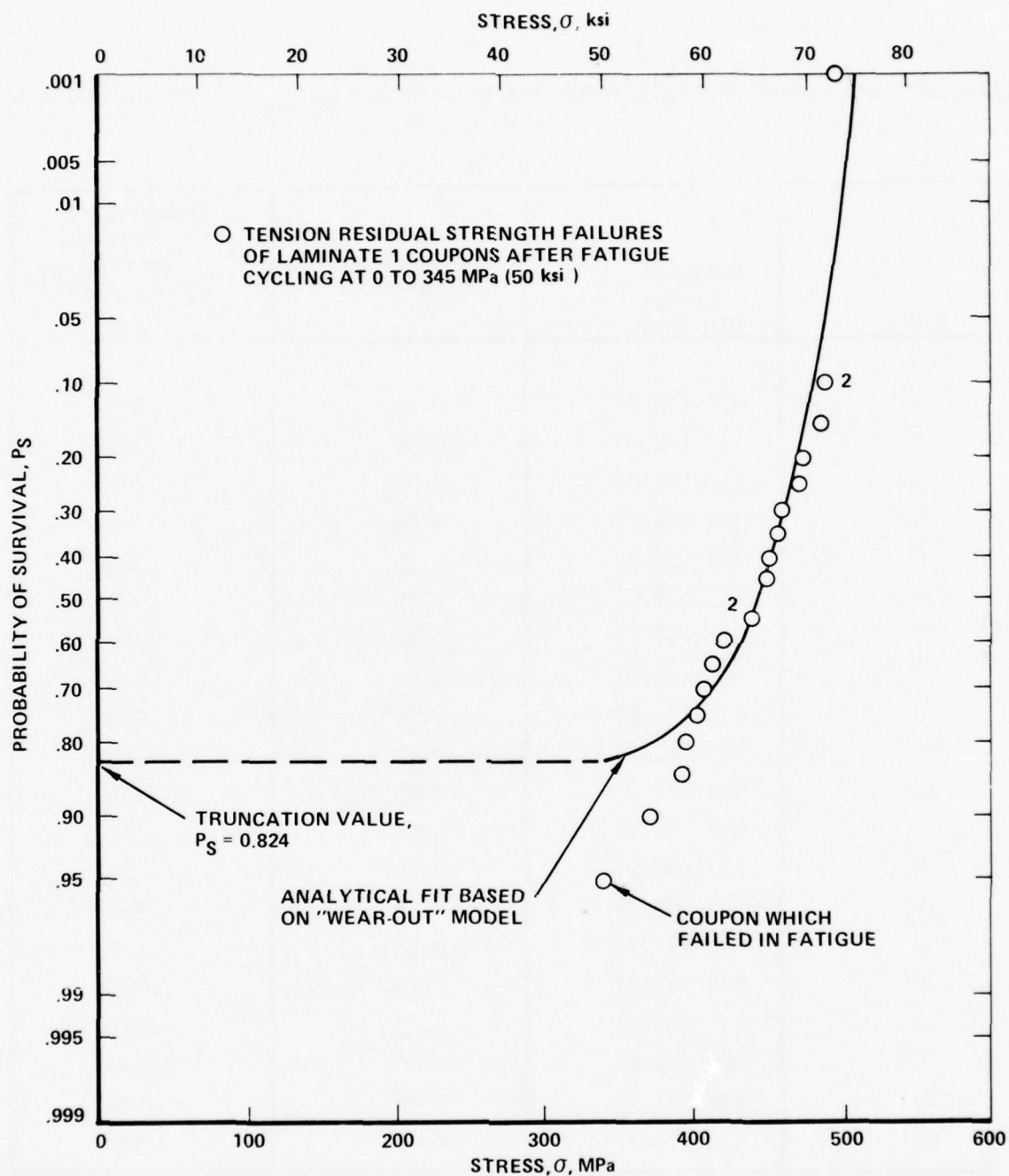
Figure 83. Comparison Between Analytical Fit and Laminate 1 Static
Tension Residual Strength Data for Specimens Prior Fatigue
Tested at 0 to 345 MPa (50.0 ksi)
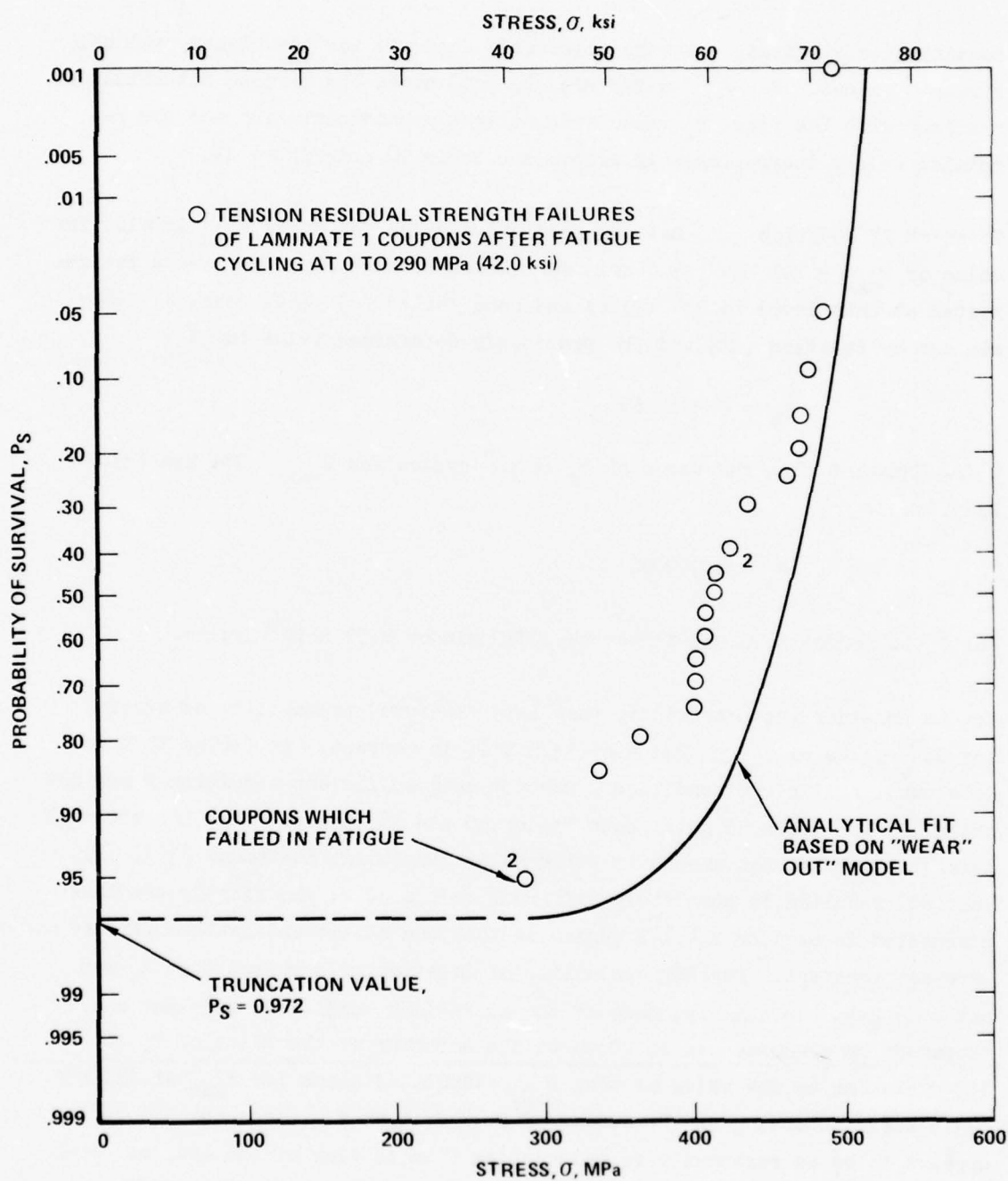
Figure 84. Comparison Between Analytical Fit and Laminate 1 Static Tension Residual Strength Data for Specimens Prior Fatigue Tested at 0 to 290 MPa (42.0 ksi)

conservative at first, but were reasonably accurate for the higher residual strength values. For $F_{max}$ = 290 MPa (42 ksi) data, the reverse situation occurred with the first $P_s$ value being slightly unconservative and the remaining values increasingly in error, see Table 36 and Figure 84.

To check if Equation (21) has any predictive value for other $F_{max}$ levels, the value of $F_{max}$ = 231 MPa (33.5 ksi) was chosen because 20 coupons were fatigue tested at this level to $10^6$ cycles and none failed. In this case, $\bar{t}$ = 1667 min and by Equation (18) and the previously determined value for $\bar{A}_4$:

$$\hat{t}_b = 44371 \text{ min}$$

Using Equation (21), the value of $P_s$ at $10^6$ cycles for $F_{max}$ = 231 MPa (33.5 ksi) is:

$$P_s = 0.999006$$

For $P_s$ to reduce to 0.95, t must be 10849 min or 6.51 x $10^6$ cycles.

Let us consider the possibility that this predicted probability of survival for $10^6$ cycles at $F_{max}$ = 231 MPa (33.5 ksi) is correct. As Tables 35 and 36 showed, sufficient condition 1 was not met; sufficient condition 2 was not satisfied for Table 35 data; both Tables 35 and 36 indicate that the residual strength data are not smooth if failures are included; Equations (16), (19) and (20) resulted in completely different values of r; and finally previous discussion in Section 7.4.1.1 suggested that the static and fatigue failure modes were not constant. Further, evaluation of Equation (17) showed that $A_4$ was not constant. In summary, none of the sufficient conditions were met and therefore no credence can be given to the accuracy of the value of $P_s$ at $10^6$ cycles or to the value of t at $P_{.95}$ calculated above for $F_{max}$ of 231 MPa (33.5 ksi). Guessing at the values of $P_{.90}$ or t at $P_{.95}$ from the S-N curve appears to be as reasonable as calculating them in view of the lack of correlation between the experimental data and that predicted by the model. This latter point can, of course, only be proven by actually testing a large coupon sample size to failure at $F_{max}$ = 231 MPa (33.5 ksi).

198

To explore the last question more fully, one can inquire whether the data obtained at $F_{max}$ = 400 MPa (58 ksi) and $F_{max}$ = 345 MPa (50 ksi) can be used to predict the known residual strength distribution for $F_{max}$ = 290 MPa (42 ksi). In this case, $\alpha_f$ = 2.34 and by Equation (16) r = 6.15, and $\overline{A}_4$ is 3.9885 x $10^{-5}$. From Equation (18), $\hat{t}_b$ for $F_{max}$ = 290 MPa (42.0 ksi) is calculated to be 587 min which is unrealistically low compared to the actual value of 3321 min. The calculated truncated value of $P_s$ corresponding to t = 606.7 min is 0.336 which is much lower than the actual value of 0.95. This lack of consistency is not unexpected since the sufficient conditions were not met and because the data above $F_{max}$ = 345 MPa (50 ksi) were previously noted to be apparently dominated by $\sigma_{max}$ while at lower stress levels, $\Delta\sigma$ was dominant. The lack of correlation at $F_{max}$ = 290 MPa (42 ksi) between the actual probability of survival value, 0.95, and the predicted value, 0.336, is a further indication of the inadequacy of the present formulation of the model to correctly describe the data obtained in this program.

In view of these disappointments, one is led to reconsider how well the data presented in Reference [24] actually fit the model formulation. The data of Reference [24], Figures 9 and 10, are reproduced in Figures 85 and 86. Figure 85 appears to indicate that, as expected, the boundary conditions were met. Between the limits of $P_s$, the predicted residual strength distribution fits the actual data, at best, poorly. The data of Figure 85 do not support the formulation of the wear-out model as given by Equation (21). The values of r = 5.64 and $\alpha_o$ = 12.3 are given in Reference [24] for these data. Therefore, from Equation (20), $\alpha_f$ can be found to be 1.32 which also checks with Equation (16). No indication is given in Reference [24] whether or not the failure modes remained constant or whether the residual strength distributions were smooth when the fatigue failures were included.

The data in Figure 85 again indicate, as expected, that the boundary conditions are met. As discussed above, that these conditions were met does not constitute sufficient support for the accuracy of Equation (21). Between the extremes of $P_s$, the fit of the model curve to the data appears to be reasonably good
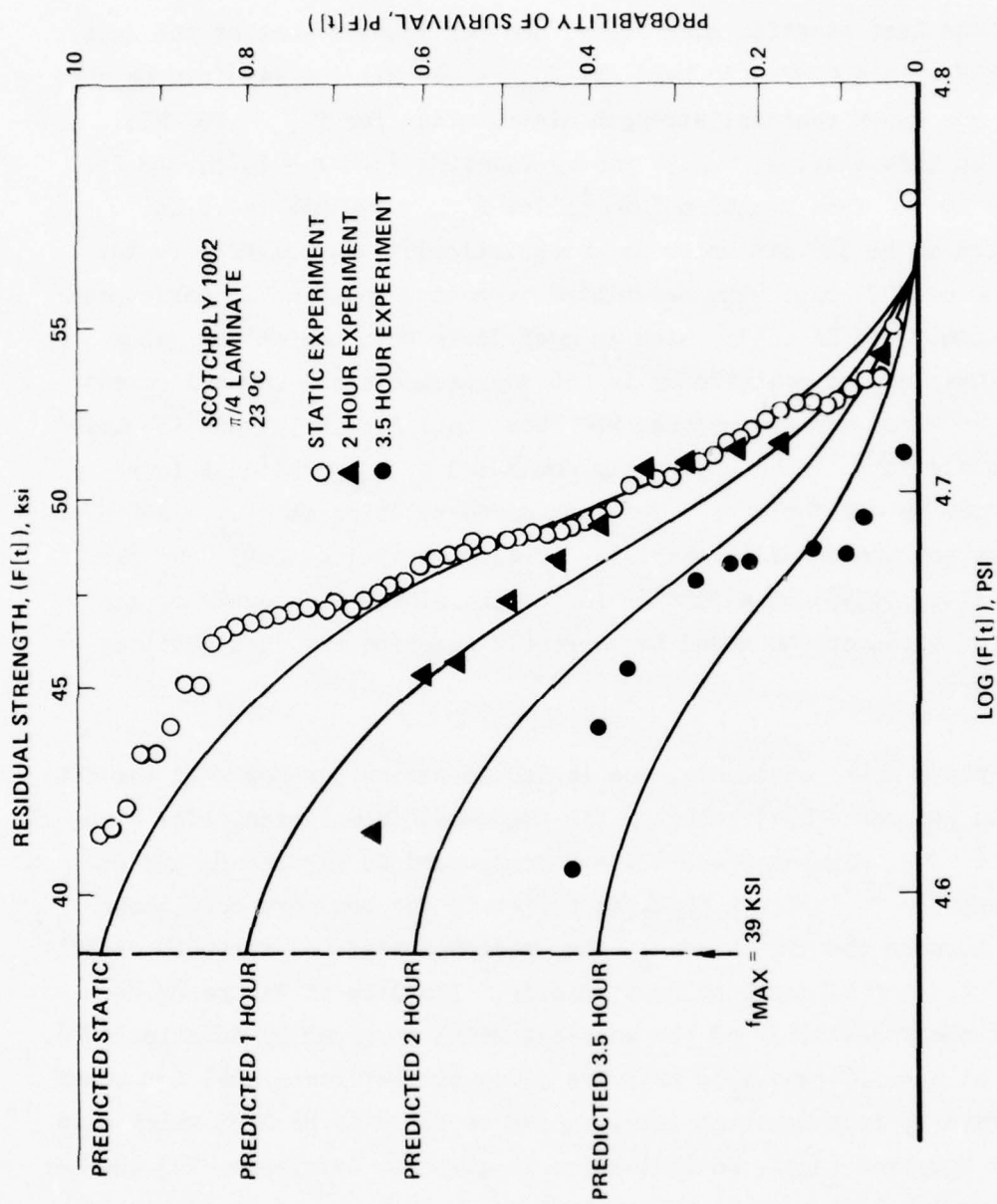
Figure 85. Residual Strength Degradation with Time for a Composite Material; Comparison Between Theory and Experiment (Figure Duplicates Figure 9 of Reference 24)

200
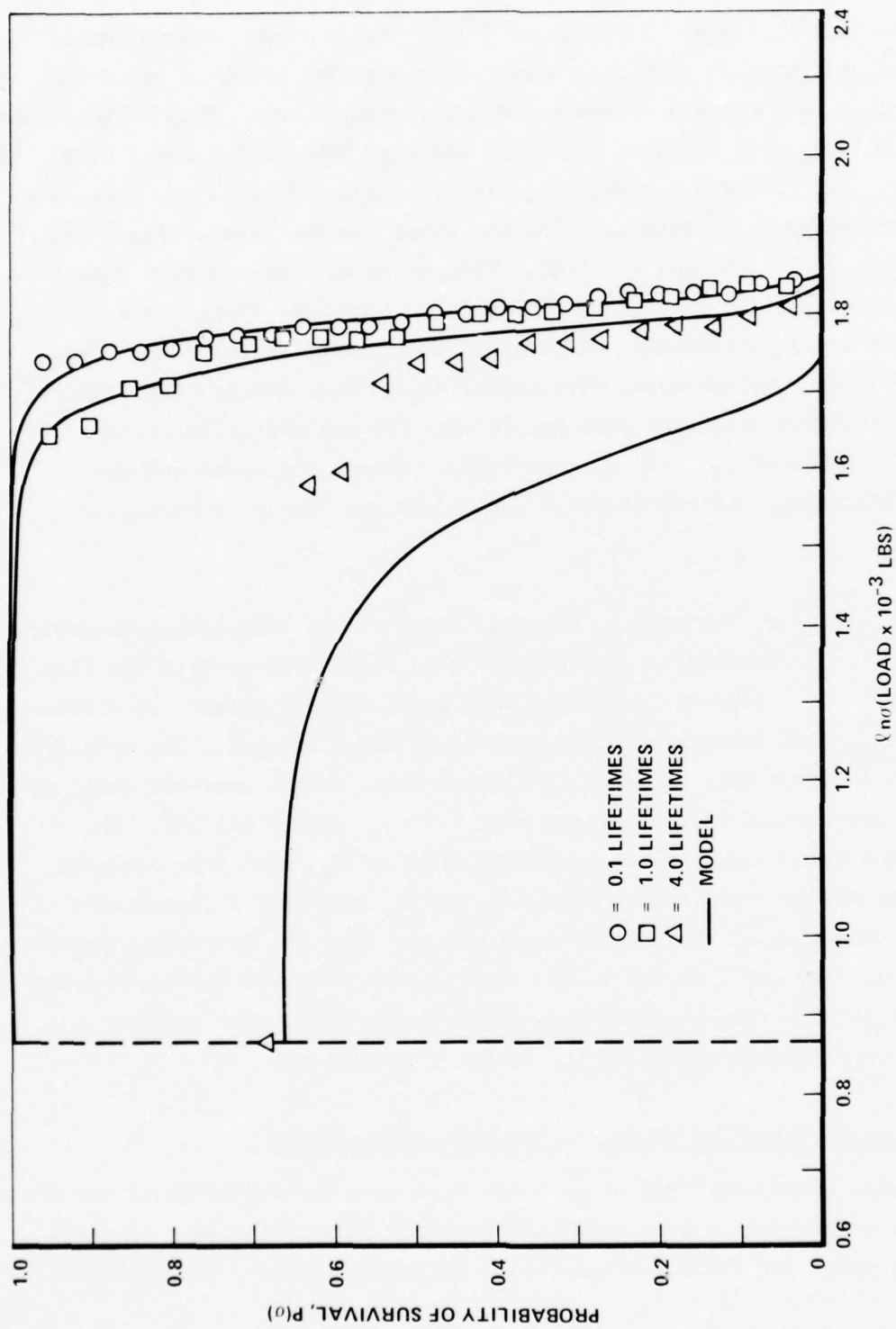
Figure 86. Residual Strength Degradation and Truncation with Time for a Bonded Joint; Comparison of Theory and Experiment (Figure Duplicates Figure 10 of Reference 24)

201

for the 0.1 lifetime data. However, at 1 lifetime, a close examination of the data as presented in this figure reveals a poor fit which is partially masked by this form of data presentation. For example, at $\sim$ 26.9 kN (6050 lbs) ($\ln \sigma = 1.80$), $P_s$ from the data is $\simeq$ 0.39 and from the model curve $\simeq$ 0.09. At 4 lifetimes, the fit of the model curve is clearly inadequate. In Reference [24] the coefficients of Equation (21) are given for the data of Figure 86 as $\alpha_o = 32.5$, $\alpha_f = 4.35$, and $r = 4.73$. This value of r checks with Equation (16), but Equation (19) gives $r = 15.75$ and Equation (20) gives $r = 1.45$. These values are inconsistent. No information is given in Reference [24] as to whether the failure modes were indeed constant or whether the distributions of residual strengths were smooth when the fatigue failures were included. In view of the lack of correlation between the model and the data, see Figure 86, neither of these conditions are likely to have been satisfied.

Summarizing the above discussion, the real value of any formulation to describe the wear-out or strength degradation rate is to accurately predict the time to first failure of coupons or components undergoing fatigue loading at different levels of $F_{max}$ than those previously used to obtain life data. The data from this report indicate that any such prediction based on the wear-out model as formulated above would have a low accuracy and thus little utility. The fact that the model predicts the truncated value of $P_s$, with fair accuracy, for the data set or sets used to obtain $\alpha_f$ and $\hat{t}_b$ is simply a fulfillment of a boundary condition of the derived equations and does not constitute proof of the model. The model is not needed for prediction of the truncated value of $P_s$, because this value is already known from the data. The model is inadequate beyond satisfaction of the boundary conditions.

### 7.4.3 Summary; Direction of Future Research and Analysis

The discussion given above had as an overall purpose ascertainment of the characteristics required of a successful mathematical formulation of a strength degradation model for fibrous composites. Any model requires the mathematical

expression of three assumptions: 1) the nature of the degradation rate; 2) the criterion of failure; 3) the relationship between failure modes under static and dynamic loading. In order to discern the required complexity of the model an outline of physical observations and principles was described which included: distribution of damage growth and failure modes in unnotched coupons; a determination of the microstructural reasons for the limited success of strength degradation models in metals; description of the nature of the fibrous composite microstructure and comparison to metals; and a short investigation of the complexity of observed damage growth and failure modes in notched composites.

The discussion of the physical principles underlying composite strength degradation led to a number of expected mechanical responses for a composite which were observed in this research program. The general conclusion of this study is that the form of the mathematical expressions necessary for successful prediction of strength degradation in composites should be expected to be quite complex. The reason for this is due to the fact that damage zone sizes of practical consideration will usually be significantly smaller than the dominant microstructural detail which is the ply. Essentially, damage growth and failure properties are macrostructurally complex in composites requiring the development of relatively complicated rate and failure formulations.

Because of the disturbing nature of this general conclusion for engineering analysis and component life prediction, one proposed relatively simple model of strength degradation was appraised to discern if the conclusion was indeed valid. The appraisal of the simple model strongly showed that the form of this model for strength degradation was inadequate for engineering utility. Although other simple strength degradation models [59] were not assessed, they should be carefully evaluated in the light of physical principles discussed here and the results of the appraisal of the degradation model of Reference [24]. Most likely, other such simple models will show superficial success which will not stand up to rigorous examination.

Because of the conclusions reached in this discussion section, the question naturally arises as to what can be substituted for simple models of strength degradation in composites. One must recognize three basic points before this question can be answered: 1) no successful formulation is likely to be simple or even general; 2) development of new formulations will be difficult; 3) no viable solutions are presently available as substitutes. In view of these three points, life and strength degradation prediction for composites will have to rely in the near future on experimentally generated static and fatigue data just as is true for most metal components.

Over the longer term, this discussion section has indicated the considerations necessary for successful analyses and mathematical formulations, namely; emphasize the macroscopically inhomogeneous nature of fibrous composites; consider in detail the general characteristics of damage growth; carefully observe, describe and record failure modes. Analytical derivations which carefully consider the above described considerations will lead to phenomenological explanations of fatigue life and fracture strength prediction rather than more general degradation models such as those in References [24-28 and 55-57]. Numerous attempts at developing such phenomenological explanations and theories, using finite elements, linear elastic fracture mechanics, and other concepts, have been considered some of which are listed in References [38-46, 52, and 60-64].

Unfortunately, none of these attempts are adequate, because the derived mathematical formulations contain two or more experimentally based parameters without real physical significance. The formulations, which are in many cases relatively complex, are primarily curve fitting procedures which only apply to a restricted set of experimental results (see Reference 65 for a more complete discussion of this point). What is needed is a mathematical model with predictive and extrapolative capability which incorporates the various micromechanical failure processes [65]. The model developed by Kannenen, Rybicki and Griffith [66] attempts to solve the problems raised in this discussion section by treating the material as heterogenous where microstructural effects predominate and as a homogenous anisotropic continuum where they are not. Perhaps their paper best indicates the direction for future effort.

204

## 7.5   Applications to Design

All of the results discussed in this report apply only to narrow unnotched coupons. The major question for the application of composites to aerospace structural usage is whether test results on small laboratory coupons can be directly or indirectly applied to structural analysis and design. The situation for composites is analogous to that of metals where the application of laboratory coupon results to practical design questions remains a problem. However, within reasonable limitations, several procedures have been success-fully applied in metals to scale-up laboratory coupon test results.

Two problems are of major concern when considering the data of this report. First, because only unnotched coupons were used, the data must be used with caution because in practical application fatigue failures originate in the region of notches. Second, the question arises as to whether fatigue or static test results for narrow coupons are the same for wide panels. In regard to the second problem, because of the apparent differences in the two fatigue failure modes for the two laminates considered in this program, test results for wide panels compared to narrow coupons are expected to be different for the two laminates. Scaling to wide panels from narrow coupons is probably laminate dependent. Future composite research must be oriented, in part, towards ascertaining the extent of the difference in mechanical behavior between wide panels and narrow coupons.

In regards to employing insights into material properties gained from programs such as this one, the reference by Anthony [67] is pertinent. Anthony made a number of observations in 1972 most of which have been confirmed by this pro-gram. Quoting at length, Anthony observed:

1.   The fracture of composites and the fatigue of both metals and composites appears to be statistical in nature.

2.   Of prime importance in statistically defining material behavior is the low probability of failure tail of the strength distribution.

3. A large number of statistical distribution functions are available for defining material behavior.
4. Despite the availability of many mathematical expressions or distribution functions, it is difficult to accurately define property distributions in the tail regions.
5. The extensive data generation required to improve the definition of tail regions is expensive.
6. Since there are usually a number of possible failure locations the allowable probability of failure at any one location is lower than that for the aircraft.
7. For composites some relatively low loads have a degrading effect.

His proposed solution to the problem of handling the tail of the data distribution is interpolation from a threshold strength rather than extrapolation from a curve fit.

A research question which should be of future interest is whether or not a threshold for fatigue failures exists in a practical sense. Since at most of the stress levels examined in this study, scatter in the fatigue data was large, the question of the existence of a practical threshold should be of major interest to the designer. Possibly, potential service failures due to fatigue can be prevented by restricting ultimate strains below the threshold value. This concept is similar to that proposed [67] for static strength values. The concept of a threshold seems to be of far more value to the designer of aircraft than the concept of strength degradation.

# SECTION VIII

## CONCLUSIONS AND RECOMMENDATIONS

### 8.1    Conclusions

Based on the results of this program, several major conclusions have been drawn. Conclusions pertain specifically to narrow width coupons of a type similar to that used in this research program. However, with proper concern for complexity scale-up, the conclusions are believed to have some general validity.

o   Consistent well-controlled coupons were manufactured with low variability in geometry and material characteristics such as void content and fiber volume.

o   The tensile stress-strain response of laminate 1 coupons was linear followed by a curved region prior to a brittle-like failure while that of laminate 2 was essentially linear to failure.

o   Laminate 1 coupons exhibited more delamination after static tensile failure than laminate 2 coupons.

o   In some laminates, off-axis plies can dominate the failure mode even though they make up only one-third of all plies in the laminate.

o   The static tensile strength and apparent modulus of laminate 2 coupons were higher than laminate 1 coupons and exhibited slightly more scatter, but the strains to failure were similar.

o   Variation in tensile strength among the same laminates made from different batches of the same material manufactured early in batch shelf life was small.

o   The static compression strength and modulus of laminate 2 exceeded that of laminate 1 and had somewhat less scatter.

o   The Poisson's ratio of laminate 2 was approximately 0.63 and that of laminate 1 approximately 0.28.

o   Both laminates showed large data scatter during fatigue loading and a dependence of fatigue life on maximum stress. This was especially noticeable for laminate 1.

207

o   Compression markedly reduces fatigue life with a greater reduction corresponding to a larger compression load excursion.

o   The effect of compression can not be reliably correlated over all stress levels on either stress range or maximum stress.

o   A fatigue life endurance limit appears to exist, but is not definitively proven.

o   Fatigue data scatter was greater for laminate 2 than for laminate 1.

o   Laminate 2 coupons subjected to fatigue are susceptible to first cycle failures at strain levels significantly below that necessary for static failure.  This response was not true of laminate 1 coupons.   The cause of this effect remains unknown.

o   The tensile and compressive residual strengths of laminate 1 coupons degraded due to fatigue cycling.

o   The tensile residual strength of laminate 2 coupons did not degrade after $10^6$ fatigue load cycles at stress levels at which other coupons failed in fatigue.

o   The compressive residual strength of laminate 2 coupons at the stress range studied degraded after $10^6$ fatigue load cycles.

o   The apparent modulus of elasticity of laminate 2 coupons under compressive loading increased.  This was most likely due to moisture absorption and redistribution of residual stresses.

o   The difference in mechanical response between laminate 1 and laminate 2 was large.  The nature of the difference appeared to be similar to that observed in different heat treatments of a metal alloy and thus there is hope that such differences can be analyzed and understood.

o   Differences in the mechanical response of composite laminates may possibly be more easily correlated on the basis of the average strain to failure as opposed to the average ultimate stress.

o   A 3-parameter Weibull fit to fatigue data appears to be significantly superior to a 2-parameter fit at high probability of survival levels.

o   Extrapolation of fatigue (and possibly static) data to the most important region of concern to aerospace designers, namely in excess of $P_{99}$, appears to be, at present, inadequate even using a 3-parameter Weibull fit.

o The recommended minimum number of coupons needed to describe the extent of fatigue scatter inherent in presently used composites is 20. However, even this number only allows calculation to a probability of survival level equivalent to $P_{.95}$. To determine $P_{.99}$, 100 coupons may have to be tested.

o Present models of residual strength degradation are inadequate.

o A major question remains as to whether test results obtained using small coupons can be extended to large coupons or structural panels.

## 8.2   Recommendations

Based on the conclusions listed in Section 8.1, the following recommendations for future research work in composite materials are suggested.

o Determine whether the mechanical response of wider and larger coupons is the same as for narrow coupons.

o Investigate the techniques needed to improve prepreg, panel fabrication, and machining quality such that mechanical property scatter is reduced.

o Investigate those material properties which can result in fatigue failure of some coupons under loading conditions which do not degrade the properties of other coupons.

o Determine the cause of laminate 2 first cycle fatigue failures.

o Further investigate the possibility of using strain as a comparison parameter instead of stress.

o Investigate the effect of environment and temperature upon the scatter of the data and the response of the material to compressive load excursion during fatigue loading.

o Investigate the effect of holes and notches under similar loading conditions as those used in the research program.

o Extend analytical and experimental investigations into the phenomenological characteristics of damage growth and failure for developing strength and life prediction models.

o Investigate whether a threshold for fatigue failure exists in a practical sense and determine whether or not the threshold value for different layups can be related on the basis of strain.

T300/934 GRAPHITE/EPOXY LAMINATE AND
TEST SPECIMEN FABRICATION PROCEDURE
AFML Contract F33615-75-C-5118

1. Material Storage - All material shall be stored in sealed moisture-proof bags in refrigerators maintained at -18 ± 12°C (0 ± 10°F). Storage time shall not exceed six months.

2. Open Time - All material shall be laid up and cured within a total cumulative time of 72 hours out of refrigerators. Material shall be removed from refrigerators for at least one hour before removal from covering bag.

3. Receiving Tests - Each batch of prepreg shall be sampled and tested in accordance with Lockheed Material Specification C-22-1379/111.

4. Tool and Caul Plates for Curing - All tool plates used for curing laminates shall be aluminum. Thickness of the caul plate shall be 12.7 mm (0.500 in.) with a tolerance of ± 0.08 mm (± 0.003 in.), flat and parallel. Caul plates used on top surface of laminate under the vacuum bag shall be aluminum sheet (1.62 mm (0.064 in.) standard thickness).

5. Lay-Up Procedure - Panels shall be laid up using 305 mm (12 in.) wide prepreg graphite/epoxy (T300/934) tape as the base material. Tape shall be laid with a gap tolerance of 0 to 0.8 mm (0 to 0.031 in.). A check-off system shall be used by the lay-up operator to assure proper orientation of the tape edge (within ± 2° of an oriented template) and stacking sequence of each ply in the laminate. All panels shall be laid up oversize to allow for 25.4 mm (1.0 in.) trim minimum on all edges of the panel to avoid edge taper and resin content variables of panels as laminated.

Laminate 1 panels shall be approximately 610 x 660 mm (24 in. x 26 in.) while Laminate 2 panels shall be approximately 965 x 1372mm (38 x 54 in.).

6. Bleeding and Bagging Procedure - The bleeding and bagging materials used for curing laminates 16 plies thick are listed in sequence starting from surface of curing plate as follows:

    (1) Release film (Teflon)
    (2) Two plies Mochburg CW1850 Bleeder paper
    (3) One ply of porous Teflon-coated glass cloth (duPont Armalon)
    (4) Graphite/epoxy laminate (Laminate 1 or 2)
    (5) One ply porous Teflon-coated glass cloth (duPont Armalon)
    (6) Two plies Mochburg CW1850 bleeder paper
    (7) Release film (Teflon)
    (8) Caul plate (aluminum 1.62 mm (0.064 in.) thick).
    (9) Glass boat cloth (vacuum distribution)
    (10) Nylon bag (Vac-Pac 0.076 mm (0.003 in. thick))

The nylon bag is sealed to the cure plate with sealing putty (Presstite No. CS12-4). The bag seal and bag shall be carefully checked for leaks under vacuum before the cure cycles are started.

7. Cure Procedure - The thermocouple shall be placed on the caul plate adjacent to the laminate and the complete time-temperature history of each laminate monitored and recorded on a strip chart. The cure cycle used for T300/934 material shall be as follows:

    (1) Apply full vacuum 88-98 x $10^3$ Pa (26-29 in.Hg)
    (2) Raise temperature to 121°C (250°F) at average of 1-2°C (3-4°F) per minute
    (3) Dwell at 121°C (250°F) for 15 minutes with vacuum pressure
    (4) Apply 0.69 MPa (100 psi) pressure plus vacuum and hold at 121°C (250°F) for 45 minutes
    (5) Raise temperature to 177°C (350°F) at 2-3°C (3-5°F) per minute
    (6) Hold at 177°C (350°F) and 0.69 MPa (100 psi) plus vacuum for 2 hours

212

(7) Cool to 82.2°C (180°F) under vacuum and pressure while recording cool-down rate

(8) Cool to 65.6°C (150°F) under vacuum only while recording cool-down rate.

8. Resin Content and Voids - The average resin and void content of each panel fabricated shall be determined. Resin content shall be maintained at 28-31 wt.% (60-65 vol.% fiber). Void content shall be 2.0% max. by volume.

9. Non-Destructive Inspection - Each panel shall be inspected using ultrasonic C-scan techniques. Results for Laminate 1 panels shall be compared to a reference panel standard containing known voids at specified depths and of specified sizes as shown in Figure 1A. For Laminate 2 panels, results will be compared to known voids placed in each panel as shown in Figure 2A.

10. Fabrication and Bonding of Glass Fabric/Epoxy Grip Tabs - Grip tab sheet material shall be fabricated by laminating eight plies of 1581 glass/ fabric/epoxy to make a laminate 1.65-1.78 mm (0.065-0.070 in.) thick. The material to be used is Fiberite Corp. MXB-7701/1581 glass fabric/ epoxy prepreg conforming to Lockheed material specification LCM C22-1032/ 131. This material is to be cured at 121°C (250°F) for one hour under a pressure of 0.34 MPa (50 psi) plus vacuum.

The glass fabric/epoxy laminate shall be cut into 76.2 mm (3 in.) wide strips to be located on graphite panels in preparation for bonding as shown in Figures 3A and 4A. After all preliminary machining is done, glass tabs shall be thoroughly cleaned by wiping with methyl-ethyl-ketone solvent. The adhesive film shall then be cut to size and applied to glass/epoxy tab strips which are located on the test laminate with 1.59 mm (0.0625 in.) rivets placed in pre-drilled holes in trim area on the panel.

The adhesive used shall be American Cyanamid Co. FM-137 film 0.96 Kg/m$^2$ (0.06 lb/ft$^2$) conforming to Lockheed Specification LCM 30-1085 Type II, Grade A. Spacers used between tabs next to curing plate shall be constructed of the same glass fabric epoxy sheet used for fabricating tabs using 0.127 mm (0.005 in.) Teflon film next to graphite/epoxy laminate.

The laid up panels shall be bagged and cured in an autoclave at 121$^o$C (250$^o$F) for one hour with a pressure 0.34 MPa (50 psi) plus vacuum.

11. Panel and Coupon Identification - All panels and coupons shall be clearly marked before and after application of tabs to indicate the bag side of the graphite/epoxy laminate as originally cured. Panels shall be identified with a number including material code and autoclave run number. Coupons shall be identified with panel number from which cut and dash numbers.

    Example: ILY 556-1A

    Coupons shall be numbered consecutively as they are cut from panels to indicate relative location in the panel (see Figure 3A for Laminate 1 and Figure 4A for Laminate 2).

12. Machining of Coupons - Coupons of the configuration shown in Figure 5A shall be machined from each panel as per Figure 3A or Figure 4A. Coupons shall be machined dry using a 152.4 mm (6 in.) diameter, 40 tooth carbide cutter at 250 ± 10 rpm and at a feed rate of 304.8 ± 25.4 mm/min (12 ± 1 in./min).

13. Performance Requirements - Laminate panels shall be rejected if review of fabrication records reveals that prepreg did not meet Item 3 and laminates did not meet Items 9 and 10 of this fabrication procedure. In addition, finished coupons shall be measured for width in four (4) places and for thickness in eight (8) places as per Figure 6A. Coupons shall be rejected if all width measurements are not 22.22 ± 0.07 mm (0.875 ± 0.003 in.) and if thickness is not within ± 0.05 mm (± 0.002 in.) of the average of eight thickness measurements.

214
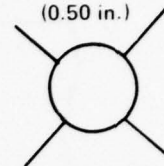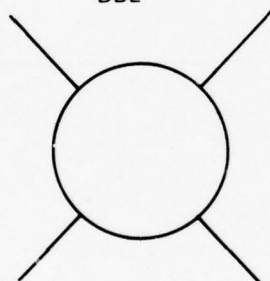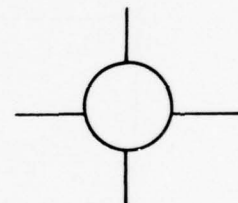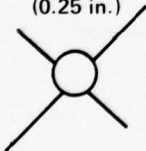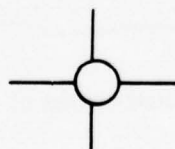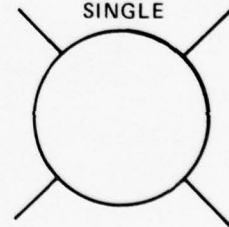
Figure 1A. Template for Laminate 1 Panels
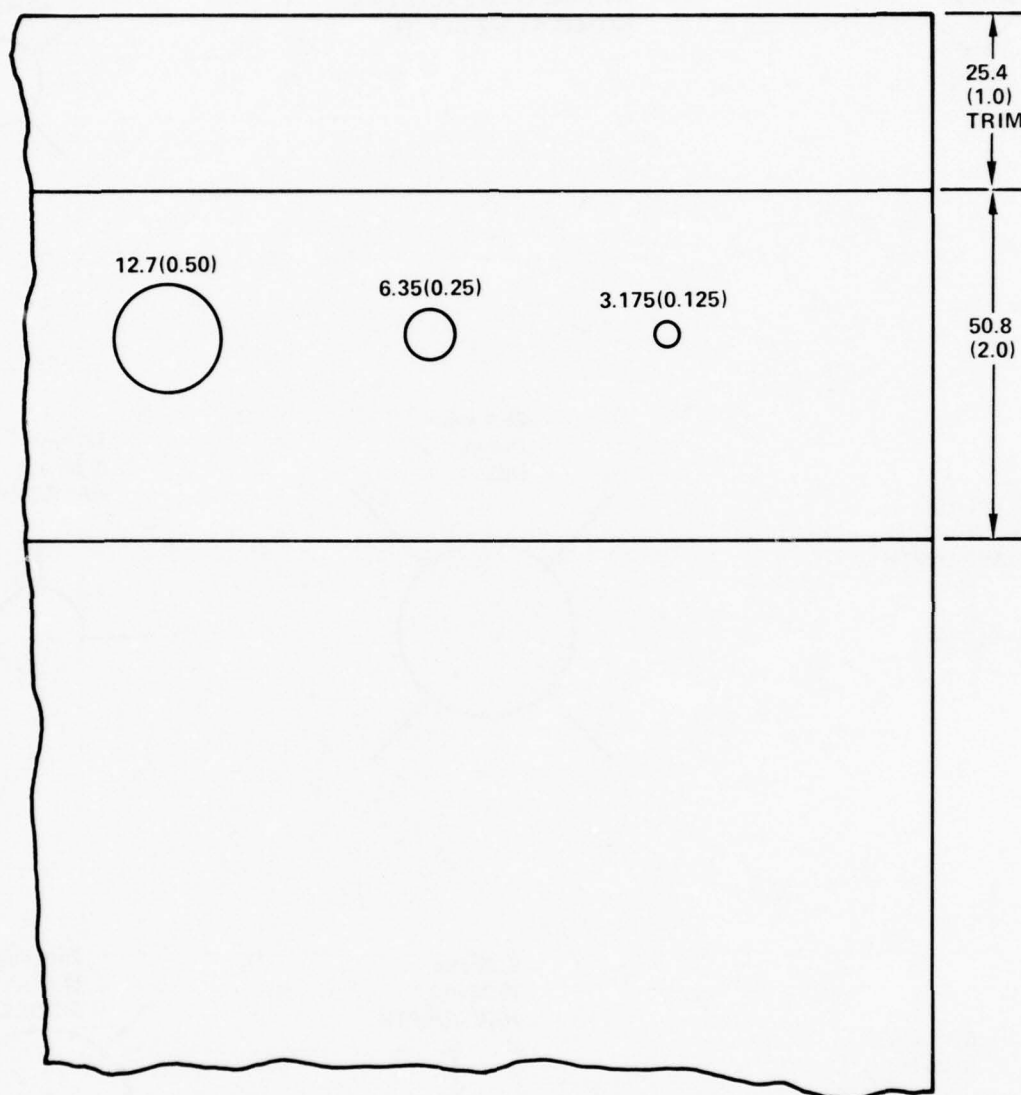
**DIMENSIONS IN** mm (in.)

Figure 2A. Template for Laminate 2 Panels

216
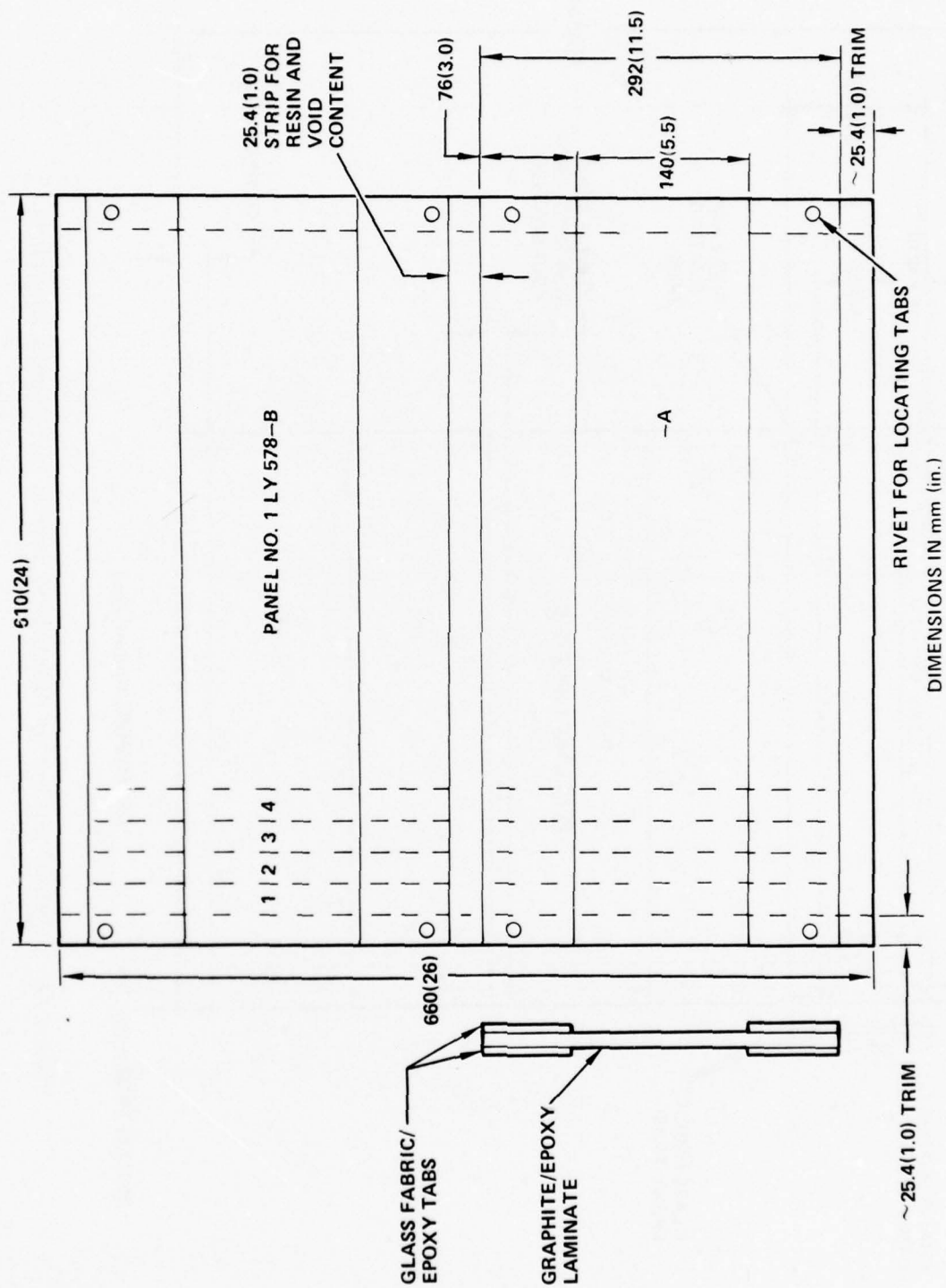
Figure 3A. Identification of Laminate 1 Panels and Coupon Locations
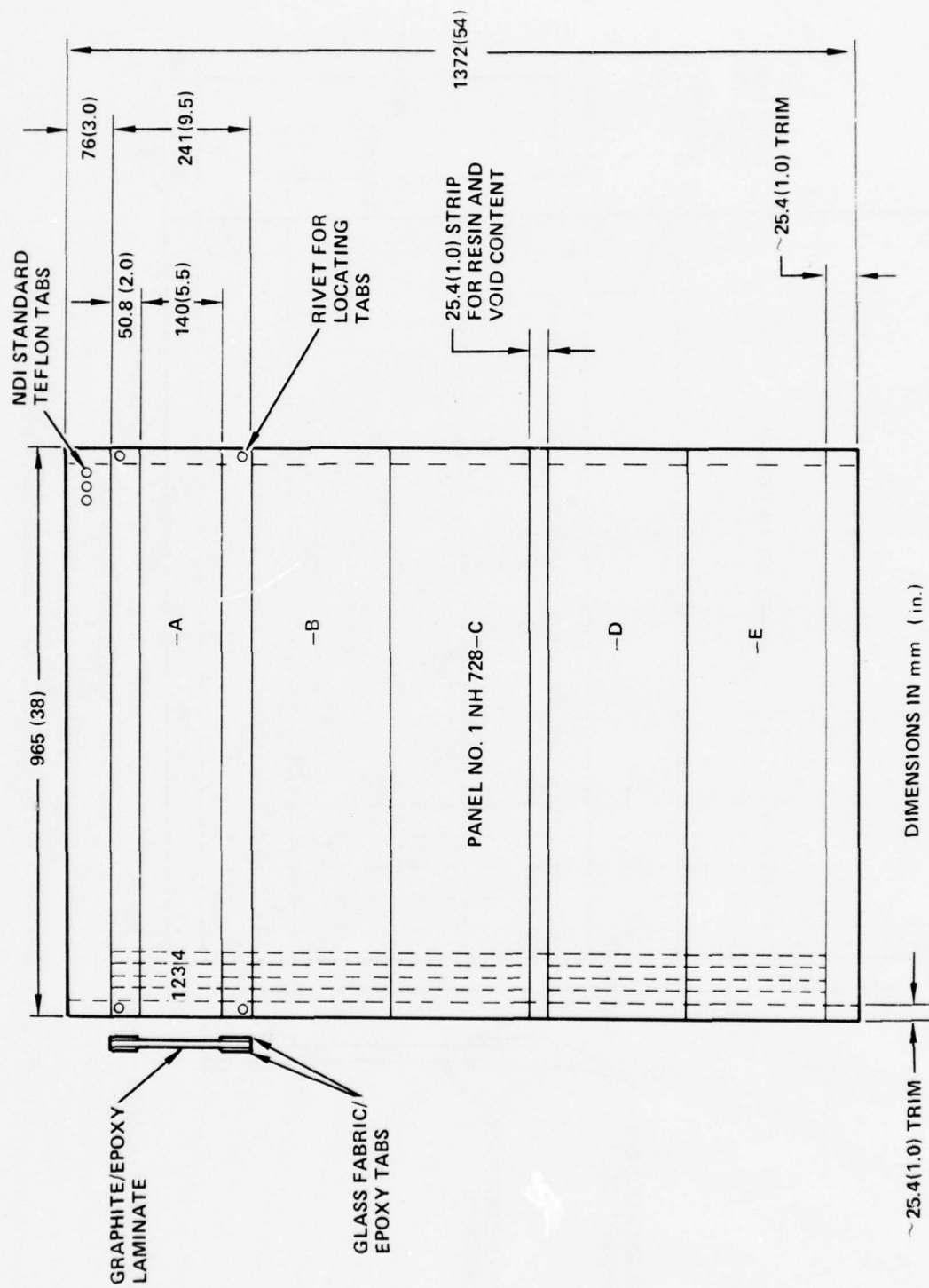
Figure 4A. Identification of Laminate 2 Panels and Coupon Locations

218

1.6 (0.06)

22.225 ( 0.875 )
± 0.07 (±0.003)

139.7 ± 2.5 (5.50 ± 0.1)

215.9 ± 2.5 (8.50 ± 0.1)

292.1 ± 2.5 (11.50 ± 0.1)

76.0 ± 2.0
(3.0 ± 0.1)

ALL DIMENSIONS IN mm (in.)
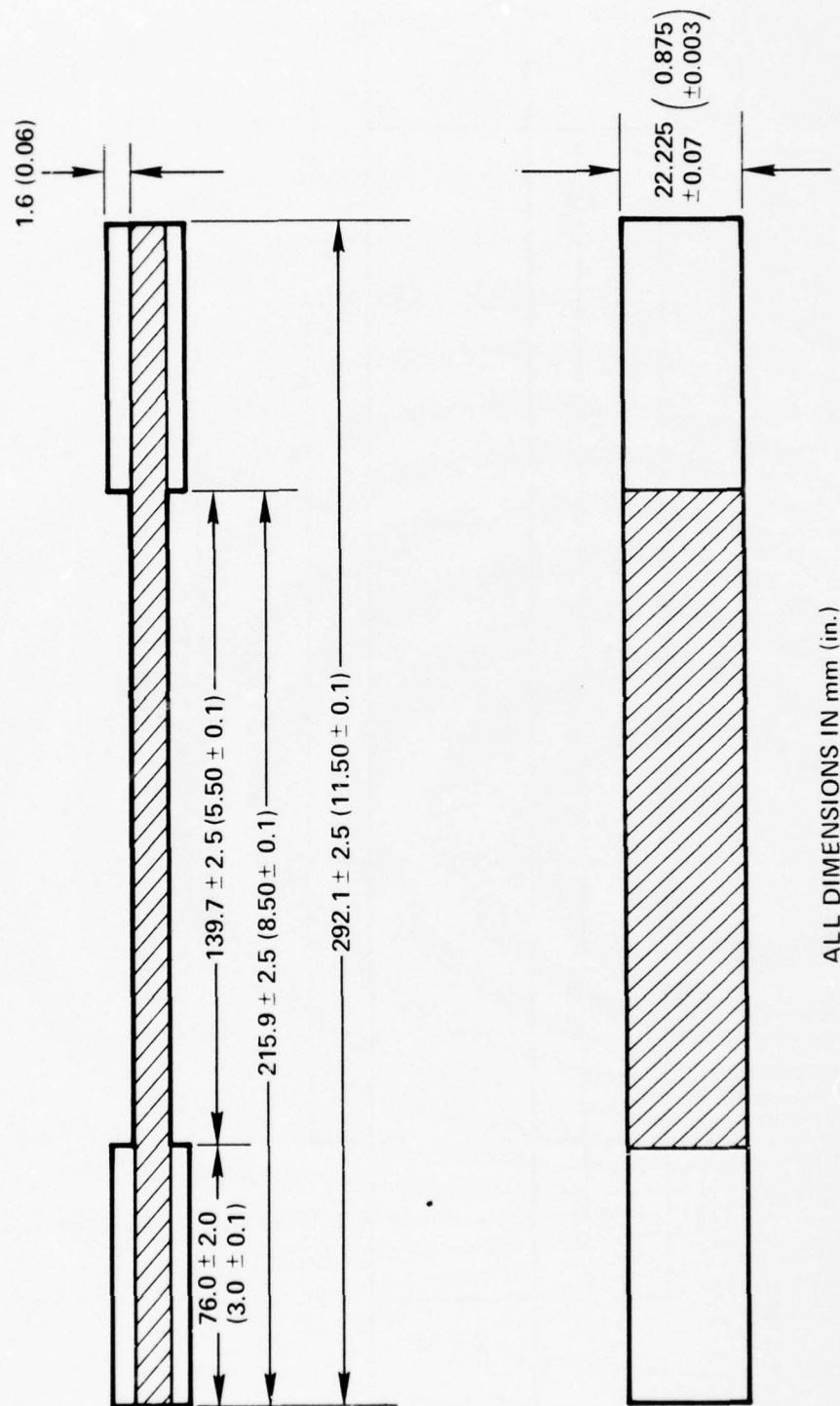
Figure 5A.  Coupon Geometry
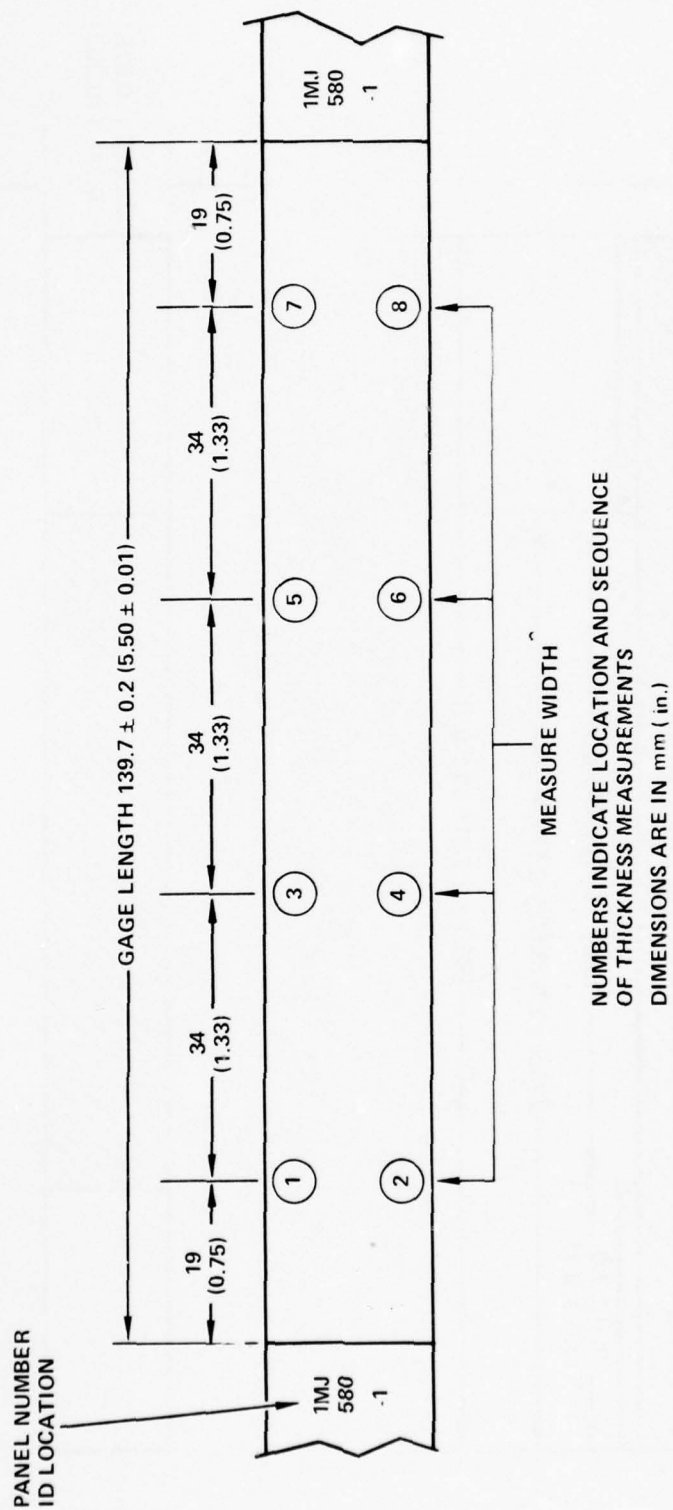
Figure 6A. Location of Thickness and Width Measurements

APPENDIX B

This appendix lists all of the fatigue data generated during this
research investigation.

TABLE 1B

STRESS LIFE SCAN

TENSION-TENSION FATIGUE TEST RESULTS

OF LAMINATE 1

$\sigma_{min}$ = 0 ksi, f = 10 Hz

| Sample ID | Minimum Area, in.$^2$ | Maximum Stress, $\sigma_{max}$, ksi | Cycles to Failure, $N_F$ | Cycles to Delamination, $N_{DL}$ (Approximate) |
|---|---|---|---|---|
| 601- 7B | 0.0822 | 62.0 | 2,079 | - |
| 603-18A | 0.0825 | 62.0 | 229 | - |
| 606- 2B | 0.0823 | 62.0 | 3 | - |
| 578-10A | 0.0840 | 58.0 | 1,664 | - |
| 578-25B | 0.0852 | 58.0 | 1,643 | - |
| 580- 2A | 0.0846 | 58.0 | 5,705 | - |
| 580-21A | 0.0812 | 54.0 | 30,520 | - |
| 603-26B | 0.0815 | 54.0 | 7,798 | - |
| 604- 4A | 0.0806 | 54.0 | 9,888 | - |
| 583-26A | 0.0815 | 50.0 | 512,600 | 222,500 |
| 601-24B | 0.0811 | 50.0 | 58,530 | - |
| 606-21A | 0.0810 | 50.0 | 367,644 | 95,000 |
| 596-13A | 0.0843 | 46.0 | 564,726 | 60,000 |
| 594-20B | 0.0822 | 46.0 | 351,900 | 36,000 |
| 583-23A | 0.0808 | 46.0 | 279,440 | - |
| 582-25A | 0.0820 | 42.0 | 864,420 | - |
| 582- 9A | 0.0821 | 42.0 | 1,698,100 | 1,400,000 |
| 594-21A | 0.0819 | 42.0 | 2,876,860 | 1,100,000 |

## TABLE 2B

## STRESS LIFE SCAN

## TENSION-COMPRESSION FATIGUE TEST RESULTS

## OF LAMINATE 1

$$f = 10 \text{ Hz}$$

| Sample ID | Min Area, in.$^2$ | Maximum Stress, $\sigma_{max}$, ksi | Minimum Stress, $\sigma_{min}$, ksi | Cycles to Failure, $N_F$ | Cycles to Delamination, $N_{DL}$ (Approximate) |
|---|---|---|---|---|---|
| 578-20A | 0.0835 | 62.0 | -10.0 | 810 | - |
| 604-23A | 0.0813 | 62.0 | -10.0 | 1,127 | - |
| 606-15B | 0.0841 | 62.0 | -10.0 | 10 | - |
| 580-26A | 0.0837 | 58.0 | -10.0 | 4,840 | 3,000 |
| 594- 1A | 0.0809 | 58.0 | -10.0 | 4,980 | - |
| 603-10A | 0.0815 | 58.0 | -10.0 | 1,675 | - |
| 596-23B | 0.0823 | 54.0 | -10.0 | 10,500 | 9,500 |
| 582- 2B | 0.0810 | 54.0 | -10.0 | 11,055 | 7,200 |
| 601-18B | 0.0821 | 54.0 | -10.0 | 6,997 | - |
| 601-20B | 0.0818 | 50.0 | -10.0 | 10,651 | - |
| 580-16B | 0.0837 | 50.0 | -10.0 | 16,030 | 16,000 |
| 596-26A | 0.0869 | 50.0 | -10.0 | 10,000 | 9,000 |
| 582- 3A | 0.0823 | 46.0 | -10.0 | 25,520 | 25,180 |
| 603-18B | 0.0834 | 46.0 | -10.0 | 36,500 | - |
| 604- 5A | 0.0824 | 46.0 | -10.0 | 78,710 | 35,000 |
| 578-21A | 0.0846 | 42.0 | -10.0 | 130,720 | 125,500 |
| 583-13A | 0.0849 | 42.0 | -10.0 | 78,290 | 73,500 |
| 606-19B | 0.0829 | 42.0 | -10.0 | 188,887 | 38,000 |
| 594-22B | 0.0818 | 38.0 | -10.0 | 111,600 | - |
| 583- 7B | 0.0833 | 38.0 | -10.0 | 414,560 | 407,000 |
| 601-21A | 0.0819 | 38.0 | -10.0 | 485,190 | 436,020 |
| 582-25B | 0.0808 | 34.0 | -10.0 | 1,047,000 | 899,000 |
| 578-16B | 0.0868 | 34.0 | -10.0 | 1,322,440 | 677,000 |
| 596- 3A | 0.0816 | 34.0 | -10.0 | 2,104,510 | 1,241,000 |
| 580-26B | 0.0859 | 58.0 | -16.0 | 1,402 | - |
| 594-7A | 0.0845 | 58.0 | -16.0 | 3,251 | - |
| 601-17A | 0.0856 | 58.0 | -16.0 | 1,010 | - |
| 578-22A | 0.0849 | 50.0 | -16.0 | 10,906 | - |
| 582- 5B | 0.0817 | 50.0 | -16.0 | 11,445 | 2,500 |
| 604-24B | 0.0808 | 50.0 | -16.0 | 3,981 | 2,900 |
| 580-22A | 0.0827 | 38.0 | -16.0 | 213,539 | 187,000 |
| 603-16A | 0.0823 | 38.0 | -16.0 | 55,380 | 42,000 |
| 606-12A | 0.0832 | 38.0 | -16.0 | 43,485 | 38,000 |
| 604-16B | 0.0873 | 34.0 | -16.0 | 123,672 | 104,600 |
| 580-15A | 0.0821 | 34.0 | -16.0 | 749,444 | - |
| 606- 3A | 0.0803 | 34.0 | -16.0 | 638,880 | - |

# TABLE 3B

## STRESS LIFE SCAN

### TENSION-TENSION FATIGUE TEST RESULTS

### OF LAMINATE 2

$\sigma_{min}$ = 0 ksi, f = 10 Hz

| Sample ID | Average Area, in.$^2$ | Maximum Stress, $\sigma_{max}$, ksi | Cycles to Failure, $N_F$ |
|---|---|---|---|
| 696-10B | 0.1293 | 118.0 | 664,690 |
| 727-15A | 0.1267 | 118.0 | 90 |
| 728-32C | 0.1296 | 118.0 | 761,130 |
| 696- 5B | 0.1275 | 112.0 | 2,350 |
| 696- 6B | 0.1286 | 112.0 | 268,060 |
| 727-31C | 0.1269 | 112.0 | $10^6$ NF[a] |
| 727- 5A | 0.1273 | 112.0 | 1.1 x $10^6$ NF |
| 696- 2C | 0.1270 | 106.0 | 210 |
| 728-29A | 0.1292 | 106.0 | 933,780 |
| 728-30B | 0.1310 | 106.0 | $10^6$ NF |
| 696-36C | 0.1265 | 106.0 | 15,400 |
| 696-29A | 0.1291 | 100.0 | 1.069 x $10^6$ NF |
| 699-30B | 0.1235 | 100.0 | $10^6$ NF |
| 727-24A | 0.1290 | 100.0 | $10^6$ NF |
| 699-34B | 0.1276 | 94.0 | 1 |
| 727- 6B | 0.1270 | 94.0 | 991,880 NF |

a - NF indicates No Failure.

TABLE 4B

STRESS LIFE SCAN

TENSION-COMPRESSION FATIGUE RESULTS

OF LAMINATE 2

$\sigma_{min}$ = -30 ksi, f = 10 $H_z$

| Sample ID | Average Area, in.$^2$ | Maximum Stress, $\sigma_{max}$, ksi | Cycles to Failure, $N_F$ |
|---|---|---|---|
| 699-26B | 0.1270 | 100.0 | Tab adhesive Failure |
| 699- 6B | 0.1281 | 100.0 | Tab adhesive Failure |
| 728- 9B | 0.1322 | 100.0 | Tab adhesive Failure |
| 696-23B | 0.1273 | 90.0 | Tab adhesive Failure |
| 727-27C | 0.1248 | 90.0 | Tab adhesive Failure |
| 728-11A | 0.1286 | 90.0 | $10^6$ NF$^a$ |
| 696-10C | 0.1261 | 80.0 | $10^6$ NF |
| 699-19C | 0.1299 | 80.0 | $10^6$ NF |
| 696-22A | 0.1286 | 70.0 | $10^6$ NF |
| 727- 3A | 0.1255 | 70.0 | $10^6$ NF |
| 728-24A | 0.1301 | 70.0 | 380,800 |

a - NF indicates No Failure

TABLE 5B

TENSION-TENSION FATIGUE RESULTS OF LAMINATE 1

AT A MAXIMUM STRESS OF 25 ksi

$\sigma_{min}$ = 0 ksi, f = 10 H$_z$

(Number of Tests = 20)

| Sample ID | Minimum Area, in.$^2$ | Number of Testing Cycles, N |
|---|---|---|
| 578-13B | 0.0873 | $10^6$ |
| 578-19B | 0.0847 | $10^6$ |
| 580-6A | 0.0825 | $10^6$ |
| 580-16A | 0.0828 | $10^6$ |
| 582-8A | 0.0824 | $10^6$ |
| 582-3B | 0.0814 | $10^6$ |
| 583-23A | 0.0809 | $10^6$ |
| 583-26B | 0.0820 | $10^6$ |
| 594-4A | 0.0811 | $10^6$ |
| 594-25A | 0.0818 | $10^6$ |
| 596-9A | 0.0831 | $10^6$ |
| 596-26B | 0.0816 | $10^6$ |
| 601-8B | 0.0827 | $10^6$ |
| 603-4A | 0.0810 | $10^6$ |
| 603-13A | 0.0841 | $10^7$ |
| 604-11A | 0.0836 | $10^7$ |
| 604-12A | 0.0836 | $10^6$ |
| 606-9B | 0.0836 | $10^7$ |
| 606-10B | 0.0844 | $10^7$ |
| 606-23B | 0.0803 | $10^6$ |

NOTE: All tests ran out, no failures, no delamination.

## TABLE 6B

### TENSION-TENSION FATIGUE RESULTS
### OF LAMINATE 1 AT A MAXIMUM STRESS OF 33.5 ksi

$\sigma_{min}$ = 0 ksi, f = 10 Hz

(Number of Tests = 20)

| Sample ID | Minimum Area, in.$^2$ | Number of Testing Cycles, N |
|---|---|---|
| 578-13A | 0.0827 | $10^6$ |
| 578-23A | 0.0827 | $10^6$ |
| 580-21A | 0.0821 | $10^6$ |
| 580-11B | 0.0831 | $10^6$ |
| 582-4A | 0.0809 | $10^6$ |
| 582-16A | 0.0827 | $1.468 \times 10^6$ |
| 582-13B | 0.0818 | $10^6$ |
| 594-22A | 0.0814 | $1.039 \times 10^6$ |
| 594-1B | 0.0796 | $1.039 \times 10^6$ |
| 596-21A | 0.0817 | $10^6$ |
| 596-14B | 0.0832 | $10^6$ |
| 596-24B | 0.0816 | $1.468 \times 10^6$ |
| 601-12A | 0.0817 | $10^6$ |
| 601-13A | 0.0832 | $10^6$ |
| 603-7A | 0.0814 | $10^6$ |
| 603-9B | 0.0830 | $10^6$ |
| 603-11B | 0.0833 | $10^6$ |
| 604-26A | 0.0817 | $10^6$ |
| 606-2A | 0.0810 | $10^6$ |
| 606-16B | 0.0840 | $10^6$ |

NOTE: All tests ran out, no failures, no delaminations.

227

## TABLE 7B

### TENSION-TENSION FATIGUE RESULTS

### OF LAMINATE 1 AT A MAXIMUM STRESS OF 42 ksi

$\sigma_{min}$ = 0 ksi, f = 10 Hz

(Number of Tests = 20)

| Sample ID | Minimum Area, in.$^2$ | Cycles to Failure, $N_F$ | Cycles to Delamination, $N_{DL}$ (Approximate) |
|---|---|---|---|
| 578-25A | 0.0835 | 1,872,851 | 142,000 |
| 578-17B | 0.0869 | 1,437,800 | 500,000 |
| 580-15B | 0.0835 | 215,984 | 185,000 |
| 580-18B | 0.0829 | 2,359,300 | 142,000 |
| 582- 9A | 0.0821 | 1,698,100 | 1,528,100 |
| 582-25A | 0.0820 | 864,420 | - |
| 583- 1B | 0.0823 | 1,291,505 | 197,000 |
| 583- 2B | 0.0824 | 1,186,800 | 560,000 |
| 594-21A | 0.0819 | 2,876,860 | 1,100,000 |
| 594- 6B | 0.0817 | 3,347,500 | 1,983,800 |
| 596- 2A | 0.0823 | 1,416,509 | 830,200 |
| 596-16A | 0.0832 | 1,967,170 | 1,790,600 |
| 601- 1A | 0.0799 | 632,406 | 326,000 |
| 601-11A | 0.0827 | 245,455 | - |
| 603-14A | 0.0845 | 350,363 | - |
| 603- 5B | 0.0823 | 2,628,300 | 1,271,000 |
| 604-13B | 0.0848 | 1,354,800 | 1,175,000 |
| 604-22B | 0.0824 | 1,216,000 | 702,000 |
| 606-25A | 0.0814 | 4,951,832 | 861,000 |
| 606-20B | 0.0818 | 3,542,157 | 1,091,000 |

228

TABLE 8B

TENSION-TENSION FATIGUE RESULTS

OF LAMINATE 1 AT A MAXIMUM STRESS OF 50 ksi

$\sigma_{min}$ = 0 ksi, f = 10 Hz

(Number of Tests = 20)

| Sample ID | Minimum Area, in.$^2$ | Cycles to Failure, $N_F$ | Cycles to Delamination, $N_{DL}$ (Approximate) |
|---|---|---|---|
| 578- 4A | 0.0850 | 87,373 | 70,000 |
| 578-18B | 0.0859 | 11,491 | - |
| 580- 2B | 0.0830 | 59,320 | 48,000 |
| 580- 5A | 0.0825 | 60,912 | - |
| 582- 2A | 0.0818 | 81,571 | 37,000 |
| 582-26B | 0.0823 | 51,848 | 40,000 |
| 583-26A | 0.0815 | 512,600 | 222,500 |
| 583-22B | 0.0822 | 69,711 | 37,000 |
| 594- 7B | 0.0823 | 54,187 | 50,000 |
| 594- 2A | 0.0819 | 71,400 | 43,500 |
| 596- 5A | 0.0820 | 116,667 | - |
| 596- 7A | 0.0824 | 64,070 | 42,750 |
| 601-19A | 0.0827 | 70,049 | 35,000 |
| 601-24B | 0.0811 | 58,530 | - |
| 603-12B | 0.0833 | 17,578 | - |
| 603-25B | 0.0830 | 40,270 | - |
| 604- 9A | 0.0837 | 44,830 | - |
| 604- 6B | 0.0823 | 41,200 | - |
| 606- 8A | 0.0839 | 70,497 | - |
| 606-21A | 0.0810 | 367,644 | 95,000 |

TABLE 9B

TENSION-TENSION FATIGUE RESULTS

OF LAMINATE 1 AT A MAXIMUM STRESS OF 58 ksi

$\sigma_{min}$ = 0 ksi, f = 10 Hz

(Number of tests = 20)

| Sample ID | Minimum Area, in.$^2$ | Cycles to Failure, $N_F$ | Cycles to Delamination, $N_{DL}$ (Approximate) |
|---|---|---|---|
| 578-10A | 0.0840 | 1664 | - |
| 578-25B | 0.0852 | 1643 | - |
| 580- 2A | 0.0846 | 5705 | - |
| 580- 3A | 0.0836 | 5329 | - |
| 582-22A | 0.0814 | 7954 | 4650 |
| 582- 4B | 0.0812 | 6430 | 3500 |
| 583- 6A | 0.0833 | 8430 | - |
| 583-15A | 0.0848 | 7232 | - |
| 594- 2B | 0.0810 | 690 | - |
| 594-16B | 0.0823 | 100 | - |
| 596-12A | 0.0838 | 1121 | - |
| 596-20B | 0.0822 | 5347 | - |
| 601- 3A | 0.0802 | 359 | - |
| 601-14B | 0.0828 | 61 | - |
| 603- 1A | 0.0817 | 1588 | - |
| 603-22A | 0.0825 | 528 | - |
| 604-18A | 0.0843 | 3558 | - |
| 604-21B | 0.0817 | 9590 | - |
| 606- 7B | 0.0831 | 4930 | - |
| 606-25B | 0.0822 | 9060 | - |

TABLE 10B

TENSION-COMPRESSION FATIGUE RESULTS OF LAMINATE 1

AT A MAXIMUM STRESS OF 26 ksi

$\sigma_{min}$ = -16 ksi, f = 10 Hz

(Number of Tests = 20)

| Sample ID | Minimum Area, in.$^2$ | Cycles to Failure, $N_F$ |
|---|---|---|
| 580-14A | 0.0827 | 7,204,500 [a] |
| 582-1B | 0.0801 | 3,173,500 |
| 582-11B | 0.0837 | 489,800 |
| 582-27B | 0.0833 | 2,595,200 |
| 594-14A | 0.0827 | 3,533,600 |
| 594-17A | 0.0823 | 2,582,000 |
| 594-22A | 0.0815 | 3,118,000 |
| 594-1B | 0.0796 | 1,598,200 |
| 594-12B | 0.0811 | 2,107,000 |
| 603-8A | 0.0825 | 7,137,590 |
| 604-17A | 0.0830 | 5,963,240 |
| 604-3B | 0.0813 | 1,994,110 |
| 604-10B | 0.0838 | 1,769,470 |
| 606-9A | 0.0841 | 806,000 |
| 606-24A | 0.0804 | 2,622,000 |
| 606-22B | 0.0813 | 152,390 |
| 693-11A | 0.0854 | 6,985,600 |
| 693-16B | 0.0880 | 559,030 |
| 693-11C | 0.0860 | 4,373,425 |
| 693-26C | 0.0867 | 2,076,100 |

a - Failed due to equipment malfunction

## TABLE 11B

### TENSION-COMPRESSION FATIGUE RESULTS OF LAMINATE 1
### AT A MAXIMUM STRESS OF 42 ksi

$$\sigma_{min} = -16 \text{ ksi}, \ f = 10 \text{ Hz}$$

(Number of Tests = 20)

| Sample ID | Minimum Area, in.$^2$ | Cycles to Failure, $N_F$ | Cycles to Delamination, $N_{DL}$ (Approximate) |
|---|---|---|---|
| 578- 8A | 0.0855 | 35,764 | 28,000 |
| 578-12B | 0.0860 | 7,980 | - |
| 580- 3B | 0.0846 | 20,400 | - |
| 580- 6B | 0.0838 | 25,121 | 16,000 |
| 582- 9B | 0.0824 | 39,580 | - |
| 582-16B | 0.0835 | 23,400 | - |
| 583- 9B | 0.0839 | 41,520 | 37,000 |
| 583-14B | 0.0858 | 40,100 | 39,000 |
| 594-23A | 0.0805 | 30,785 | 28,900 |
| 594- 4B | 0.0808 | 20,340 | - |
| 596-14A | 0.0831 | 38,600 | 33,500 |
| 596- 8B | 0.0815 | 40,000 | 27,000 |
| 601- 2A | 0.0804 | 21,610 | - |
| 601- 1B | 0.0796 | 27,850 | - |
| 603-15A | 0.0832 | 18,550 | 12,500 |
| 603- 8B | 0.0832 | 72,935 | - |
| 604- 7A | 0.0829 | 23,468 | - |
| 604-25A | 0.0826 | 23,100 | - |
| 606-22A | 0.0814 | 27,111 | - |
| 606-17B | 0.0836 | 56,000 | - |

## TABLE 12B

### TENSION-COMPRESSION FATIGUE RESULTS OF LAMINATE 1

### AT A MAXIMUM STRESS OF 50 ksi

$$\sigma_{min} = -16 \text{ ksi, } f = 10 \text{ Hz}$$

(Number of Tests = 20)

| Sample ID | Minimum Area, in.$^2$ | Cycles to Failure, $N_F$ | Cycles to Delamination, $N_{DL}$ (Approximate) |
|---|---|---|---|
| 578-22A | 0.0849 | 10,906 | - |
| 578- 1B | 0.0856 | 142 | - |
| 580-12B | 0.0828 | 3,671 | - |
| 580-24B | 0.0824 | 5,586 | - |
| 582- 5B | 0.0817 | 11,445 | 2,500 |
| 582-10B | 0.0828 | 9,274 | - |
| 583- 2A | 0.0827 | 11,960 | 9,670 |
| 583-11B | 0.0841 | 1,650 | - |
| 594-11B | 0.0817 | 8,490 | 4,500 |
| 594-19B | 0.0825 | 21,774 | 7,800 |
| 596- 4B | 0.0820 | 14,094 | 12,000 |
| 596-17A | 0.0832 | 19,320 | - |
| 601- 9B | 0.0829 | 13,655 | 12,000 |
| 601-10B | 0.0830 | 7,833 | - |
| 603- 4B | 0.0811 | 14,720 | - |
| 603-19B | 0.0834 | 16,008 | - |
| 604- 5B | 0.0826 | 7,002 | - |
| 604-24B | 0.0808 | 3,981 | 4,400 |
| 606-15A | 0.0847 | 8,580 | - |
| 606-21B | 0.0806 | 700 | - |

233

## TABLE 13B

### TENSION-COMPRESSION FATIGUE RESULTS OF LAMINATE 1

### AT A MAXIMUM STRESS OF 58 ksi

$$\sigma_{min} = -16 \text{ ksi, } f = 10 \text{ H}_z$$

(Number of Tests = 20)

| Sample ID | Minimum Area, in.$^2$ | Cycles to Failure, $N_F$ | Cycles to Delamination, $N_{DL}$ (Approximate) |
|---|---|---|---|
| 578-21B | 0.0843 | 1,473 | - |
| 578-24B | 0.0832 | 3,453 | - |
| 580- 7A | 0.0817 | 3,406 | - |
| 580-26B | 0.0859 | 1,402 | - |
| 582- 1A | 0.0790 | 1,930 | - |
| 582-13A | 0.0822 | 330 | - |
| 583-21B | 0.0824 | 57 | - |
| 583-10A | 0.0819 | 2,685 | 580 |
| 594- 7A | 0.0845 | 3,251 | - |
| 594-13A | 0.0834 | 1,167 | 300 |
| 596- 5B | 0.0818 | 1,385 | - |
| 596-10A | 0.0838 | 2,356 | 1,100 |
| 601- 7A | 0.0817 | 71 | - |
| 601-17A | 0.0832 | 1,010 | - |
| 603-11A | 0.0828 | 316 | - |
| 603-20A | 0.0818 | 2,186 | - |
| 604-11B | 0.0835 | 1,510 | - |
| 604-12B | 0.0832 | 5 | - |
| 606-18A | 0.0844 | 3,430 | - |
| 606-26B | 0.0803 | 1,740 | - |

234

TABLE 14B

TENSION-TENSION FATIGUE RESULTS OF LAMINATE 2

AT A MAXIMUM STRESS OF 100 ksi

$\sigma_{min}$ = 0 ksi, f = 10 Hz

(Number of Tests = 51)

| Sample ID | Average Area, in.$^2$ | Cycles to Failure, $N_F$ | Sample ID | Average Area, in.$^2$ | Cycles to Failure, $N_F$ |
|---|---|---|---|---|---|
| 696- 5A | 0.1286 | $10^6$ NF [a] | 727-24A | 0.1290 | $10^6$ NF |
| 696-16A | 0.1286 | $10^6$ NF | 727-26A | 0.1255 | 1.055 x $10^6$ NF |
| 696-23A | 0.1279 | 930,000 | 727-30A | 0.1270 | $10^6$ NF |
| 696-24A | 0.1253 | $10^6$ NF | 727- 1B | 0.1195 | $10^6$ NF |
| 696-29A | 0.1291 | $10^6$ NF | 727- 7B | 0.1195 | $10^6$ NF |
| 696- 2B | 0.1239 | $10^6$ NF | 727-15B | 0.1274 | $10^6$ NF |
| 696-20B | 0.1262 | $10^6$ NF | 727-16B | 0.1275 | $10^6$ NF |
| 696-31B | 0.1282 | 495,040 | 727- 1C | 0.1188 | 1 |
| 696-35B | 0.1270 | $10^6$ NF | 727- 9C | 0.1284 | $10^6$ NF |
| 696-11C | 0.1256 | $10^6$ NF | 727-11C | 0.1270 | 1.358 x $10^6$ NF |
| 696-28C | 0.1276 | $10^6$ NF | 727-23C | 0.1285 | $10^6$ NF |
| 696-29C | 0.1264 | $10^6$ NF | 727-25C | 0.1260 | 910 |
| 696-34C | 0.1280 | $10^6$ NF | 727-33C | 0.1276 | $10^6$ NF |
| 699- 1A | 0.1201 | $10^6$ NF | 728- 6A | 0.1287 | 826, 940 |
| 699-21A | 0.1266 | $10^6$ NF | 728-37A | 0.1300 | $10^6$ NF |
| 699-29A | 0.1284 | 2,000 | 728- 2B | 0.1236 | $10^6$ NF |
| 699-33A | 0.1296 | $10^6$ NF | 728- 6B | 0.1290 | $10^6$ NF |
| 699-34A | 0.1302 | $10^6$ NF | 728- 7B | 0.1304 | 1.47 x $10^6$ NF |
| 699- 1B | 0.1176 | 1 | 728-26B | 0.1288 | 1.212 x $10^6$ NF |
| 699-22B | 0.1318 | $10^6$ NF | 728-27B | 0.1271 | $10^6$ NF |
| 699-30B | 0.1235 | $10^6$ NF | 728-34B | 0.1300 | $10^6$ NF |
| 699-37B | 0.1266 | $10^6$ NF | 728- 9C | 0.1306 | $10^6$ NF |
| 699- 1C | 0.1171 | $10^6$ NF | 728-27C | 0.1265 | 1880 |
| 699-10C | 0.1295 | $10^6$ NF | 728-31C | 0.1282 | $10^6$ NF |
| 699-21C | 0.1307 | $10^6$ NF | 728-33C | 0.1302 | $10^6$ NF |
| 699-28C | 0.1269 | 1 | | | |

a - NF indicates No Failure

235

TABLE 15B

TENSION - TENSION FATIGUE RESULTS OF LAMINATE 2

AT A MAXIMUM STRESS OF 112 ksi

$\sigma_{min}$ = 0 ksi, f = 10 Hz

(NUMBER OF TESTS = 20)

| Sample ID | Average Area, in.$^2$ | Cycles to Failure, $N_F$ |
|---|---|---|
| 696-34A | 0.1270 | 164,980 |
| 696-5B | 0.1275 | 2,350 |
| 696-6B | 0.1286 | 268,060 |
| 696-13C | 0.1261 | $10^6$ NF[a] |
| 696-23C | 0.1281 | 599,330 |
| 699-3A | 0.1276 | 1.036 x $10^6$ NF |
| 699-15A | 0.1135 | $10^6$ NF |
| 699-28A | 0.1270 | $10^6$ NF |
| 699-11C | 0.1285 | 25,000 |
| 699-20C | 0.1255 | $10^6$ NF |
| 727-5A | 0.1273 | 1.1 x $10^6$ NF |
| 727-19A | 0.1283 | 910 |
| 727-17B | 0.1287 | $10^6$ NF |
| 727-31C | 0.1269 | $10^6$ NF |
| 727-36C | 0.1255 | 390 |
| 728-31A | 0.1285 | 17,191 |
| 728-19B | 0.1294 | 1 |
| 728-10C | 0.1299 | 574,260 |
| 728-17C | 0.1320 | 1.065 x $10^6$ NF |
| 728-26C | 0.1263 | $10^6$ NF |

a - NF indicates No Failure

236

TABLE 16B

TENSION-COMPRESSION FATIGUE RESULTS OF LAMINATE 2

AT A MAXIMUM STRESS OF 70 ksi

$\sigma_{min}$ = -30 ksi, f = 10 Hz

(Number of Tests = 48)

| Sample ID | Average Area, in.$^2$ | Cycles to Failure, $N_F$ | Sample ID | Average Area, in.$^2$ | Cycles to Failure, $N_F$ |
|-----------|----------|----------|-----------|----------|----------|
| 696-19A | 0.1279 | $10^6$ NF[a] | 727-6A | 0.1270 | $10^6$ NF |
| 696-22A | 0.1286 | $10^6$ NF | 727-21A | 0.1295 | $10^6$ NF |
| 696-27A | 0.1264 | $10^6$ NF | 727-4B | 0.1258 | 1.198 x $10^6$ NF |
| 696-30A | 0.1292 | $10^6$ NF | 727-22B | 0.1291 | $10^6$ NF |
| 696-33A | 0.1269 | $10^6$ NF | 727-35B | 0.1268 | 696,420 |
| 696-1B | 0.1146 | $10^6$ NF | 717-5C | 0.1282 | $10^6$ NF |
| 696-7B | 0.1285 | $10^6$ NF | 727-14C | 0.1257 | $10^6$ NF |
| 696-8B | 0.1279 | $10^6$ NF | 727-16C | 0.1282 | 504,510 |
| 696-16B | 0.1286 | $10^6$ NF | 727-17C | 0.1270 | $10^6$ NF |
| 696-18C | 0.1295 | $10^6$ NF | 727-26C | 0.1243 | $10^6$ NF |
| 699-31A | 0.1283 | $10^6$ NF | 727-28C | 0.1264 | $10^6$ NF |
| 699-32A | 0.1304 | $10^6$ NF | 727-34C | 0.1289 | $10^6$ NF |
| 699-37A | 0.1304 | $10^6$ NF | 728-1A | 0.1150 | $10^6$ NF |
| 699-7B | 0.1290 | $10^6$ NF | 728-10A | 0.1300 | $10^6$ NF |
| 699-13B | 0.1268 | $10^6$ NF | 728-20A | 0.1312 | 53,090 |
| 699-14B | 0.1258 | $10^6$ NF | 728-24A | 0.1301 | 380,800 |
| 699-18B | 0.1280 | $10^6$ NF | 728-28A | 0.1268 | $10^6$ NF |
| 699-33B | 0.1288 | $10^6$ NF | 728-34A | 0.1292 | $10^6$ NF |
| 699-24C | 0.1299 | $10^6$ NF | 728-1B | 0.1177 | $10^6$ NF |
| 699-26C | 0.1269 | $10^6$ NF | 728-22B | 0.1320 | $10^6$ NF |
| 699-32C | 0.1292 | $10^6$ NF | 728-25B | 0.1284 | $10^6$ NF |
| 699-35C | 0.1299 | $10^6$ NF | 728-29B | 0.1300 | $10^6$ NF |
| 727-3A | 0.1255 | 1.044 x $10^6$ NF | 728-37B | 0.1258 | 1.120 x $10^6$ NF |
| 727-4A | 0.1259 | $10^6$ NF | 728-23C | 0.1317 | $10^6$ NF |

a - NF indicates No Failure

237

APPENDIX C


This appendix lists all of the results of the static residual strength
tests conducted during this research investigation.

## TABLE 1C

### RESIDUAL TENSION STRENGTH
### TEST RESULTS OF LAMINATE 1 COUPONS
### FATIGUE TESTED AT 0 to 42 ksi

Coupons fatigue tested to 364,000 cycles equal to a probability of survival, $P_s$, of 0.9.  (Number of coupons static tested = 20)

| Sample ID | Min. Area, in.$^2$ | Ultimate Load, $P_{ult}$, lbs. | Ultimate Stress, $\sigma_{ult}$, ksi | Ultimate Strain, $\varepsilon_{ult}$, in 2.0 in. | Apparent Initial Modulus, $E_a$, psi X $10^6$ |
|---|---|---|---|---|---|
| 578- 6A | 0.0821 | 5970 | 72.4 | 0.0097 | 7.61 |
| -26B | 0.0849 | 5140 | 60.5 | 0.0090 | 6.93 |
| 580-20B | 0.0826 | 5680 | 68.8 | 0.0100 | 7.12 |
| -21B | 0.0809 | 5630 | 69.6 | 0.0098 | 6.87 |
| 582-21A | 0.0813 | 4830 | 59.4 | - | 7.03 |
| - 6B | 0.0821 | 5240 | 63.8 | 0.0096 | 6.41 |
| 583-21A | 0.0821 | 5840 | 71.1 | 0.0091 | 6.41 |
| -10B | 0.0836 | 5770 | 69.0 | 0.0102 | 6.64 |
| 594-10A | 0.0834 | 4850 | 58.2 | 0.0081 | 7.04 |
| -16A | 0.0826 | Coupon failed at 51,792 cycles | | | |
| - 9B | 0.0815 | 5050 | 62.0 | 0.0088 | 6.82 |
| 595-15A | 0.0838 | 4900 | 58.5 | 0.0084 | 7.02 |
| -22A | 0.0813 | 5520 | 67.9 | 0.0092 | 7.45 |
| 601-23A | 0.0810 | 4310 | 53.2 | 0.0079 | 6.86 |
| - 3B | 0.0824 | Coupon failed at 245,030 cycles | | | |
| -16B | 0.0821 | 5350 | 65.2 | 0.0091 | 7.16 |
| 603- 9A | 0.0823 | 4900 | 59.5 | 0.0088 | 6.40 |
| -22B | 0.0822 | 4040 | 49.2 | 0.0074 | 6.76 |
| 604-20A | 0.0838 | 4910 | 58.6 | 0.0090 | 6.63 |
| -13A | 0.0838 | 5200 | 62.0 | - | 6.63 |
| 606- 8B | 0.0842 | 4900 | 58.2 | 0.0093 | 6.60 |
| -14B | 0.0835 | 5070 | 60.7 | 0.0091 | 6.47 |
| Average | | | 62.4 | 0.0090 | 6.84 |
| | | | +10.0 | +0.0012 | +0.77 |
| | | | -13.2 | -0.0016 | -0.43 |

## TABLE 2C

### RESIDUAL TENSION STRENGTH
### TEST RESULTS OF LAMINATE 1 COUPONS
### FATIGUE TESTED AT 0 TO 50 ksi

Coupons fatigue tested to 31,400 cycles equal to a probability of survival, $P_s$, of 0.9. (Number of coupons Static Tested = 20.)

| Sample ID | Min. Area, in.$^2$ | Ultimate Load, $P_{ult}$, lbs. | Ultimate Stress, $\sigma_{ult}$, ksi | Ultimate Strain, $\varepsilon_{ult}$, in./in. in 2.0 in. | Apparent Initial Modulus, $E_a$, psi X $10^6$[a] |
|---|---|---|---|---|---|
| 578- 7A | 0.0836 | 5640 | 67.5 | 0.0092 | 7.04 |
| - 3B | 0.0839 | 4580 | 54.6 | 0.0079 | 6.81 |
| 580  8A | 0.0829 | 5700 | 68.8 | - | 6.70 |
| -12A | 0.0815 | Coupon failed at 21,600 cycles | | | |
| - 9B | 0.0833 | 5360 | 64.4 | 0.0102 | 7.06 |
| 582-23A | 0.0820 | 5880 | 71.7 | 0.0099 | 7.17 |
| -21B | 0.0815 | 5380 | 66.0 | 0.0092 | 7.22 |
| 583- 3A | 0.0821 | 5740 | 69.9 | 0.0105 | 6.77 |
| -16A | 0.0837 | 5800 | 69.3 | 0.0098 | 7.03 |
| 594- 9A | 0.0817 | 5410 | 66.2 | 0.0091 | 7.16 |
| -15B | 0.0822 | 4740 | 57.7 | 0.0087 | 6.63 |
| 596-11A | 0.0832 | 5360 | 64.4 | 0.0093 | 7.07 |
| -16B | 0.0840 | 5090 | 60.6 | 0.0079 | 7.68 |
| 601- 4A | 0.0804 | 5780 | 71.4 | 0.0099 | 7.32 |
| -13B | 0.0830 | 6030 | 72.6 | 0.0102 | 7.09 |
| 603.23A | 0.0817 | 4820 | 59.0 | 0.0092 | 6.80 |
| - 3B | 0.0808 | 4830 | 59.8 | 0.0094 | 6.51 |
| 604- 2B | 0.0833 | 4820 | 57.9 | 0.0084 | 6.86 |
| -17B | 0.0833 | 5580 | 67.0 | 0.0096 | 7.06 |
| 606- 6B | 0.0824 | 5910 | 71.7 | 0.0099 | 7.14 |
| -18B | 0.0835 | 5140 | 61.6 | 0.0088 | 7.04 |
| Average | | | 65.1 | 0.0093 | 7.01 |
| | | | + 7.5 | +0.0012 | +0.31 |
| | | | -10.5 | -0.0014 | -0.38 |

241

## TABLE 3C

### RESIDUAL TENSION STRENGTH
### TEST RESULTS OF LAMINATE 1 COUPONS
### FATIGUE TESTED AT -16 TO 42 ksi

Coupons fatigue tested to 14,400 cycles equal to a probability of survival, $P_s$, of 0.9. (Number of coupons Static Tested = 20.)

| Sample ID | Min. Area, in.$^2$ | Ultimate Load, $P_{ult}$, lbs. | Ultimate Stress, $\sigma_{ult}$, ksi | Ultimate Strain, $\varepsilon_{ult}$, in./in. in 2.0 in. | Apparent Initial Modulus, $E$, psi X $10^6$ [a] |
|---|---|---|---|---|---|
| 578- 6B | 0.0838 | 5830 | 69.6 | 0.0097 | 7.23 |
| -11B | 0.0850 | 5600 | 65.9 | 0.0100 | 6.92 |
| -15B | 0.0862 | Coupon failed at 1,220 cycles | | | |
| 580-20A | 0.0826 | 5950 | 72.0 | 0.0102 | 7.12 |
| -25B | 0.0813 | 5320 | 65.4 | 0.0092 | 7.24 |
| 582- 5A | 0.0819 | 6440 | 78.6 | 0.0107 | 7.51 |
| -17B | 0.0839 | 5780 | 68.9 | 0.0094 | 7.22 |
| 583- 5B | 0.0848 | 5960 | 70.3 | 0.0097 | 6.21 |
| -15B | 0.0825 | 5980 | 72.5 | 0.0101 | 7.13 |
| 594-20A | 0.0821 | 5860 | 71.4 | 0.0100 | 7.16 |
| -13B | 0.0830 | 5300 | 63.9 | 0.0093 | 7.13 |
| 596- 6B | 0.0811 | 4900 | 60.4 | 0.0083 | 7.71 |
| - 7B | 0.0812 | 5440 | 67.0 | 0.0093 | 7.21 |
| 601- 5B | 0.0819 | 5430 | 66.3 | 0.0088 | 7.63 |
| - 9A | 0.0832 | 5600 | 67.3 | 0.0094 | 7.07 |
| 603-17A | 0.0831 | 5280 | 63.5 | 0.0093 | 7.08 |
| -19A | 0.0821 | 5780 | 70.4 | - | 7.16 |
| 604-15B | 0.0843 | 5460 | 64.8 | 0.0095 | 6.78 |
| - 3A | 0.0809 | Coupon failed at 12,289 cycles | | | |
| -16A | 0.0823 | 5120 | 62.2 | 0.0092 | 7.15 |
| 606-17A | 0.0848 | 5000 | 59.0 | 0.0077 | 7.37 |
| -11B | 0.0850 | 5540 | 65.2 | 0.0090 | 7.35 |
| Average | | | 67.2 | 0.0094 | 7.17 |
| | | | +11.4 | +0.0013 | +0.54 |
| | | | - 8.2 | -0.0017 | -0.96 |

## TABLE 4C

### RESIDUAL TENSION STRENGTH
### TEST RESULTS OF LAMINATE 1 COUPONS
FATIGUE TESTED AT -16 TO 50 ksi

Coupons fatigue tested to 2,150 cycles equal to a probability of survival, $P_s$, of 0.90. (Number of coupons Static Tested = 20.)

| Sample ID | Min. Area, in.$^2$ | Ultimate Load, $P_{ult}$, lbs. | Ultimate Stress, $\sigma_{ult}$, ksi | Ultimate Strain, $\varepsilon_{ult}$, in./in. in 2.0 in. | Apparent Initial Modulus, $E_a$, psi X 10$^6$ [a] |
|---|---|---|---|---|---|
| 578- 1A | 0.0835 | 5880 | 70.4 | 0.0088 | 7.21 |
| -19A | 0.0821 | 5900 | 71.9 | 0.0101 | 7.16 |
| 580-17B | 0.0834 | 5860 | 70.3 | 0.0097 | 7.05 |
| -17A | 0.0824 | 5840 | 70.9 | 0.0092 | 7.58 |
| 582- 7B | 0.0824 | 5560 | 67.5 | 0.0097 | 7.14 |
| -24B | 0.0805 | 5490 | 68.2 | 0.0093 | 7.10 |
| 583-11A | 0.0822 | 4960 | 60.3 | - | 7.16 |
| -24A | 0.0802 | 5120 | 63.8 | 0.0094 | 6.93 |
| 594-18A | 0.0820 | 5300 | 64.6 | 0.0106 | 6.42 |
| -17B | 0.0825 | 5900 | 71.5 | 0.0107 | 6.73 |
| 596-25A | 0.0807 | 5160 | 63.9 | 0.0095 | 6.70 |
| -24A | 0.0825 | 5520 | 66.9 | 0.0095 | 7.13 |
| 601- 2B | 0.0819 | 6000 | 73.3 | 0.0099 | 7.40 |
| - 4B | 0.0817 | 5790 | 70.9 | 0.0093 | 7.65 |
| -15B | 0.0824 | Coupon failed at 940 cycles | | | |
| 603-12A | 0.0830 | 5520 | 66.5 | 0.0097 | 7.09 |
| -17B | 0.0843 | 5880 | 69.8 | 0.0097 | 6.98 |
| 604- 2A | 0.0819 | 5280 | 64.5 | 0.0088 | 7.63 |
| -21A | 0.0819 | 5560 | 67.9 | 0.0094 | 6.98 |
| 606- 7A | 0.0816 | 5890 | 72.2 | 0.0103 | 7.21 |
| -13B | 0.0844 | 4920 | 58.3 | 0.0084 | 7.40 |
| Average | | | 67.7 | 0.0095 | 7.13 |
| | | | + 5.6 | +0.0012 | +0.50 |
| | | | - 9.4 | -0.0011 | -0.71 |

243

TABLE 5C

RESIDUAL COMPRESSION STRENGTH TEST RESULTS OF
LAMINATE 1 COUPONS FATIGUE TESTED AT 0 TO 42 ksi

Coupons fatigue tested to 364,000 cycles equal to a probability of
survival, $P_s$, of 0.90. (Number of coupons Static Tested = 20.)

| Sample ID | Min. Area, in.$^2$ | Ultimate Load, $P_{ult}$, lbs. | Ultimate Stress, $\sigma_{ult}$, ksi | Ultimate Strain, $\varepsilon_{ult}$, in./in. in 2.0 in. | Apparent Initial Modulus $E_a$, psi x 10$^6$ | Amt. of Strain at Peak Load, $\varepsilon$, in./in. in 2.0 in. |
|---|---|---|---|---|---|---|
| 578-26A | 0.0852 | 5310 | 62.3 | 0.0108 | 6.34 | 0.0006 |
| -22B | 0.0831 | 5620 | 67.6 | 0.0129 | 6.68 | 0.003 |
| 580-11A | 0.0821 | 3400 | 41.4 | 0.0069 | 6.25 | -$^a$ |
| - 5B | 0.0820 | 3870 | 47.2 | 0.0091 | 6.25 | 0.0027 |
| 582- 7A | 0.0822 | 4280 | 52.1 | 0.0090 | 6.08 | 0.00045 |
| -15B | 0.0836 | 4440 | 53.1 | 0.0101 | 6.64 | 0.0021 |
| 583- 1A | 0.0838 | 4680 | 55.8 | 0.0096 | 6.63 | 0.0006 |
| -12A | 0.0833 | Coupon failed at 99,400 cycles | | | | |
| -14A | 0.0854 | 3620 | 43.4 | 0.0079 | 5.85 | 0.0009 |
| 594-24B | 0.0794 | 4830 | 60.8 | 0.0105 | 5.60 | - |
| -26B | 0.0804 | 4240 | 52.7 | 0.0086 | 5.92 | - |
| 595-10B | 0.0838 | 5020 | 59.9 | 0.0093 | 7.23 | - |
| -22B | 0.0823 | 5870 | 71.3 | 0.0120 | 5.93 | 0.00045 |
| 601-16A | 0.0831 | 4290 | 51.6 | 0.0093 | 6.17 | 0.0019 |
| - 8A | 0.0825 | Coupon failed at 238,061 cycles | | | | |
| -20A | 0.0828 | 5440 | 65.7 | 0.0113 | 6.36 | 0.0006 |
| -12B | 0.0816 | Coupon failed at 118,000 cycles | | | | |
| 603- 2A | 0.0825 | 4920 | 59.6 | 0.0102 | 6.22 | 0.0006 |
| -24A | 0.0804 | 5230 | 65.0 | 0.0109 | 6.91 | 0.0009 |
| 604-10A | 0.0844 | 5630 | 66.7 | 0.0109 | 6.67 | 0.0006 |
| -18B | 0.0833 | 4410 | 52.9 | 0.0078 | 6.67 | 0.0005 |
| 606- 4A | 0.0809 | 5530 | 68.4 | 0.0114 | 6.34 | 0.0012 |
| -26A | 0.0813 | 3800 | 46.7 | 0.0077 | 6.65 | 0.0006 |
| Average | | | 57.2 | 0.0098 | 6.37 | |
| | | | +14.1 | +0.0031 | +0.86 | |
| | | | -10.5 | -0.0029 | -0.77 | |

a - A dash (-) indicates no strain at peak load, sharp brittle fracture

TABLE 6C

RESIDUAL COMPRESSION STRENGTH TEST RESULTS OF
LAMINATE 1 COUPONS FATIGUE TESTED AT 0 TO 50 ksi

Coupons fatigue tested to 31,400 cycles equal to a probability of
survival, $P_s$, of 0.90    (Number of coupons Static Tested = 20.)

| Sample ID | Min. Area, in.$^2$ | Ultimate Load, $P_{ult}$, lbs. | Ultimate Stress, $\sigma_{ult}$, ksi | Ultimate Strain, $\epsilon_{ult}$, in./in. in 2.0 in. | Apparent Initial Modulus $E_a$, psi x 10$^6$ | Amt. of Strain at Peak Load, $\epsilon$, in./in. in 2.0 in. |
|---|---|---|---|---|---|---|
| 578- 5A | 0.0836 | 6010 | 71.9 | 0.0123 | 6.65 | -$^a$ |
| - 2B | 0.0838 | Coupon failed at 14,200 cycles | | | | |
| -14B | 0.0817 | 5580 | 68.3 | 0.0119 | 6.44 | 0.0006 |
| 580- 4A | 0.0830 | 5240 | 63.1 | 0.0097 | 7.09 | - |
| - 8B | 0.0835 | 5620 | 67.3 | √$^b$ | 6.30 | √ |
| 582-14A | 0.0835 | 5630 | 67.4 | 0.0112 | 6.65 | 0.00045 |
| -19A | 0.0835 | 5130 | 61.4 | √ | √ | √ |
| 583- 8B | 0.0835 | 5640 | 67.5 | 0.0108 | 6.14 | - |
| -20B | 0.0831 | 5310 | 63.9 | 0.0107 | 6.50 | - |
| 594- 5A | 0.0812 | 5600 | 69.8 | 0.0116 | 6.32 | 0.0006 |
| - 8A | 0.0828 | 5330 | 64.4 | 0.0117 | 6.53 | - |
| 595-17B | 0.0832 | 5280 | 63.5 | 0.0103 | 6.68 | - |
| -21B | 0.0817 | 5080 | 62.2 | 0.0097 | 6.80 | - |
| 601- 5A | 0.0828 | 4270 | 51.6 | 0.0072 | 8.05 | 0.0006 |
| -17B | 0.0827 | 5810 | 70.2 | 0.0109 | 6.72 | 0.0006 |
| 603- 3A | 0.0810 | Coupon failed at 28,800 cycles | | | | |
| -16B | 0.0828 | Coupon failed at 5,350 cycles | | | | |
| -23B | 0.0809 | 5510 | 68.1 | 0.0110 | 6.68 | - |
| -24B | 0.0810 | 4720 | 58.3 | √ | 6.86 | √ |
| 604- 7B | 0.0833 | 5350 | 64.2 | 0.0108 | 6.49 | - |
| -14B | 0.0847 | 5000 | 59.0 | 0.0108 | 6.56 | - |
| 606-10A | 0.0840 | 4650 | 55.4 | 0.0093 | 6.44 | - |
| - 1B | 0.0815 | 4540 | 55.7 | 0.0093 | 6.29 | - |
| Average | | | 63.7 | 0.0111 | 6.64 | |
| | | | + 8.2 | +0.0012 | +1.41 | |
| | | | -12.1 | -0.0039 | -0.50 | |

a - A dash (-) indicates no strain at peak load, sharp brittle fracture.
b - A check (√) indicates not properly recorded by the measuring
apparatus.

245

## TABLE 7C

### RESIDUAL COMPRESSION STRENGTH TEST RESULTS OF LAMINATE 1 COUPONS FATIGUE TESTED AT -16 TO 42 ksi

Coupons fatigue tested to 14,400 cycles equal to a probability of survival, $P_S$, of 0.90. (Number of coupons Static Tested = 20.)

| Sample ID | Min. Area, in.$^2$ | Ultimate Load, $P_{ult}$, lbs. | Ultimate Stress, $\sigma_{ult}$, ksi | Ultimate Strain, $\varepsilon_{ult}$, in./in. in 2.0 in. | Apparent Initial Modulus $F_a$, psi x 10$^6$ | Amt. of Strain at Peak Load, $\varepsilon$, in./in. in 2.0 in. |
|---|---|---|---|---|---|---|
| 578-14A | 0.0866 | 4960 | 57.3 | 0.0103 | 5.92 | -$^a$ |
| - 7B | 0.0833 | 5740 | 68.9 | 0.0117 | 6.67 | 0.0006 |
| - 9B | 0.0861 | Coupon failed at 9,550 cycles | | | | |
| 580-14B | 0.0842 | 5400 | 64.1 | 0.0102 | 6.99 | 0.0010 |
| - 7B | 0.0822 | 6260 | 76.2 | √$^b$ | 6.58 | - |
| 582- 6A | 0.0807 | 5520 | 68.4 | 0.0105 | 6.88 | 0.0006 |
| -11A | 0.0823 | 5770 | 70.1 | 0.0118 | 6.75 | 0.0004 |
| 583-17B | 0.0841 | 5500 | 65.4 | 0.0109 | 6.61 | 0.0008 |
| -19B | 0.0836 | 6340 | 75.8 | 0.0130 | 6.64 | 0.0009 |
| 594-19A | 0.0826 | 5860 | 70.9 | 0.0119 | 6.72 | 0.0006 |
| - 8B | 0.0816 | 5070 | 62.1 | 0.0103 | 6.62 | 0.0008 |
| 595- 2B | 0.0818 | 5060 | 61.9 | 0.0111 | 6.79 | 0.0012 |
| -13B | 0.0835 | 5240 | 62.8 | 0.0099 | 6.65 | 0.0003 |
| 601-14A | 0.0836 | 5970 | 71.4 | 0.0118 | 6.64 | 0.00045 |
| -15A | 0.0829 | 5300 | 63.9 | 0.0102 | 6.52 | - |
| 603-26A | 0.0819 | 5510 | 67.3 | 0.0111 | 6.78 | 0.0006 |
| -10B | 0.0843 | 5400 | 64.1 | 0.0104 | 6.98 | - |
| 604-15A | 0.0812 | Coupon failed at 11,800 cycles | | | | |
| - 4B | 0.0808 | 5100 | 63.1 | 0.0096 | 6.88 | 0.0004 |
| - 9B | 0.0839 | 4980 | 59.4 | √ | √ | √ |
| 606-16A | 0.0847 | 4450 | 52.5 | 0.0084 | 6.56 | 0.0006 |
| - 4B | 0.0814 | 4940 | 59.5 | 0.0111 | 6.30 | 0.0009 |
| Average | | | 65.2 | 0.0108 | 6.66 | |
| | | | +11.0 | +0.0022 | +0.32 | |
| | | | -12.7 | -0.0024 | -0.74 | |

a - A dash (-) indicates no strain at peak load, sharp brittle fracture.

b - A check (√) indicates not properly recorded by the measuring apparatus.

246

TABLE 8C

RESIDUAL COMPRESSION STRENGTH TEST RESULTS OF
LAMINATE 1 COUPONS FATIGUE TESTED AT -16 TO 50 ksi

Coupons fatigue tested to 2,150 cycles equal to a probability of
survival, $P_s$, of 0.9. (Number of coupons Static Tested = 20.)

| Sample ID | Min. Area, in.$^2$ | Ultimate Load, $P_{ult}$, lbs. | Ultimate Stress, $\sigma_{ult}$, ksi | Ultimate Strain, $\varepsilon_{ult}$, in./in. in 2.0 in. | Apparent Initial Modulus $E_a$, psi x 10$^6$ | Amt. of Strain at Peak Load, $\epsilon$, in./in. in 2.0 in. |
|---|---|---|---|---|---|---|
| 578-12A | 0.0849 | 4880 | 57.5 | 0.0102 | 6.19 | 0.0003 |
| - 4B | 0.0840 | 5560 | 66.2 | 0.0114 | 6.61 | 0.00075 |
| 580-13A | 0.0842 | 6660 | 79.1 | 0.0125 | 6.60 | 0.0005 |
| - 1B | 0.0864 | 5200 | 60.2 | 0.0094 | 6.43 | - a |
| 582-26A | 0.0826 | 5860 | 70.9 | 0.0116 | 6.73 | 0.00045 |
| -22B | 0.0813 | 5700 | 70.1 | 0.0113 | 6.65 | - |
| 583-22A | 0.0823 | 5630 | 68.4 | 0.0114 | 6.75 | 0.00045 |
| - 4B | 0.0821 | 5990 | 73.0 | 0.0112 | 5.80 | 0.0006 |
| 594- 5B | 0.0798 | 5610 | 70.3 | 0.0108 | 7.37 | - |
| -18B | 0.0821 | 5700 | 69.4 | 0.0108 | 6.41 | - |
| 596- 8A | 0.0821 | 5830 | 71.0 | 0.0116 | 6.96 | 0.0005 |
| -18B | 0.0835 | 5330 | 63.8 | 0.0102 | 6.65 | - |
| 601-22A | 0.0820 | 5730 | 69.9 | 0.0102 | 7.17 | - |
| -25B | 0.0804 | 5850 | 72.8 | 0.0116 | 6.91 | 0.0005 |
| 603- 1B | 0.0823 | 5800 | 70.5 | √ b | √ | - |
| - 6B | 0.0801 | 6020 | 75.2 | 0.0114 | 6.94 | 0.0003 |
| 604- 8A | 0.0833 | 5500 | 66.0 | 0.0109 | 6.67 | 0.0006 |
| - 1B | 0.0823 | 4650 | 56.5 | 0.0087 | 6.75 | 0.0006 |
| 606-11A | 0.0844 | 5800 | 68.7 | 0.0117 | 6.58 | 0.0006 |
| - 5B | 0.0819 | 5900 | 72.0 | 0.0117 | 6.43 | 0.0006 |
| Average | | | 68.6 | 0.0110 | 6.66 | |
| | | | +10.5 -12.1 | +0.0015 -0.0023 | +0.71 -0.86 | |

a - A dash (-) indicates no strain at peak load, sharp brittle fracture
b - A check (√) indicates not properly recorded by the measuring
   apparatus.

247

TABLE 9C

RESIDUAL TENSION STRENGTH  TEST RESULTS OF LAMINATE 2 COUPONS
FATIGUE TESTED AT 0 TO 100 ksi

(Number of coupons Static Tested = 20)

| Sample ID | Average Area, in.$^2$ | Ultimate Load, $P_{ult}$, lbs | Ultimate Stress, $\sigma_{ult}$, ksi | Ultimate Strain, $\epsilon_{ult}$, in./in. in 2.0 in. | Apparent Modulus of Elasticity, $E_a$, psi x$10^6$ | Amt. of Strain at Ultimate Load, $\epsilon$, in./in. in 2.0 in. |
|---|---|---|---|---|---|---|
| 696- 5A | .1236 | 18050 | 140.4 | .0090 | 15.6 | .0004 |
| 696-24A | .1253 | 15150 | 120.9 | .0080 | 15.1 | .0005 |
| 696-29A | .1291 | 18150 | 140.6 | .0092 | 15.3 | .0005 |
| 696- 2B | .1239 | 16650 | 134.4 | .0084 | 16.0 | .0004 |
| 696-29C | .1264 | 19000 | 150.3 | .0088 | 17.1 | .0005 |
| 699- 1A | .1201 | 18550 | 154.5 | .0096 | 16.1 | .0005 |
| 699-34A | .1302 | 19900 | 152.8 | .0093 | 16.4 | $-^a$ |
| 699-22B | .1318 | 19650 | 149.1 | .0096 | 15.5 | - |
| 699-30B | .1235 | 17200 | 139.3 | .0084 | 16.6 | - |
| 699- 1C | .1171 | 16900 | 144.3 | .0091 | 15.8 | .0005 |
| 727-24A | .1290 | 18050 | 139.9 | .0094 | 14.9 | - |
| 727-26A | .1255 | 16000 | 127.5 | .0089 | 14.3 | .0005 |
| 727- 7B | .1270 | 19000 | 149.6 | .0097 | 15.4 | .0005 |
| 727-16B | .1275 | 20300 | 159.2 | .0102 | 15.6 | $0^b$ |
| 727-11C | .1270 | 17300 | 136.2 | .0091 | 15.0 | .0005 |
| 728-37A | .1300 | 18000 | 138.5 | .0093 | 14.9 | - |
| 728- 2B | .1236 | 18250 | 147.7 | .0096 | 15.4 | - |
| 728- 7B | .1304 | 18550 | 142.2 | .0087 | 16.3 | - |
| 728-26B | .1288 | 19700 | 153.0 | .0093 | 16.5 | - |
| 728- 9C | .1306 | 19600 | 150.1 | .0097 | 15.5 | - |
| Average | | | 143.5 +15.7 -22.6 | .0092 +.0010 -.0012 | 15.7 +1.4 -1.4 | |

a – A dash (-) indicates that the strain at ultimate load was not recorded.

b – A zero (0) indicates that no strain at ultimate load was observed.

248

TABLE 10C

RESIDUAL TENSION STRENGTH TEST RESULTS OF LAMINATE 2 COUPONS
FATIGUE TESTED AT -30 TO + 70 ksi
(Number of coupons Static Tested = 20)

| Sample ID | Average Area, in.$^2$ | Ultimate Load $P_{ult}$, lbs | Ultimate Stress, $\sigma_{ult}$, ksi | Ultimate Strain, $\epsilon_{ult}$, in./in. in 2.0 in. | Apparent Modulus of Elasticity, $E_a$, psi x $10^6$ | Amt. of Strain at Ultimate Load, $\epsilon$, in./in. in 2.0 in. |
|---|---|---|---|---|---|---|
| 696-22A | .1286 | 16700 | 129.9 | .0092 | 14.1 | .0005 |
| 696-27A | .1264 | 17250 | 136.5 | .0085 | 16.1 | .0005 |
| 696-33A | .1269 | 18100 | 142.6 | .0086 | 16.6 | .0003 |
| 696- 8B | .1279 | 18700 | 146.2 | .0103 | 14.3 | 0 [a] |
| 696-20B | .1262 | 18750 | 148.6 | .0096 | 15.5 | .0005 |
| 699- 7B | .1290 | 19700 | 152.7 | .0098 | 15.6 | .0005 |
| 699-14B | .1258 | 18600 | 147.8 | .0106 | 13.9 | 0 |
| 699-24C | .1299 | 18400 | 141.6 | .0094 | 15.1 | .0004 |
| 699-26C | .1269 | 18550 | 146.2 | .0093 | 15.7 | .0004 |
| 727- 3A | .1255 | 18000 | 143.4 | .0094 | 15.3 | .0005 |
| 727- 6A | .1270 | 18300 | 144.1 | .0093 | 15.5 | .0003 |
| 727-4B | .1258 | 17200 | 136.7 | .0085 | 16.1 | .0004 |
| 727- 5C | .1282 | 19600 | 152.9 | .0099 | 15.4 | .0004 |
| 727-28C | .1264 | 16600 | 131.3 | .0087 | 15.1 | .0005 |
| 728-10A | .1302 | 20100 | 154.6 | .0104 | 14.9 | 0 |
| 728-34A | .1292 | 18450 | 142.8 | .0090 | 15.9 | .0004 |
| 728- 1B | .1177 | 18300 | 155.5 | .0097 | 16.0 | .0004 |
| 728-22B | .1320 | 18700 | 141.7 | .0095 | 14.9 | .0005 |
| 728-37B | .1258 | 17000 | 135.1 | .0091 | 14.8 | .0002 |
| Average | | | 143.7 +11.8 -13.8 | .0094 +.0012 -.0009 | 15.3 +1.3 -1.4 | |

a - A zero (0) indicates that no strain at ultimate load was observed.

249

## TABLE 11C

RESIDUAL COMPRESSION STRENGTH TEST RESULTS OF LAMINATE 2 COUPONS FATIGUE TESTED AT 0 TO 100 ksi

(Number of coupons Static Tested = 20)

| Sample ID | Average Area, in.$^2$ | Ultimate Load, $P_{ult}$, lbs. | Ultimate Stress, $\sigma_{ult}$, ksi | Ultimate Strain, $\epsilon_{ult}$, in./in. in 2.0 in. | Apparent Modulus of Elasticity, $E_a$, psi x 10$^6$ | Amt. of Strain at Ultimate Load, $\epsilon$, in./in. in 2.0 in. | Secant Modulus at 70 ksi, $E_{sec}$, psi x 10$^6$ |
|---|---|---|---|---|---|---|---|
| 696-35B | .1270 | 12050 | 94.9 | .0072 | 13.1 | .0008 | 13.72 |
| 11C | .1256 | 10700 | 85.2 | .0062 | 13.5 | 0$^b$ | 13.86 |
| 28C | .1276 | 14800 | 116.0 | .0093 | 11.9 | .0008 | 13.21 |
| 34C | .1280 | 11000 | 85.9 | .0066 | 12.6 | .0014 | 13.46 |
| 699-21A | .1266 | 13200 | 104.3 | .0080 | 12.9 | .0006 | 13.73 |
| 33A | .1296 | 13550 | 104.6 | .0087 | 12.2 | 0 | 12.96 |
| 37B | .1266 | 12500 | 98.7 | .0078 | 12.4 | .0003 | 13.21 |
| 10C | .1295 | 12700 | 98.1 | .0077 | 12.5 | .0011 | 13.46 |
| 21C | .1307 | 10150 | 77.7 | .0057$^a$ | 13.3 | 0 | 13.08 |
| 727-30A | .1270 | 11250 | 88.6 | $^{\underline{a}}$ | - | - | - |
| 1B | .1195 | 11200 | 93.7 | .0061 | 14.2 | .0009 | 15.20 |
| 9C | .1284 | 13150 | 102.4 | .0081 | 12.1 | .0011 | 13.46 |
| 15B | .1274 | 13500 | 106.0 | .0084 | 12.4 | .0007 | 13.59 |
| 33C | .1276 | 11800 | 92.5 | .0081 | 13.2 | .0010 | 12.50 |
| 728-6B | .1290 | 12850 | 99.6 | .0078 | 12.5 | .0009 | 13.46 |
| 27B | .1271 | 10800 | 85.0 | .0067 | 11.8 | .0003 | 12.50 |
| 34B | .1300 | 13550 | 104.2 | .0083 | 12.6 | 0 | 13.86 |
| 31C | .1282 | 16125 | 125.8 | .0101 | 11.9 | .0007 | 13.21 |
| 33C | .1302 | 16250 | 124.8 | .0099 | 12.4 | 0 | 13.73 |
| Average | | | 99.3 +26.5 -2.6 | .0078 +.0023 -.0021 | 12.7 +1.5 -0.9 | | 13.46 +0.40 -0.96 |

a - A dash (-) indicates this value was not recorded.

b - A zero (0) indicates that no strain at ultimate load was observed.

250

TABLE 12C

RESIDUAL COMPRESSION STRENGTH TEST RESULTS OF LAMINATE 2 COUPONS FATIGUE TESTED AT -30 TO +70 ksi

(Number of coupons Static Tested = 20)

| Sample ID | Average Area, in.$^2$ | Ultimate Load, $P_{ult}$, lbs | Ultimate Stress, $\sigma_{ult}$, ksi | Ultimate Strain, $\epsilon_{ult}$, in./in. in 2.0 in. | Apparent Modulus of Elasticity, $E_a$, psi x 10$^6$ | Amt. of Strain at Ultimate Load, $\epsilon$, in./in. in 2.0 in. | Secant Modulus at 70 ksi, $E_{sec}$, psi x 10$^6$ |
|---|---|---|---|---|---|---|---|
| 696-19A | .1279 | 15400 | 121.3 | .0094 | 12.8 | .0008 | 13.86 |
| 30A | .1292 | 12900 | 99.8 | .0084 | 12.7 | .0010 | 13.73 |
| 1B | .1146 | 10550 | 92.1 | .0070 | 13.2 | - | 13.73 |
| 16B | .1286 | 13250 | 103.0 | .0081 | 12.2 | .0008 | 13.59 |
| 18C | .1295 | 13400 | 103.5 | -a | 13.8 | - | 12.96 |
| 699-31A | .1283 | 16600 | 129.4 | .0109 | 11.6 | .0008 | 13.33 |
| 37A | .1204 | 12250 | 101.7 | .0078 | 12.9 | .0009 | 13.86 |
| 18B | .1280 | 12050 | 94.1 | .0071 | 12.9 | 0b | 13.73 |
| 33B | .1288 | 11950 | 92.8 | .0072 | 13.0 | .0009 | 13.86 |
| 35C | .1299 | 11250 | 86.6 | .0066 | 12.7 | .0011 | 13.59 |
| 727-4A | .1259 | 13100 | 104.0 | .0088 | 12.1 | .0015 | 13.59 |
| 21A | .1295 | 11500 | 88.8 | .0066 | 12.9 | .0012 | 13.46 |
| 22B | .1291 | 10400 | 80.6 | .0061 | 13.2 | .0010 | 13.46 |
| 26C | .1243 | 10950 | 88.1 | .0066 | 12.7 | .0010 | 13.21 |
| 34C | .1289 | 10620 | 85.9 | - | - | - | - |
| 728-28A | .1268 | 11650 | 91.9 | .0076 | 12.0 | .0008 | 12.84 |
| 25B | .1284 | 10600 | 82.6 | .0077 | 11.2 | .0011 | - |
| 29B | .1300 | 16750 | 128.8 | .0106 | 11.9 | .0007 | 14.00 |
| 23C | .1317 | 13550 | 102.9 | .0081 | 12.9 | 0 | 13.73 |
| Average | | | 98.8 +30.0 -18.2 | .0079 +.0030 -.0018 | 12.6 + 1.2 - 1.4 | | 13.56 +0.44 -0.72 |

a – A dash (-) indicates this value was not recorded.

b – A zero (0) indicates that no strain at ultimate load was observed.

TABLE 13C

COMPRESSION STRENGTH TEST RESULTS OF LAMINATE 2 COUPONS TESTED IN OCT, 1976

(No Prior Fatigue)   (Number of coupons Static Tested = 20)

| Sample ID | Average Area, in.² | Ultimate Load, $P_{ult}$, lbs | Ultimate Stress, $\sigma_{ult}$, ksi | Ultimate Strain, $\epsilon_{ult}$, in./in. in 2.0 in. | Apparent Modulus of Elasticity, $E_a$, psi x 10⁶ | Amt. of Strain at Ultimate Load, $\epsilon$, in./in. in 2.0 in. | Secant Modulus at 70 ksi, $E_{sec}$, psi x 10⁶ |
|---|---|---|---|---|---|---|---|
| 696- 4A | .1298 | 12900 | 99.4 | .0077 | 12.4 | .0005 | 13.21 |
| 17B | .1287 | 14000 | 108.8 | .0087 | 12.4 | .0006 | 13.21 |
| 21B | .1282 | 14000 | 109.2 | .0087 | 12.4 | 0ᵇ | 13.08 |
| 15C | .1296 | 15250 | 117.7 | .0093 | 12.8 | .0011 | 13.72 |
| 30C | .1289 | 15300 | 118.7 | .0093 | 12.6 | .0005 | 13.72 |
| 699- 6A | .1295 | 14100 | 108.9 | .0092 | 11.8 | .0009 | 12.73 |
| 11A | .1300 | 15750 | 121.2 | .0099 | 11.9 | .0008 | 13.70 |
| 20A | .1318 | 15150 | 114.9 | .0099 | 11.4 | - | 12.96 |
| 28B | .1293 | 15500 | 119.9 | .0101 | 12.2 | .0008 | 13.46 |
| 6C | .1293 | 15150 | 117.2 | .0099 | 11.7 | .0011 | 12.84 |
| 727-16A | .1284 | 14200 | 110.6 | .0087 | 12.4 | 0 | 13.21 |
| 14B | .1256 | 15000 | 119.4 | .0102 | 11.3 | .0008 | 12.61 |
| 31B | .1290 | 15500 | 120.2 | .0099 | 11.7 | .0007 | 13.26 |
| 2C | .1239 | 13600 | 109.8 | .0085 | 12.8 | .0007 | 14.00 |
| 29C | .1287 | 15000 | 116.6 | .0099 | 12.2 | .0010 | 13.72 |
| 728-22A | .1323 | 15200 | 114.9 | .0099 | 11.5 | .0006 | 12.96 |
| 25A | .1285 | 14950 | 116.3 | -ᵃ | 11.6 | - | 12.73 |
| 8B | .1312 | 15150 | 115.5 | .0099 | 12.0 | .0010 | 12.73 |
| 7C | .1317 | 12850 | 97.6 | .0077 | 12.5 | .0011 | 12.96 |
| 9C | .1303 | 14600 | 112.0 | .0090 | 12.2 | .0008 | 13.46 |
| Average | | | 113.4 | .0093 | 12.1 | | 13.21 |
| | | | + 15.2 | +.0014 | + 0.7 | | + 0.79 |
| | | | - 10.0 | -.0011 | - 0.8 | | - 0.48 |

a - A dash indicates this value was not recorded

b - A zero indicates that no strain at ultimate load was observed

252

REFERENCES

1.  Kaminski, B. E., "Narmco 5208/T300:  A Graphite-Epoxy System Engineered for High-Performance Aircraft Structures," 5th National SAMPE Technical Conference, October, 1973.

2.  Doner, Douglas R., and Novak, R. C., "Structural Behavior of Laminated Graphite Filament Composites," Proceedings of the Society of the Plastics Industry 24th Annual Technical Conference, February, 1969.

3.  Sattar, S. A., and Kellog, D. H., "The Effect of Geometry on the Mode of Failure of Composites in the Short Beam Shear Test," Composite Materials: Testing and Deisgn, ASTM STP 460, American Society for Testing and Materials, 1969.

4.  Pagano, N. J., and Pipes, R. Byron, "Some Observations on the Interlaminar Strength of Composite Laminates," Int. J. Mech. Sci., Vol. 15, 1973.

5.  Lakman, L. M., et al, "Advanced Composites Data for Aircraft Structural Design, Vol. IV:  Material and Basic Allowable Development-Graphite/Epoxy," AFML TR 70-58, September, 1972.

6.  Pagano, N. J., and Pipes, R. B., "Some Observations on the Interlaminar Strength of Composite Laminates," Int. J. Mech. Sci., Volume 15, 1973.

7.  Spiegel, M. R., Theory and Problems of Statistics, Schaum's Outline Series, McGraw-Hill, 1961.

8.  Gumbel, E. J., Statistics of Extremes, Columbia University Press, New York, 1958.

9.  Bowie, G. E., Pettit, D. E., Ryder, J. T., and Krupp, W. E., "NDI Life Analysis Interface," Lockheed-California Company Report LR 27013, September,1974.

10. Advanced Composites Design Guide, Vol. IV, Test Methods Sec. 4.2, prepared by Rockwell International Corporation for the United States Air Force, January 1973, pp. 3-6.

11. " Test Methods - High Modulus, High Strength Graphite Materials and Assemblies," Specification IT-50, Revision B, Code Ident. No. 76823, Northrop Corporation, Aircraft Division, May 22, 1972.

12. "Material Specification, Cloth, Graphite Yarn, Epoxy Resin Impregnated, Fleet Ballistic Missile," Code Ident. 10001, prepared by Lockheed Missiles and Space Company, Inc. for Department of the Navy, Strategic Systems Project Office, Washington, D. C., April 5, 1974.

13. "Hercules Incorporated Graphite Composite Testing Procedures," HD-SG-2-6002B, Hercules Incorporated, Bacchus Works, Magna, Utah, January, 1975, pp. 14-16.

14. "Material Specification - Graphite Fiber Tape and Sheet, Epoxy Resin Impregnated," 207-8-410A, Vought Systems Division, LTV Aerospace Corporation, Dallas, Texas, June 3, 1974.

15. "Specification for Advanced Composite Material - Multiply Graphite/Epoxy Prepreg Broodgoods," LB0130-XXX, Code Ident. No. 43999, Rockwell International Corporation, B-1 Division, February 3, 1976.

16. "General Specification for Graphite Fiber Non-Woven Tape and Sheet, Resin Impregnated," C-22-1379, Lockheed-California Company, Burbank, California, November 12, 1975.

17. "Standard Method of Test for Compressive Properties of Oriented Fiber Composites," American Society for Testing and Materials, Designation: D3410-75.

18. "Standard Method of Test for Compressive Properties of Rigid Plastics," American Society for Testing and Materials, Designation: D695-69.

19. Halpin, J. C., Jerina, K. L., and Johnson, T. A., "Characterization of Composites for the Purpose of Reliability Evaluation," AFML, Technical Report No. AFML-TR-73-289, December, 1972.

20. Valluri, S. R., "Unified Engineering Theory of High Stress Level Fatigue," Aerospace Engineering, Vol. 20, No. 20, October, 1961.

21. Halpin, J. C., and Jerina, K. L., "Statistical Stress Concentration Effects in Composites," presented at UCLA Symposium, November, 1972.

22. Reed, D. L, and Eisenmann, J. R., "Reliability Aspects of a Composite Bolted Scarf Joint," <u>Composite Reliability</u>, ASTM STP 580, American Society for Testing and Materials, 1975, pp. 90-101.

23. <u>Advanced Composites Design Guide</u>, AFML, Advanced Development Division, Vol. IV, Third Edition, 1973.

24. Halpin, J. C., Jerina, K. L., and Johnson, T. A., "Characterization of Composites for the Purpose of Reliability Evaluation," <u>Analysis of Test Methods for High Modulus Fibers and Composites</u>, ASTM STP 521, American Society for Testing and Materials, 1973, pp. 5-64.

25. Berens, A. P., and West, B. S., "Evaluation of an Accelerated Characterization Technique for Reliability Assessment of Adhesive Joints," <u>Composite Reliability</u>, ASTM STP 580, American Society for Testing and Materials, 1975, pp. 90-101.

26. Berens, A. P., Johnson, P. E., and West, B. S., "Experimental Evaluation of a Reliability Assessment Model for Adhesively Bonded Joints," Air Force Materials Laboratory, Technical Report AFML-TR-74-120, June, 1974.

27. Halpin, J. C., "Structural Reliability Characterization of Advanced Composites," <u>Proceedings of the Colloquium on Structural Reliability: The Impact of Advanced Materials on Engineering Design,</u> Conducted with the cooperation of the U. S. Air Force Materials Laboratory, AFSC, held at Carnegie-Mellon University, 9-12 October, 1972, pp. 275-307.

28. Waddoups, M. E., and Halpin, J. C., "The Fracture and Fatigue of Composite Structures," <u>Computers and Structures</u>, Vol. V, 1974, pp. 659-673.

29. Air Force Military Standard, "Aircraft Structural Integrity Program, Airplane Requirements," MIL-STD-1530, U. S. Air Force Aeronautical Systems Command, Wright-Patterson AFB, Ohio, September, 1972.

30. Lavengood, R. E., and Ishai, O., "The Mechanical Performance of Cross-Plied Composites," <u>Polymer Engineering and Science</u>, Vol. 11, No. 3, May, 1971, pp. 226-232.

31. Reed-Hill, R. E., <u>Physical Metallurgy Principles</u>, D. Von Nostrand Company, Inc., Princeton, New Jersey, 1964.

32. Hoeppner, D. W., and Krupp, W. E., "Prediction of Component Life by Application of Fatigue Crack Growth Knowledge," <u>Engineering Fracture Mechanics</u>," Vol. 6, 1974, pp. 47-70.

33. Irwin, G. R., "Fracture Mechanics," <u>Structural Mechanics</u>, Pergamon Press, New York, 1960, p. 557.

34. Rice, J. R., and Rosengren, G. F., <u>Journal of the Mechanics and Physics of Solids</u>, Vol. 16, 1968, pp. 1-12.

35. Begley, J. A., and Landes, J. D., "The J Integral as a Fracture Criterion," <u>Fracture Toughness, Proceedings of the 1971 National Symposium on Fracture Mechanics</u>, Part II, ASTM STP 514, American Society for Testing and Materials, 1972, pp. 1-20.

36. Landes, J. D., and Begley, J. A., "The Effect of Specimen Geometry on $J_{IC}$," <u>Fracture Toughness, Proceedings of the 1971 National Symposium on Fracture Mechanics, Part II</u>, ASTM STP 514, American Society for Testing and Materials, 1972, pp. 24-39.

37. Ryder, J. T., "Fracture Control of H-O Engine Components," National Aeronautics and Space Administration Report, NASA CR-135137, February, 1977.

38. Adsit, N. R., and Waszczak, J. P., "Fracture Mechanics of Boron/Aluminum Coupons Containing Stress Risers," <u>Fracture Mechanics of Composites</u>, ASTM STP 593, American Society for Testing and Materials, 1975, pp. 163-176.

39. Slepetz, J. M., and Carlson, L., "Fracture of Composite Compact Tension Specimens," <u>Fracture Mechanics of Composites</u>, ASTM STP 593, American Society for Testing and Materials, 1975, pp. 143-162.

40. Konish, H. J., Jr., "Mode I Stress Intensity Factors for Symmetrically-Cracked Orthotropic Strips," <u>Fracture Mechanics of Composites</u>, ASTM STP 593, American Society for Testing and Materials, 1975, pp. 99-116.

41. Zimmer, J. E., "Fracture Mechanics of a Fiber Composite," J. Composite Materials, Vol. 6, April, 1972, p. 312.

42. Konish, H. J., Jr., and Swedlow, J. L , "On Fracture Phenomena in Advanced Fiber Composite Materials," Presented at the 13th Structures, Structural Dynamics, and Materials Conference, Sponsored by AIAA/ASME/ SAE, San Antonio, Texas, April 10-12, 1972.

43. Beaumont, P. W. R., and Phillips, D. C., "Tensile Strengths of Notched Composites," J. Composite Materials, Vol. 6, January, 1972, p. 32.

44. Hancock, J. R., and Swanson, G. D., "Toughness of Filamentary Boron/Aluminum Composites," Composite Materials:  Testing and Design (Second Conference) ASTM STP 497, American Society for Testing and Materials, 1971, p. 299.

45. Cooper, C. A., "The Fracture Toughness of Composites Reinforced with Weakened Fibers," J. Material Science, Fol. 5, 1970, pg. 645.

46. Beaumont, P. W. R., and Tetelman, A. S., "The Fracture Strength and Toughness of Fibrous Composites," Reports Group, School of Engineering and Applied Science, University of California, Los Angeles, August, 1972.

47. Pettit, D. E., Ryder, J. T., Krupp, W. E., and Hoeppner, D. W., "Investigation of the Effects of Stress and Chemical Environments on the Prediction of Fracture in Aircraft Structural Materials," Air Force Materials Laboratory Report, AFML-TR-74-183, December, 1974.

48. Nuismer, R. J., and Whitney, J. M., "Uniaxial Failure of Composite Laminates Containing Stress Concentrations," Fracture Mechanics of Composites,  ASTM STP 593, American Society for Testing and Materials, 1975, pp. 117-142.

49. Roderick, G. L., and Whitcomb, J. D., "Fatigue Damage of Notched Boron/ Epoxy Laminates Under Constant Amplitude Loading," presented at the Symposium on Filamentary Composites sponsored by ASTM in Denver, Colorado, November, 1976.

50. Chang, F. H., Gordon, D. E., and Gardner, A. H., "A Study of Fatigue Damage in Composites by Nondestructive Testing Techniques," presented at the Symposium on Filamentary Composites sponsored by ASTM in Denver, Colorado, November, 1976.

51. Freeman, R. B., and Durchlaub, E. C., "Designing for the Fracture Strength and Failure Modes of Notched Boron-Epoxy Composites," Proceedings of the Conference on Fibrous Composites in Flight Vehicle Design, AFFDL-TR-72-130, Dayton, Ohio, 26-28 September 1972, pp. 739-755.

52. Kulkarni, S. V., McLaughlin, P. V., Jr., Pipes, R. B., and Rosen, B. W., "Fatigue of Notched Fiber Composite Laminates: Analytical and Experimental Evaluation," Composite Materials: Testing and Design (Fourth Conference), ASTM STP 617, American Society for Testing and Materials, 1977.

53. Reifsnider, K. L., "Fatigue in Composite Materials," North Atlantic Treaty Organization, Advisory Group for Aerospace Research and Development, AGARD, Report AGARD-R-638, February, 1976.

54. Reifsnider, K., Stinchcomb, W. E., and O'Brien, T. K., "Frequency Effects on a Stiffness Based Failure Criterion in Flawed Composite Specimens," Presented at the Symposium on Filamentary Composites Sponsored by ASTM in Denver, Colorado, November, 1976.

55. Halpin, J. C., "Structure- Property Relations and Reliability Concepts," J. Composite Materials, Vol. 6, April, 1972, pp. 208-231.

56. Halpin, J. C., Waddoups, M. E., and Johnson, T. A. "Kinetic Fracture Models and Structural Reliability," Int. J. Fracture Mechanics, Vol. 8, 1972, pp. 465-468.

57. Eisenman, J. R., Kaminski, B. E., Reed, K. L., Wilkens, D. J., "Toward Reliable Composites: An Examination of Design Methodology," J. Composite Materials, Vol. 7, 1973, pp. 298-308.

58. Paris, P. C., "The Growth of Cracks Due to Variations in Loads," Ph.D Thesis, Lehigh University, 1962.

59. Yang, J. N., "Analysis of Fatigue Data," presented at the Mechanics of Composites Review sponsored by the Air Force Materials Laboratory, Nonmetallic Materials Division and the Air Force Office of Scientific Research, Directorate of Aerospace Sciences in Dayton, Ohio, 26-28 October, 1976

60. Wu, E. M., "Strength and Fracture of Composites," Composite Materials, Vol. 5, Academic Press, 1974.

61. Rosen, B. W., and Zweben, C. H., "Tensile Failure Criteria for Fiber Composite Materials," NASA CR-2057, 1972.

62. Zweben, C. H., "Fracture Mechanics and Composite Materials: A Critical Analysis," Analysis of Test Methods for High Modulus Fibers and Composites, ASTM STP 521, American Society for Testing and Materials, 1972, pp. 65-97.

63. Kulkaini, S. V., and Rosen, B. W., "Design Data for Composite Structure Safe Life Prediction Analysis Evaluation, AFML-TR-73-225, 1973.

64. Zweben, C. H., "A Bounding Approach to the Strength of Composite Materials," J. Engineering Fracture Mechanics, Vol. 4, No. 1, March 1972, pp. 1-8.

65. Kanninen, M. F., Rybicki, E. F., and Brenson, H. F., " A Critical Look at Current Applications of Fracture Mechanics to the Failure of Fibre-Reinforced Composites," Composites, January, 1977, pp. 17-22.

66. Kanninen, M. F., Rybicki, E. F., and Griffith, W. L., "Preliminary Development of a Fundamental Analyses Model for Crack Growth in a Fibre-Reinforced Composite Material," Composite Materials: Testing and Design (Fourth Conference), ASTM STP 617, American Society for Testing and Materials, 1977.

67. Anthony, F. M., "Discussion of the Colloquium on Structural Reliability," Proceedings of the Colloquium on Structural Reliability: The Impact of Advanced Materials on Engineering Design, Conducted with the cooperation of the U. S. Air Force Materials Laboratory, AFSC, held at Carnegie-Mellon University, 9-12 October, 1972, pp. 527-534.